MAY 1971

MDC G2134

MASTER

NUCLEAR SHUTTLE

SYSTEM DEFINITION STUDY, PHASE III

FINAL REPORT

VOLUME II
Concept and Feasibility Analysis

PART A
Class 1 Hybrid RNS

BOOK 1
System Analysis and Operations

PREPARED FOR NASA-MSFC
UNDER CONTRACT NAS8-24714,
DRL NO. MSFC-DRL-196,
LINE ITEM 3

COPY NO. 52

MCDONNELL DOUGLAS ASTRONAUTICS COMPANY

MCDONNELL DOUGLAS
CORPORATION

DISTRIBUTION OF THIS DOCUMENT UNLIMITED

DISCLAIMER

This report was prepared as an account of work sponsored by an agency of the United States Government. Neither the United States Government nor any agency Thereof, nor any of their employees, makes any warranty, express or implied, or assumes any legal liability or responsibility for the accuracy, completeness, or usefulness of any information, apparatus, product, or process disclosed, or represents that its use would not infringe privately owned rights. Reference herein to any specific commercial product, process, or service by trade name, trademark, manufacturer, or otherwise does not necessarily constitute or imply its endorsement, recommendation, or favoring by the United States Government or any agency thereof. The views and opinions of authors expressed herein do not necessarily state or reflect those of the United States Government or any agency thereof.

DISCLAIMER

Portions of this document may be illegible in electronic image products. Images are produced from the best available original document.

MASTER

MCDONNELL DOUGLAS

NUCLEAR SHUTTLE SYSTEM DEFINITION STUDY
PHASE III FINAL REPORT
VOLUME II
Concept and Feasibility Analysis
PART A
Class 1 Hybrid RNS
BOOK 1
System Analysis and Operations

MAY 1971

MDC G2134

PREPARED FOR NASA-MSFC
UNDER CONTRACT NAS8-24714
DRL NO. MSFC-DRL-196
LINE ITEM 3

MCDONNELL DOUGLAS ASTRONAUTICS COMPANY

5301 Bolsa Avenue, Huntington Beach, CA 92647

DISTRIBUTION OF THIS DOCUMENT UNLIMITED

NOTICE
This report was prepared as an account of work sponsored by the United States Government. Neither the United States nor the United States Energy Research and Development Administration, nor any of their employees, nor any of their contractors, subcontractors, or their employees, makes any warranty, express or implied, or assumes any legal liability or responsibility for the accuracy, completeness or usefulness of any information, apparatus, product or process disclosed, or represents that its use would not infringe privately owned rights.

FOREWORD

This document contains the results of the operations and design analysis effort performed during the Phase III Nuclear Shuttle Definition Study for the Class 1 Hybrid Reusable Nuclear Shuttle (RNS) concept. This work was accomplished for the National Aeronautics and Space Administration, George C. Marshall Space Flight Center, Huntsville, Alabama, under Contract NAS8-2714. The final report was generated to fulfill the requirements of DRL No. MSFC-DRL-196, Line Item 3, and it covers the period from May 1, 1970 to May 1, 1971.

The study effort described in this volume was performed under the direction of Dr. R. J. Holl and Dr. K. P. Johnson, with responsibility for specific activities as follows:

G. I. Abrams — Astrionics and System Analysis
M. P. Billings — Radiation Shielding Analysis
C. B. Boehmer — Reliability and Safety
R. Chen — Thermal and Structures Analysis
R. S. Cowls — Mission Analysis
P. A. Ferguson — Operations Analysis
L. B. Goda — Structures Design and Analysis
C. Goetz — Radiation Shielding Analysis
J. P. Harland — Trajectory Analyses
R. Hauver — Flight Dynamics Analyses
R. Luna — Reliability Analyses
R. F. Manoske — Propulsion Analysis
M. Mayer — Computing Analyses
G. Montoya — Astrionics Design
W. C. Nowak — Navigation and Guidance Analysis
Y. Oster — Propulsion Design and Analysis
R. G. Riedesel — Operations Analysis
J. Salontai — Thermal Analysis
D. A. Schow — Radiation Effects
R. G. Seibert — Navigation and Guidance Analysis
R. van't Riet — Structural Dynamics and Flight Control

DISTRIBUTION OF THIS DOCUMENT UNLIMITED

BLANK

PREFACE

The material contained in this document represents a portion of the final report documentation for the Phase III Nuclear Shuttle System Definition Study. The study effort was performed as a 12-month extension to the existing Nuclear Flight System Definition Study Contract (NAS8-24714), with the objective of establishing Phase A conceptual definition for two classes of reusable nuclear shuttle concepts. The first concept class is characterized as a 33-ft-diameter configuration that is launched integrally to orbit by a Saturn V INT-21 vehicle. The second concept class is characterized as a modular configuration which is assembled in earth orbit from modules carried to orbit in a space shuttle.

The final report documentation has been organized to provide separable information for the two concepts, where appropriate, and to combine report material common to both concepts in singular documents. The total documentation for the study is listed below, with this document identified in the left margin.

o	Volume I:	Executive Summary
	Volume II:	Concept and Feasibility Analysis
		Part A — Class 1 Hybrid RNS
●		Book 1 — System Analysis and Operations
o		Book 2 — System Definition
		Part B — Class 3 RNS
o		Book 1 — System Analysis and Operations
o		Book 2 — System Definition
	Volume III:	Program Support Requirements
o		Part A — Class 1 Hybrid RNS
o		Part B — Class 3 RNS
o		Part C — Test Program Analyses and SRT Requirements
	Volume IV:	Cost Data
o		Part A — Class 1 Hybrid RNS
o		Part B — Class 3 RNS
o	Volume V:	Schedules, Milestones, and Networks
o	Volume VI:	Reliability and Safety Analysis
o	Volume VII:	RNS Project Requirements

CONTENTS

FIGURES

Number		Page

TABLES

Section 1
INTRODUCTION

1.1 SCOPE

This document contains the technical analyses, tradeoffs, and descriptions of the design and operations of a Reusable Nuclear Shuttle (RNS), generated by McDonnell Douglas Astronautics Company under a System Definition Study as a 12-month extension to Contract NAS8-24714, designated here as Phase III.

The results of the previous Phase I and II activities of the Nuclear Flight System Definition Studies provided a sound basis for Phase III. Although Phase I concerned an expendable nuclear stage (NFPM), an advanced stage concept was selected which included a reusable shuttle mission as a design requirement. Phase II entailed a total reorientation to reusable systems, and surveyed a broad spectrum of potential RNS system and subsystem concepts. From these, two RNS concepts were selected for further evaluation during Phase III: (1) Class 1 Hybrid, a 33-ft-diameter configuration launched to orbit by a Saturn INT-21, but with NERVA launched to orbit separately as a propulsion module by the space shuttle; and (2) Class 3, a modular configuration assembled in orbit from modules launched by the space shuttle. The distinctions between these concepts were maintained within the context of parallel evaluations, which are reported as separate self-contained volumes. The design and operations activities on the Class 1 Hybrid RNS are reported herein, and those for the Class 3 RNS are contained in Volume II, Part B.

A baseline RNS configuration was established at an orientation meeting, held at the inception of the Phase III study. RNS operations (launch, orbital, flight, etc.) were evaluated for this baseline, and the configuration and subsystem design requirements were revised accordingly. These resulted in additional subsystem trade studies, some of which were intimately related to the sequence and interrelation of operations (such as startup of the RNS), and more complete definition of system and subsystem operational parameters. The design effort concluded with definition of the hardware tree and a description of the design details.

Documentation of the results of these activities has been organized in this volume in a manner which permits the reader to focus on each aspect of the system definition as an entity. Section 1.2 concisely summarizes the final baseline design. Section 2 defines the RNS mission applications and the reference lunar shuttle mission. Section 3 incorporates the complete set of RNS operations from prelaunch through the reference mission, establishing the basis for RNS design requirements and interfaces with other planned systems. Section 4 contains the design analyses performed in response to these. Book 2 describes the resulting RNS design as an integrated system. It also describes the RNS modules and subsystems and the recommended NERVA/stage interface.

1.2 DESIGN SUMMARY

This section contains a brief description of the RNS Class 1 Hybrid (1-H) concept. The vehicle is based in low earth orbit and provides transportation in a shuttle mode to more distant destinations. Its design mission is a round trip to a 60-nmi lunar polar orbit, operating from a 260 nmi, 31.5 degree inclination earth orbit. It is maintained and replenished there by the space shuttle.

A sketch of the Class 1 Hybrid RNS configuration is shown in Figure 1.2-1, which illustrates the selected configuration and provides a locator for some of the features which were evaluated. It consists of three distinct modules which can be assembled and disassembled in space. The aft module, called the propulsion module, contains NERVA and a small run tank of propellant. The propellant module provides the main propellant tank and minimal propellant management subsystems. At the forward end of the stage is a command and control module (CCM) which contains most of the functional equipment and all of the expendables except for main stage LH_2. The auxiliary propulsion engines are located on outriggers on the CCM, which are visible

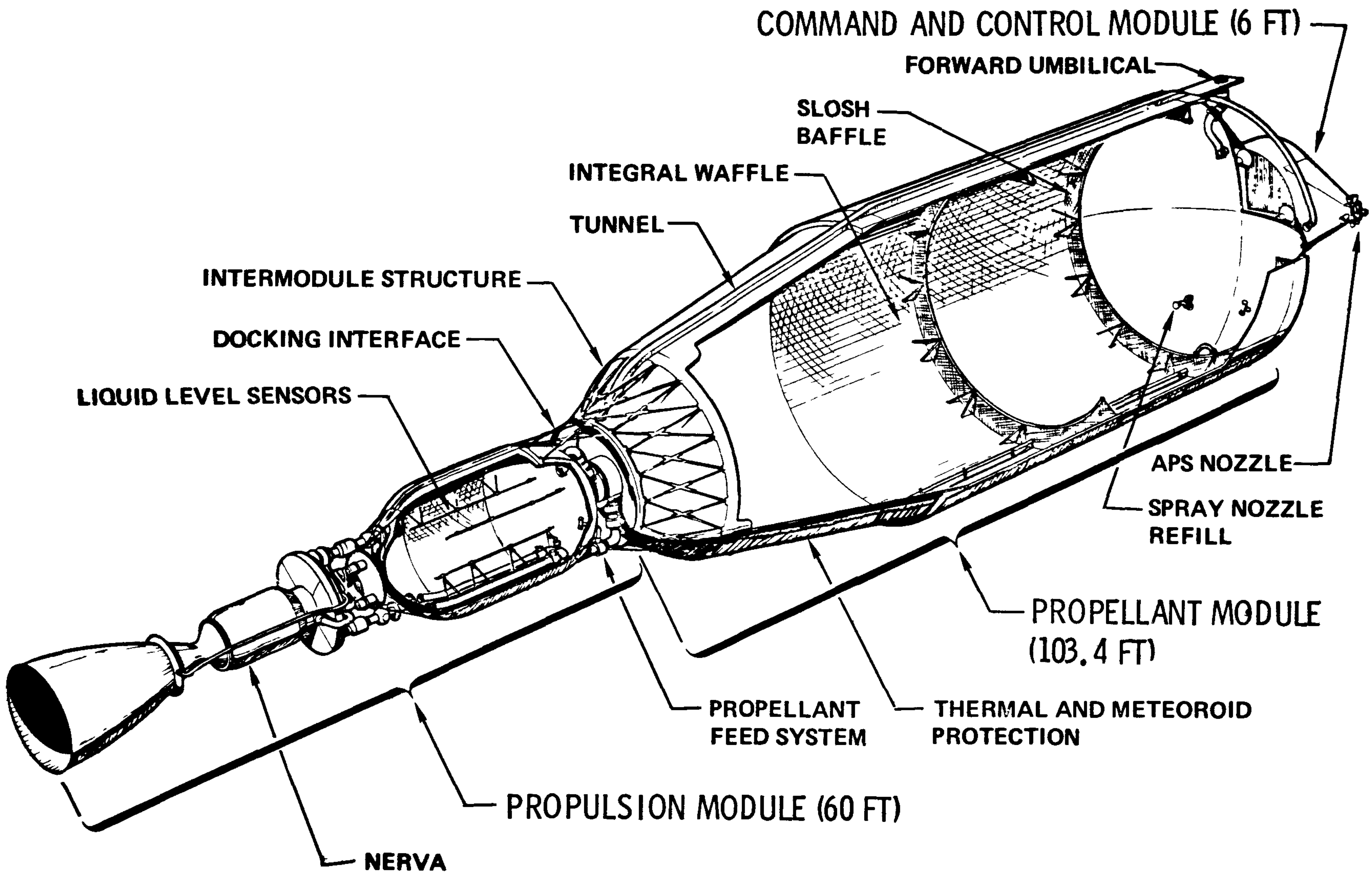

Figure 1.2-1. Class 1 Single-Module Hybrid RNS

in the sketch. This module is replaced between missions in earth orbit, thereby effecting a replenishment of expendables and all scheduled maintenance.

Both the propulsion module and the CCM are designed to be transported to earth orbit within the cargo bay of the space shuttle. This facilitates replacement of the CCM, as noted, and of NERVA, as might be required because of failure or to extend the lifetime of the RNS beyond that of the engine. The RNS is resupplied with LH_2 in earth orbit by the space shuttle between missions.

The total propellant capacity of the stage is 300,000 lb LH_2, of which 10,850 lb LH_2 is contained in the run tank on the propulsion module. The modules are contained within a 10-degree half-angle cone subtended by the NERVA reactor, determined from a combined optimization of structural and shield weights during Phase II. The location of the CCM is selected for ease of replacement. The run tank diameter on the propulsion module is constrained to 160 in. to limit the radiation shield weight but still provide adequate volume to allow autonomous operation during startup, shutdown, and aftercooling. This autonomy simplifies the operating requirements imposed on the stage and reduces the RNS development requirements.

The RNS design and operations concept minimizes orbital support requirements. The space shuttle is utilized to deliver replacement modules and resupply propellant. A space tug is utilized to support assembly and replacement of modules and to safely dispose of expended propulsion modules. No permanent, manned, orbital facilities are required for maintenance or propellant resupply.

A weight statement for the RNS Class 1 Hybrid vehicle is given in Table 1.2-1.

Table 1.2-1

WEIGHT SUMMARY – CLASS 1 HYBRID RNS

Code	Description	Modules: Pro-pellant	Pro-pulsion	Command & Control	Total Vehicle Weight (lb)
2.00	Structure	(21,110)	(1,300)	(720)	(23,130)
2.01	Propellant Tank Assembly	17,150	570	---	
2.02	Thrust Structure	470	170	---	
2.03	Forward Skirt	620	250	---	
2.04	Aft Skirt	720	---	---	
2.05	Tunnel and Fairings	490	---	---	
2.06	Exterior Finish and Sealer	210	20	---	
2.07	Antislosh Baffles	360	60	---	
2.08	Equipment Support Structure	230	160	360	
2.09	Equipment Module Structure	---	---	360	
2.10	Additional Structure				
	Payload Adapter	640	---	---	
	Access	220	70	---	
3.00	Meteoroid/Thermal Protection	(6,250)	(710)	(110)	(7,070)
3.01	Insulation	2,470	430	---	
3.02	Meteoroid Protection	3,780	280	110	
4.00	Docking/Clustering	(280)	(80)	(280)	(640)
4.01	Forward Docking Structure	80	80	80	
4.02	Aft Docking Structure	200	---	200	
4.03	Clustering Structure	---	---	---	
5.00	Main Propulsion	(520)	(30,630)	(560)	(31,710)
5.01	NERVA Engine	---	27,300	500	
5.02	External Disc Shield for NERVA	---	2,900	---	
5.03	Purge System	---	---	---	
5.04	Propellant Scavenging System and Sensors	---	---	---	
5.05	Propellant Feed System	110	140	---	
5.06	Pressurization System	70	60	---	
5.07	Prepressurization System	---	---	---	
5.08	Pneumatic System	---	---	---	
5.09	Fill and Drain/Orbit Refueling	120	60	60	
5.10	Ground and Emergency Vent	160	---	---	
5.11	Flight Vent	60	50	---	
5.12	Integrated Chilldown System	---	70	---	
5.13	Refill System	---	50	---	

Table 1.2-1 (Continued)

Code	Description	Modules: Pro-pellant	Pro-pulsion	Command & Control	Total Vehicle Weight (lb)
6.00	Auxiliary Propulsion	---	(160)	(950)	(1,110)
6.01	Reaction Control System	---	160	950	
6.02	Retro System	---	---	---	
6.03	Ullage System	---	---	---	
7.00	Astrionic System/Astrionics	(255)	(345)	(1,905)	(2,505)
7.01	Guidance, Navigation and Control		20	310	
7.02	Instrumentation	35	15	210	
7.03	Command and Control	10	10	140	
7.04	Electrical Power	40	130	785	
7.05	Electrical Networks	160	150	85	
7.06	Environmental Control	---	---	---	
7.07	Propellant Management	---	10	---	
7.08	Onboard Checkout	5	5	60	
7.09	Data Management	5	5	315	
8.00	Safety/Ordnance System	---	---	---	---
8.01	Safety System	---	---	---	
8.02	Ordnance System	---	---	---	
9.00	Contingency	(1,480)	(150)	(200)	(1,830)
	Subtotal	29,865	33,375	4,725	67,995
10.00	RCS Propellant	---	---	(1,250)	(1,250)
11.00	Residual Propellant	(9,030)	(440)	---	(9,470)
11.01	Liquid Propellant	400	100	---	
11.02	Vapor Vented	---	---	---	
11.03	Vapor	8,630	340	---	
12.00	Reserve Flight Performance				(1,700)
13.00	Propellant Boiloff	---	---	---	---
14.00	Impulse Propellant (Startup, Mainstage, Shutdown, Cooldown) Baseline 6-Burn Mission Profile				(288,830)
14.01	Leave Earth				174,330
14.02	Arrive Moon				37,960
14.03	Leave Moon				26,210
14.04	Arrive Earth				50,330
	Total	NA	NA	NA	369,245

Section 2
MISSION APPLICATIONS

Three classes of missions are proposed for the RNS: interorbital shuttle (lunar and geosynchronous), unmanned planetary, and manned planetary. These are all performed in a reusable shuttle mode. The lunar shuttle mission provides the basis for RNS design requirements in this study. The other mission classes are described only in the context of future applications. However, the RNS designed for the lunar shuttle mission possesses the functional capability to perform the other missions, except for transplanetary operations. More detailed mission descriptions and performance data are documented in the Mission Planning Handbook. All mission performance are based on the following NERVA performance figures and a 300,000-lb LH_2 capacity RNS:

Thrust Mode	Thrust (lb)	Specific Impulse (sec)
Full Thrust	75,000	825
Throttle	45,000	825
Idle	1,000	500
Aftercooling	302	431

2.1 MISSION DESCRIPTIONS

2.1.1 Lunar Shuttle

The lunar shuttle mission entails transfer of cargo and men to and from a 60-nmi polar lunar orbit, operating from a low circular earth orbit. An approximate 260-nmi circular earth orbit, inclined at 31.5 degrees, provides both lunar phase and daily ground rendezvous compatibility, permitting repetitively rendezvousing with a facility in lunar orbit. This model provides two coplanar round trip opportunities for each 54.6-day cycle. During this cycle the moon completes two orbits about the earth while the earth operational orbit regresses a total of one cycle. These two coplanar opportunities are characterized by an 18-day lunar and 15-day earth-orbit stay on the first coplanar round trip and four days and three days, respectively, on the second round trip. In order to have a finite launch window, the capability of performing orbital plane changes at the moon must be introduced. For the purpose of identifying RNS design requirements, a plane change requirement of 30 degrees was imposed for both the lunar orbit insertion and translunar injection maneuvers. This is equivalent to an earth or lunar-departure launch window of about one to three days, depending upon the specific transfer opportunity in question, assuming an attendant variation in transit time.

The characteristics of the lunar shuttle design mission are schematically portrayed in Figure 2.1-1, indicating a total of eight main stage burns, one each for translunar and earth orbit injection, and three each for lunar orbit and transearth injection. The orbital plane change maneuvers conducted at the moon are accomplished near apoapsis in an intermediate elliptical orbit.

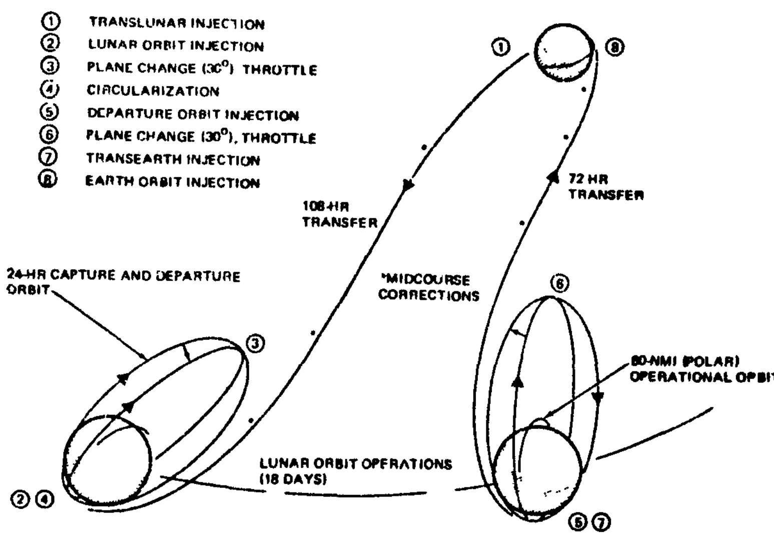

Figure 2.1-1 LUNAR SHUTTLE DESIGN MISSION PROFILE

The orbital period of this orbit (24 hours) was selected because of its characteristics of providing for an efficient plane rotation maneuver (low apoapsis speeds) and not being unduly large in regard to the earth-induced perturbations. Ideal velocity requirements associated with this design profile, as well as with the normal operational profile (four burns), are summarized in Table 2.1-1. Because of the short burn time required for the plane change maneuver, NERVA is operated in the throttle mode.

Table 2.1-1

VELOCITY SUMMARY FOR LUNAR SHUTTLE MISSION

	Profile (fps)	
	8-Burn	4-Burn
Translunar injection (108-hr transfer, $C_3 = 1.912\ km^2/sec^2$, 300 fps flight geometry reserve)	10,372	10,372
Midcourse correction	50	50
Lunar orbit injection ($C_3 = 0.808\ km^2/sec^2$)	3,150	2,760
24-hr orbit	(929)	---
30-deg plane change	(320)	---
Circularize at 60 nmi	(1,831)	---
Lunar orbit operations	---	---
Transearth injection (72-hour transfer)	3,590	3,200
24-hour orbit	(1,831)	---
30-deg plane change	(390)	---
Injection ($C_3 = 1.486\ km^2/sec^2$)	(1,369)	---
Midcourse correction	50	50
Earth orbit injection ($C_3 = 1.378\ km^2/sec^2$, 300 fps flight geometry reserve)	10,454	10,454
Flight performance reserve (3/4 percent of total ΔV)	207	201
TOTAL	27,873	27,087

ANSC A-1-M 27195

SNSOW A 28700

2.1.2 Geosynchronous Shuttle

The geosynchronous shuttle mission entails transfer of men and equipment between low circular and equatorial geosynchronous (19,323 nmi) orbit altitudes. This mission requires four main stage maneuvers for each mission round trip, as is depicted in Figure 2.1-2. A 2.4-degree plane change is incorporated into the 260 nmi departure and arrival maneuvers. Course corrections via NERVA idle mode are required on the ascending and descending mission legs. Major mission phase times include 5.25-hour transfer between the 260-nmi baseline departure orbit and synchronous altitude, and 30 days (design value) on station at geosynchronous altitude.

2.1.3 Unmanned Planetary

A variety of transplanetary injection missions, characterized by a broad range of earth-departure velocity requirements, is being considered for the RNS. The ideal velocity requirements of these missions range from about 12,000 fps for Mars surface sample retrieval missions to about 28,000 fps

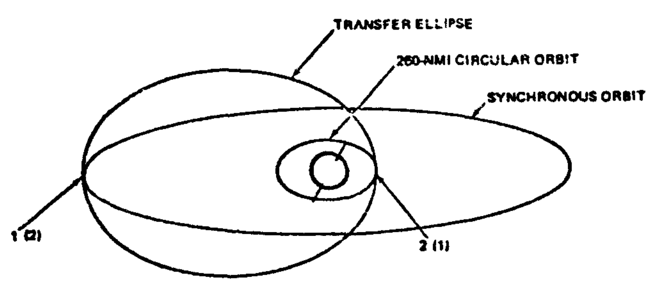

		*Velocity (fps)
ASCENT:		
(1)	INJECTION INTO 260 BY 19 325 NMI TRANSFER ELLIPSE—ORBITAL PLANE IS CHANGED 2.4 DEG	6014
(2)	ORBIT IS CIRCULARIZED AT 19,325 NMI, ORBITAL PLANE IS CHANGED 29 1 DEG	7885
DESCENT:		
1	INJECTION INTO 260 BY 19,325 NMI TRANSFER ELLIPSE—ORBITAL PLANE IS CHANGED 29.1 DEG	7885
2	ORBIT IS CIRCULARIZED AT 260 NMI ORIBTAL PLANE IS CHANGED 2.4 DEG	6014

*Ideal velocity requirement. Excludes in- transit midcourse correction allowance of 50 fps each for outbound and inbound mission legs.

Figure 2.1-2 GEOSYNCHRONOUS SHUTTLE MISSION (above 260-nmi circular speed) for grand tour missions. The basic requirement imposed upon the RNS is to accelerate the mission spacecraft from the 260-nmi circular speed to the desired hyperbolic transfer trajectory. Subsequently, the RNS is to (1) separate from the spacecraft, (2) dispose of itself via placing it on a safe trajectory relative to the spacecraft, or (3) perform the required propulsive maneuvers to return it to a 260-nmi orbit. In the case where the RNS is used in an expendable mode, energy provided by the aftercooling phase following injection and separation from the spacecraft would provide sufficient separation to avoid interference with the spacecraft. In the case where the RNS is required to return to the 260-nmi circular orbit following injection of the mission spacecraft on to the desired escape hyperbola, sufficient propellant reserves must be retained to permit recapture of the RNS into the earth's sphere of influence.

Figure 2.1-3 schematically illustrates the required maneuvers for the shuttle mode. The first maneuver following injection (ΔV-2) rotates the velocity vector along the hyperbola to an angle coincident with an intermediate buffer ellipse. This maneuver is accomplished near perigee of the buffer not So

- ΔV_1 - RNS Injects Spacecraft Onto Escape (Hyperbolic) Trajectory
- ΔV_2 - Following RNS-Spacecraft Separation, RNS Injects Onto Buffer Ellipse
- ΔV_3 - RNS Circularizes Orbit at 260 NMi

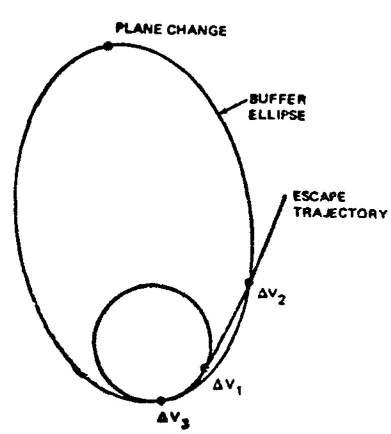

Figure 2.1-3 ESCAPE INJECTION MISSION SCHEMATIC

ellipse. Near apogee of the buffer ellipse, a plane change maneuver will be performed to adjust for the relative regression between the elliptical buffer orbit and a desired 260-nmi orbital plane (approximately 6 degrees, or 500 fps, for a 48-hour period buffer ellipse). This would be accomplished with an idle mode operation of the NERVA engine. Subsequently, the second major maneuver following transplanetary injection (ΔV-3) would be performed near perigee of the buffer ellipse placing the RNS again into the 260-nmi earth orbit. The second maneuver (ΔV-3) could be broken into two phases to permit establishing an immediate elliptical orbit which would provide phase correction between an earth-orbit facility and the RNS. As the velocity increments are mission-dependent, they are not indicated on the figure. The relationships between these velocities and the mission injection velocity requirements are discussed and displayed parametrically in the Mission Planning Handbook.

2.1.4 Manned Planetary

Two reference manned Mars landing missions are evaluated and described in the Mission Planning Handbook. The missions are described briefly as follows.

2.1.4.1 1990 Mars Conjunction Class

The heliocentric flight profile (Figure 2.1-4) indicates trajectory phase time, planetary nuclear propulsion system propellant requirements, and ideal mission velocity requirements. The launch date (middle of August 1990), 1,005-day total trip time, and 13 May 1993 arrival date are based on the optimum earth-departure date. The profile is optimum in a sense that the initial mass in earth orbit is minimized based on a propulsion vehicle configured for retrieval of the leave-earth stages. The planetary mission module is assumed carried throughout the entire mission to return to earth orbit, while all other items are assumed jettisoned while in Mars orbit. The earth departure is from a 260-nmi circular orbit. The 12-hour Mars orbit has a periapsis altitude of 270 nmi and an apoapsis altitude of 9,700 nmi, and the earth arrival orbit (24-hour period) has a perigee altitude of 270 nmi, and an apogee altitude of 38,420 nmi.

MANEUVER	ΔV (1000 FPS)	W_P (1000 LB)
LV-EARTH	13.72	876*
MIDCOURSE	0.50	31
ARV-MARS	4.71	151
ORBIT TRIM	0.15	7
LV-MARS	6.55	98
MIDCOURSE	0.50	10
ARV-EARTH	5.42	59
TOTAL	31.55	1,232*

*FOR RETRIEVAL OF LV-EARTH STAGES, PROPELLANT = 949,000 LB, TOTAL IS 1,305,000 LB

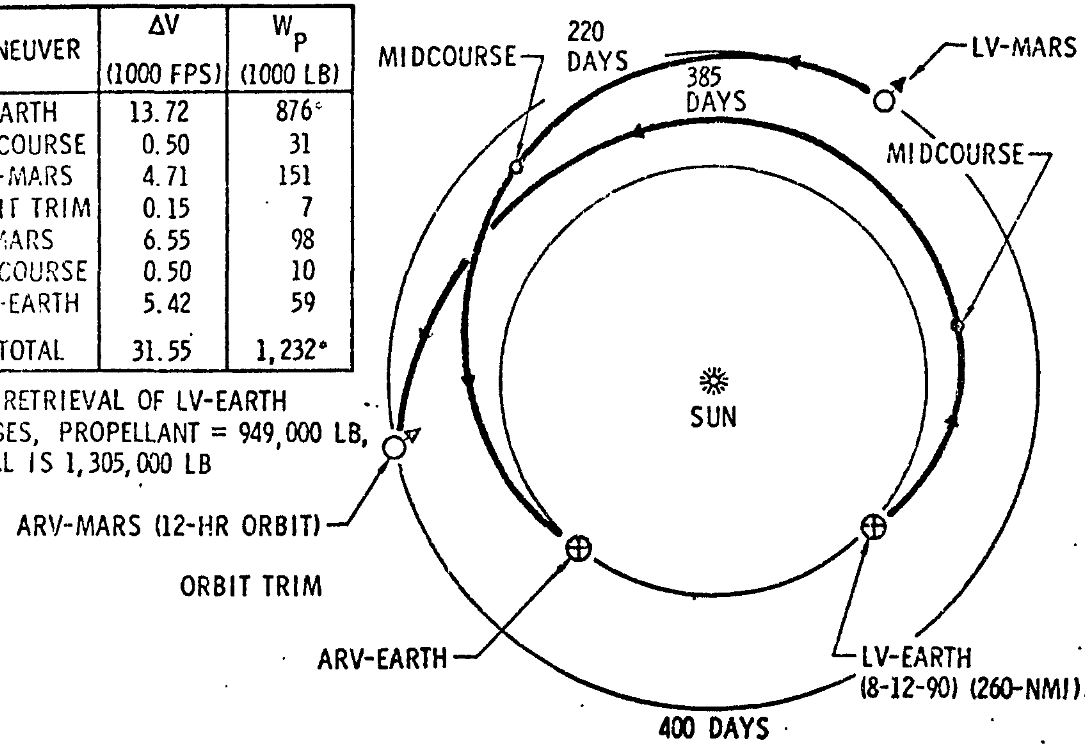

Figure 2.1-4 PLANETARY MISSION PERFORMANCE — 1990 MARS CONJUNCTION

2.1.4.2 1986 Mars Opposition Class (Outbound Venus Swingby Mode)

The heliocentric profile for the 1986 outbound Venus swingby manned planetary mission is shown in Figure 2.1-5. Mission velocity and phase time requirements are based on the optimum earth departure date. It is optimum in the sense that initial mass in earth orbit is minimized when it is based on an orbital launch vehicle configured for retrieval the leave-earth stages. Midcourse and Mars orbit trim propulsion maneuvers are assumed to be performed with a NERVA operating in the idle mode. Earth departure is from a 260-nmi circular orbit. The Mars capture orbit has a periapsis altitude of 270 nmi and an apoapsis altitude of 9,700 nmi, and the earth arrival orbit has a perigee altitude of 270 nmi and an apogee altitude of 38,420 nmi.

2.2 PERFORMANCE

2.2.1 Lunar Shuttle

The RNS performance is shown in Figure 2.2-1 for both the 4-burn and 8-burn lunar shuttle missions. The 4-burn profile is representative of the coplanar mission model (discussed in Section 2.1.1), repeating once every 54.6 days.

MANEUVER	ΔV (1000 FPS)	W_P (1000 LB)
LV-EARTH	14.08	1222*
MIDCOURSE	0.50	39
ARV-MARS	11.05	431
ORBIT TRIM	0.15	6
LV-MARS	6.88	113
MIDCOURSE	0.50	11
ARV-EARTH	8.95	101
TOTAL	42.11	1923*

*FOR RETRIEVAL OF LV-EARTH STAGES, PROPELLANT = 1,493,000 LB, TOTAL IS 2,194,000 LB

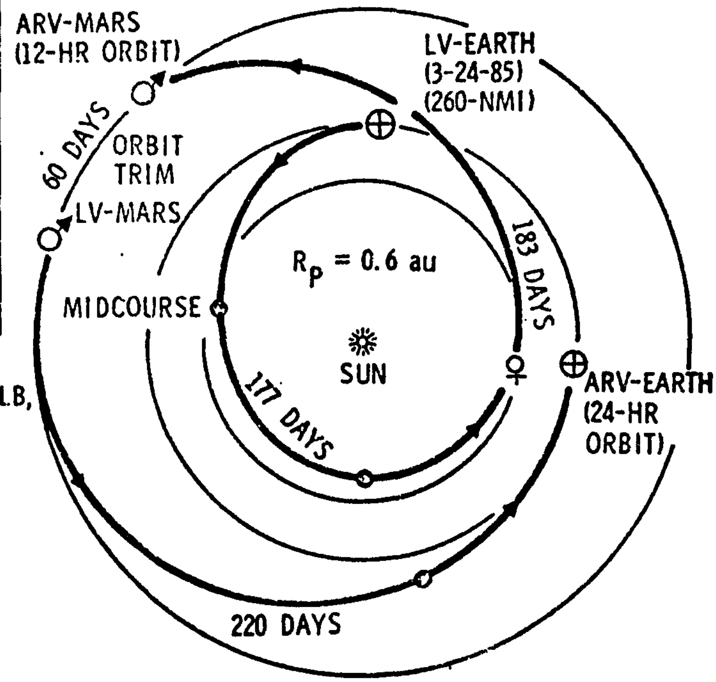

Figure 2.1-5 PLANETARY MISSION PERFORMANCE --
1986 MARS OPPOSITION (OUTBOUND VENUS SWINGBY MODE)

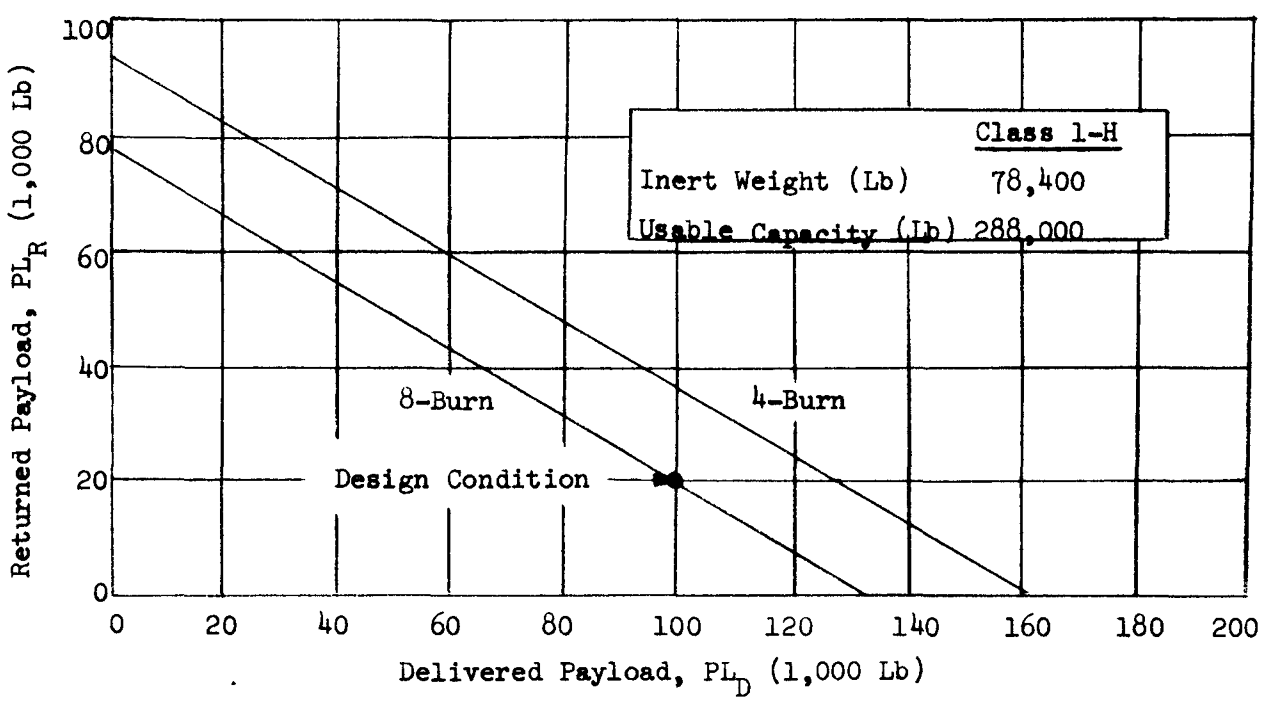

Figure 2.2-1 LUNAR SHUTTLE PERFORMANCE

This profile is used for operations and cost analyses. The 8-burn profile reflects a design condition. The performance data shown reflect total utilization of the cooldown impulse for the over all mission velocity requirement. Return payload (PL_R) is defined as the total payload carried above the RNS on the transearth leg of the mission while, correspondingly, delivered payload (PL_D) is defined as the total payload carried above the RNS on the translunar leg of the mission. Table 2.2-1 presents a variety of performance sensitivities to various parameters for the lunar shuttle mission. The reference mission model considers return of only the crew module (20,000 lb). The 300,000-lb LH_2 capacity RNS can deliver 98,000 lb of payload to the moon in this case for the 8-burn profile or 127,000 lb for the 4-burn profile. Based on a space shuttle launch cost of $5 million per launch and a mission rate of six per year, this corresponds to a transportation cost of $578/lb of payload in lunar orbit for the 4-burn profile (see Volume IV, Section 2.1, Cost Data).

2.2.2 Geosynchronous Shuttle

Mission performance for the geosynchronous mission is shown in Figure 2.2-2 based on the minimum velocity sum for the two primary transfer maneuvers between the low 260-nmi (31.5-degree inclination) orbit, at a geosynchronous equatorial orbit. Maneuver velocity requirements were as noted in Section 2.1.2. Return payload is defined as the total payload above the RNS on the descent leg of the mission, while delivered payload is defined as the total payload forward of the RNS on the ascent leg of the mission. The performance data shown for this mission are conservative in the sense that impulse derived from the aftercooling is not credited toward the overall mission velocity requirement.

2.2.3 Unmanned Planetary

RNS escape injection performance is shown in Figure 2.2-3 for three operating modes. These are: (1) RNS-only, no retrieval — the RNS is used in the expendable mode, requiring only separation from the spacecraft and establishment of a safe trajectory (relative to the spacecraft) through application of

Table 2.2-1

LUNAR SHUTTLE MISSION SENSITIVITIES

Sensitivity	8-burn	4-burn
$\partial PL_D/\partial PL_R$ (lb/lb)	-1.70	-1.73
$\partial PL_D/\partial$RNS Inert (lb/lb)	-2.70	-2.73
$\partial PL_R/\partial$RNS Inert (lb/lb)	-1.59	-1.58
$\partial PL_D/\partial W_P$ (lb/lb)		
∂RNS Inert/∂W_P = 0 lb/lb	1.18	1.30
∂RNS Inert/∂W_P = 0.125 lb/lb	0.84	0.96
$\partial PL_R/\partial W_P$ (lb/lb)		
∂RNS Inert/∂W_P = 0 lb/lb	0.69	0.75
∂RNS Inert/∂W_P = 0.125 lb/lb	0.49	0.56
$\partial PL_D/\partial$vented propellant (lb/lb)		
Translunar coast	-1.82	-2.02
Capture orbit	-1.91	-
60-nmi circular orbit	-2.09	-2.31
Departure orbit	-2.26	-
Transearth	-2.43	-2.69
$\partial PL_D/\partial$Jettisoned weight (lb/lb)		
Translunar coast	-0.65	-0.72
Capture orbit	-0.73	-
60-nmi circular orbit	-0.92	-1.01
Departure orbit	-1.08	-
Transearth	-1.26	-1.39
$\partial PL_D/\partial\Delta V$ (lb/fps)		
Outbound	-	- 26
Inbound	-	- 18
$\partial PL_D/\partial$Isp (lb/sec)	~ 700	~ 700

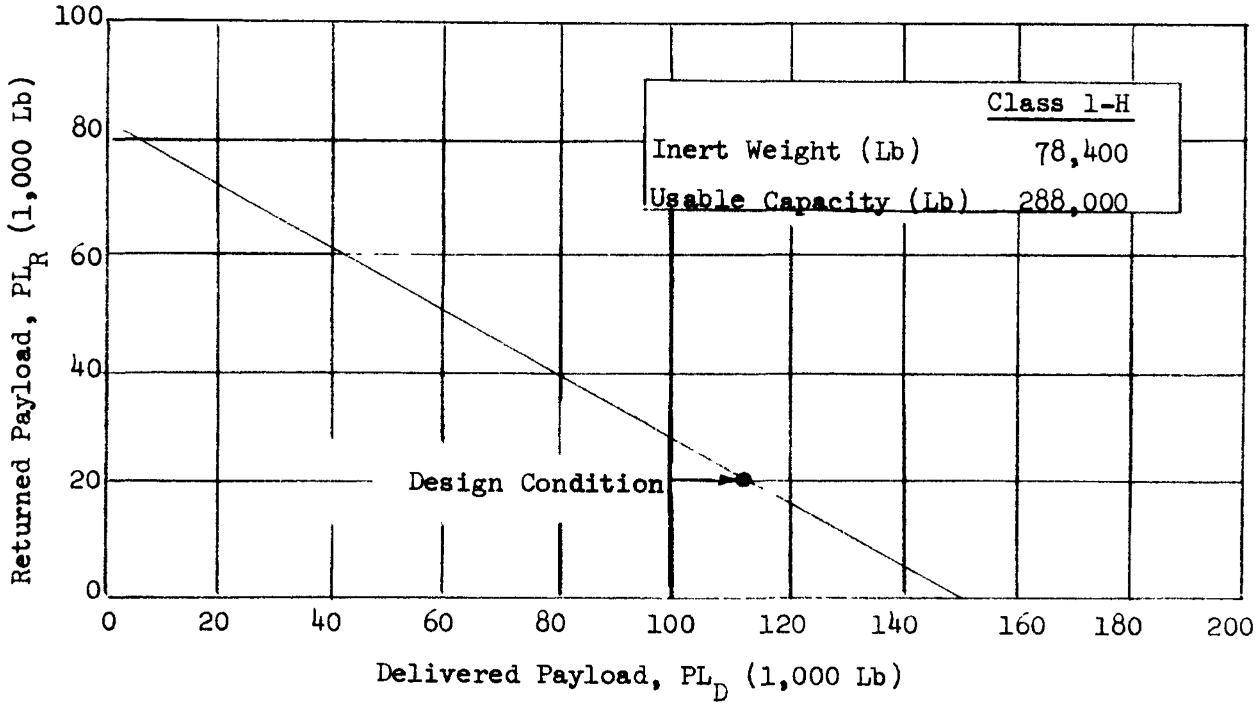

Figure 2.2-2 GEOSYNCHRONOUS SHUTTLE PERFORMANCE

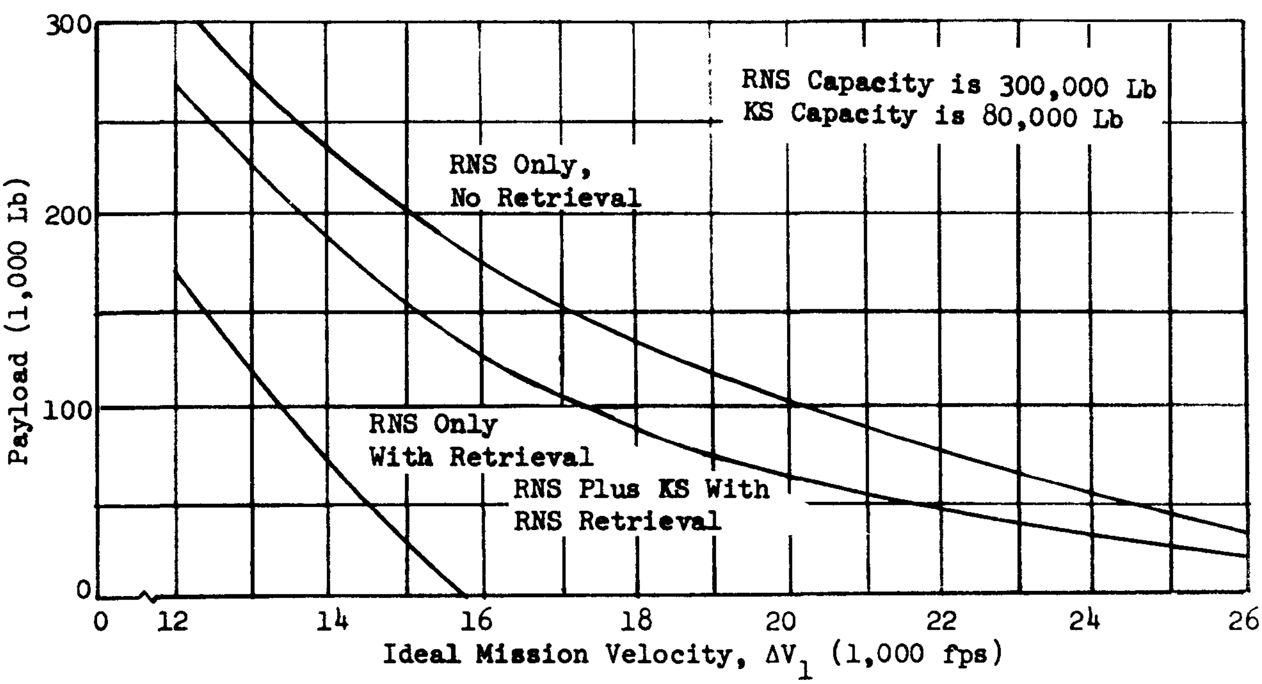

Figure 2.2-3 RNS ESCAPE INJECTION PERFORMANCE - MODE COMPARISON

the cooldown thrust; (2) RNS-plus-kick-stage with RNS retrieval – the RNS returns to the initial 260-nmi departure orbit following burnout and staging, with the chemical kick stage providing the remainder of the required mission velocity; and (3) RNS-only with retrieval – the RNS provides the total mission injection velocity requirement, followed by return to the initial 260-nmi departure orbit. Parameters pertinent to the representative chemical kick stage include the following:

Specific Impulse	460 sec
Structural Efficiency (λ')	0.86
RNS/KS Interstage	2,000 lb
Usable Propellant	80,000 lb

2.2.4 Manned Planetary

Mission performance requirements, in terms of number of stages and propellant in the 260 nmi assembly orbit, are identified for various operating modes in the Mission Planning Handbook.

2.3 MISSION TIMELINES

2.3.1 Lunar Shuttle

Table 2.3-1 presents the mission timeline for the lunar shuttle mission as related to the various propulsion maneuver requirements. The reference time is the translunar injection maneuver. The propellant consumption requirements and associated phase times are those utilized for design purposes (for example, see Section 3.10). With exception of the outbound and inbound midcourse and outbound and inbound plane change maneuvers (LOI-2 and TEI-2), the maneuvers are conducted at full thrust. The timeline is for the first of the two coplanar mission opportunities of the 54.6-day cycle previously discussed (Section 2.1.1), indicating an 18-day stay in lunar orbit.

Table 2.3-1

MISSION TIMELINE – CLASS 1 HYBRID

Event	Initiation Time (hr)	Propulsion Parameters				
		Impulse Propellant[1] (lb)	Cooldown Propellant (lb)	Steady-State Time (sec)	Total Run Time[1] (sec)	Cooldown Time[2] (hr)
TLI	0	166, 026	7, 300	1, 750	2, 700	108
Midcourse[3]	15, 37, 67 (typ)	1, 000	-	500	500	-
LOI-1	108	10, 730	770	70	330	12
LOI-2[4]	120	5, 370	400	25	260	12
LOI-3	132	19, 330	1, 250	160	460	27
TEI-1	518	11, 860	850	82	350	12
TEI-2[4]	530	3, 900	300	0	230	5
TEI-3	542	8, 200	600	43	290	11
Midcourse[3]	552, 577, 595 (typ)	500	-	250	250	-
EOI	614	47, 910	2, 800	470	930	45
TOTAL		274, 826	14, 270			

TLI Translunar injection
LOI-1 Lunar orbit injection (into 24-hour elliptical capture orbit)
LOI-2 30-deg plane change maneuver
LOI-3 Circularization maneuver at 60 nmi
TEI-1 Injection maneuver to elliptical departure orbit
TEI-2 30-deg plane change maneuver
TEI-3 Transearth injection
EOI Earth orbit injection (260 nmi)

NOTES

(1) Including chilldown (56 sec) through PSOV closure.
(2) Or time to next maneuver, whichever is less.
(3) Idle mode operation.
(4) Throttle mode operation, 30-deg plane change.

Activities occurring during the recycle operation in earth orbit are summarized in Table 2.3-2. In this case, the total time available for earth orbit turnaround of 84.2 days corresponds to a mission model with a 6-mission-a-year frequency. For this mission model two RNS systems alternately perform lunar shuttle missions at a combined rate of once each 54.6 days (every two lunar cycles). Since the missions are performed alternately by the two RNS, 84.2 days are spent in earth orbit by each RNS between mission applications. In order to minimize, if not eliminate, the requirement to perform recycling operations simultaneously in the two RNS, only a portion of this is allocated for the performance of the major operations of propellant refueling and mission payload launch and integration. Two blocks of time are allocated in the profile shown to perform uncheduled maintenance. The first block of time (960 hours) immediately follows the completion of cooldown operations and mission crew retrieval. This block of time provides for major maintenance such as propellant module replacement. A similar, but smaller, block of time is allocated following exchange of the RNS command and control module and subsystem verification and integrated tests. The extent to which the first unscheduled maintenance period is used correspondingly infringes upon the performance of turnaround operations on the alternate RNS, and would impose a greater burden because of increased space shuttle launch frequency and orbital activity. The table indicates the combined launch of the new command and control module and mission crew. This approach is taken to maximize the use of the space shuttle payload capability. Should future investigations indicate this approach untenable because of extended crew time required in earth orbit (additional 14 days of on-orbit time), the crew could be launched separately, following launch and integration of the unmanned payload, at the expense of an added space shuttle launch. A space shuttle launch rate of one each three days is required to filfill these objectives.

Table 2.3-3 identifies major mission operations from, and including, lunar orbit insertion through transearth injection. No lunar orbit operations are assumed to be conducted until completion of cooldown following the lunar orbit injection maneuver. Thus, the timeline could be compressed if necessary by accomplishing rendezvous and docking between pulses once the no-pulse duration becomes sufficiently large. The time allowed for payload

Table 2.3-2

EARTH ORBIT TIMELINE

(6 missions per year)

Event	Initiation Time (hr)	Duration (hr)
Injection into 260-nmi circular earth orbit	0	-
Cooldown operations	0	45
Deploy earth-return cargo/crew*	45	4
Post-flight checkout	49	24
Contingency for unscheduled mainten.	73	960
LH_2 refueling (10 space shuttle launches)	1,033	648
CCM exchange/mission crew up	1,681	4
Subsystem verification, integrated test	1,685	72
Contingency for unscheduled maintenance	1,757	96
Launch and integrate unmanned payload (three launches)	1,853	144
Integrated test, flight readiness test, countdown	1,997	24
Translunar injection	2,021	-

*Alternative is deployment of crew during cooldown phase.

Space shuttle launch rate is 3 days per launch.

deployment and exchange (10 hours) is considered representative in the case where the cargo delivered is palletized, requiring no EVA. A contingency is seen even for the shorter 4.5-day lunar orbit stay, which is the shorter of the two coplanar mission opportunities occurring during the 54.6-day cycle, thus giving confidence that both opportunities are available for missions. It should be noted that the timeline has provisions for LOI and TEI by way of an intermediate 24-hour ellipse to provide the capability of a 30-degree plane change. In the event the nominal coplanar opportunities

Table 2.3-3

LUNAR ORBIT TIMELINE

Event	Initiation Time (hr)	Duration (hr)
Injection into 24-hr elliptical capture orbit	0	-
Cooldown operations	0	12
Plane change (30 deg)	12	-
Cooldown operations	12	12
Injection into 60-nmi circular orbit	24	-
Cooldown operations	24	27
Rendezvous with orbital facility or space tug	51	4
Cargo deployment/exchange	55	10
Contingency	65	339*
Integrated, flight readiness tests, countdown	404	6
Injection into 24-hr elliptical departure orbit	410	-
Cooldown operations	410	12
Plane change	422	-
Cooldown operation	422	5
Transearth injection	434	-

*13 hr for 4.5-day lunar stay

are achieved, this would be unnecessary, thereby freeing an added 48 hours for lunar orbit operations.

2.3.2 Other Missions

The top-level timelines for the geosynchronous shuttle, unmanned planetary, and manned planetary missions are defined in Sections 2.1 as mission descriptions.

Section 3
RNS OPERATIONS

3.1 SUMMARY

Prelaunch, launch, and mission phases of RNS system operations have been analyzed to establish a basis for the RNS design and are defined in this section. The philosophy and tradeoffs involved in establishing the baseline mode of operations will be described. The approach to the study and its reporting is to focus on how the operations lead to design requirements for the RNS. These will then be reflected in the design criteria indicated for each of the subsections within Section 4, RNS Analyses, and Book 2, RNS System Definition. Another output of the operations analyses is the identification of the RNS interface with other planned systems, which is reported in Section 3.17.

The functional flow of operations and method of reporting is summarized in Figure 3.1-1 for major categories of operations: ground and prelaunch operations, launch operations, orbital operations, etc. These categories have been abstracted from the top and first level functional flow diagrams, which are reported in Volume VII. The corresponding box within the functional flow diagram is indicated here outside the box at its upper right-hand corner by the designation "FF". The figure also establishes a correspondence between study task numbers and sections of the report. Task numbers are designated by "T" and report sections are designated by "S". These are indicated for the appropriate entries within the operations boxes. Under the major heading of each box, the issues dealt with in the study are cited with identifications as indicated. The terminology for some of these issues correspond to specific study tasks called out under Subtask 2.3.1, Orbital Operations, and Subtask 2.3.2, Flight Operations, but the lower level subtask breakdown is not included in the figure.

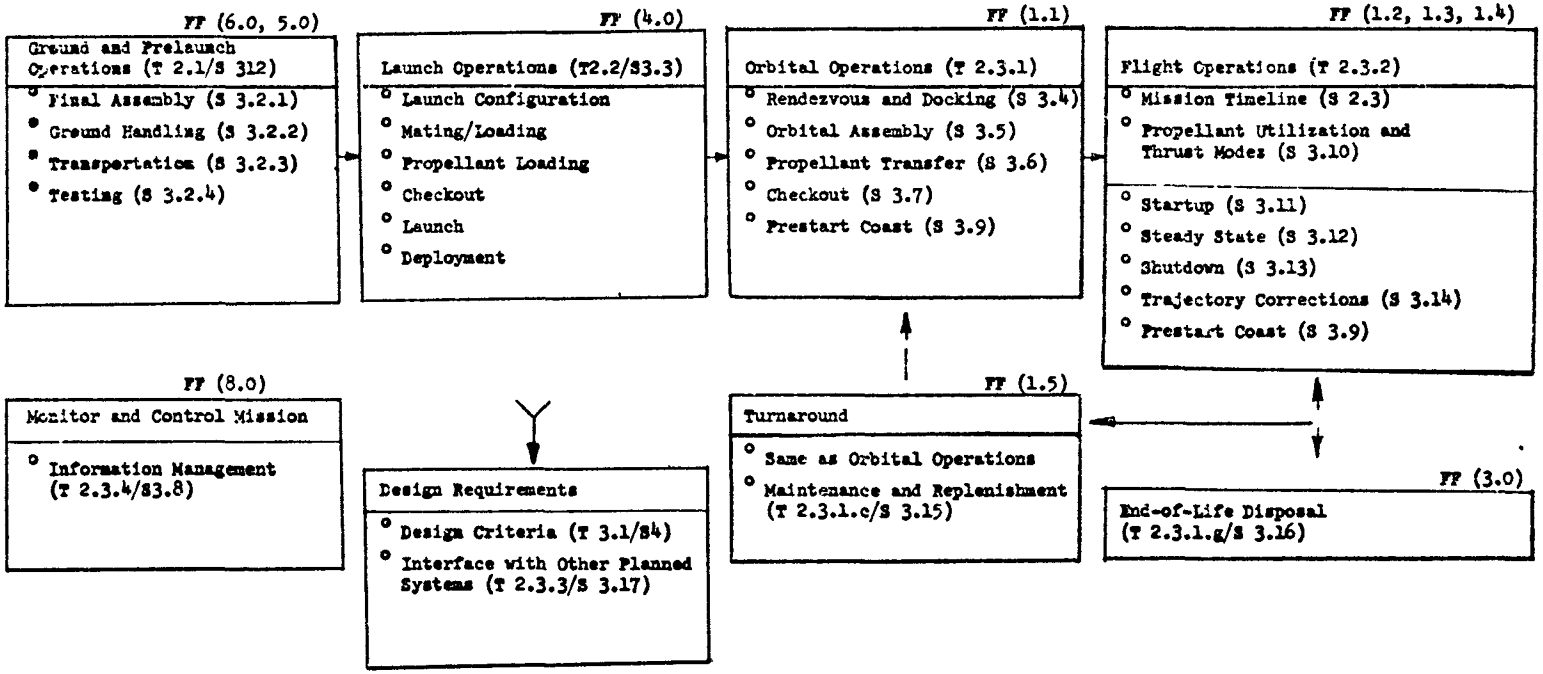

Figure 3.1-1 RNS OPERATIONS SUMMARY

3.2 GROUND AND PRELAUNCH OPERATIONS

The operations on the RNS system during final assembly, ground handling, and testing generate design requirements for the system. The operations are described in the following sections to provide an integrated statement of the basis for the design requirements and criteria cited in the system description and hardware trees.

The sequence of operations, selection of manufacturing and test sites, and methods of transportation are discussed in detail in other sections of this report. The manufacturing is discussed in Volume III, Part A, Section 3, and the acceptance testing and the modes of transportation are discussed in Volume III, Part A, Section 5.2.3.

3.2.1 Final Assembly

3.2.1.1 Propellant Module

The baseline program features propellant module final assembly at Michoud. The propellant module will be capable of being picked up by a crane at the forward end of the tank for transfer to and from the hydrostatic test pit prior to final assembly, and for transfer to and from a vertical position for final assembly, integration, and checkout. The aft heat block/interstage mating plane will be designed to be compatible with placement on a 33-ft-diameter special fixture for performing the subsystems installation, vehicle integration, and checkout operations. These final assembly operations will be conducted in a clean room atmosphere. The tank will be designed for installation of desiccants to prevent contamination of the inner walls after assembly and cleaning. The high-performance insulation blankets will be purged with an inert gas after installation, and a protective cover will be placed over the exterior of the module to prevent atmospheric contamination of the high-performance insulation during subsequent prelaunch operations.

3.2.1.2 Propulsion Module

The current baseline program assumes that the detail fabrication and final assembly of the stage portion of the propulsion module will take place at

Huntington Beach. Subsequently, it will be mated to NERVA at KSC during prelaunch operations. The run tank will be capable of being picked up and rotated from a horizontal to a vertical position for transfer to and from the hydrostatic test pit prior to final assembly, and for transfer to and from a vertical position for placement in and removal from final assembly, integration, and checkout towers. The final assembly and checkout will be accomplished with the tank in a horizontal position. The tank will be supported by a special fixture at each end of the cylindrical section of the tank. These final assembly operations will be conducted in a clean room atmosphere. The tank will be designed for installation of desiccants to prevent contaminations of the inner walls after assembly and cleaning. The high-performance insulation blankets will be purged with an inert gas after installation, and a protective cover will be placed over the exterior of the module to prevent atmospheric contamination of the high-performance insulation during subsequent prelaunch operations.

3.2.1.3 Command and Control Module

The current baseline program assumes that the detail fabrication and final assembly of the CCM will be performed at Huntington Beach. The module will be outfitted with functional subsystems while in a vertical position at the manufacturing site. The module will be placed on a support fixture with a diameter equivalent to that of the CCM, with the aft interface plane of the module being the load carrying surface. The final assembly, integration, and checkout operations will be conducted in a clean room atmosphere. Fuel cell reactant tanks and auxiliary propulsion hydrogen and oxygen tanks will be designed to allow installation of desiccants to prevent contamination after assembly and cleaning. The high-performance insulation blankets on the tanks will be purged with an inert gas after installation, and a protective cover will be placed over the exterior of the module to prevent atmospheric contamination of the high-performance insulation and damage to the module subsystems during subsequent prelaunch operations.

3.2.2 <u>Ground Handling</u>

3.2.2.1 Propellant Module

The module will be structurally designed for handling without pressure stabilization in both a vertical and horizontal position after completion of the final assembly and checkout operations at the manufacturing site. During time periods when the module is not being tested, it will be placed on a mobile transporter in a horizontal position, with loads being transmitted from the module to the transporter through load rings located at stations compatible with the forward and aft heat blocks of the module. The exterior protective cover and tank desiccant are kept in place during all ground handling operations unless the module is being readied for test.

3.2.2.2 Propulsion Module

The module will be structurally designed for handling without pressure stabilization in both a vertical and horizontal position after completion of the final assembly and checkout operations at the manufacturing site. During time periods when the module is not being tested, it will be placed on a mobile transporter in a horizontal position, with loads being transmitted from the module to the transporter through pickup points at the aft end of thrust structure and the forward end of the fiber glass strut forward skirt. The exterior protective cover and tank desiccant are kept in place during all ground handling operations unless the module is being readied for test.

3.2.2.3 Command and Control Module

The module will be structurally designed to be handled in both a vertical and horizontal position after completion of the final assembly and checkout operations at the manufacturing site. During time periods when the module is not being tested, it will be placed on a mobile transporter in a vertical position, with loads being transmitted from the module to the transporter through pickup points located around the circumference of the module. The exterior protective cover and tank desiccants are kept in place during all ground handling operations unless the module is being readied for test.

3.2.3 Transportation

3.2.3.1 Propellant Module

The propellant module will be designed to be moved on a mobile transporter and to be carried on river and ocean-going barges. The mobile transporter will be used for movement between the manufacturing site and barge, as well as movement at test sites and at KSC between the barge and VAB. The propellant module will be transported by barge between the manufacturing site, production acceptance test site, and KSC. The baseline concept as currently defined involves final assembly at Michoud, production acceptance testing at the Mississippi Test Facility, and launch operations at KSC. In addition, one production article will be shipped by barge from Michoud to southern California, and, subsequently, ferried by helicopter to NRDS for all systems testing. The exterior protective cover and tank desiccant are kept in place during all transportation periods.

3.2.3.2 Propulsion Module

The run tank module will be designed to be moved on a mobile transporter, to be carried on river and ocean-going barges, and to be transported in the cargo hold of aircraft (such as the Super Guppy). The mobile transporter will be used for movement between the manufacturing site and barge or aircraft, as well as movement at test sites and at KSC between the barge or aircraft and the VAB. The propulsion module will be transported by aircraft between the manufacturing site and production acceptance test site, and by barge between the production acceptance test site and KSC, assuming the baseline concept as described above. The NERVA will not be mated to the propulsion module during transportation between the various sites. An all-systems test article will also be flown from the manufacturing site to NRDS by aircraft. The exterior protective cover and tank desiccant are kept in place during all transportation periods.

3.2.3.3 Command and Control Module (CCM)

The CCM will be designed to be moved on a mobile transporter and to be transported in the cargo hold of aircraft (such as the Super Guppy). The mobile transporter will be used for movement between the manufacturing site and aircraft, as well as movement at test sites and at KSC between the aircraft and the VAB. The CCM will be transported by aircraft between the manufacturing site at Huntington Beach and KSC, assuming the baseline concept as described above. In addition, an all systems test article will be flown from the manufacturing site to NRDS by aircraft. The exterior protective cover and tank desiccant are kept in place during all transportation periods.

3.2.4 Testing

3.2.4.1 Propellant Module

Under the current baseline manufacturing and test programs, each production propellant module will undergo post manufacturing checkout at Michoud, during which time it will be integrated with a CCM. The automatic checkout system of the CCM will be used to operate the functional systems of the propellant module. Subsequent testing will be performed on the integrated assembly at the Mississippi Test Facility, which will include, as a minimum, a tanking, pressurization, and detanking operation utilizing LH_2. Functional systems will be exercised, using the CCM as the master control element. The propellant module purge system will be active during the test activities which involve liquid hydrogen. The current program does not require a propulsion module for conducting the production acceptance test of the propellant module. Additional all systems testing will be performed on a minimum of one production propellant module at NRDS, in combination with a propulsion module and a CCM, to demonstrate integrated system operation.

3.2.4.2 Propulsion Module

The current baseline program assumes that the production run tank modules will undergo post-manufacturing checkout at Huntington Beach, during which time they will be mated to a master tool simulating the engine/stage interface and the propellant module/propulsion module interface planes for dimensional verification. Subsequent testing will be performed at the Mississippi Test

Facility, where the modules will be tanked, pressurized, and detanked with LH_2 to verify structural integrity of the module under a cryogenic environment. Specifically, the weld areas of the propellant tanks will be checked for leakage. Additional all systems testing will be performed on a minimum of one production propulsion module at NRDS, in combination with a propellant module and a CCM, to demonstrate integrated system operation. Engine mating and interface verification tests will be conducted on each propulsion module at KSC.

3.2.4.3 Command and Control Module

The current baseline program assumes that post-manufacturing checkout operations will be performed on each production CCM at Huntington Beach. This includes dimensional checks of the CCM/propellant module interfaces, as well as astrionics circuitry checks, alignment, calibration and redundancy verification. Subsequent to this checkout, the CCM's will be shipped to KSC, where they will undergo receiving inspection and prelaunch checkout tests before being placed in the space shuttle orbiter. All systems testing will be performed on a minimum of one production CCM at NRDS, in combination with a propellant module and a propulsion module, as discussed above.

3.3 LAUNCH

3.3.1 Baseline Launch Mode

The Class 1 Hybrid RNS is launched to orbit initially as three separate modules. The propellant module is launched by the Intermediate-21 launch vehicle which consists of the S-IC and S-II stages. The NERVA propulsion module and the CCM are launched to orbit inside the cargo bay of the space shuttle. This approach minimizes the impact of the RNS on the INT-21 and acknowledges required replacement of these modules. The propellant module can be launched to orbit with only a partial loading of propellant, about 155,000 lb. Thus, assembly of the complete RNS vehicle and preparation for initial flight would require additional propellant launched by a space shuttle. The net initial launch cost for the three modules, excluding credit for propellant, is $117.5 million for each RNS.

3.3.1.1 Propellant Module

The launch configuration for the propellant module on the Intermediate-21 launch vehicle is depicted in Figure 3.3-1. The 341-ft overall height presents no facility height problems (VAB hook height is 410 ft). The vehicle injects the propellant module into the operational 31.5-degree inclination, 260-nmi orbit in a direct ascent mode with a delivered payload forward of the S-II/RNS interstage of approximately 192,000 lb. The RNS propellant module is designed to comply with the INT-21 ground, launch, and ascent design load envelope, compatible with current design loads for the S-IC and S-II stages. This imposes a policy of utilizing a wind-biased launch trajectory and accepting a minimum seasonal launch availability of 84 percent for winter winds.

An alternate launch concept can be considered with the CCM and propellant module launched as an integral unit by the INT-21. In this configuration the payload envelope is increased by 12 ft and the launch availability would be reduced to 80 percent.

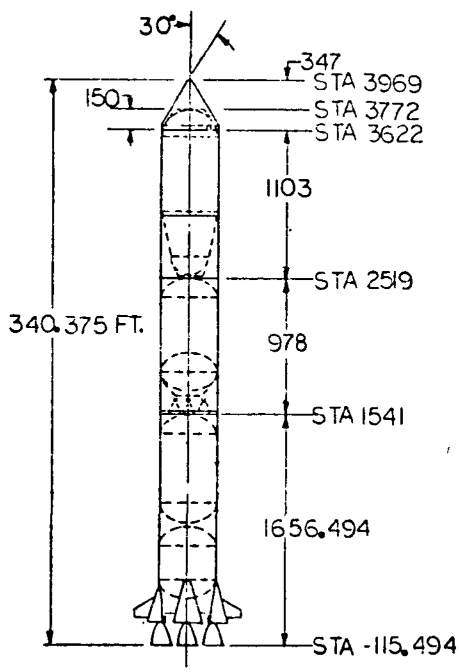

Figure 3.3-1 BASELINE LAUNCH CONFIGURATION

In preparation for launch the propellant module undergoes receiving inspection in the low bay of the VAB while in the horizontal position on a mobile transporter. The protective exterior cover and tank desiccant will be removed inside the VAB during the launch preparation sequence. The module and interstage will be mated in the VAB with both elements in a vertical position. The combined module and interstage will be stacked and mechanically mated with the launch vehicle in the VAB high bay. The propellant module will be fueled on the launch pad.

3.3.1.2 Propulsion Module

The launch configuration for the NERVA propulsion module inside the cargo bay of the space shuttle is in a normal vertical attitude, as depicted in Figure 3.3-2. It is deployed in orbit using the standard space shuttle payload deployment mechanism. Launch support, including provision of lateral restraint, are defined in Section 4.2.9. The module is launched with its propellant tank dry and unpressurized. Umbilical panels are provided by the space shuttle for power, data acquisition, checkout, and helium purges.

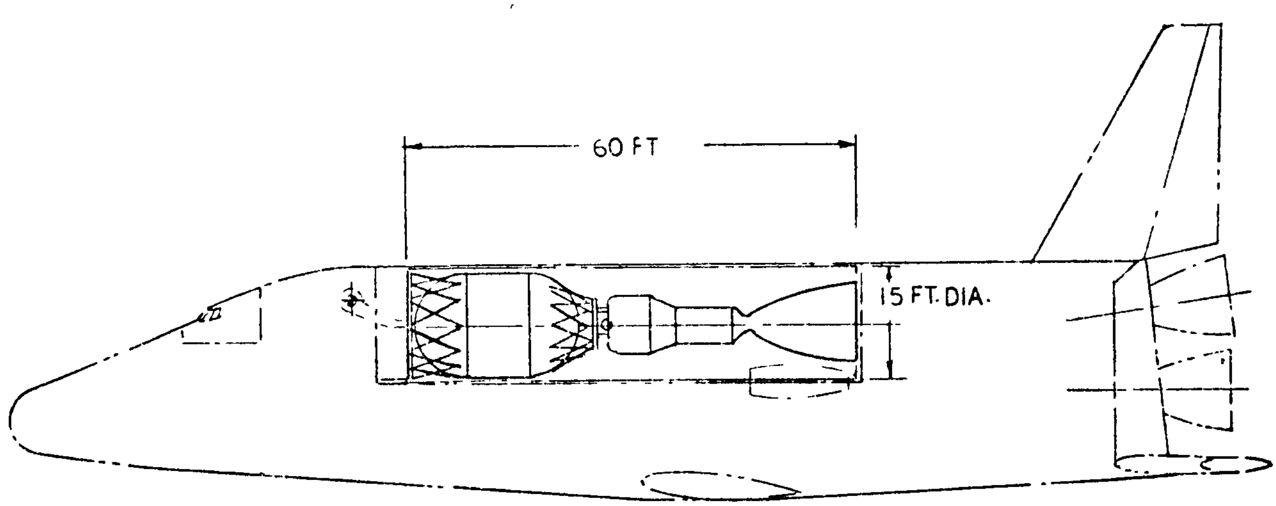

Figure 3.3-2 PROPULSION MODULE IN ORBITER CARGO BAY

In preparation for launch, the propulsion module will undergo receiving inspection in the low bay of the VAB while in the horizontal position on a mobile transporter. The protective exterior cover and tank desiccant will be removed inside the VAB during the launch preparation sequence. The module will be mated with the NERVA in the VAB with both elements in a vertical position. The completed module will subsequently be loaded into the cargo bay of the space shuttle orbiter while both are in a horizontal attitude, with load pickup attach points being compatible with stations of the module thrust structure, forward skirt, and the NERVA. The orbiter is subsequently erected in a vertical attitude on the booster. Environmental conditioning is provided by the space shuttle.

Poison wires are installed in NERVA during core assembly for safety during transportation and launch operations. A removal mechanism is attached to the cargo bay aft bulkhead, consisting of an electric motor, reel, and line.

This is attached to the poison wires during loading of the propulsion module into the cargo bay. The wires and a fiberglass nozzle throat sheath are withdrawn prior to deployment of the module in orbit.

3.3.1.3 Command and Control Module

For initial assembly and recycling of the RNS after each mission, the CCM is launched to orbit inside the cargo bay of the space shuttle. Because the APS motors are located on outriggers which exceed the 15-ft-diameter envelope, the CCM must be launched with its axis perpendicular to the cargo bay. The launch configuration is shown in Figure 3.3-3, with the CCM mounted on a rack which is attached to the standard payload deployment mechanism. The rack is deployed with the module and is utilized for retrieval of the CCM for recycling. Umbilical panels are provided by the space shuttle for power, data acquisition, checkout, LH_2 and LO_2 transfer, GH_2 and GO_2 venting, and helium purges.

In preparation for launch, the CCM will undergo receiving inspection and subsystem checkout in the low bay of the VAB, while in a horizontal position

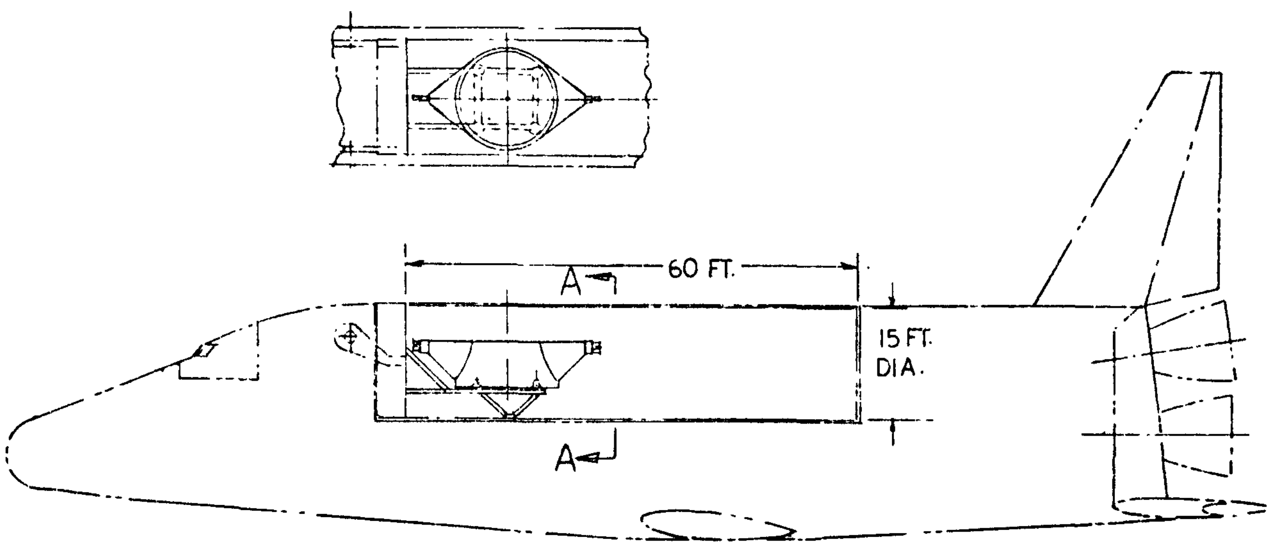

Figure 3.3-3 COMMAND AND CONTROL MODULE IN ORBITER CARGO BAY

on a mobile transporter. The protective cover and tank desiccants will be removed inside the VAB. The module will be loaded into the cargo bay of the space shuttle orbiter while both are in a horizontal attitude, with load pickup attach points compatible with the aft end of the module. The orbiter is subsequently erected in a vertical attitude on the booster. The tankage for fuel cell reactants and auxiliary propulsion propellants will be filled while the module is in a vertical attitude inside the cargo bay. Environmental conditioning is provided by the space shuttle.

3.3.2 Alternate Integral Launch Mode

The three modules of the Class 1 Hybrid RNS (propellant, propulsion, and CCM) are initially launched to orbit as a single unit by the INT-21 launch vehicle which consists of the S-IC and S-II stages. The propulsion module is launched to orbit dry and unpressurized, and the propellant module can be launched with only a partial loading of propellant, about 120,000 lb. Thus, preparation for initial flight would require additional propellant launched by a space shuttle. The net initial launch cost for the system, excluding credit for propellant, is $107.5 million for each RNS. The CCM is launched to orbit separately inside the cargo bay of the space shuttle for each subsequent mission, and recycled to the ground for maintenance and replenishment.

The integral RNS launch configuration on the INT-21 launch vehicle is depicted in Figure 3.3-4. The overall vehicle height including the 30-degree nose cone (approximately 410 ft less 10 ft below station zero) is just within the 410-ft VAB hook height limit. The vehicle injects the RNS into the operational 31.5-degree inclination, 260-nmi orbit in a direct ascent mode with a delivered payload forward of the S-II/RNS interstage of approximately 192,000 lb.

The RNS is designed to comply with the INT-21 ground, launch, and ascent design load envelope, compatible with current design loads for the S-IC and S-II stages. This imposes a policy of utilizing a wind-biased launch trajectory and accepting a minimum seasonal launch availability of 60 percent for winter winds. This constraint for launch availability is much more severe than for the baseline launch mode without the propulsion module,

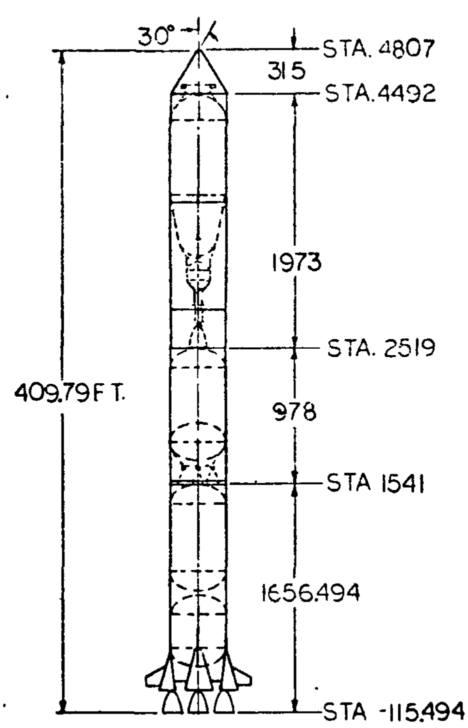

Figure 3.3-4 INTEGRAL LAUNCH CONFIGURATION

which is 60 ft shorter. Lateral restraint of the propulsion module may be required during launch in the integral mode (Section 4. 8. 2).

The launch preparation sequences for all modules are identical to those described for the baseline launch mode. All of the modules and the interstage will be mated in the VAB with all elements in a vertical position. The combined modules and interstage will be stacked and mechanically mated with the launch vehicle in the VAB high bay. The propellant module will be fueled on the launch pad.

The CCM and the propulsion module would be launched as described in Section 3. 3. 1 for recycling and replacement.

3.4 RENDEZVOUS AND DOCKING

The RNS and its modules will experience numerous rendezvous and docking operations during their life history, including those for initial assembly operations, orbital injection maneuvers, and turnaround operations in earth orbit. The vehicle dynamics and flight mechanics for these operations are described in this section. The additional operations required to accomplish RNS orbital assembly are defined in Section 3. 5. Evaluation of sensor and thrustor accuracies in this section indicates that these are adequate for an automated rendezvous and docking operation.

3.4.1 Vehicle Dynamics

3.4.1.1 RNS Assembly

It is desirable that the RNS be maintained in a gravity-gradient-stable, local-vertical orientation during all rendezvous and docking maneuvers (when the RNS is the passive element) to minimize RNS attitude control propellant consumption. The dynamics of the RNS during the orbital assembly phase have been analyzed to identify attitude control requirements. Dynamics of the complete configuration at various payload and propellant loadings have been evaluated.

The Class 1 RNS is delivered to orbit as three separate modules. A space shuttle first places the CCM in the assembly orbit. Next the INT-21 boosts the partially loaded propellant tank into the close vicinity of the CCM. The CCM performs a micro-rendezvous and docks with propellant module. Finally, the propulsion module is delivered by the space shuttle. After it is deployed, it can separate itself from the space shuttle and maintain a stable attitude using its cold gas attitude control system. The RNS assemblage, self-propelled, then docks to the propulsion module. During CCM replacement, the old CCM removes itself, allowing the RNS to oscillate as gravity-gradient forces dictate. The CCM rotates the configuration into the correct attitude and then nulls the attitude rates as accurately as possible. The residual RNS attitude rates that would cause the cluster to tumble were calculated. If the residual attitude rates about the pitch, roll, and yaw axes are equal and the vehicle has no alignment errors, residual rates of 0.08 deg/sec would result in tumbling in the pitch plane (minimum gravity-gradient restoring torques) if all the rotational energy were concentrated in that plane. Based on the need for quiescent storage of the CCM, the resultant minimum impulse-bit requirement for the CCM APS to preclude tumbling is approximately 130 lb-sec or less. The current design easily meets this requirement, having a minimum impulse bit size of 3 lb-sec.

The design criteria for the propulsion module attitude control system will be primarily dictated by the requirement to stabilize module rates induced by a disturbing force, such as, a missed docking attempt. As currently envisioned, this cold-gas attitude control system has a thrust level of 10 lb, moment arms of 80 in. for roll control and 300 in. for pitch and yaw, and a minimum impulse bit of 0.5 lb-sec. It is capable of stabilizing the propulsion module if the missed docking attempt induced rates are on the order of 5 deg/sec or less, compared to anticipated induced rates of 1 deg/sec or less. A secondary function of this control system is to stabilize the RNS when the CCM is being replaced. The critical situation is again that of a missed docking attempt. In this configuration the pitch and yaw control moment arms are assumed to be 665 in., and the control system is capable of stabilizing the RNS if the rates are on the order of 3 deg/sec or less, compared to anticipated induced rates of 0.5 deg/sec or less.

3.4.1.2 Orbital Storage

The complete RNS configuration will spend the majority of its lifetime in the gravity-gradient-stable, local-vertical orientation. During storage in both lunar and earth orbits, the propellant consumption for the attitude control system will be minimized in this orientation. Following a given active operation the RNS is rotated into the local-vertical orientation and the attitude rates damped by the RNS attitude control system. If attempted docking to the RNS fails, the RNS attitude control system must restabilize the vehicle. Residual rates not removed by the control system that might result in tumbling are 0.08 deg/sec for earth orbit and 0.06 deg/sec for lunar orbit. Again it is assumed the rates about all three axes are equal and that all the rotational energy is transferred to the pitch plane. These rates are considered to be quite insensitive to both propellant loading and payload weight as, in all operational plans, the complete RNS has equal pitch and yaw inertias (it is symmetrical about the roll axis) and the roll inertia is very small in comparison to the pitch-yaw inertias. These characteristics make the tumbling rate threshold only a function of the gravity-gradient profile.

The ability of the RNS attitude control system to preclude tumbling is determined by its minimum impulse bit, shown by the relationship between maximum possible pitch angle amplitude and minimum bit size in Figure 3.4-1 for a particular control authority in earth orbit. The 3 lb-sec minimum impulse bit capability of the RNS attitude control system can limit the amplitude to 0.2 degree (period equal to the orbital period) which is more than adequate. Similarly, considering the comparable tumbling threshold rate, the system is adequate in lunar orbit.

The possibility of the RNS spinning about the roll axis has not been investigated. Gravity-gradient restoring torques are the smallest about this axis and, if the configuration is symmetrical, are zero. In addition, the period of pitch and yaw oscillation for the complete configuration is approximately equal to the orbital period and therefore the possibility of amplifying the oscillation exists. This should be investigated in future studies.

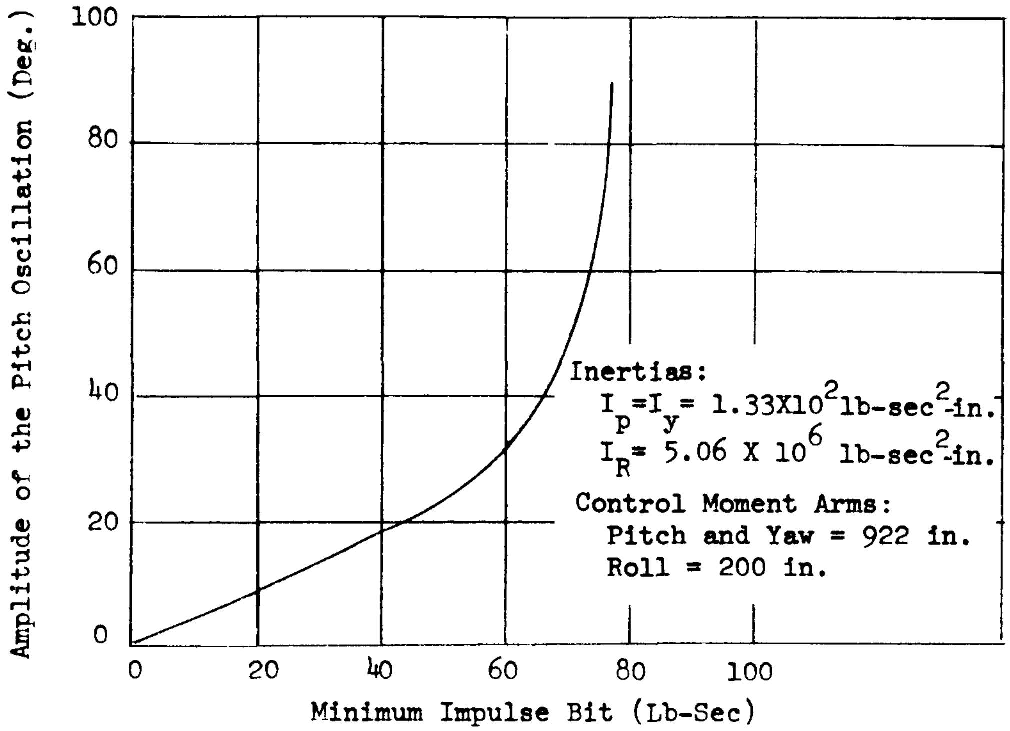

Figure 3.4-1 EFFECT OF CONTROL SYSTEM CAPABILITY -- GRAVITY GRADIENT OSCILLATION

3.4.2 Flight Mechanics

3.4.2.1 RNS Assembly

This section describes the flight mechanics of rendezvous and docking operational requirements associated with the initial assembly of the RNS in the 260-nmi operational earth orbit. The space shuttle orbiter delivers the CCM and propulsion modules to the orbit and performs a rendezvous with the RNS staging and assembly area. A payload module is deployed from the orbiter and the space tug docks with it, removes it from the orbiter, and transports the module to the RNS where it is docked to the assemblage, which separates itself from the orbiter, permitting the space tug to transfer and dock the RNS to it.

Space Shuttle Rendezvous

Rendezvous constitutes arrival of the orbiter in the proximity (500 ft) of the RNS staging and assembly area. The mode described here is common to all modules and is that presently envisioned for rendezvous of the space shuttle orbiter with the earth orbiting space station as well. The first module to be orbited in the RNS assembly sequence provides the focal point of rendezvous for subsequent module launches. The rendezvous operations (Figure 3.4-2) consist of (1) establishment of a circular parking orbit (100 nmi), (2) phase catch-up in the parking orbit, (3) transfer to the final approach co-elliptic orbit, and (4) two phases of terminal rendezvous with the RNS. The first three steps in this sequence are open loop, accomplished without contact with the target point or RNS assemblage. The two phases of terminal rendezvous are closed loop, utilizing laser radar acquisition of the RNS assemblage.

The circular parking orbit is maintained until correct phasing is established with the RNS for initiation of the first Hohmann transfer orbit insertion (TOI) burn. The objective of phasing is to bring the orbiter within the range of terminal rendezvous sensor for as broad a range of initial target phase angles as possible. The location of the target point is biased below and behind the RNS assembly area to allow for dispersions in the orbiter position and yet maintain the assembly area in a known direction for the circular-

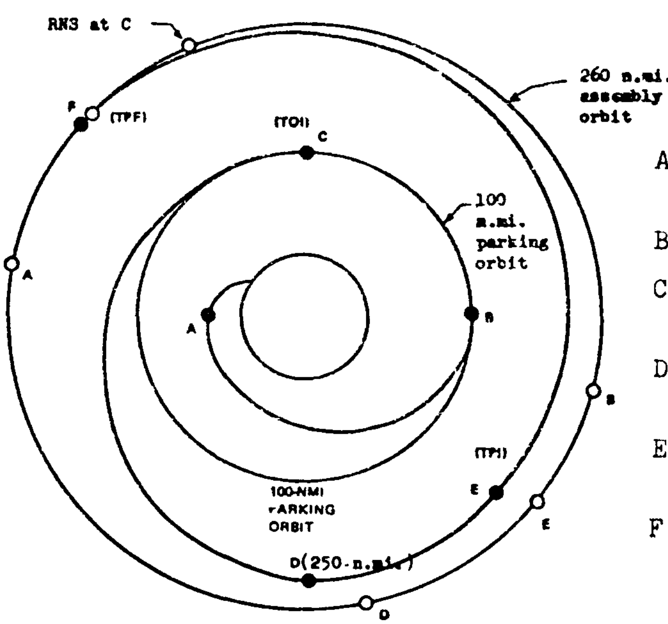

A. Insertion into 50 X 100 N Mi Phasing Orbit Perigee

B. Circularization at 100 N Mi

C. Transfer Orbit Insertion (Range to go = 450 N.Mi)

D. Coelliptic Maneuver (Circularization)

E. Terminal Rendezvous Phase Initiation

F. Braking (500 ft. from RNS)

Figure 3.4-2 BASELINE RENDEZVOUS PROFILE ization maneuver. This facilitates laser lock-on and provides time for navigation and computation of the terminal phase initiation (TPI) maneuver.

Terminal rendezvous is a closed loop sequence of maneuvers beginning with TPI maneuver and ending 500 ft from the RNS assemblage. Typical intercept trajectories are shown in Figure 3. 4-3.

Braking is the most important of the terminal rendezvous maneuvers. For a typical profile, the command pilot nulls the line-of-sight rate when the range to go is approximately 3 nmi. The orbiter then drifts in at a closing velocity of 25 fps until the range to go is approximately 0. 5 nmi, at which time the first braking maneuver reduces the closing rate to 10 fps. When the range to go is reduced to 1, 000 ft, a second braking maneuver reduces the closing rate to 5 fps. When the range reaches 500 ft, the command pilot executes the final braking maneuver to null the range rate.

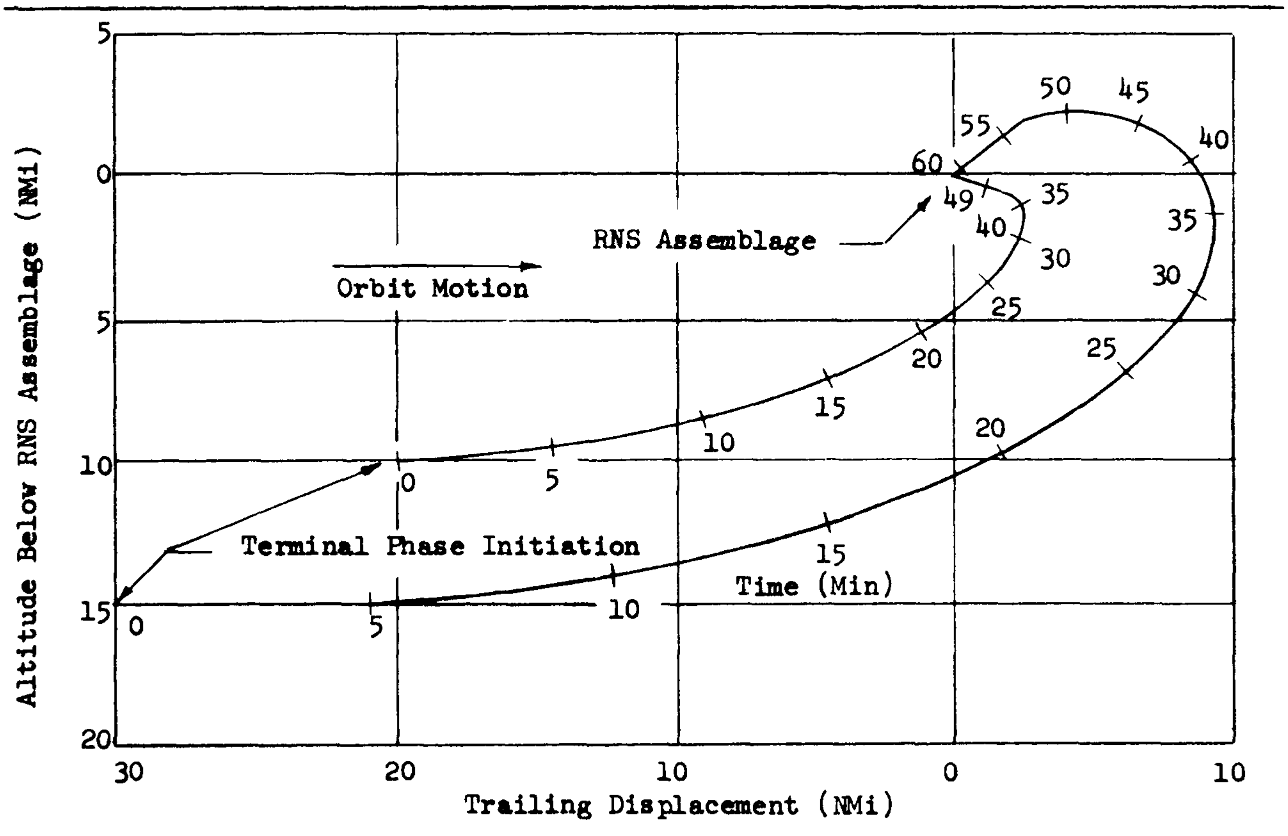

Figure 3.4-3 TERMINAL RENDEZVOUS PROFILE

Space Tug Docking

The space tug docking phase embraces the activities from initial erection and deployment of the payload modules (or CCM) from the space shuttle orbiter up to docking of the given module to the RNS assemblage. The sequence of required operations has been already described. The orbital transfer module is essentially line of sight over the 500-ft range from the orbiter to the RNS. The docking controller in the tug grossly aligns the module to the assemblage, stopping about 200 ft from the assemblage to make the necessary vernier adjustments and then apply a small velocity to effect the docking.

Docking system requirements are inferred by the performance characteristics of the tug APS. A limiting case of a CCM-derivative tug (minimum bit pulse of 10 lb-sec) employed to attach a payload module to the RNS assemblage results in the maximum rates at the docking interface of the propellant module shown in Table 3.4-1, where the CCM rates are also shown.

Table 3.4-1
SUMMARY OF DOCKING CONDITIONS

	Payload Module	CCM
Longitudinal Velocity (fps)	0.02	0.25
Lateral Velocity (fps)	0.02	0.02
Pitch Angular Velocity (deg/sec)	0.04	0.08
Roll Angular Velocity (deg/sec)	0.03	1.0
These are based on:		
Weight (lb)	38,200	5,200
Inertia (slug-ft^2)		
Pitch-yaw	374,000	4,500
Roll	33,500	9,050
Moment Arm (ft)		
Pitch-yaw	26	7.5
Roll	7.5	7.5

3.4.2.2 Orbital Injection Maneuvers

This section considers the rendezvous modes required to accomplish earth orbit and lunar orbit injection maneuvers. The cooldown spiral (as discussed in Section 3.13.4.2) provides the required course rendezvous capability. Off-nominal performance during the cooldown phase is accommodated by way of stage rotation (for the high-impulse case) or NERVA idle mode operation (for the low-impulse case). Refinements in orbital position following completion of cooldown will be accomplished by way of a combination of the NERVA idle and APS maneuvers (see Section 3.14.2) in the case of a requirement for close positioning or docking with a manned orbital facility. In this case the final braking maneuver is accomplished with the APS while the RNS is in a retrograde orientation to keep the facility within the RNS shadow cone.

Noting that approximately 45 hours (or 28-1/2 orbital revolutions) are required to complete the cooldown phase for the EOI maneuver, the question is raised as to the possibility of crew deployment before the termination of the cooldown phase. Two approaches to accomplishing this were investigated: (1) injecting the RNS at a lower initial orbit to permit spiraling down to 260 nmi more quickly, followed by deploying the crew and allowing the RNS to complete the cooldown phase on its own; and (2) intercepting the RNS early in the cooldown phase at a higher orbit with another stage, such as in the chemical tug and returning the crew to 260 nmi. In the latter case, the RNS would continue its downward spiral to 260 nmi following deployment of the crew.

Performance penalties were determined for these concepts for a NERVA steady-state operating time of 600 seconds, which is characteristic of an EOI maneuver. If a 260-nmi insertion were desired at the end of two orbital revolutions (following 40 cooldown pulses), injection must occur in an orbit with a 394-nmi apogee and 320-nmi perigee. This compares with the 437 by 365 nmi initial injection orbit, which would use all the cooldown prior to circularization of 260 nmi, as was previously discussed. Adopting this approach in effect results in depriving the RNS of the useful impulse occurring following circularization at 260 nmi. The lunar orbit payload impact of this higher energy requirement is 950 lb.

The tug intercept concept considered retrieval of the 20,000-lb crew module with a tug weighing 12,000 lb (inert weight, as specified in NASA guidelines) at a specific impulse of 460 seconds. No velocity penalties were assigned beyond the ideal Hohmann transfer requirement. The tug propellant requirement to accomplish this sequence of events (10.2 lb/nmi between 260 nmi and the intercept orbit) was converted to equivalent payload delivered to lunar orbit at the rate of 112,000 lb of payload for 300,000 lb of propellant, or 0.373 lb/lb resulting in a 200-lb penalty. This approach would require that the crew module be physically mounted in front the RNS/payload combination and that a provision for separation of the crew module exists. Additional velocity penalties would be incurred to assure maintenance of the crew module within the shadow cone of the RNS during the early separation phase.

3.4.2.3 Orbital Turnaround

Turnaround activities in earth orbit require multiple rendezvous maneuvers with the space shuttle orbiter to provide propellant refueling, CCM replacement and cargo deployment and installation prior to departure on a subsequent mission. The rendezvous procedures must be designed to prohibit exceeding orbiter crew radiation maximums. During the majority of time in earth orbit the RNS will be in a gravity-gradient-stabilized mode with the NERVA engine pointing down. Exceptions to this will be during propellant transfer when the RNS/orbiter combination are oriented perpendicular to the orbital plane, and during pre-injection operations and procedures.

Considering the gravity-gradient orientation of the RNS, a procedure has been identified to permit approach by the orbiter to the RNS which minimizes the requirements on the RNS APS, while observing radiation considerations. The initial portion of rendezvous will be as described for orbital assembly of the RNS in Section 3.4.2.1. The difference is that while the mode described for vehicle assembly requires rendezvous of the space shuttle orbiter at the assembly area, the orbiter will in this case rendezvous at a co-altitude position with the RNS at, for example, 20-nmi distance. This distance will depend on the time following the last full-power engine operation. In all cases this will not occur prior to the completion of NERVA cooldown from the preceding EOI maneuver. Thus it would be no sooner than approximately 45 hours following the last full-power burn. In this case the 20-nmi separation would yield a maximum dose per mission (one day) to the orbiter crew of less than 10^{-3} rem, if the orbiter were viewing the NERVA from the side. CCM replacement and cargo handling operations by the space tug are then analogous to those for RNS assembly.

For propellant resupply, following rendezvous with the 20-nmi position, the terminal closure maneuver would be initiated. During the final phase of the closure, it is necessary to assure that NERVA is pointed away from the orbiter. A stable orbit maneuver is used because the final portion of the trajectory is straight, thus making it easier for the orbiter to keep within the shadow cone of the RNS. This portion of the maneuver is depicted in Figure 3.4-4. The characteristic of this type of closure is that it has a low relative line-of-sight change during the final phase and thus allows the orbiter to stay within the shadow cone. This can be assured through activation of the RNS attitude control system during this final closure phase. The

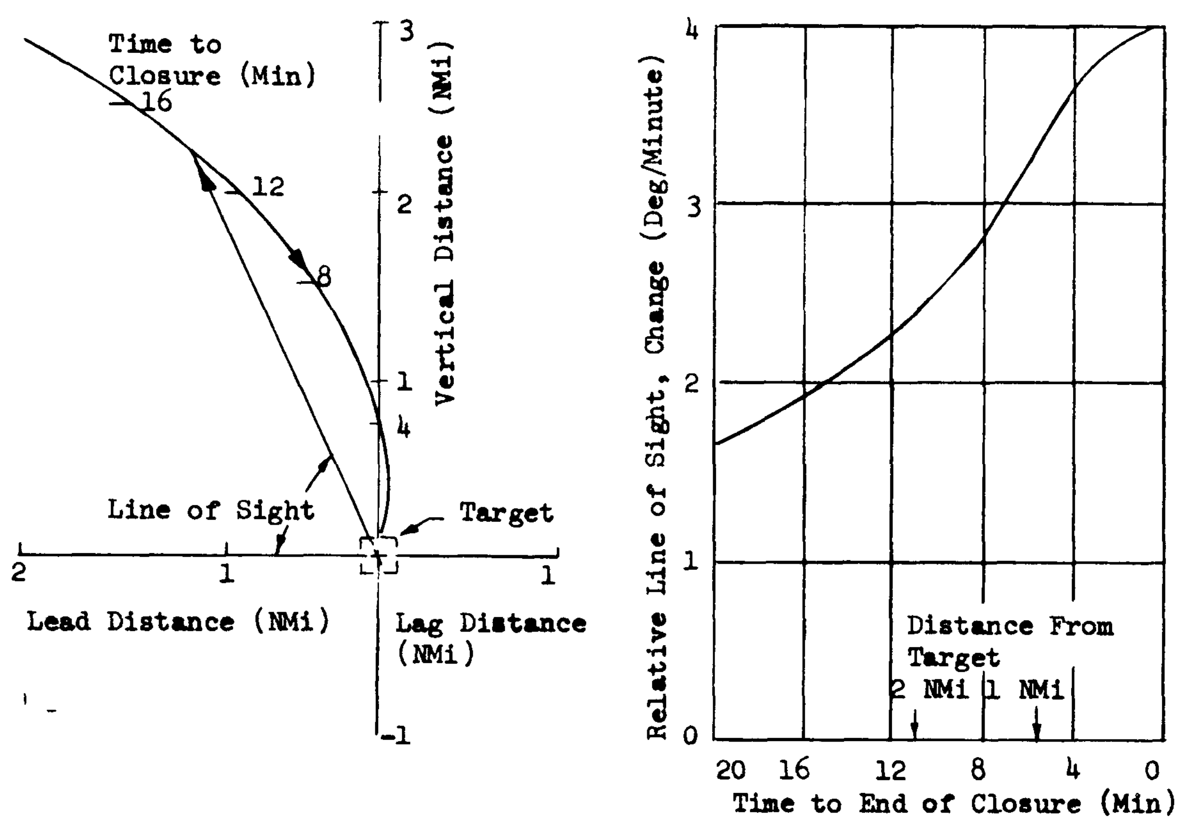

Figure 3.4-4 STABLE ORBIT CLOSURE

dominant factor, in terms of radiation exposure, will be the integrated dose received by the orbiter crew bringing the first load of LH_2 up. Subsequent trips will encounter substantially lower doses (one and more orders of magnitude) due to the added time from engine shutdown and increased fuel level in the RNS. The dose received by the first crew, docking 48 hours after shutdown, and staying 24 hours, would be about 1 rem. The RNS will be in a gravity-established mode at the time of rendezvous and dock. In the case of propellant transfer, this will be followed by rotation of the orbiter/RNS to a orientation normal to the orbital plane in order to conduct propellant transfer operations (Section 3. 6). This mode minimizes the resultant orbital perturbations to a wobble in inclination and node.

3. 4. 3 Rendezvous and Docking Sensors

The investigation of rendezvous and docking requirements focused on the implications of use of a laser radar system selected in Phase II for acquisition and gross rendezvous as well as terminal docking. The scanning laser radar system currently being developed for NASA by ITT was used as a reference for this evaluation. The equipment located on the chaser or active vehicle consists of a transmitter and receiver and scanners which position these components. The transmitter consists of a semiconductor laser. The receiver consists of optical lenses and filters and an image detector. The beam steerer consists of solid-state devices and optical lenses. The ITT scanning laser radar system requires that the target be cooperative and contain functional equipment to assist the rendezvous. The required equipment consists of a corner cube reflector. With such a cooperative target, the baseline system could allow the chaser to acquire and track the target out to a range of approximately 75 miles adequate for baseline RNS operations. If the system were noncooperative, it would be limited to a 1-mile range. The ITT specifications (Reference 4-47) are reproduced in Table 3. 4-2 indicating a potentially high accuracy system.

It was considered that provision of active functional equipment on the target vehicle might not be desirable for RNS operation, since that would require attitude control and provision of power on the target during the entire

Table 3.4-2

ESTIMATED SYSTEM PERFORMANCE CHARACTERISTICS OF THE SCANNING LASER RADAR

Range	0 to 120 km (75 miles)
Range Accuracy (3σ)	±0.2% or ±10 cm (whichever is greater)
Range-Rate	0 to 5 km/sec (28,800 mph)
Range-Rate Accuracy	±1.0% or ±0.5 cm/sec (whichever is greater)
Angle Coverage without Gimbals	±15 degree pitch ±15 degree yaw ±90 degree relative roll
Angle Accuracy	
Pitch and Yaw	±0.02 degree
Roll Index	±1.0 degree
Acquisition Scan Time	1 to 150 seconds
Angle-Rate	
Acquisition Mode	0 to 0.4 degree/second
Track Mode	0 to 10 degree/second
Angle-Rate Accuracy	±1.0% or ±0.01 degree/second (whichever is greater)

rendezvous and docking operation. A system could be defined with passive systems located at each interface requiring only the active laser radar system at the CCM. Such an approach requires multiple laser radar units located around the circumference of the vehicle to establish the geometry. Thus, the full accuracy of the ITT system could be utilized and, in addition, the roll index accuracy would be reduced to 0.05 percent. The use of multiple units would provide redundancy without using the backup of a different technology system such as radar or TV. The accuracy of the alignment system would not produce any limitations on the rendezvous or assembly operations.

3.5 ORBITAL ASSEMBLY

This operations phase provides for assembly of the three distinct modules into the RNS vehicle. It includes structural assembly and the hookup of fluid and electrical lines. The baseline launch modes were established in Section 3.3 and the techniques for accomplishing rendezvous and docking were described in Section 3.4. This operational phase will terminate with the RNS vehicle in a fully functional form, but prior to completing propellant loading in earth orbit and final vehicle checkout. This operational phase will be described by first establishing the assembly concept and then describing the operations selected for assembling the propellant module with the command and control module into a subassembly, and then assembling this with the propulsion module.

3.5.1 Assembly Concept

The launch mode, established in Section 3.3, consists of launching each module independently. The CCM and the propulsion module are both launched within the cargo bay of the space shuttle. The propellant module is launched on the INT-21 launch vehicle. The different alternatives for launch sequence were assessed in terms of operational complexity and support element requirements. With the sequence selected — CCM, propellant module, then propulsion module — no support elements are required to aid in the RNS assembly and the minimum complexity of operations are encountered.

Since the CCM contains the processing and control functions for the RNS, electric power, auxiliary propulsion, and the laser ranging radar system, starting the assembly with this module allows use of these RNS systems. Thus, the CCM will be launched first, activated, and deployed from the space shuttle in the assembly orbit.

The propellant module will be launched next and inserted into the assembly orbit by the INT-21 launch vehicle. The propellant module will be stabilized by the launch vehicle while the CCM rendezvous and docks with it. Following assembly of these two modules, the launch vehicles will be jettisoned.

The propulsion module will be launched by the space shuttle which will rendezvous with the first two modules in the assembly orbit. The propulsion module will be activated so that it can stabilize itself during subsequent operations. It will then be deployed from the space shuttle and the CCM will control docking the aft end of the propellant module with it. While these operations make maximum use of the existing system elements, the INT-21 launch vehicle and the space shuttle, no additional capability is required from these elements to accomplish these operations.

3.5.2 Propellant/Command and Control Modules Assembly

The CCM is launched first into the assembly orbit by the space shuttle. While still within the cargo bay, it is activated and performs sufficient self-check to verify its power, command and control, and auxiliary propulsion capabilities. It is then deployed into the assembly orbit and the space shuttle orbiter returns to earth. The propellant module is then launched by the INT-21 launch vehicle. It is injected into the assembly orbit by the launch vehicle to within an accuracy of 10 miles from the CCM. The propellant module attitude is preassigned and stored within the launch vehicle IU. The IU also performs status monitoring functions for the propellant module. However, no cooperative action other than stabilization is required from the IU during the terminal rendezvous and docking maneuvers. The nose cone was jettisoned during launch so that the forward docking structure attached to the payload adapter is exposed together with the four corner cube assemblies needed to assist the final docking maneuver. The propellant module remains stabilized by the launch vehicle while the CCM rendezvous with it. After accomplishing this rendezvous to within 500 ft, the CCM verifies the attitude and condition of the propellant module before terminal docking. During the final docking approach an uplink signal from ground is provided to deactivate the limit cycling on the propellant module. Final closure is accomplished by a stable orbit rendezvous maneuver.

The CCM is provided with docking probes on its aft end which engage with conical dorgues on the propellant module. The assembly is shown schematically in Figure 3.5-1. Engagement of the soft probe within the drogue is accomplished by the acquisition latch. The kinetic energy of impact is dissipated by shock absorbers. The modules come to rest with approximately a 3-in. separation. Screw jacks are utilized, reacting against the acquisition latch of the soft probe to draw the bearing surfaces of the modules together. After the circumferential bearing surfaces are aligned and joined hook-type latches located at 12 points around the interface are activated simultaneously by a single cable driven by a reversible motor and drum assembly. A braking system on the motor holds the latches in either the closed over center or open positions. Following structural latching, the modules are in a final, stable structural configuration.

Following structural assembly the electrical hookup is accomplished to provide control to the CCM of propellant module subsystems which need to cooperate during fluid lines coupling and to provide power to the propellant module. The electrical hookup is accomplished by deployment of a single

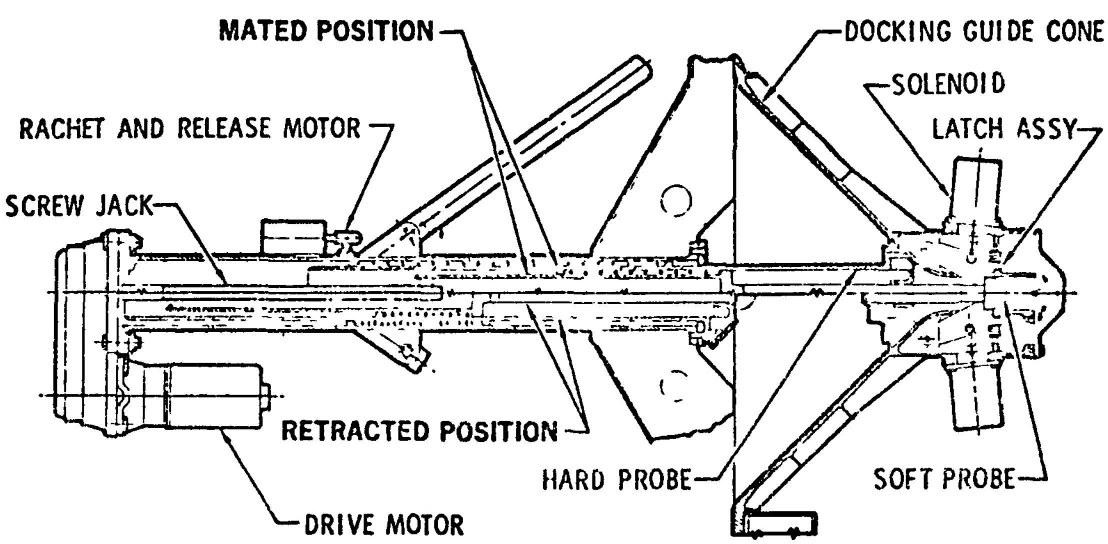

Figure 3.5-1 DOCKING DROGUE AND PROBE ASSEMBLY

panel from the CCM to a mating panel on the propellant module. The final module drawup used for structural latching also engaged the coarse level guide pins for the electrical panel mating. The initial panel deployment aligns the panels by the coarse guide pins and engages the fine alignment guides. The second phase of panel deployment aligns the terminal pins with their sockets by use of the fine alignment guides. The final deployment phase inserts the electrical pin connectors. All probes and pins are located on the CCM side of the interface. All power, data, and control connections are made by the single panel deployment. However, use of data bus for communication within the RNS reduces data and control signal hookup to a single connector assembly with four pins. The power hookup also employs one connector with four pins. The major electrical assembly requirement is the coupling of 8 connectors containing approximately 100 pins each for the emergency detection system. Seven of these connectors are provided to meet the current NERVA EDS requirements. One is provided for stage purposes. A schematic of the panel alignment and assembly is shown in Figure 3.5-2.

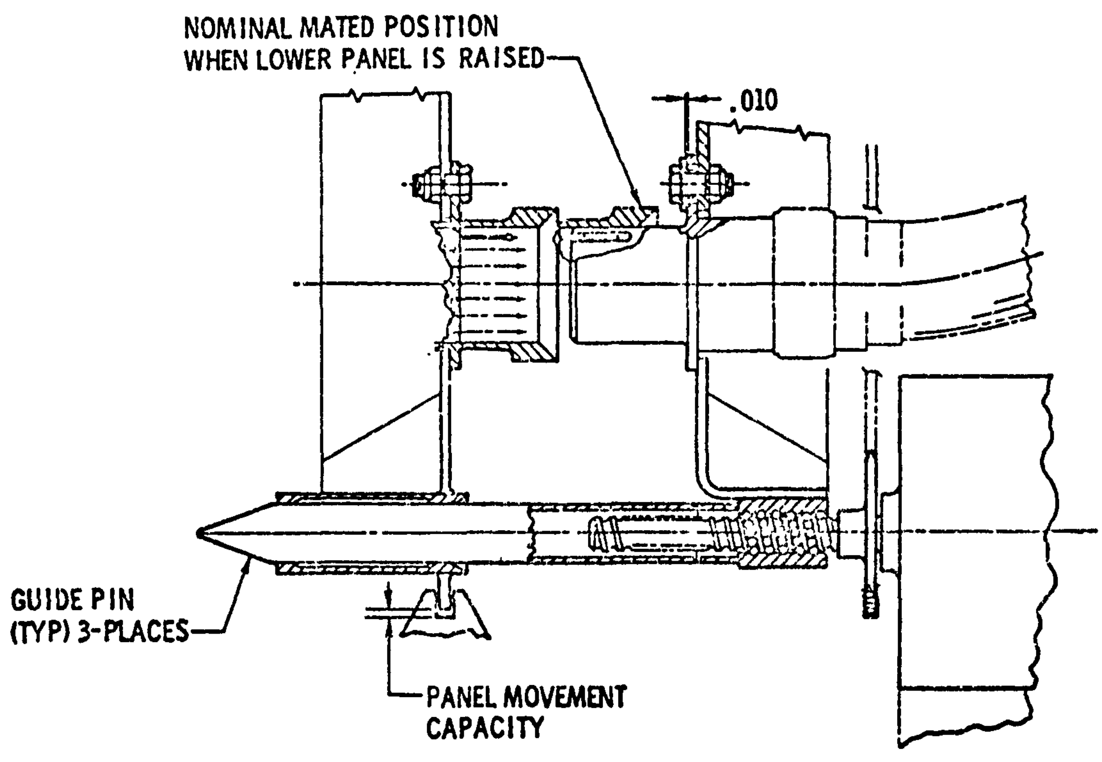

Figure 3.5-2 ELECTRICAL PANEL ASSEMBLY

Following electrical assembly of the CCM to the propellant module, control of the assembly is assumed by the CCM. An initial checkout is accomplished to ensure that the propellant module responds to all command signals and provides necessary data. Following this, the S-II stage and IU are jettisoned.

The only fluid line assembly required between the CCM and the propellant module is the propellant feedthrough for orbital fill. No fluid lines cross this interface which are needed for RNS operation. The feedthrough is assembled by first deploying a section of duct from the CCM to a mating flange on the propulsion module and then coupling the flanges with a V-coupling located on the propellant module. The deployment and coupling mechanism is shown schematically in Figure 3.5-3 while details of the alignment and coupling mechanism are shown in Figure 3.5-4. The drawup needed to accomplish structural latching was used to engage the alignment pilot for this duct. A total of 3 in. is provided with a linear compensator in the duct on the CCM accommodating this motion. The coupling of the flanges is accomplished subsequent to their mating by activation of the two

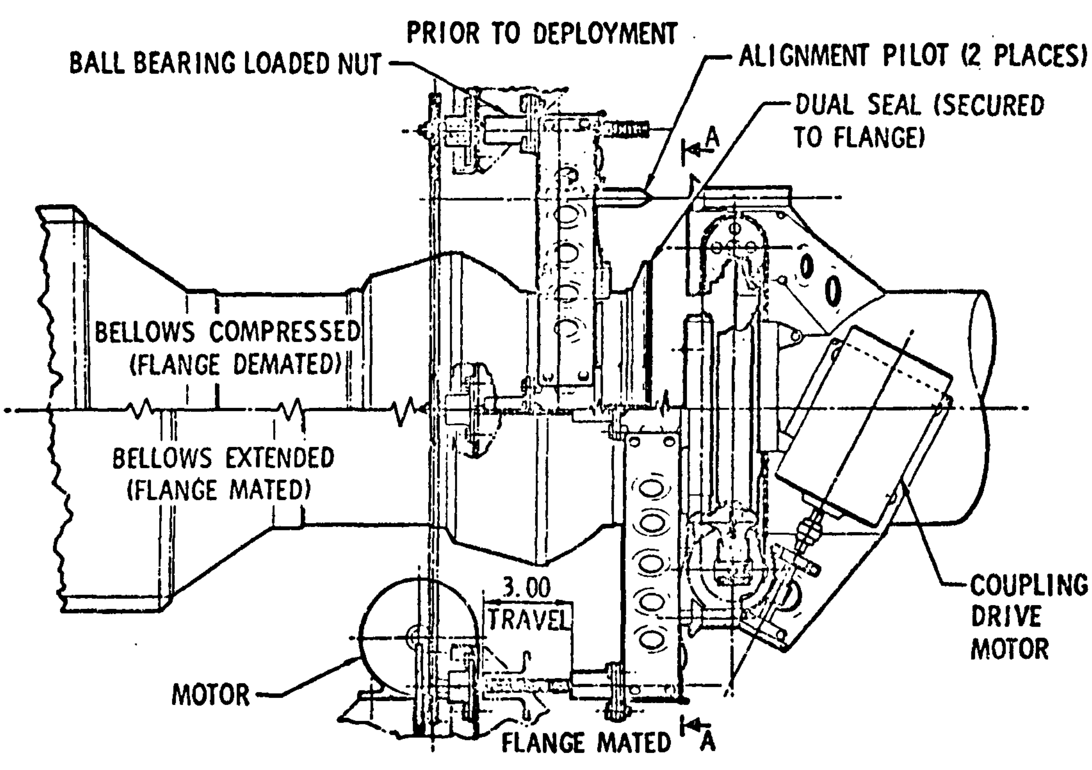

Figure 3.5-3 DEPLOYMENT AND COUPLING MECHANISMS

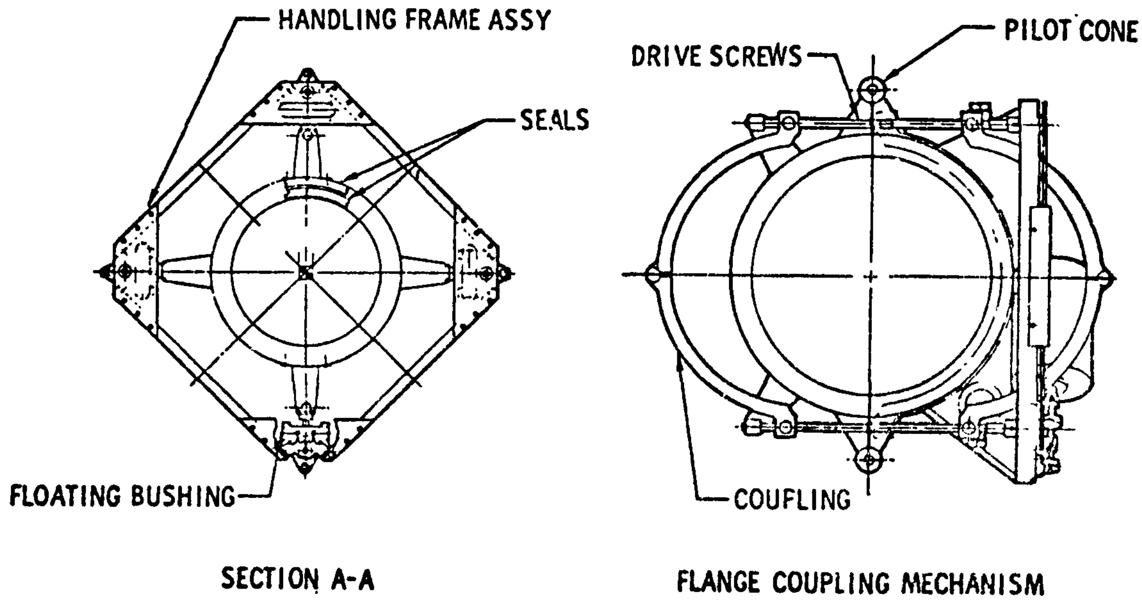

Figure 3.5-4 ALIGNMENT AND COUPLING MECHANISM DETAILS

V-couplings sections illustrated in Figure 3.5-4. They are supported and operated by left- and right-hand threaded drive screws. Sealing is accomplished by dual metallic pressure actuated seals. This operation completes assembly of the CCM with the propellant module.

3.5.3 Propellant/Propulsion Modules Assembly

The propulsion module is launched into the assembly orbit within the cargo hold of the space shuttle. The space shuttle accomplishes final rendezvous to within 500 ft of the partially assembled RNS. The propulsion module is then deployed from the cargo hold of the space shuttle and its stabilization system, utilizing stored gas attitude control, is activated prior to severance from the space shuttle. The forward docking interface on the propulsion module contains docking cones and the passive corner cube assembly needed for final rendezvous and docking. The terminal docking is under the control of the command and control module.

All subsequent operations of structural latching, electrical hookup, and fluid line hookup are the same as those described in Section 3. 5. 2 for the assembly of the command and control module with the propellant module with the following exceptions: the electrical panel assembly includes coupling of a 1-1/4-in. diameter pressurant line, the main flow line assembly is also described in Section 3. 5. 2, but in this case assembly of the main 12-in. feed duct is accomplished rather than merely an orbital fill line. Completion of this operation concludes the assembly phase of the RNS orbital operations.

3. 6 PROPELLANT TRANSFER

3. 6. 1 Concept

Propellant resupply is required to perform multiple missions with the RNS. It is a major operation affecting orbital support of the RNS and the overall economics of the space transportation system, since the RNS applications which have been evaluated typically result in a supporting traffic by the space shuttle consisting of 75 percent LH_2 resupply. The baseline RNS propellant resupply concept utilizes the space shuttle, configured as an integral tanker, to transfer propellant directly to the RNS under linear acceleration.

During Phase II, a number of system approaches (space shuttle tankers, propellant modules, orbital tank farms) and propellant transfer systems (acceleration, dielectrophoresis, etc.) were evaluated with the option of refilling or replacing depleted tankage (Reference 3-1). It was established that a reservoir of propellant tankage in orbit, either as a tank farm or larger RNS fleet, is required to smooth out propellant delivery to orbit and minimize the number of relatively expensive space shuttle vehicles which must be dedicated to propellant resupply for the RNS. Use of a larger RNS fleet was considered attractive since it provides reservoir capacity as well as mission flexibility.

The implications of propellant transfer system technology were assessed for the RNS in Phase II. Five transfer system concepts were evaluated: linear acceleration, rotating acceleration, surface tension, dielectrophoresis (DEP), and bladder expulsion. A linear acceleration transfer was found to be most economical and compatible with the RNS system. The liquid residual for acceleration transfer is reduced by employing flow control and other design strategies to minimize suction dip. The impact of acceleration on the orbit is reduced to only a slight wobble by orienting the thrust vector perpendicular to the orbit and transferring the propellant in an integral number of orbits. A spray nozzle inlet is provided in the RNS tank to collapse the ullage and allow propellant transfer without RNS venting.

The relation between the space shuttle cargo bay volume (15 ft diameter by 60 ft long) and its payload weight delivery capability (nominally 33,000 lb) impacts the selection of a propellant resupply mode. An initial evaluation during Phase II concluded that for either a volume-limited or weight-limited space shuttle it would be both simpler and more economical to use an integral propellant module and deploy a propellant transfer line from the space shuttle to engage the RNS tank fill system, than to deploy propellant modules from the space shuttle. This conclusion reflects the inert weight penalty (about 3,000 lb) for the additional design requirements of a deployed propellant tank, which include rendezvous and docking systems, thermal and meteoroid protection, and increased tank design pressure. Also, the available propellant volume is reduced for a deployed tank to provide clearance for feed lines and meteoroid protection. A further evaluation of the propellant resupply mode, was made during Phase III for the Class 3 RNS (see Section 3.6.2 in Volume II, Part B) to clarify weight and volume implications and confirm that propellant transfer was superior to replacement of depleted tanks. It was found that even if the propellant modules could be deployed from the space shuttle at a low orbit and delivered by a space tug to the RNS operational orbit (260 nmi and 31.5-degree inclination), direct transfer from the space shuttle would still be most attractive.

3.6.2 Propellant Transfer Operations

Propellant transfer operations will occur before the initial RNS mission to top off the propellant module and fill the dry propulsion module and between missions to resupply both tanks. In both cases, initial chilldown of a warm tank (nominally 370°R) must be accommodated by the design and operations. A nonvented propellant transfer operation is provided. However, the thermal protection system evaluation in Section 4.3.11 imposes a venting operation on the propellant resupply sequence to reject tank conditioning propellant and orbital heating incurred prior to final topping off. This permits design of the insulation system for the duration of mission operations and a short full tank orbital coast.

The RNS is passive for propellant resupply operations, requiring only actuation of orbital fill system valving and data management. The burden of operations is placed on the space shuttle tanker. It will provide acceleration for both the normal propellant transfer and the venting operation imposed prior to topping off. The baseline operations concept will be described briefly. Propellant resupply operations cannot be initiated until completion of engine cooldown, 53 hours after completion of the earth orbit injection burn. Payload deployment could be accomplished during that period or impose an additional time interval before tanking. Thus, the radiation environment will impose minimal constraints on the propellant resupply operation. Rendezvous and docking are accomplished by the space shuttle at the RNS operational orbit in the manner defined in Section 3.4, while the passive RNS maintains a gravity gradient stabilized local vertical attitude. An "I" formation for tanking is recommended, as shown in Figure 3.6-1, permitting the space shuttle orbiter to remain within the shadow cone of the RNS shield for both rendezvous and propellant transfer operations. This approach limits the dose rate to the orbiter crew to less than 0.1 rem/hr for 48 hours after shutdown, and a further reduction by an order of magnitude occurs after an additional 8 days.

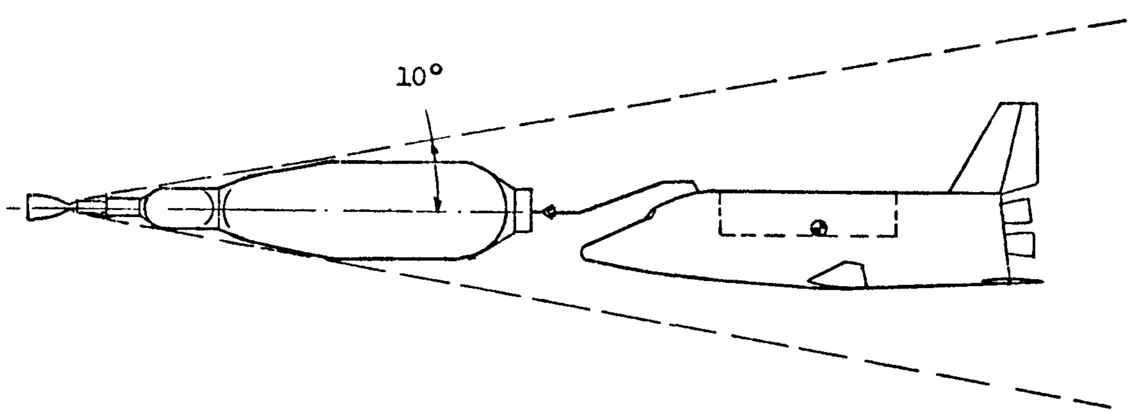

Figure 3.6-1 SPACE SHUTTLE TANKER IN "I" FORMATION WITH R.N.S.

The docking interface between the space shuttle and RNS for tanking remains to be defined, pending resolution of the orbiter configuration and payload interfaces. A single probe-drogue docking mechanism could be utilized, integrated with the orbital transfer lines. Fluid couplings could be accomplished similar to the design approach for RNS assembly shown in Section 3.5. Two alternatives are considered for the location of the line deployed from the orbiter: (1) the line can be deployed from the cargo bay over the top of the crew compartment, as depicted in Figure 3.6-1; or (2) a fixed portion of the line could be located inside the orbiter, running under the crew compartment and emerging at the top of the nose. The latter approach could be less complicated, since the distance from the front of the cargo bay to the tip of the nose of the orbiter is about 50 ft. Transfer line chilldown could be implemented without propellant losses with a pump-fed recirculating chilldown system similar to that used for RNS feed system chilldown, described in Section 4.5.5.

A linear acceleration transfer is used, with thrust provided by the space shuttle. Prior to propellant settling and transfer, the docked vehicles are rotated perpendicular to the orbit plane. The impact of acceleration on the orbit is then reduced to only a slight wobble by transferring the propellant in an integral number of orbits. It is anticipated that the orbiter would deliver 1,000-lb thrust in the forward direction for its normal operations. This results in an acceleration level from 1.7×10^{-3} to 3×10^{-3} g, depending on whether the RNS is full or empty. Accordingly, the corresponding Bond number in the 15-ft-diameter space shuttle propellant tank ranges from 3,000 to 5,300. In the propulsion module it is 15 percent lower, and in the propellant module it is about 5 times as large. A comprehensive discussion of propellant settling (Section 3.11.2) indicates that this acceleration level is at least an order of magnitude higher than is desired for efficient propellant settling. The propellant must be settled in both the donor and receiver tanks for the transfer. At the 1,000-lb orbiter thrust level, necessary settling would be accomplished within 10 minutes. The propellant transfer could then be accomplished ideally in about 20 minutes (based on transferring

30,000-lb LH_2 at 1,500 lb/min through a 4-in. line). Transfer line chill-down would be accomplished during the settling period. Thus, at high thrust the transfer could be completed within a single orbit period (1.6 hours). However, it is expected that a lower thrust level would be utilized if the space shuttle were designed for RNS propellant resupply operations. Alternatively, the thrust requirement could be imposed on the RNS. Initial settling would then take up to an hour, and the transfer operation would be designed for efficient reduction of liquid residuals from suction dip in the tanker by flow control and other strategies which could increase the transfer time by a factor of 10 or more. Accordingly, three orbit periods (4.8 hours) are allocated for propellant settling and transfer from the space shuttle.

The sequence of events and time budget for each propellant resupply operation is summarized in Table 3.6-1. Thus, except for the qualification on orbiter APS thrust, it appears that at this conceptual level no major constraints would be imposed on either the RNS or space shuttle design or operations.

Table 3.6-1

PROPELLANT RESUPPLY OPERATION SUMMARY

Event	Time Allocation (Hr)
Rendezvous (from 4 nmi)	1.0
Docking	0.5
Fluid Coupling and Checkout	1.0
Attitude Maneuver	0.5
Propellant Settling and Transfer Line Chilldown	1.0
Propellant Transfer	3.8
Attitude Maneuver	0.5
Separation (to 4 nmi)	1.0
Total	9.3

3.6.3 Propellant Logistics

Propellant resupply histories were defined to assess logistics implications and establish thermal protection requirements. Figure 3.6-2 identifies the required space shuttle launch rate to complete RNS turnaround in earth orbit within available time, based on a total 14 shuttle launches required. Ten launches are required for resupplying 300,000-lb LH_2 and four for CCM replacement and payload assembly. No credit was taken for space shuttle tanker performance gains without full payload return to the ground, so propellant delivery was 30,000 lb per launch. The sequence of these activites is: (1) refuel; (2) replace CCM; (3) perform unscheduled maintenance (4 days); (4) assemble payload; (5) perform checkout and countdown (1 day); and (6) initiate TLI. Propellant venting and final topping off can be performed as required for the mission during the period assigned to performing unscheduled maintenance. The total time available depends on the lunar shuttle annual mission rate as follows:

Annual mission rate (missions/year)	2	4	6	8
Time available for turnaround (days)	138.8	69	54.6	42.1

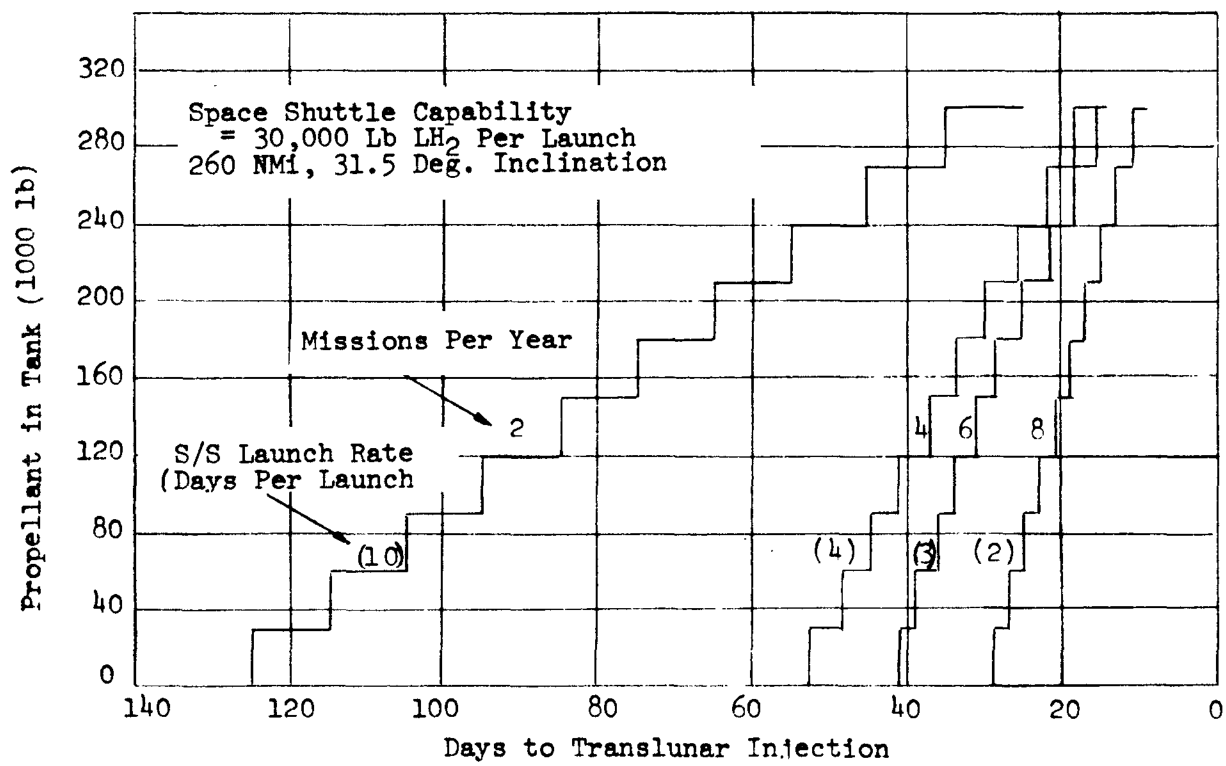

Figure 3.6-2 EFFECT OF MISSION RATE ON RNS PROPELLANT LOADING HISTORY

A single RNS is assigned to the two-lunar-shuttle-missions-per-year case, while two RNS are assigned for the higher rates. The uninterrupted available time between missions is used to complete turnaround activities without interference to turnaround of the other RNS. The turnaround sequence is scheduled for completion as close as possible to the translunar injection opportunity to minimize the hold time in a ready condition. However, in the 8 missions-per-year case, it was necessary to service the RNS immediately following return from the mission in some cases to prevent interference with the second RNS. Variations of schedule to accommodate the launch window requirements of missions such as unmanned planetary probes were not considered.

The 4 days per space shuttle launch case was used as a baseline for evaluating thermal protection requirements. Propellant resupply is initiated 53 days before the mission begins in that case.

3.7 CHECKOUT

Table 3.7-1 summarizes the checkout requirements for the various mission phases. This section concerns on-orbit checkout portion of these requirements. Ground checkout operations are defined in Volume III, Section 2. The RNS based equipment satisfies the requirements of onboard checkout in orbit only and for ground operations is complemented by the requisite GSE. Section 4.7.4 evaluates the point of control for on-orbit checkout and the role of ground. It concludes that the procedures and processing should be on board, with uplink and downlink capability to allow for ground evaluation of checkout results, procedure modification, and the use of special diagnostics for situations that were not preprogrammed or anticipated. Section 4.7.4 also defines the processing and storage requirements for the onboard data management function, the emergency detection system (EDS), and the requirements for fault prediction.

Table 3.7-1

CHECKOUT REQUIREMENTS BY PROGRAM PHASE

Requirement	Program Phase: On Orbit	Ground Recycle	Production Checkout	Launch
Functional check all subsystems/ components	All modules	All modules	All modules	---
Verify redundancies	Space resident modules	CCM	All modules	---
Process previous mission data for fault prediction	All module data processed on ground		Provides data base for all modules	---
Interface checks (Leak check and electrical continuity)	For orbital connections made and valve seals	For ground connections made and valve seals	For all connections and seals (including permanent)	EOS connections made
Instrumentation calibration	Space resident modules	CCM	All modules	---
Equipment alignment	---	CCM	All modules	---
Proof test	---	---	All modules	---

Four discrete phases of onboard checkout can be identified:

A. During orbital assembly or refurbishment, assembly verification will be made for those modules that are involved in assembly (including payload). Rechecks on all broken fluid connections and on the dynamic seals of all critical valves will be made. The interface between modules and specific subsystems which are best checked during this phase of the operation will be verified.

B. During the orbital countdown all subsystem and component checkout will occur, including the verification of all redundancies for space resident modules. This will be accomplished by the systematic performance of a series of procedures stored in the data management subsystem.

C. During the operational phase of the mission continuous status, monitoring of a limited set of functions will occur. The status of these functions will be compared to some predetermined standard to ensure that the vehicle health is as expected. During the operational phase, data must be collected to accomplish fault prediction.

D. Following the mission the fault prediction data will be utilized to determine the potential of impending failures on space resident hardware, and the ground will process the mission data to identify anomalies.

The onboard checkout system is required to perform a functional checkout of the RNS in both earth and lunar orbit. It must provide stimuli and evaluate the responses of the stage to determine if it is operationally ready to begin its mission. To insure a high probability of success for completion of the mission, the checkout of redundancies is required. The checkout system must also be able to isolate to a replacement module level consistent with the maintenance policy. All procedures are stored and processing is accomplished by the centralized processor in the data management subsystem (DMS). The NDICE included in the CCM will effect checkout of the NERVA. The propellant module will utilize the capability of the onboard checkout system in the CCM to verify its flight readiness.

The nature of a reusable stage dictates that during the life of this stage impending failures must be detected in advance of the catastrophic failure. This requirement creates a need for fault prediction techniques on those functional components which may cause such catastrophic failures. Since the propellant module is a space resident element, fault prediction sensors are included. The propulsion module also being space resident will have the same characteristic requirements for checkout as the propellant modules. The issues of maintenance, fault isolation and fault prediction are dealt with more extensively in Section 3. 15.

The principal components of the onboard system are the procedures or software programs stored in the bulk storage of the DMS which cover checkout of each RNS subsystem and of the RNS as an integral system. These procedures must be functionally compatible with the centralized DMS approach which has been chosen as baseline.

3.7.1 Orbital Assembly

3.7.1.1 Assembly Operations Checkout

Three candidate checkout approach candidates for assessing successful assembly were identified during the course of this study. All three assumed that each module will be thoroughly checked-out before launch from earth (including all redundancies).

The first candidate approach requires orbital checkout of components within a module prior to translation of that module to the RNS assembly area. This checkout could be performed either by the space shuttle or the space tug. The second candidate employs sequential checkout of each module as it becomes assembled to the RNS using the RNS onboard checkout system. Both electrical and fluid interfaces would be verified upon completion of each docking operation. The CCM should necessarily be the first module upon which the complete cluster would be built upon if the onboard checkout subsystem resident capabilities are to be used. The third checkout approach candidate is based on performing checkout of the integrated RNS only. That is, no checkout will be performed for assembly verification until the total assembly operation is completed. This candidate uses the same software and hardware that the onboard checkout subsystem would use during recycle checkout.

For the Class 1 Hybrid RNS, unlike the Class 3, the CCM is up first and interface verification can be effected by the CCM onboard procedures; first between the CCM and the propellant module, which prior to CCM mating is monitored and controlled by the INT-21 IU, and subsequently the interface to the propulsion module.

3.7.1.2 Leak Check Concepts

For this system one of the main concerns during assembly verification checkout is to establish the integrity of the fluid interfaces and to insure that no unacceptable propellant losses occur due to improper mating. Four approaches may be taken to satisfy this concern:

A. Indirect methods of determining joint integrity other than direct leakage measurements can be used. Examples are torque measurements and position indications. These parameters can be correlated to ground test data establishing confidence levels for the integrity of the connection.

B. Pressure decay analysis could be performed after assembly. Pressure decay analysis measures the rate of pressure drop in a calibrated volume. No quantitative measurement of leakage is attempted. Ground data correlations are used to establish a go or no-go action. Prohibitive pressure rise would require repair procedures to be initiated.

C. A quantitative leak check across dual seal flanges could be performed using leak detection ports on all intermodule fluid interfaces. This is accomplished with a flow meter pressure and temperature transducer combination. This system permits determination of the quantity of leakage. Possible actions include the recycling of connections and releak check or replacement of the module.

D. Acoustic emission sensors could be used to monitor gas leaks across the seals or flanges.

The third approach, leak check across dual seal flanges, is favored for the RNS. Dynamic seal integrity will be checked on the ground before installation on the stage. Only intermodule connections will be checked in orbit. This approach requires only minor additional instrumentation at the intermodule interfaces.

3.7.2 Orbital Countdown

3.7.2.1 Checkout Operations

To assess the impact of onboard checkout on operational RNS subsystems, the propellant management system was selected as a representative system to develop specific checkout requirements and procedures. Implications of two alternative approaches to checkout were assessed: (1) component functional checkout, and (2) simulation of operations were assessed for orbital checkout.

Component Functional Checkout

Approaches to component functional checkout are defined for three general classes of propellant management subsystem configurations. Similar considerations apply to the APS. The first class is represented by quad-redundant valve configurations imposed on certain flight systems for reliability. No additional checkout valves are required and fluid losses are minimized if the checkout approach consists of sequencing valve actuation and verifying talkbacks. This approach requires independent control of the valves.

The second class of propellant management subsystems is represented by the LH_2 feed system. For this system, blocking valves isolate each module interface, permitting actuation of the dual feed valves. Similarly, the chill-down and refill pumps could be run with the discharge valves closed. These checkout operations could be performed at convenient times in the operations profile, which include the propellant resupply period and the normal feed system chilldown during the startup ramp to minimize the impact of these operations.

The third class of checkout items consists of ground-only functions such as the fill-and-drain and ground vent systems. These are locked for flight, and orbital checkout is not required.

Simulated Operations

Although the simulation of actual subsystem operations is characteristic of ground checkout operations accomplished on previous programs to determine flight readiness, substantial penalties could be incurred using this approach for orbital checkout. In order to verify the propellant management subsystem in orbit settling of propellants, feed system chilldown and NERVA criticality for pressurization gas would be necessary. This would require the use of consumables and, should maintenance be required, cause delays or interference with other operations during NERVA cooldown. Alternately, a separate pressurization system could be employed implying equipment penalties.

The possibility of integrating this system simulation philosophy with the required prestart operations was assessed. The primary difficulty with this approach is that the thrust buildup ramp would necessarily be initiated. Should anomalies occur at this point in the prestart, they would likely be sensed by the EDS and corrective procedures taken at any point in the prestart cycle.

Selection

Component functional checkout was chosen over simulated operations on the basis of minimum operational penalties, the lack of additional major design requirements, and the ability of this approach to verify the design integrity of the RNS. The chosen approach avoids the possible requirement for a separate propellant settling operation. Minimum fluid flow and virtually no expendable loss will be incurred during checkout by establishing a component sequence of operation that will satisfy both of these goals. Additionally, some components would be checked at times when minimum loss is incurred. For example, the spray nozzle fill valves may be checked during orbital refueling, propellant isolation valves after refueling and pressure control valves prior to refueling. Simulated operations is an attractive approach for certain subsystems in the astrionics system where these penalties do not accrue. The use of a built-in test equipment (BITE) concept is incorporated in the data management subsystem only with the self test approach.

No additional valves are required for checkout purposes. Component operation will be verified by monitoring operational instrumentation and precision talkbacks. No additional instrumentation requirements for checkout purposes were identified. The only additional control capability identified specifically was that of provisions for individual control of redundant valves. This separate control is required to verify redundancies and preclude expendable loss.

3.7.2.2 Subsystem Requirements

Operational considerations and checkout approaches for RNS elements are summarized by module in Table 3.7-2. Three major phases of checkout are characterized: checkout following orbital assembly (OA), whether initially or following CCM recycle; checkout prior to translunar injection (PTLI); and ground checkout, whether before initial launch or during CCM recycle.

The types of checkout identified are: (1) functional—the actual activation of a component under electrically powered conditions, verifying its response and effect on interfacing systems; (2) calibration—establishing output level relationship to standard or predetermined levels; (3) alignment—physical orientation determination and comparison to expected indications or measurement, (4) redundancy verification— check operational status of primary as well as backup components; (5) output quality verification— measurement and analysis of signal characteristics such as frequency, format or power level and comparison of these measurements with predetermined standards; (6) leak check— search, detection, and potentially quantification of fluid loss by leakage. Additionally, preliminary definition of the functional requirements of the ground checkout procedures are given where they complement similar onboard procedures.

Table 3.7-2

CHECKOUT APPROACH SUMMARY

Element	QA	PTLI	G	Functional Checks	Calibration or Alignment	Other Tests
				CCM		
Electrical Networks	X	X		By implication on other tests		
			X			Verify installation and redundancies. Check connection and insulation resistances.
Environmental Control	X	X	X	Temperature measurement during operation.		
Onboard Checkout		X		By implication on other tests	Verify EDS sensing levels during instrumentation calibration	
			X	Performance verification on system integration RNS simulators. Check software procedures and hardware EDS.	Verify parameter limit assignments both in software and in EDS hardware.	Quality fault isolation procedures. Verify EDS automatic operation by simulating failures.
Data Management	X	X	X	Diagnostic self-test (BITE), and verification by implication.		Check automatic switchover of processor and data bus elements performance.
			X			Verify redundancies
				PROPELLANT MODULE		
Structures	X	X				Fault predicting—acoustic detection of structural integrity and cracks.
Docking/Clustering			X	Same as for CCM		
Propellant Feed and Pressurization systems	X	X		Activate isolation and blocking valves - limit switches		
			X			Leak check all connections.
Orbital Refueling		X		Verify component operation during refueling.		Leak check refueling valves after refuel by pressure and temperature measurement in quad-valve cavities.
			X	Component actuation—limit switches		Leak check all connections.
Vent System	X	X		Component actuation—limit switches		Verify redundancies and leak check by pressure and temperature measurements in quad-valve cavity.
Astrionics	X	X		Same as for CCM where applicable	Same as for CCM	Same as for CCM-add redundancy checks

Table 3. 7-2 (Continued)

Element	O A	P T L I	G	Functional Checks	Calibration of Alignment	Other Tests
PROPULSION MODULE						
Docking/Clustering			X	Same as for CCM		
Propellant Feed, Pressurization, and Orbital Refueling System				Same as for Propellant Module		
Chilldown System	X	X		Chilldown pump operation for 1 minute—verify speed speed developed. Component cycling-limit switch verification		Verify redundancies of valves and pumps. No propellant settling required.
Chilldown System			X	Pump operation with liquid flow. Verify performance by discharge pressure and speed measurement.	Pump inverter frequency calibration.	Leak check of all connections. Verification of operating and instrumentation redundancies.
Refill System	X	X	X	Same as for chilldown system.	Same as chilldown inverters.	Same as for chilldown system.
Astrionics	X	X		Same as for CCM	Same as for CCM	Same as for CCM—add redundancy checks.
INTERFACES						
Automatic Mating Panels and Mechanism			X	Verify operability by mating with test panels.	Mechanical alignment torque level calibration to achieve tight connections.	Redundancy verification
Fluid		X		By implication during orbit refueling		
	X	X		Verification of torque level at connecting points.		Leak check by measuring flow at dual seal flange leakage ports.
Electrical	X			By implication during other tests exercising components and verifying instrumentation.		
			X			Continuity and isolation resistance measurements on test lines.

3.7.3 Astrionics and Software Impact

Reviewing the various subsystems, orbital checkout, and utilizing S-IVB test data, it is estimated that 25,000-word storage will require for the checkout procedures. This includes both subsystem and emergency procedures. Although the bulk of the procedures are performed off the peak data processing load time (orbital operations or coast phases), there is a requirement to perform specific checkout — related operations during peak (anticipated during engine burn). Reviewing the checkout functions that must be performed during peak, a total of 8,200 equivalent adds per second (ops) have been identified. These primarily include the data management self-check procedures, guaranteeing the health of the processor, and trend analysis operations to detect impending failures which potentially would preclude an emergency situation. Additionally, a small amount of processing will be used for a general health monitor or status monitoring capability included in the data management functions. A review of specific subsystems indicates that the existing vehicle operational data acquisition capability can generally be used as a primary data source to evaluate the performance of each subsystem during the checkout phase. Additionally, the control to stimulate these subsystems/components can be effected by the nominal control lines of the RNS. A minimum of additional instrumentation and control will be required for checkout. Exceptions to this are the requirement that position indications be supplied for all components to verify the performance of the component upon simulation and discrete instrumentation and control be provided for all redundancies. Because CCM checkout is assisted by ground support equipment, the addition of test connectors will be required for access to critical test points for the verification of these subsystems and the associated redundancies.

3.8 INFORMATION MANAGEMENT

This section is concerned with the information flow between the RNS and external system elements. The data flow internal to the RNS, the associated processing and storage requirements, the RNS system architecture, and data bus concept are described in Section 4.7.6. The Phase II study established the instrumentation list used as a basis for the data flow evaluation and selected PCM/PSK coding and RF transmission in the S-band based on the compatibility with the Deep Space Information Facility (DSIF/MSFN) and the maximum anticipated data rate of 0.5 MHz.

3.8.1 External Systems Informational Interfaces

Table 3.8-1 summarizes the informational flow with the leading external system elements by RNS function. The largest quantity of information flow occurs between the RNS and ground. Minimal information flow exists for short periods of time between other program elements and the RNS.

3.8.1.1 Ground Interfaces

The ground will monitor the RNS performance and intermittently uplink information to the RNS. Uplink requirements exist throughout all mission phases to allow for direct control of RNS operations or for program changes that are determined necessary during the space residence of the RNS. Ground processing of RNS data is necessary for evaluation of the previous mission performance to assess vehicle status and establish unscheduled maintenance requirements. In non-real time the ground will process the stored, compressed performance data transmitted by the RNS to perform fault prediction or trend analysis evaluation between missions. The results of this evaluation will determine what maintenance operations must be effected prior to initiation of subsequent missions. A limited number of critical functions are anticipated to be monitored in real time to provide for ground intervention in special situations. The projected capabilities of the DSIF/MSFN are assumed to include an average of five ground stations per orbit and 160 minutes per day viewing time.

3.8.1.2 Space Shuttle Interfaces

While the ground interfaces are characterized by RF transmissions, the space shuttle interface is characterized by a hard-line connection to the RNS data bus. During launch and module return maneuvers, the space shuttle will connect into the RNS data bus directly to effect the gathering of information and control of RNS module components. During propellant transfer operations, the space shuttle will physically connect to the RNS and using the

Table 3.8-1

RNS INFORMATIONAL INTERFACE WITH OTHER PLANNED SYSTEM ELEMENTS

Operational Interface (RNS Functions) / System Element	Rendezvous and Docking for Assembly, Maintenance, and Replenishment	Navigation and Guidance	Checkout	Instrumentation Command and Control	Data Management
DSIF/MSFN (Ground)	Monitor operations – data transmitted from RNS, INT 21 or space shuttle	Backup capib. to baseline autonomous RNS. N&G update on position and velocity	Processing of previous mission data for trend analysis/fault prediction. Operational monitor of limited number of critical functions	Uplink to the RNS for program change or direct command	Store and monitor data compressed and transmitted by RNS
Space Shuttle	RNS passive – space shuttle maneuvers to allow for LH_2 replenishment	Not required	Not required	Monitor and control of modules during launch phase using RNS data bus	Process module data from RNS data bus during launch
INT-21	RNS passive – must hold constant attitude – CCM maneuvers for assembly operations	Not required	Not required	Monitor and control of module during launch and assembly phase using RNS data bus	Process module data from RNS data bus during launch and assembly operations

data bus control operate the required components to effect transfer of LH_2. Information transfer occurs between the RNS and the space shuttle only during these phases of the mission. The requirement for compatibility of the RNS and space shuttle data bus implementation is implied.

3.8.1.3 Payload Interfaces

The payload interfaces with the RNS are represented by a capability to accept data both hard line and via a compatible data bus and to provide for manned payload control of RNS functions again using the capability of the data bus in addition to hard-line control effected through the EDS. The RNS is independent of the payload and these interfaces provide an override capability in the case of manned payloads.

3.8.1.4 INT-21 Interfaces

For the Class 1 Hybrid RNS, the INT-21 launch vehicle is postulated for the launch of the propellant module. No intelligence is attributed to the propellant module; consequently, the INT-21 is required to provide control and monitoring of propellant module functions during launch. Additionally, the INT-21 will provide stable orientation so that the CCM deployed from the space shuttle can dock to the propellant module and take over control before separation.

3.8.1.5 NERVA Interfaces

The NERVA interface is an internal interface to the RNS and is covered in detail in Section 4.7.5 and in Section 7.2.3 of Book 2. In summary, this interface is primarily accomplished between the NDICE located forward in the RNS and the data bus terminal dedicated for engine control and instrumentation located on the propulsion module. The RNS data bus is utilized for transmission of this data and no independent engine interface exists outside of the RNS. All data are integrated into the data management function of the RNS.

3.8.2 Data Flow

The data flow between the RNS and ground was evaluated and several conclusions derived. Although numerous data interfaces can be established between the RNS and other space program elements, the primary recurring communication exists between the RNS CCM and the ground. Two approaches were evaluated: (1) using a direct RF link to ground stations, and (2) using an RF link to ground via a communications satellite. With relatively low data rates, a dump of data over each ground station can be used requiring storage of real time data when out of view of a ground station. With high data rates, communication satellites must be used to establish continual data flow to earth in real or near real time.

3.8.2.1 Requirements

Based on the data requirements identified in Phase II and presented in Section 4.7.1 for an operational vehicle, it can be determined that there is an expected 8,800 samples per second. For ten bits per sample, approximately 90,000 bits per second of data would be generated. For a typical RNS earth orbit, the total data acquired would then be at a rate of 5×10^8 bits/orbit. For transmission from lunar distances where the ground stations are essentially in continuous view, a data acquisition rate of 9×10^4 bits/sec applies.

3.8.2.2 Bandwidth Reduction Approaches

There is a strong motivation to reduce the total quantity of data transmitted to earth without reducing the informational content of these data. Techniques of data compression to achieve this objective are well known. Alternately, data elimination could be practiced. This would take the form of having multiple data modes for the various mission phases each of which would contain only a subset of the RNS parameter list. It is estimated that about eight discrete phases would be established, each having a characteristic subset of data. Data not relevant to the particular mission phase would be neither sampled nor transmitted. The possibility of eliminating the least significant binary bits, thus shorting the word length, also exists. Data compression techniques and multimode data approaches evaluated in Phase II are presented in Section 2.2.3 of Reference 3-2.

3.8.2.3 Approach Evaluation and Selection

Using data compression techniques which do not reduce the informational content a reduction of the total data transmitted from orbit can be achieved. Gemini data compression simulations have demonstrated compression ratios of about 100 to 1 for the type of data anticipated for the RNS. Assuming five ground stations would be available and the total transmission time over these ground stations were 160 minutes per day, a transmission rate to ground using data compression would be 8.5×10^3 bits per second. Data compression requirements on the data management function represents one of the largest processing requirements. However, it is considered totally within the capability of a conventional processor (see Section 4.7.5). During the life of the RNS this represents an overwhelming quantity of data to be received, processed or stored in ground facilities. This suggests that extensive data elimination may be also desirable. Alternatively the data may be disposed of, unprocessed after some period of time.

The relatively low transmission rate indicates that there is no requirement for communication satellite relay to transmit full information content to ground. However, their availability would allow for essentially continuous viewing of the RNS. Furthermore, the low data rate is compatible with the use of a subcarrier of the unified S-band transmission system. This would typically be the 1.024-MHz telemetry subcarrier of the 2,287.5-MHz carrier presently dedicated to the CSM. This provides substantial additional bandwidth capability for data on the same carrier, including low rate TV coverage for operations and experiments in the early phases of the program.

3.9 PRESTART COAST

Prestart coast covers the period prior to stage main propulsive maneuvers in earth orbit, lunar orbit, and in transit according to the mission timeline defined in Section 2.3. The stage functions required include navigation and guidance, attitude control, attitude maneuvers, and separation from target facilities prior to NERVA operation.

3.9.1 Navigation and Guidance

The navigation and guidance subsystem will be capable of operating in three modes during orbital coast in addition to full capability operation: (1) a dormant mode, (2) a "wake-up" mode, and (3) a checkout mode. During long term coast phases in earth and lunar orbits, the RNS will be stored in a gravity-gradient-stabilized mode which obviates the requirement for attitude determination. This permits use of a dormant mode in which all N&G electronics are powered down and a predetermined environment maintained. Prior to attitude maneuvers, a "wake-up" mode will allow for initialization of attitude and position and coarse attitude hold in an otherwise dormant phase. In this mode the horizong sensor, IMU and processor will be activated to determine the local vertical and maintain a lock onto a point on the earth's horizon. Attitude error signals are then provided to operate the auxiliary propulsion system.

During coast periods, checkout operations will be performed which include calibration of the RNS sensors. During checkout and periods of payload mating or refurbishment operations, a fully operational mode will be used to determine position and attitude. Also, active periods exist during transit where the full capability of the navigation and guidance subsystem will be utilized in the guidance policy to optimize the application of aftercooling pulse.

3.9.2 Attitude Control

For long-term coast phases in earth and lunar orbits, the RNS will be stored in the gravity-gradient-stable, local-vertical orientation that precludes the necessity for active attitude control. The RNS will operate in a limit cycle mode during the translunar and transearth coast periods and both of the 24-hour lunar orbits.

The total impulse for limit cycle operation about pitch, roll and yaw axes over the entire mission is plotted as a function of minimum impulse bit for three values of the deadband angle in Figure 3.9-1. Gravity-gradient capture considerations constrain the minimum impulse bit to less than 190 lb-sec. The lower bound is set by the APS motor valve actuation considerations which restrict firing time to approximately 0.030 second. For a thrust level of 100 lb selected in Section 4.6.2, the resulting minimum impulse bit is 3 lbs-sec. This value has been adopted for the current RNS design. In addition, a deadband of 1-degree has been assumed to limit dispersions and performance loss during cooldown thrusting.

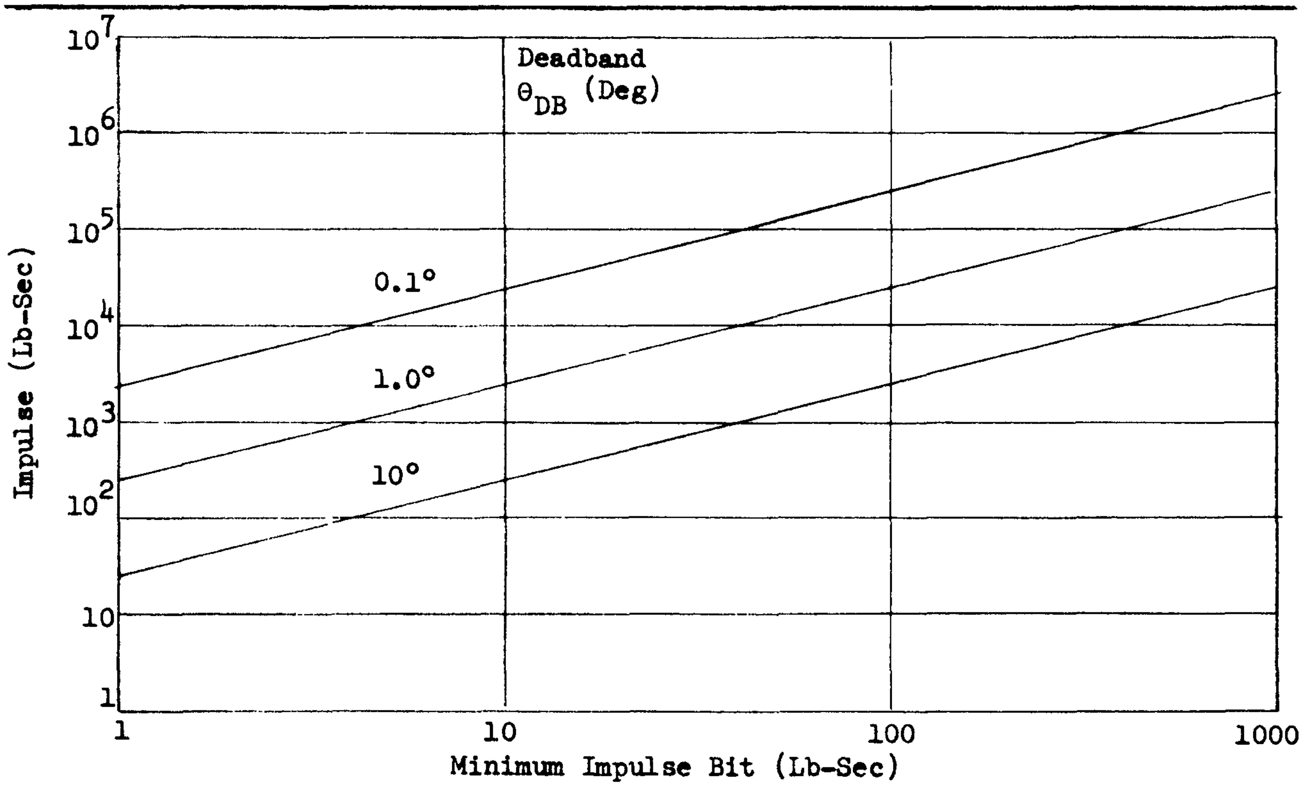

Figure 3.9-1 COAST PHASE ATTITUDE CONTROL REQUIREMENTS

The limit cycle impulse requirements about each axis and the time between thrustor firings are presented for each of the four affected coast phases in Table 3.9-1. The total impulse requirement to be used in the APS sizing was 1,850 lb-sec. This impulse requirement is dependent on the thrust level selected, since the minimum impulse bit is thrust-dependent. However, this requirement is such a small part of the total requirement that reduction does not appear warranted for other considerations, such as powered flight roll control authority, attitude maneuver times, and contingency conditions.

3.9.3 Attitude Maneuvers

For the lunar mission there is a large number of candidate attitude maneuvers. The impulse requirement is generated in establishing and cancelling the attitude rate at which the maneuver is performed. In Figure 3.9-2 the time to perform a 30-degree pitch or yaw maneuver at a constant maneuver rate is presented for the impulse required to initiate and terminate the pitch or yaw rate. The S-IVB uses a maneuver rate of 0.3 degree/second. For the RNS a rate of 0.1 degree/second has been selected. This rate should provide a reasonable time to complete pitch

Table 3.9-1

CLASS 1 COAST ATTITUDE CONTROL IMPULSE REQUIREMENTS*

Coast Phase	Time (hr)	Impulse Requirements (lb-sec)				Frequency of Firing (hr)
		Pitch	Yaw	Roll	Total	
Translunar	108	42	42	266	350	1
24-hr lunar orbit at arrival	24	9	9	59	77	1
24-hr lunar orbit at departure	24	79	79	144	302	0.2
Transearth	72	238	238	647	1,123	0.2
					1,852	

*Deadband = 1 degree; minimum impulse bit = 3 lb-sec.

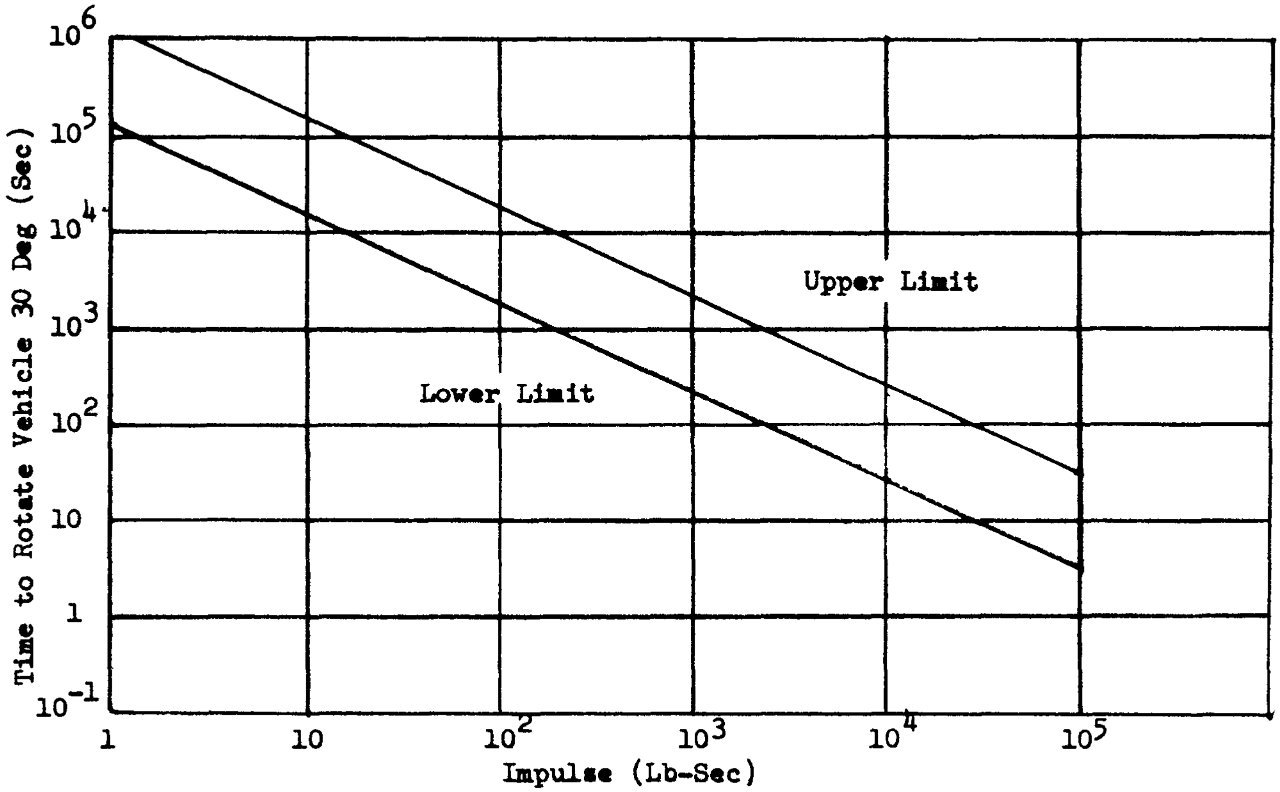

Figure 3.9-2 TIME TO MANEUVER (PITCH OR YAW)
(Time to Achieve and Cancel Rate Excluded)

or yaw maneuvers (a half-hour to rotate 180 degrees) at a relatively small cost (from 500 to 8,200 lb-sec/maneuver).

For this study 36 attitude maneuvers have been assumed for the reference mission profile. These are identified in Table 3.9-2, with their impulse expenditure. Based on this schedule, the maneuver impulse requirement to be used for APS sizing is 145,000 lb-sec.

Based on studies of the dynamics of the attitude maneuvers, a thrust level of between 10 and 100 lb will give reasonable maneuver time. A nominal 100-lb thrust level, about each of pitch and yaw axes, was selected in this study. Two 50-lb motors were used in each plane to achieve this thrust level. The pitch and yaw/roll motors are all 50-lb thrust. With this size motor, maximum roll control authority was achieved without causing limit cycle

Table 3.9-2

ATTITUDE MANEUVERS

Mission Phase		Maneuver	Impulse (lb-sec)
Pre-TLI	1.	Acquire coast attitude	6,800
	2.	Reorient for separation	6,800
	3.	Reorient after separation	6,800
	4.	Orient for TLI burn	6,800
Translunar coast	5.	Acquire coast attitude	7,000
	6.	Orient for midcourse	7,000
	7.	Acquire coast attitude	7,000
	8.	Orient for midcourse	7,000
	9.	Acquire coast attitude	7,000
	10.	Orient for midcourse	7,000
	11.	Acquire coast attitude	7,000
	12.	Orient for first lunar orbit injection burn	7,000
Intermediate lunar orbit coast	13.	Acquire coast attitude	7,000
	14.	Orient for lunar plane change burn	7,000
	15.	Acquire coast attitude	7,000
	16.	Orbit for second lunar orbit injection burn	7,000
Lunar orbit operations	17.	Acquire coast attitude	8,200
	18.	Orient for rendezvous maneuver	8,200
	19.	Orient for gravity-gradient storage	8,200
	20.	Orient for separation maneuver	500

Table 3.9-2 (Continued)

Mission Phase		Maneuver	Impulse (lb-sec)
	21.	Acquire coast attitude	500
	22.	Orient for third lunar orbit burn	500
Second intermediate lunar orbit coast	23.	Acquire coast attitude	500
	24.	Orient for second lunar orbit plane change burn	500
	25.	Acquire coast attitude	500
	26.	Orient for TEI burn	500
Transearth coast	27.	Acquire coast attitude	500
	28.	Orient for midcourse correction	500
	29.	Acquire coast attitude	500
	30.	Orient for midcourse	500
	31.	Acquire coast attitude	500
	32.	Orient for midcourse	500
	33.	Acquire coast attitude	500
	34.	Orient for EOI burn	500
Earth orbit coast	35.	Acquire coast attitude	500
	36.	Orient for rendezvous maneuver	500
	37.	Orient for gravity-gradient storage	500
		TOTAL	144, 800

consumption to become large. As will be shown in Section 4.6.3, a configuration could be selected which would provide complete redundancy in yaw and contingency operation (in case of a motor failure) in pitch.

3.9.4 Separation

In the event the RNS is in the vicinity of a manned facility prior to an-orbit departure maneuver, the RNS must leave its vicinity before initiating full-thrust NERVA operation because of the radiation problem. The separation maneuver described in Reference 3-1 imposes a severe impulse requirement on the APS (ΔV = 22 fps in the earth orbit case assuming the NERVA engine, operating in the idle mode, provides half the impulse).

Previously in Phase II, a safe separation distance (tentatively identified as 160 nmi) was achieved by Hohmann transfer with RNS moving above and behind the space station. The cost of achieving the 160-nmi separation distance in terms of impulsive velocity (ΔV) and altitude difference is shown in Figure 3.9-3 as a function of time to attain the safe distance. An altitude

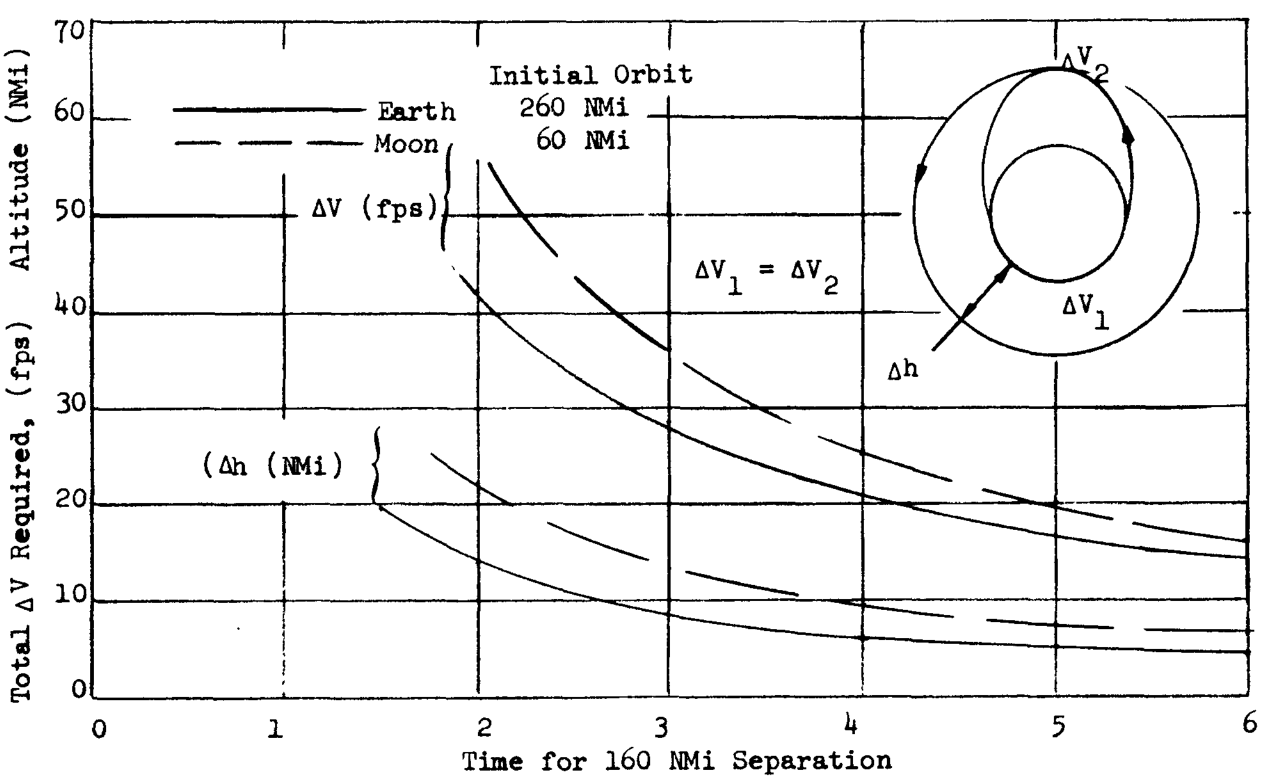

Figure 3.9-3 SEPARATION MANEUVER REQUIREMENTS

difference of 5 nmi was assumed which resulted in a ΔV cost of 31 fps that was provided by the APS. The sensitivity of impulse to ΔV of 10,000 lb-sec/fps made this maneuver a logical candidate for impulse reduction. Half of the impulse requirement can be transferred from the APS to the main propulsion system by using the NERVA engine operating in the idle mode to provide the prograde circularization burn at apogee, since the station is shielded from the engine by the RNS. Further reduction in APS impulse is obtained by using the APS to provide a small separation that would nevertheless allow the NERVA (in the idle mode) to complete the initial injection maneuver. This is accomplished using the APS to provide a prograde ΔV of 2.5 fps. The resulting elliptic orbit places the RNS 7 nmi behind, co-altitude with the space station after one orbit. The NERVA engine then provides that ΔV, over and above the 2.5 fps, that is required to establish an elliptic orbit with the desired altitude difference. This maneuver is also a prograde burn, so again the space station is within the shielded cone angle of the RNS. This mode of obtaining the separation distance takes one orbit longer than the previously used mode but requires a ΔV of only 2.5 fps from the APS for each maneuver. The time to achieve separation is now a function of main stage impulse expended rather than APS impulse, thus providing greater flexibility. The total impulse requirement for the separation maneuvers, using this scheme, is 49,400 lb-sec.

3.10 PROPELLANT UTILIZATION AND THRUST MODES

The propellant utilization and NERVA thrust modes during the lunar shuttle mission profile, which generate various stage design requirements, are defined in Table 3.10-1. These show the propellant loadings, equilibrium ullage volume, and ullage mass in the propellant modules and the propulsion module after completion of main stage burns. Also, the aftercoolant required after completion of the burns and refilling of the propulsion module before startup are shown separately.

The NERVA thrust modes for the various mission maneuvers are indicated. The first burn, translunar injection (TLI), is performed at full thrust. The required propellant for pulsed aftercooling is contained in the propulsion module run tank. The midcourse correction is performed using the NERVA idle mode. Only the propulsion module is operated for that maneuver. The

Table 3.10-1

PROPELLANT UTILIZATION AND THRUST MODES – CLASS 1 HYBRID

Item	Propellant Tank			Run Tank			
	Loading (lb)	Ullage Volume (ft^3)	Ullage Mass (lb)	Loading (lb)	Ullage Volume (ft^3)	Ullage Mass (lb)	Thrust Mode
Initial	289,850	3,300	450	9,690	120	16	---
TLI	120,210	41,800	5,700	8,000	500	70	Full Thrust
TLI Aftercooling	118,250	42,250	5,760	2,430	1,770	240	Aftercooling
TLI Midcourse	118,250	42,250	5,760	1,400	2,010	270	Idle Mode
Refill Run Tank	109,950	44,130	6,030	9,690	120	16	---
LOI-1	100,550	46,260	6,330	8,000	500	70	Full Thrust
LOI-1 Aftercooling	100,550	46,260	6,330	7,200	680	100	Aftercooling
LOI-2	100,550	46,260	6,330	1,240	2,030	290	Throttle Mode
Refill Run Tank	92,100	48,170	6,600	9,690	120	16	---
LOI-3	73,840	52,310	7,170	8,000	500	70	Full Thrust
LOI-3 Aftercooling	73,840	52,310	7,170	6,700	820	120	Aftercooling
Refill Run Tank	70,850	52,990	7,270	9,690	120	16	---
TEI-1	60,290	55,380	7,610	8,000	500	70	Full Thrust
TEI-1 Aftercooling	60,290	55,380	7,610	7,120	700	100	Aftercooling
TEI-2	60,290	55,380	7,610	2,780	1,680	240	Throttle Mode
Refill Run Tank	53,380	56,940	7,830	9,690	120	16	---
TEI-3	46,600	58,480	8,050	8,000	500	70	Full Thrust
TEI-3 Aftercooling	46,600	58,480	8,050	7,380	640	90	Aftercooling
TEI Midcourse	46,600	58,480	8,050	6,860	760	110	Idle Mode
Refill Run Tank	43,770	59,120	8,140	9,690	120	16	---
EOI	400		8,390	4,740	1,240	180	Full Thrust
EOI Aftercooling	400		8,390	1,850	1,900	270	Aftercooling
Flight Performance Reserve Δ				100	2,300	320	---

initial elliptical lunar orbit injection maneuver (LOI-1) is also performed at full thrust. Since the run tank was depleted for TLI aftercooling and the midcourse maneuver, it must be refilled before LOI-1. The subsequent plane change maneuver at the moon (LOI-2) is performed with the NERVA throttle mode, and all of the required propellant for that maneuver and LOI-1 aftercooling is contained in the run tank. Completion of lunar orbit injection (LOI-3) is performed as a full thrust operation, requiring a refill of the run tank before startup. The same general modes of operation are applied for the remaining phases of the mission chart, including the TEI EOI maneuvers: throttle mode for the plane change at the moon and idle mode for midcourse, with full-thrust operation in the main burns. All aftercooling operations and the small maneuvers which are performed at less than full thrust are performed using only the propulsion module run tank. It is refilled before each full-thrust burn.

The NERVA thrust modes generate requirements for different stage functions, including propellant settling, feed system chilldown, prepressurization, prestart run tank refill, navigation and guidance, and thrust vector control. The various NERVA thrust operating modes are defined according to their respective parameters and required RNS functions in Table 3.10-2.

Table 3.10-2

REQUIREMENTS FOR NERVA OPERATING MODES

NERVA Operating Mode	NERVA Parameters			RNS Functions					
	Thrust (lb)	Flow Rate (lb/sec)	Isp (sec)	Propellant Settling	Feed System Chilldown	Prepressurization	Prestart Run Tank Refill	Navigation and Guidance	Thrust Vector Control
Full Power	75,000	91.9	825	X	X	X	X	X	X
Throttle Mode	45,000	55.1	825	X	X			X	X
Idle Mode	1,000	2	500					X	
Aftercooling	300	0.7	430					X	

X = Required

3.11 STARTUP

3.11.1 Operations Phasing

The sequencing and interrelation of the operations of propellant settling, propellant feed system conditioning, NERVA thrust buildup, and pre-pressurization of propellant tankage are delineated in Figure 3.11-1. Propellant settling consists of two phases. The initial phase of inviscid orientation requires a low acceleration provided by the APS. This is followed by a high-thrust, dissipative settling phase for which the necessary acceleration is provided by NERVA during its startup ramp. The operations for preconditioning the feed system include chilldown and prestart refilling of the run tank. These are accomplished during the inviscid orientation phase after an initial settling period. Prepressurization cannot be initiated until completion of the dissipative phase of settling and NERVA cannot operate above the throttle point without tankage prepressurization, so a thrust hold period at the throttle point is incorporated into the thrust buildup ramp. After prepressurization of the run tank the NERVA thrust can be increased to full

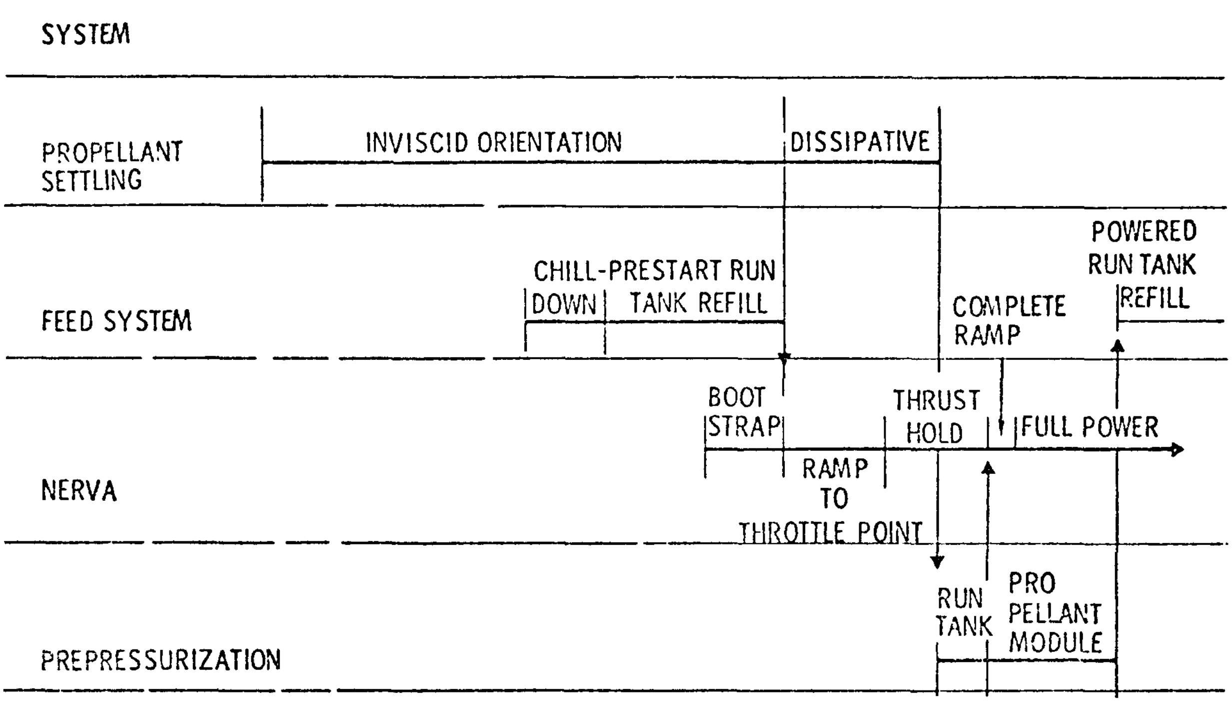

Figure 3.11-1 STARTUP OPERATIONS PHASING SCHEMATIC

power, although for some cases it could be desirable to maintain the thrust hold until completion of prepressurization of the propellant module. When the propellant module is pressurized, it can be brought on line to refill the run tank under full power. The concepts for each of these operations will be defined in the subsequent sections.

3.11.2 Propellant Settling

The Class 1 Hybrid RNS consists of two tanks with different volumes and diameters which must be settled up to ten times at various stages of loading in the course of the reference lunar shuttle mission. Consequently, optimization of the settling process becomes hypothetical and the approach adopted for the evaluation was to identify the principle phenomena which would design the settling system.

Reference 3-3 delineates the phenomena of settling phases: an initial inviscid phase for liquid orientation, followed by dissipative phases of turbulent dissipation, laminar slosh, and bubble rise. The advantage of a two-step settling process was identified. The strategy is to use a low initial acceleration to orient the liquid at the bottom of a tank while imparting the least amount of energy to it, and then raise the acceleration level to dissipate the energy and eliminate bubbles from the liquid or to stabilize the liquid gas interface. For Bond numbers much less than 10, settling times become prohibitively long, but also, the dissipative phase at high thrust is a negligible fraction of the inviscid portion of the settling time. Baffles are required to suppress initial geysering and to reduce the laminar slosh phase.

The geometric and acceleration considerations for the RNS are defined in terms of Bond number (Bo) as follows: (1) run tank - radius = 6.66 ft, acceleration (g) = 6.67×10^{-7} (Bo), length = 21 ft; and (2) Class 1 Hybrid propellant tank - radius = 16.5 ft, acceleration (g) = 1.08×10^{-7} (Bo), and length = 100 ft. Here the Class 1 Hybrid propellant tank is approximated as a cylinder with the full length of the actual ice-cream-cone-shaped tank.

The acceleration levels provided by a constant thrust and the resulting settling times are shown in Table 3.11-1, comparing two cases: initial run tank Bond numbers of 10 and 100. Typically, a full propellant tank would be critical in designing the settling system. However, as the main propellant tank becomes substantially offloaded, the run tank becomes critical for settling time.

Table 3.11-1
INVISCID SETTLING PHASE SUMMARY—CLASS 1 HYBRID

Criterion	Prior to Burn	Acceleration (g)	Settling Time (sec)
$(Bo)_{RT} = 10$,	TLI	6.7×10^{-6}	3,500
	M	1.06×10^{-5} R	1,460
3.15 lb thrust	LOI-1	1.06×10^{-5}	1,100
	LOI-2	1.10×10^{-5} R	660
	LOI-3	1.13×10^{-5}	910
	TEI-1	1.80×10^{-5}	700 R
	TEI-2	1.94×10^{-5} R	500
	TEI-3	1.99×10^{-5}	670 R
	M	2.10×10^{-5} R	480
	EOI	2.12×10^{-5}	660 R
			9,640
$(Bo)_{RT} = 100$,	TLI	6.7×10^{-5}	1,100
	M	1.06×10^{-4} R	150
31.5 lb thrust	LOI-1	1.06×10^{-4}	320
	LOI-2	1.10×10^{-4} R	210
	LOI-3	1.13×10^{-4}	290
	TEI-1	1.80×10^{-5}	220 R
	TEI-2	1.94×10^{-5} R	160
	TEI-3	1.99×10^{-5}	210 R
	M	2.10×10^{-5} R	150
	EOI	2.12×10^{-5}	210 R
			3,020

NOTE: R indicates run tank is critical.

The two-step settling process was evaluated for several strategies which are summarized in Table 3.11-2. The applicable Bond number criteria for the initial and final settling, the associated thrust levels, the inviscid and total settling times and settling propellant requirements are indicated. Here the cryogenic APS Isp is taken as 400 seconds. Alternate strategies are indicated for providing the dissipative phase of the settling thrust, i.e., use of a higher thrust level APS, or integration of the settling with the NERVA startup ramp. The dissipative phases were estimated based on previous detailed technology studies. These propellant settling requirements indicate that integrating the settling with the NERVA thrust buildup would appear to be a superior strategy, resulting in APS propellant savings of several thousand pounds and avoiding additional large settling motors.

The evaluation has resulted in selection of a 3.15-lb settling thrust to be provided by the APS, resulting in a run tank Bond number of 10 for initial inviscid settling. Additional settling for dissipation will be provided by the NERVA startup ramp. Although settling times of 1,000 seconds and larger occur for the initial TLI settling with reduced times for subsequent burns, it

Table 3.11-2

PROPELLANT SETTLING CRITERIA COMPARISON—CLASS 1 HYBRID

Bond No. Criteria		APS Thrust (lb)		Settling Time (sec)		Settling Propellant (lb)
Initial	Final	Initial	Final	Inviscid	Total	
10	10,000	3.15	3,150	9,640	9,830	1,600
10	10,000	3.15	NERVA	9,640	9,640*	80
100	10,000	31.5	3,150	3,020	3,320	2,630
100	10,000	31.5	NERVA	3,020	3,020*	240
100	100	31.5	31.5	3,020	12,080	960
1,000	10,000	315	NERVA	960	960*	760

* Dissipative phase of settling integrated with NERVA startup ramp, including a hold in the thrust buildup at the throttle point.

was found that there was no interference from aftercooling pulses, which persist through subsequent burns in most cases, and attitude control limit cycle impulses. Thruster lifetimes appear to be adequate, since with a policy of recycling the RNS command and control module to the ground on each mission, it would be possible to replace the settling thrustor.

3.11.3 NERVA Thrust Ramp

The NERVA thrust buildup ramp is summarized in Table 3.11-3, where NERVA operating conditions, acceleration level, and the required saturation pressure for 0 NPSP at the existing flow rate (defined in Section 4.5.1) are indicated at various times through the ramp. It is seen that the engine can operate up to the throttle point without prepressurization for the anticipated propellant histories (defined in Section 4.3.12), or with minor adjustments of operating procedures. There is approximately a 19-second period during the ramp-up phase until the throttle point is reached where a bootstrap NERVA startup can be employed with a zero NPSP required and providing adequate settling thrust for the dissipative phase of settling. For some of the cases

Table 3.11-3
NERVA STARTUP THRUST RAMP

Phase	Time (sec)	Flow Rate (lb/sec)	Thrust (lb)	Isp (sec)	Acceleration (g)*	PSAT for 0 NPSP (psia)
Bootstrap	0	1.2	295	253	6.3×10^{-4}	12
	25	1.2	383	331	8.1×10^{-4}	12
	30	1.8	691	375	1.5×10^{-3}	12
Ramp-up	39	29.8	17,090	572	3.6×10^{-2}	16.2
	52	55.1	44,990	816	9.6×10^{-2}	20.3 (Throttle point)
	56	91.9	75,000	816	0.16	26.0 (Full thrust)

*Full RNS at TLI

considered it was found that the required dissipative phase exceeded this ramp-up phase so that it would be necessary to hold the thrust buildup at the throttle point of 50,000-lb thrust or a lower level until settling were completed and all required prepressurization could be accomplished. In some cases it was also found desirable to hold the thrust below full thrust until the run tank could be refilled. The resulting performance losses as a function of the duration of the thrust hold were determined over a 300-second period for the two most critical burns as: -2.0 lb/sec for TLI, and -0.4 lb/sec for LOI. Thus, while employing a thrust hold at the throttle point can facilitate RNS startup operations, it has a negligible performance impact. An additional benefit of the thrust hold period is an effective increase of burn time which will reduce the impact of initial thrust vector misalignment and minimize guidance errors for the short burns in the mission profile. These are analyzed in Section 4.7.3.3 of Volume II, Part B, Book 1 for the Class 3 RNS.

3.11.4 Feed System Prestart Operations

Prior to startup, it is necessary to chill down the active portion of the RNS feed system to assure propellant conditions for NERVA and to accomplish a predictable startup operation. The feed system interfaces that require conditioning include the two legs of the NERVA feed system between the turbopump and the run tank and the interfaces between the RNS modules. These are summarized in Table 3.11-4. All the stage feed ducting uses two basic types of flexible elements, gimbal joints and linear pressure volume compensators, which account for the masses shown for those systems.

The evaluation of boiling heat transfer in hydrogen presented in Reference 3-4 indicates that film boiling occupies about 90 percent of chilldown time. Accordingly, the film boiling heat transfer correlation in Reference 3-5 was used, together with a 10 percent increment, to establish the minimum permissible time for chilldown of each duct from ambient (370°R) to hydrogen saturated conditions. A chilldown system design concept is presented in Section 4.5.5 which compensates for initial pressure surges by automatically providing an intermittent flow. Thus, an additional 100 percent margin was added to the calculated chilldown times to account for flow surge effects, resulting in the times shown in Table 3.11-4.

Table 3.11-4

CHILLDOWN REQUIREMENTS

Interface	Components	Mass (lb)	Length (ft)	Equivalent Boiloff (lb LH_2)	Chill Time (sec)
NERVA (each side)	PSOV-valve 9-in. feed duct* Turbopump PDKVA-valve	973	8.9	92	43
Run Tank/ Propellant Module	12-in. feed duct*	263	11	28	34

*Includes gimbal joints

The chilldown operation can be initiated as soon as liquid can be supplied to the chill pumps. The current system design is based on initiating chilldown at a time about 50 percent through the inviscid settling phase.

It was explained in Section 3.10 that it is necessary to refill the run tank before startup for all full-power burns to replace propellant expended for aftercooling and low-thrust maneuvers. The objectives in the design of the system are to avoid venting, to accommodate a higher pressure in run tank than in the propellant module supply, to integrate the refill operation with the normal sequence of startup operations (avoiding separate operational requirements), and to provide for delivery of up to 8,500 lb of LH_2 during the refill operation. As depicted in the startup operation phasing schematic, the refill operation will be phased subsequent to the feed system chilldown. A 20-lb/sec flow rate is desired for the refill system defined in Section 4.5.6 to avoid extending the settling period, but a lower rate would incur a minimal penalty.

3.11.5 Prepressurization

To satisfy the propellant condition requirements of NERVA (Section 4.5.2) both the run tank and propellant tank require prepressurization prior to building up to full thrust. The propellant module pressurant requirement was established for the propellant state history defined in Section 4.3.12. The module is pressurized from the saturation pressure to the nominal tank pressure at 28.7 psia, defined by the pressure control analysis in Section 3.12.2. This corresponds to a NERVA operating pressure of 26 psia and a tank design pressure of 29 psia. The propellant tank pressurant requirements are defined in Table 3.11-5 utilizing NERVA bleed gas at 225°R and a collapse factor of 1.1. The run tank pressurant requirement is less than 1 lb in each case so the expulsion pressurization system (0.58 lb/sec) is adequate for prepressurization. However, a larger prepressurization flow rate is required in the propellant module: 5 lb/sec was adopted as a baseline, considering that excessive depletion of the run tank would not occur before the propellant module was ready to be brought on line.

3.11.6 Run Tank Depletion and Refill

Although the run tank operates independently during the startup operation, it is desirable to avoid depleting its propellant level too greatly because of increased radiation dosage to equipment located at the top of the propulsion

Table 3.11-5
PROPELLANT MODULE PRESSURANT REQUIREMENTS—CLASS 1 HYBRID

Phase	Volume (ft^3)	Saturation Pressure (psia)	Pressurant Mass (lb)
TLI	3,300	18.6	20.4
LOI-1	44,130	19.6	246
LOI-3	48,170	19.8	262
TEI-1	52,990	24.6	133
TEI-3	56,940	25.0	129
EOI	59,120	26.0	98

module. The nominal run tank capacity analyzed is 9,700 lb of LH_2 and typically it is desirable to keep the run tank level above 5,000 lb of LH_2, where the dose rate is a factor of 2 higher than for the full tank. The minimum run tank level (or depletion) during the startup operations is summarized in Table 3.11-6 for the mission profile. The duration of the NERVA thrust hold to complete propellant settling and tankage prepressurization operations is also indicated. The resulting mission performance penalties are negligible. To avoid excessive depletion of the run tank for the LOI burns, it proved desirable to hold the thrust at the throttle point until completion of prepressurization. The resulting reduced flow rate before the propellant module could be brought on-line avoids excessive run tank depletion. After the propellant module is brought on-line, the run tank will be refilled during full power with the pressure head differential between the tanks by reducing the impedance of the flow control valve from its steady-state setting.

Table 3.11-6

RUN TANK DEPLETION BEFORE PROPELLANT TANK ON LINE—CLASS 1 HYBRID

Burn	NERVA Thrust Hold (sec)	Propellant Tank Prepress. Time (sec)	Run Tank Depletion (lb LH_2)	Minimum Run Tank Level (lb LH_2)
TLI	51	5	4,010	5,680
LOI-1	3 61*	58	6,240 4,110*	3,450 5,580*
LOI-3	0 59*	60	6,460 4,290*	3,230 5,400*
TEI-1	0	29	3,160	6,530
TEI-3	0	28	2,970	6,720
EOI	0	20	2,230	7,460

*Option - Maintain thrust hold through propellant tank prepressurization.

3.11.7 Navigation and Guidance

The most stringent requirements for the navigation and guidance sensors arise from the performance sensitivity to position and attitude determination prior to TLI. The accuracy requirements derived in the Phase II study, are shown in Table 3.11-7 and are based on a 50-fps midcourse budget corrected by an impulsive maneuver 20 hours after TLI or TEI. Allowance is made for impulse errors, modeling unpredictabilities, and navigation inaccuracies including sensor errors in determining the position uncertainty requirement.

The requirements for TEI is approximately 3 to 5 times less stringent than for TLI; however, for LOI an equivalent velocity error of 2 fps corresponds to a 10-nmi perilune accuracy. The comparable equivalent velocity for 10-nmi perigee accuracy at TEI is 6 fps. These requirements can be met by ground tracking, an autonomous system approach for ground-assisted approaches which are detailed and evaluated in Section 4.7. An autonomous approach was selected in Section 4.7.3 which uses a landmarker tracker for orbital parameter determination and star trackers for primary attitude determination.

Table 3.11-7

STARTUP NAVIGATION AND GUIDANCE REQUIREMENTS

RNS Activity	N&G Mode	Sensor Used	Accuracy Required
Prior to TLI or TEI	Wakeup	Horizon sensor Strapdown IMU	± 1.0 degree attitude ± 5 nmi (radial) position
TLI	Operational	2 Star trackers Landmark tracker Strapdown IMU	± 0.9 nmi (radial) position ± 2 fps velocity 10 arc second attitude
TEI	Operational	2 Star trackers, Landmark tracker Strapdown IMU	± 3 nmi (radial) position ± 6 fps velocity 10 arc second attitude

After a period of dormancy in earth or lunar orbit the "wakeup" mode described in Section 3.9.1 will initialize position and attitude. To accurately determine orbital parameters, the lankmark tracker scans a point on the earth or lunar surface to determine local vertical. After several measurements, these data are combined to refine the initial estimate of the vehicle position and velocity. The star trackers acquire stars for an inertial attitude reference. Once the navigation data thus derived compare with ground-derived estimates of the vehicle orbit, a targeting procedure using the strapdown IMU is carried out which steers the vehicle during the mission burns.

3.12 STEADY-STATE OPERATION

3.12.1 Requirements

During steady-state operation the run tank of the propulsion module acts as a surge tank. A control system is required to regulate the pressures in both the run tank and main propellant tank(s). In addition, the control system must regulate the flow rate of LH_2 into the run tank to maintain a specified liquid level. This control system must be able to: (1) regulate the startup and shutdown ramp; (2) refill the run tank after startup when the propellant module has been brought on line; (3) adjust to acceleration head changes during burn, including switching between tanks; (4) respond to flow rate changes for the NERVA emergency mode operation at 60 percent of full power; and (5) control fluctuations within controller hardware pressure bands at steady state.

Thrust vector control must be provided by engine gimbaling during powered flight to achieve vehicle attitude control. The attitude control system must compensate for initial thrust vector misalignment, vehicle center-of-gravity offset, initial vehicle rotation rates, and guidance inputs.

3.12.2 Propellant Management Control

Three parameters must be sensed by the propellant management control system: (1) ullage pressure in the propellant module, (2) ullage pressure in the propulsion module, and (3) the liquid level in the propulsion module. Each of these sensors can be tied via the data management system, to one of three controllers: (1) pressurant flow valve/vent valve on the propellant module, (2) pressurant flow valve/vent valve on the propulsion module, and (3) the LH_2 feed valve from the propellant module to the propulsion module.

A variety of concepts for connecting the control sensors and controllers were evaluated, shown in Figure 3.12-1. Control systems 1 through 6 are characterized by connecting a single sensor to each controller. Candidate 7 has the two sensors on the propulsion module connected to a single controller. Control systems 1, 2, and 7 are characterized by independent pressure control on each tank. This permits prepressurization or pressurant makeup as required in any tank and accommodates different thermodynamic states in each tank. Control system 1 is the only one which is suitable for startup and shutdown ramps to bring the propellant tank on line. It is seen that several of the concepts are subject to wide variations of control response in the coupling of the run tank liquid level to the large pressurized volume of the propellant tank.

Independent operation of the run tank would be desirable. Orbital checkout would be simplified because it would be on a discrete module basis compatible

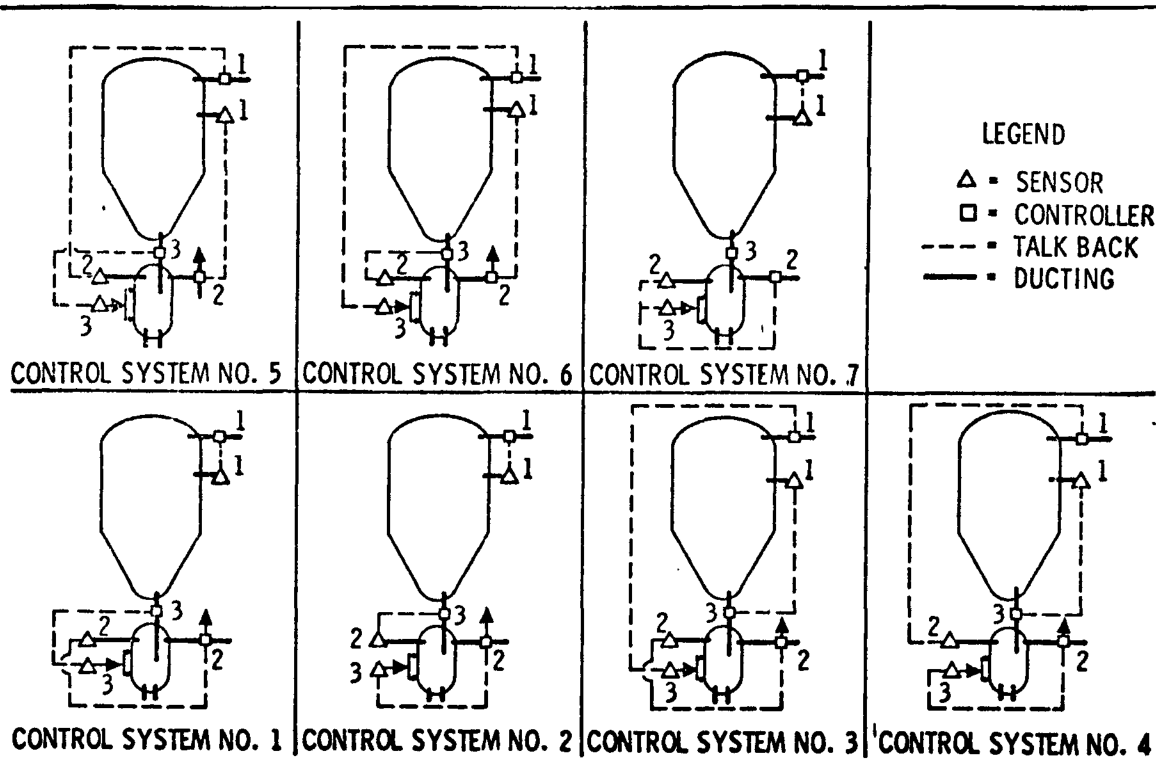

Figure 3.12-1 CANDIDATE PROPELLANT-PROPULSION MODULE CONTROL SYSTEMS

with the module assembly and replacement concept. Ground test simulation would also be simplified because the run tank could be connected to arbitrary tankage configurations and still demonstrate operation on an integral run tank. These would provide significant economic benefits to the program. Concepts 1 and 7 have the additional feature of providing direct control of tank pressure for NERVA. Control systems 1, 2, and 7 were therefore considered to be the most attractive, while the other four concepts were considered inconsistent with the simplified RNS module replacement concept.

Since control system 1 accommodates startup and shutdown ramps and also permits refilling the run tank with minimum additional pressure head built into the system, it was selected as the baseline for further evaluation. The latter consideration reflects a tank weight penalty of 500 lb per psia.

The pressure schedule and control functions are defined in Figure 3.12-2. The considerations in defining this schedule will be briefly described. The first issue is the feed system pressure drop and the resulting separation of the pressure bands between the propulsion and propellant modules. The feed system pressure drop including provision for acceleration head is defined in Section 4.5.10. The maximum steady-state value shown in the figure is 1.2 psia. The flow rate into the run tank varies as the square root of the pressure drop across the run tank feed system, while the pressures in the run tank and propellant tank can vary within the ranges of their hardware deadbands. Consequently, for a fixed impedance a wide variation from the steady-state flow rate could be incurred. A buffer δp is desired to minimize the magnitude of the allowed fluctuation. In addition, a margin must be provided for increased flow rate required while refilling the run tank during full-power, steady-state operation. A flow control margin $\delta p = 1.2$ psia is indicated in the figure. This impedance would be provided by the propellant feed control valve in the run tank. This valve permits a 40 percent increase in the flow rate above steady state for refilling the run tank.

The next consideration is the tolerances associated with the pressure sensors and control valves. Pressure schedules were developed for the tolerances associated with three hardware options: (1) pressure switch sensor with bang-bang controllers; (2) regulator valves; and (3) strain gage sensors with bang-bang control valves. The tolerance capabilities of these systems were

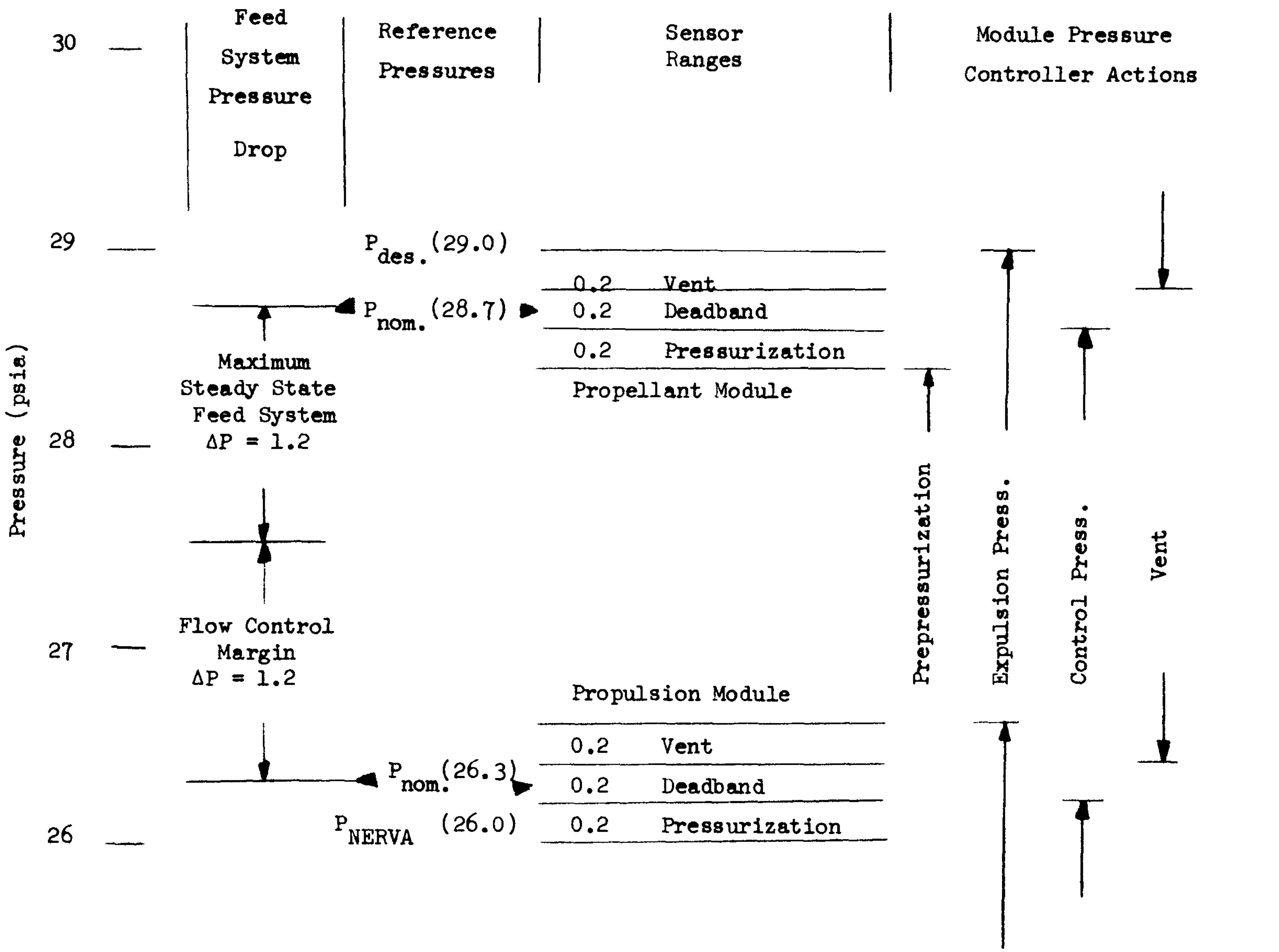

Figure 3.12-2 PRESSURE SCHEDULE AND CONTROL FUNCTIONS (CLASS 1-H)

considered to be 1.5, 0.6, and 0.2 psia, respectively. In view of the indicated tank pressure weight penalty, the most accurate control concept, strain gage sensors and bang-bang control valves, was selected. Optical point liquid level sensors have an accuracy of ±0.01 in. corresponding to 0.05 lb LH_2. Thus liquid level control does not appear limiting for control system accuracy.

The various pressurization system functions are defined in Section 4.5.7, according to the module pressure controller action strategy identified in this figure. A prepressurization function is provided for the Class 1 Hybrid propellant module. It is turned on until the bottom of the pressurization band is sensed. The expulsion pressurization function is active to the top of the module pressure control band, being turned off by activation of the vent band sensor which simultaneously actuates the control vent system. The control pressurization function is actuated by the pressurization sensor. A deadband is provided between the vent and pressurization bands within which only the expulsion pressurization function is active.

Simulations of the dynamic behavior of the run tank pressure and liquid level during startup, run tank refill, and transition to the NERVA malfunction mode were performed. A typical set of responses is shown in Figure 3.12-3, where the flow control impedance is adjusted 10 percent in response to a 50-lb liquid level sensing increment. These simulations established that the liquid level overshoot during run tank refill could be controlled, and that only a small liquid level rise would be incurred if the NERVA flow rate demand was suddenly reduced by malfunction.

3.12.3 Thrust Vector Control

A study was conducted during Phase II to determine the thrust vector control system requirements for the RNS. Preliminary engine gimbal deflections and rate limits were established based on maintaining an acceptable attitude transient. Results are presented in Section 2.6.2 of Reference 3-2. These studies and similar studies by IBM have shown that thrust vector gimbal angle requirements are largely determined by the value of thrust vector misalignment plus the vehicle center-of-gravity offset. A 1.5-degree thrust vector misalignment was allowed for in these studies. The factors investigated

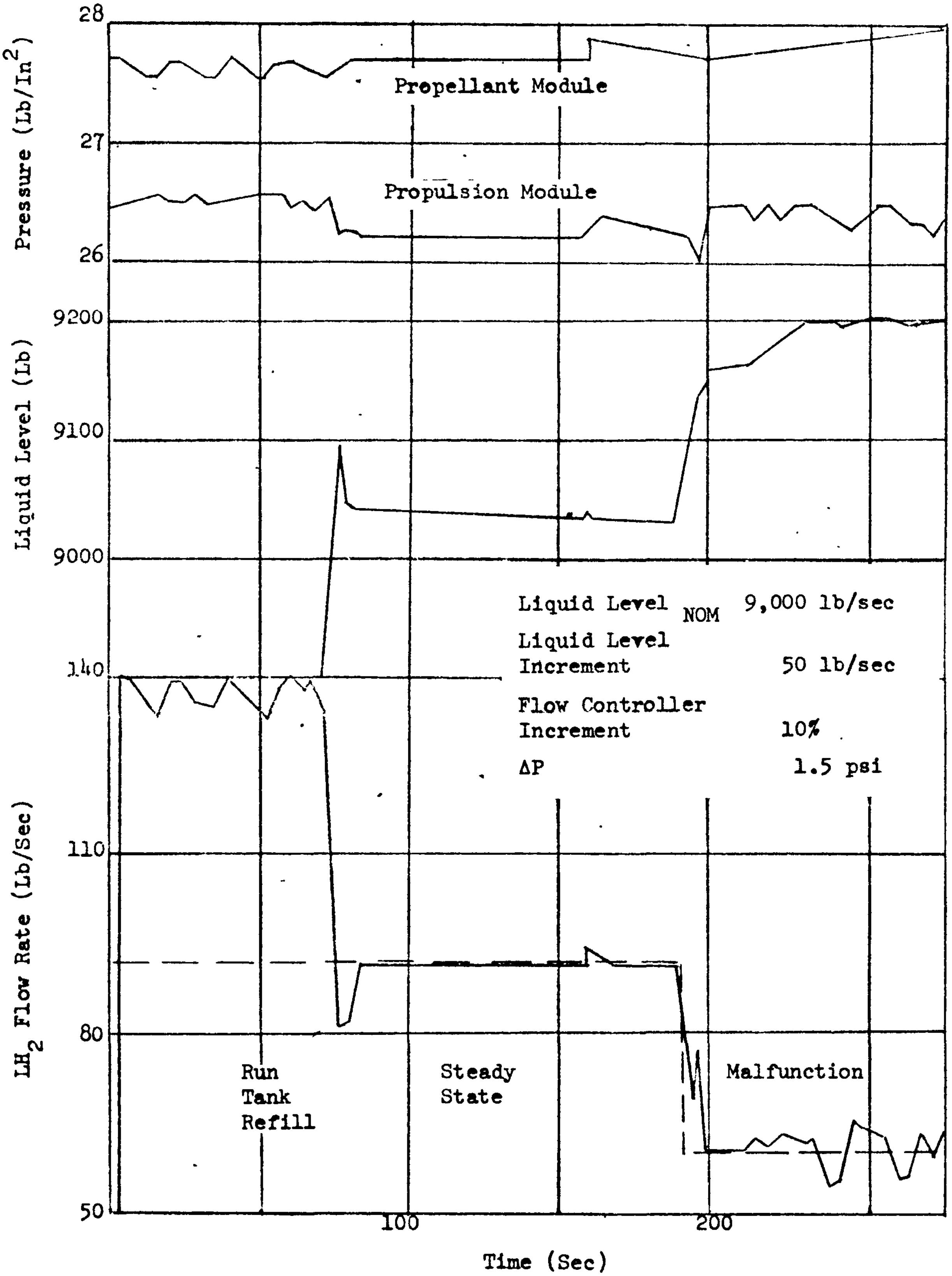

Figure 3.12-3 RUN TANK PROPELLANT MANAGEMENT CONTROL SIMULATION

included the sensitivity of the peak attitude error to engine position limits, the sensitivity to engine gimbaling rate, and the transient response. A control system similar to that currently used on the S-IVB was used for this study. Table 3.12-1 summarizes the engine gimbal requirements which were recommended during Phase II on the basis of the cited analysis.

Since it has been found that engine deflection requirements are very sensitive to the initial thrust vector misalignment, every effort should be made by the engine manufacturer to minimize it. This could result in smaller, lighter actuators, simpler engine feed lines, and smaller power requirements for engine gimbaling. Results of simulations have shown that the attitude excursions following startup can be highly reduced by pretrimming the NERVA before startup. With the first use being TLI, requiring on the order of half an hour of operation, the effect of the relatively short attitude transient (of approximately 350 seconds) on the velocity errors at cutoff will be minimal. However, for the subsequent NERVA operations, many of very short duration, the vehicle attitude transient could be reduced by pretrimming the NERVA.

3.12.4 Roll Control

The roll attitude disturbances occurring during a burn are of two types: (1) temporary roll torques resulting from the startup transient, and (2) steady-state torques resulting from NERVA operation. The first of these results from cross coupling between the pitch/yaw powered flight attitude control system transient and the roll control system through center-of-gravity offsets. The second is caused by engine exhaust gas swirl and pump gyro torques. The first is independent or burn time; the second is burn time dependent. In this study the powered flight roll control impulse allocation (Section 4.6.2) was based on 500 lb-sec for each startup + 1 lb-sec for each second of NERVA operation. The swirl torque requirement was generated by scaling propellant swirl torques experienced on S-IVB flights. Based on the above formula the total roll disturbance occurring during the burns is 11,300 lb-sec for the RNS mission.

Table 3.12-1

RECOMMENDED ENGINE GIMBAL REQUIREMENTS

Maximum engine deflection	±3 deg
Maximum engine rate	0.25 deg/sec
Maximum engine acceleration	0.5 deg/sec^2

3.13 SHUTDOWN AND AFTERCOOLING

3.13.1 Operations Phasing

The relationship of the shutdown operations for NERVA and the propellant and propulsion module propellant management systems is shown in Figure 3.13-1. The thrust level is reduced from full power to the throttle point maintaining all systems in operation. At that point, typically, the propellant module is isolated, terminating the requirement for pressurization and feed system operation for the propellant module. During the temperature retreat phase of NERVA, propellant feed is maintained through the normal NERVA feed system. Run tank pressurization can be terminated at the throttle point or continued through the temperature retreat if desired. After pump tailoff, the separate aftercooling bypass system is actuated to provide aftercooling pulses.

3.13.2 Aftercooling Concept Evaluation

Because of the long times and large number of pulses involved in providing cooldown during a mission, the requirement to provide propellant to NERVA at specified conditions during aftercooling can impose severe penalties on the RNS design. Although propellant conditions are unspecified for the current NERVA configuration, the previous hot-bleed NERVA engine required that the RNS must be capable of providing liquid hydrogen pressurized to 30 psia at its outlet with zero percent vapor during cooldown. If such a requirement is maintained, the functional requirements imposed on the RNS include settling of LH_2 and pressurization to satisfy propellant conditions. The impact of these requirements is reduced for the MDAC baseline configurations, since only the propulsion module is utilized for aftercooling. In order to evaluate the aftercooling implications for the RNS, the current cooldown data were

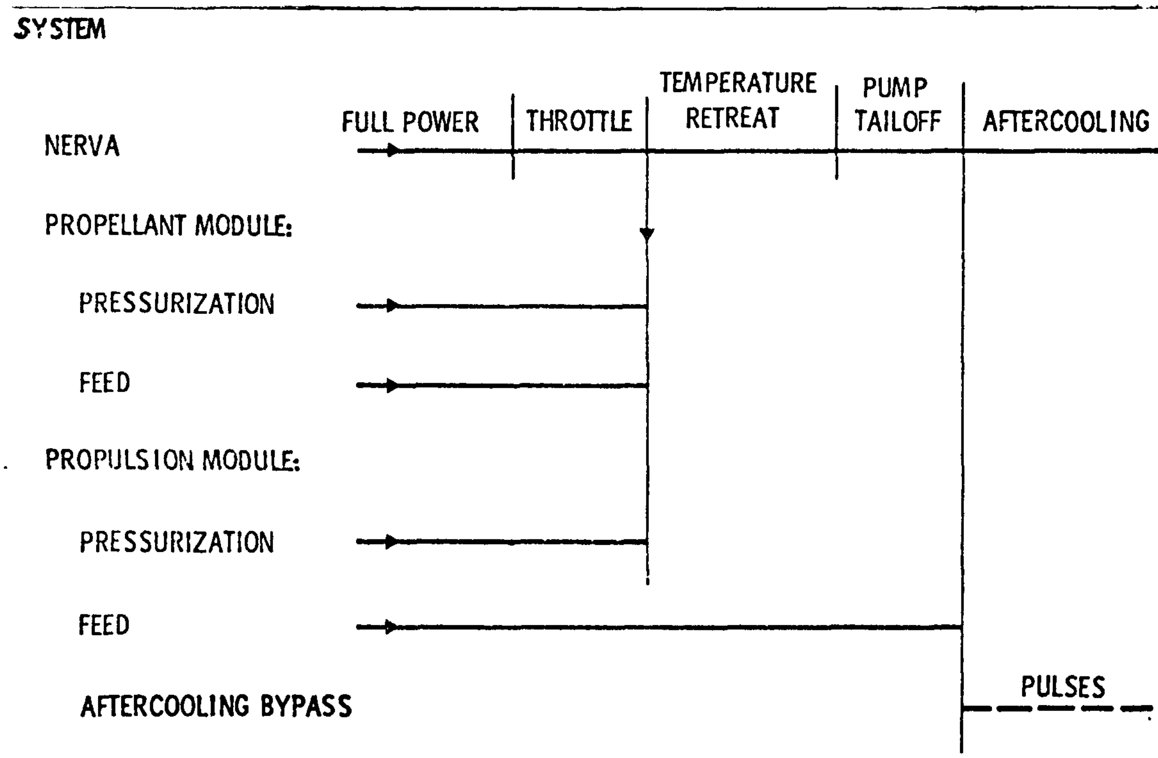

Figure 3.13-1 SHUTDOWN OPERATIONS PHASING SCHEMATIC

applied for the four-burn reference lunar shuttle mission together with the previous 100 percent liquid requirement at 30 psia, and several aftercooling system concepts were defined and evaluated which would satisfy the necessary operational requirements. Also, the sensitivity to NERVA requirements was evaluated, considering both the radiated power level and the aftercooling operating pressure, to provide greater visibility for selection of aftercooling system concepts and to identify desirable improvements in the NERVA requirements.

Table 3.13-1 summarizes the relevant NERVA aftercooling parameters for the four-burn reference mission, including aftercoolant for each burn, total aftercooling time, continuous flow duration, and the number of aftercooling pulses. The total aftercoolant propellant exceeds 5 percent of the steady-state propellant. Changes in the mission profile, including additional lunar orbit burns, would not change the conclusions of the trade study. During the initial portion of cooldown, a continuous trickle flow at 0.4 lb/sec is maintained between pulses. The resulting 186-lb thrust level is sufficient for settling, but it makes a negligible contribution to the overall settling require-

Table 3.13-1

NERVA AFTERCOOLING PARAMETERS

Full Flow Engine (April 1970), S-130

Reference Lunar Shuttle Mission

Mission Phase	Steady-State Propellant (lb)	Burn Time (sec)	Aftercooling Propellant (lb)	Total Aftercooling Time (sec)	Total Aftercooling Time (hr)	Continuous Flow Duration (sec)	Number of Pulses
Leave earth	178,100	1,940	8,000	480,000	139	1,825	182
Arrive moon	45,510	496	2,900	168,000	46.7	1,180	67
Leave moon	16,490	180	1,400	87,000	24.2	880	34
Arrive earth	41,460	450	2,700	157,000	43.6	1,130	63
Total	281,560	3,066	15,000	892,000	253.5	5,015	346

ment since it is active for only 0.4 percent of the total cooldown time. Thus, additional functional requirements are imposed on the RNS to settle propellant. After a period of time, the duration of the aftercooling pulse decays to approximately 40 seconds per pulse. The flowrate is 0.7 lb/sec during each pulse, so that the terminal pulses consume 28 lb of LH_2 per pulse. The time between pulses increases rapidly, reaching several hours for the terminal pulses. The requirement for active aftercooling down to a power level of 5 kw results in very long aftercooling durations, particularly for the leave earth burn. The large number of pulses complicates operation of the RNS systems to provide propellant conditions for each pulse. On the other hand, the long cooldown duration and the long time between pulses complicates maintaining propellant conditions continuously throughout the mission.

The evaluated aftercooling system concepts are defined in Table 3.13-2 which identifies principal features of the concepts. Three classes of concepts are distinguished by the technique used for propellant control: settling by acceleration, surface tension, and dielectrophoresis. The design criteria, characteristics, and operations of these systems concepts will be described briefly to indicate the basis for the system weight penalties assessed.

For the continuous settling concept, the acceleration level would be provided continuously for the duration of cooldown, and makeup pressurant would be added to the run tank as required to counteract the effects of ullage gas cooldown and condensation. For the pulsed settling concept, a settling impulse would be applied before each cooldown pulse cycle and a prepressurization of the run tank would be accomplished. A conservative settling criterion of a Bond number of 100 is applied, which results in an acceleration level requirement of 6.73×10^{-5} g's for the run tank. A factor of safety of 2 times the time to relocate the propellant from the top to the bottom of the run tank was applied, resulting in a settling time of 280 sec for the reference acceleration level in the run tank. The hybrid settling system is an optimum combination of continuous and pulsed settling. Continuous settling is maintained until the time between pulses exceeds the settling time. Then settling is applied prior to each pulse. Settling propellant consumption was assessed on the basis of a 300-sec specific impulse. The rotational concept could satisfy the acceleration requirements with an end-over-end tumbling of the stage at a very low rotational rate, about one revolution every 1,000 sec. Such a slow rotation, of the order of attitude limit cycling, is considered tolerable.

Table 3.13-2

AFTERCOOLING SYSTEM CONCEPT DEFINITION

	Concept	Principal Features
1	Propellant settling	Run tank LH_2 settled—Bond No. = 100
	A Continuous	Use APS for duration of aftercooling
	B Pulsed	Use APS prior to each pulse
	C Hybrid	Initially continuous, switch to pulsed
	C Rotation	Continuous end-over-end tumbling
2	Surface tension	Collect pulse liquid with screens
	A Burp tank	Discrete, pressurized tank, refill after pulse using APS
	B Pulse basket	Collect LH_2 to settle, then pressurize
3	Dielectrophoresis	Collect liquid with electrodes
	A Ullage control	Orient liquid to maintain ullage pressure
	B Pulse basket	Collect LH_2 to settle, then pressurize

The surface tension burp tank concept depicted in Figure 3.13-2 employs a small, discrete tank in the bottom of the run tank which contains LH_2, surface tension screens to collect LH_2, and its own pressurization system. The burp tank is isolated from the run tank at the beginning of a pulse and it is pressurized separately with cold (LH_2 temperature) helium to 30 psia. A settling impulse is applied by the APS upon completion of the aftercooling pulse, and the burp tank is then vented and refilled. The only pressurization requirement is for burp tank expulsion, and the run tank is not pressurized.

The surface tension pulse basket concept, also depicted in Figure 3.13-2, employs a set of screens to collect sufficient LH_2 for an aftercooling pulse. The concept would not fully satisfy NERVA pressure requirements, in the sense that it could only be used to guarantee 100 percent liquid but not the pressure level, so an effective bootstrap pressurization approach would be required.

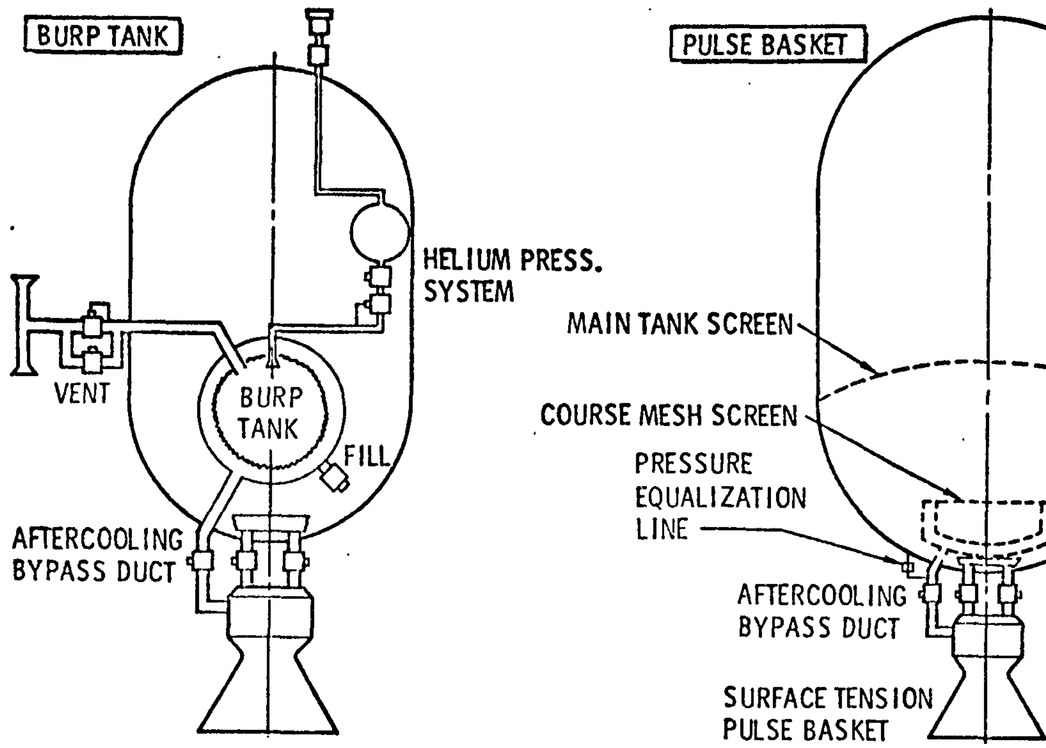

Figure 3.13-2 SURFACE TENSION CONCEPTS

Another alternative for control of the liquid and ullage locations in the run tank is to employ a dielectrophoretic (DEP) propellant collection. Two concepts were considered. For the first, an electrode configuration was conceived to locate an ullage bubble near the top of the tank so that only makeup pressurant would be required to maintain the required propellant conditions. A pulse basket concept was also considered, which would function in a manner similar to that of the surface tension pulse basket concept, but substituting an electrode grid for surface tension screens.

A weight breakdown for the different aftercooling system concepts is shown in Table 3.13-3. The hardware breakdown is differentiated between the pressurization system weight penalty and fixed weight penalties such as screens, electrodes, etc. The continuous settling mode is excessively heavy because of the long aftercooling duration, although the settling penalty would be reduced if a lower Bond number were utilized. Rotation or DEP with ullage control and the burp tank concepts are the most favorable. The system weight penalties for the other concepts are similar and excessive.

Table 3. 13-3

WEIGHT BREAKDOWN FOR AFTERCOOLING SYSTEM CONCEPTS

LUNAR SHUTTLE MISSION

NERVA PASSIVE COOLING BELOW 5 KW

Aftercooling Concept \ Weight (lb)	Settling Propellant	Makeup Pressurant	Prepressurization	Hardware (Incl He Pressurants and Combustants)	Total
1. Propellant settling					
A Continuous (B_o = 100)	35,610	790		2,370*	39,770
(B_o = 10)	3,560	790		2,370*	6,720
B Pulsed	5,143		1,945	5,835*	12,923
C Hybrid	4,752	32	1,560	4,774*	11,118
D Rotation	128	790		2,370*	3,288
2. Surface tension					
A Burp tank	475			3,015	3,490
B Pulse basket			1,945	74 5,835*	7,854
3. Dielectrophoresis					
A Ullage control		790		350 2,370*	3,510
B Pulse basked			1,945	350 5,835*	8,130

*Pressurization system weight penalty

The pressurization penalties assessed need further clarification. For continuously settled or controlled LH_2 a makeup pressurization system is required to counteract the combined effects of ullage gas cooldown and condensation. The pressure decay rate for this case was estimated utilizing NASA data (Reference 3-6) as about 3.4 psia per hour. Pressurant was then added to the run tank to counteract the pressure loss and maintain a constant tank pressure. Alternatively, in systems where the propellant orientation is not controlled between pulses, it is assumed that the ullage collapses to the liquid temperature. A prepressurization is then required to provide the proper pressure. This was based on a 5 percent initial ullage in the run tank, initial pressures of 16, 18, 24, and 30 psia for the four mission legs corresponding to the pressure profile for the Phase II insulation system, and a final pressure of 30 psia. Prepressurization and makeup pressurant system weight penalties were assessed for this comparison employing an H_2/O_2 combustor system, which has previously been found to be lighter than most conventional systems (stored gas, heated helium, etc.).

The influence of NERVA radiated power level on the aftercooling system weight penalty is shown in Figure 3.13-3. At high power levels, the continuous settling concept becomes more favorable than those concepts requiring prepressurization for each pulse. The DEP concept with ullage control and the rotation concept, both of which employ only makeup pressurization, remain the most favorable. The burp tank shows less advantage at higher power levels because the reduction in pulses is less than the reduction of time. The total aftercooling penalty includes the propellant wastefully expended during pulsed aftercooling operations, as well as the system requirements of the RNS to provide NERVA propellant conditions. Performance implications are reviewed in the next section.

Figure 3.13-4 shows the sensitivity of the aftercooling system weight to the tank pressure required during aftercooling pulses. While reduction in the tank pressure requirement does show a benefit, major operational penalties are incurred as long as it is necessary to pressurize above the liquid saturation pressure in the run tank. Thus, the major advantage of reduced pressure would be obtained only if NERVA could operate with saturated liquid at arbitrary pressures. Because the aftercoolant pulse flow bypasses the turbopumps and only flows through piping, this should be attainable in the engine

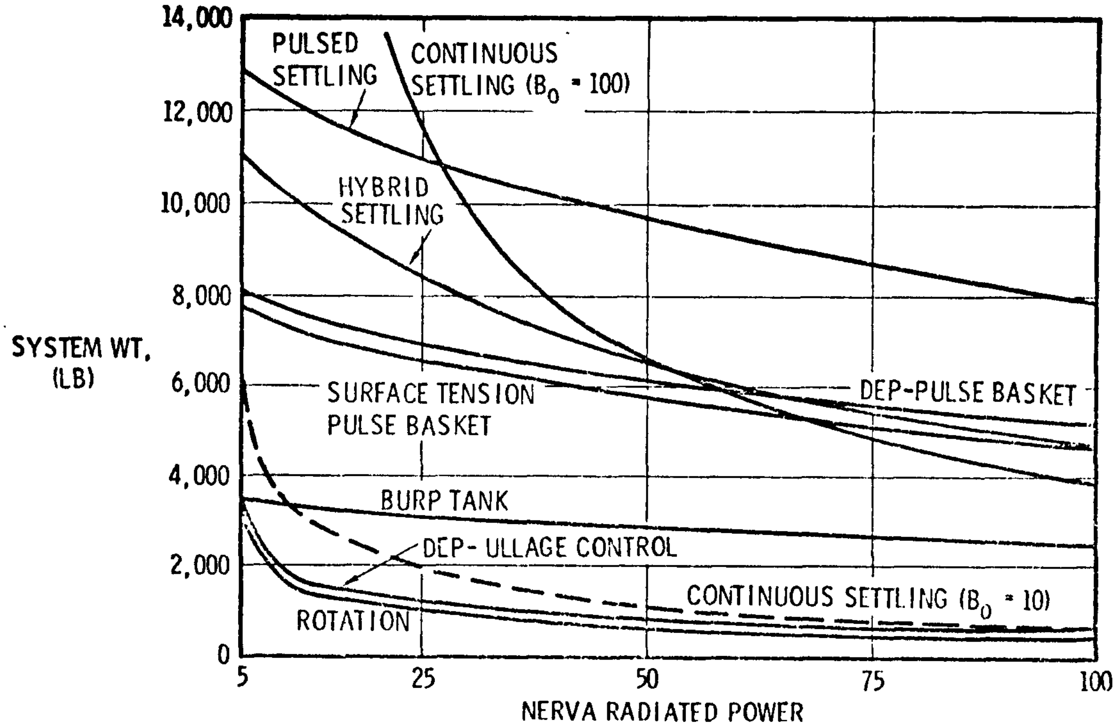

Figure 3.13-3 AFTERCOOLING SYSTEM WEIGHTS

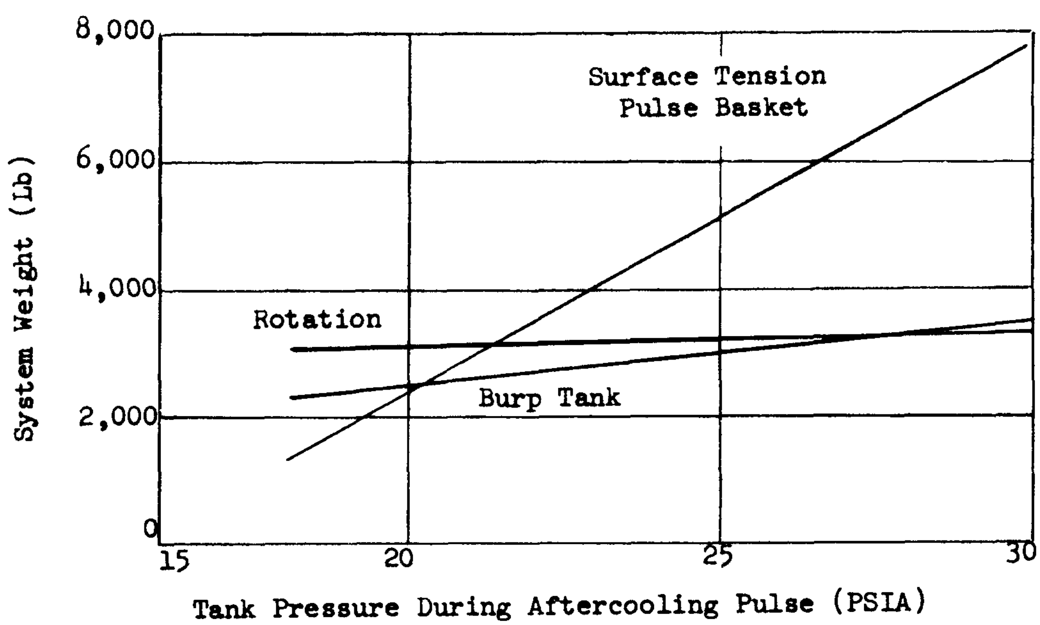

Figure 3.13-4 AFTERCOOLING SYSTEM WEIGHTS

design regardless of the power level at which aftercooling is terminated, although it might be necessary to accept reduced flow rates.

Therefore, the surface tension pulse basket concept was adopted for providing aftercooling propellant. It is the least complicated system, having no moving parts or expendables to replenish. Furthermore, based on the above considerations, the ground rule of only supplying saturated liquid conditions during aftercooling was adopted for the MDAC design.

Additional stage performance gains could be achieved if NERVA specifications were modified to permit use of a mixed phase or gas aftercooling. This would permit the utilization of residual gas, thereby reducing the stage inert weight. The savings for the Class 1 Hybrid, obtained for EOI cooldown, amounts to 2,800 lb of gaseous residual. Additional savings could be obtained for multiple-tank RNS concepts by venting depleted tanks during the mission.

3.13.3 Aftercooling Utilization

3.13.3.1 Performance Gains

NERVA aftercooling propellant is consumed at an average Isp of 430 sec (compared to 825 sec, steady state) and at nonoptimum points on the trajectory. The potential for improving mission performance (payload weight delivered to lunar orbit) by reducing the NERVA cooldown propellant requirement has been evaluated and is summarized in Table 3.13-4. The first column identifies the potential for improvement in payload delivery when the impulse derived from cooldown is credited to the required mission velocities. Conversely, given total utilization of cooldown impulse, this is the penalty that would result if the impulse were nulled out without a reduction in the propellants expended. Changes in RNS inert weight would incur additional penalties. If, instead, the requirement for cooldown propellant were somehow eliminated, the potential payload improvement shown in the right-hand column of Table 3.13-4 could be obtained. This will be offset by corresponding increases in RNS inert weight to be discussed.

Figure 3.13-5 presents the potential lunar payload gain as a function the inert weight penalty required to radiate a desired power level from NERVA. A capability to radiate 7,300 kw would eliminate the cooldown requirement after

Table 3.13-4

LUNAR PAYLOAD IMPLICATIONS OF NERVA AFTERCOOLING

Mission Maneuver	Gain by Crediting Cooldown Contribution to Mission Velocity (lb)*	Potential Gain by Cooldown Elimination (lb)*
TLI	3,380	10,452
LOI	884	3,296
TEI	900	2,502
EOI	3,240	7,288
Total	8,404	23,538

*The performance impact is shown on the RNS payload delivery capability to lunar orbit.

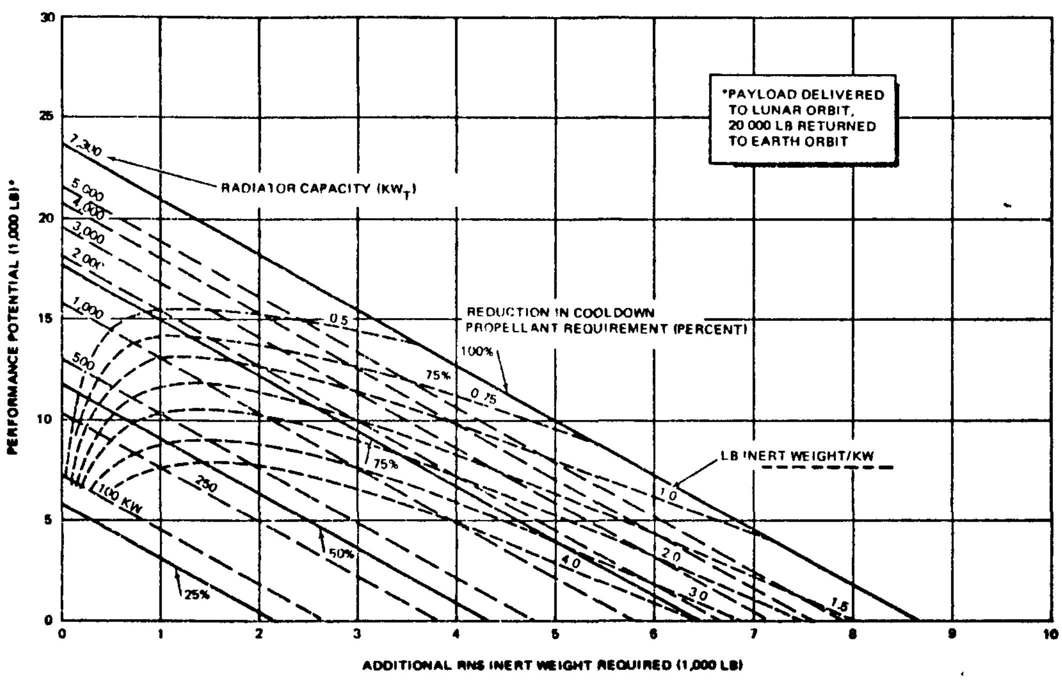

Figure 3.13-5 POTENTIAL FOR PERFORMANCE IMPROVEMENT DUE TO REDUCTION IN COOLDOWN

PSOV closure (following the TLI burn). Since the power level diminishes rapidly immediately following shutoff, substantial portions of the decay energy can still be radiated away at capacities greatly below this initial shutoff level. For example, a 500-kw capacity would radiate nearly 60 percent of the decay energy. The power level is combined with inert weight to show contours of constant radiator system specific weight in the figure.

A brief survey of the literature has indicated heat pipe radiator system concepts could be developed possessing specific weights on the order of 1 lb/kw of radiated power. Substantial performance gains at this cost are indicated in Table 3.15-5. together with minimal required radiator surface areas. It is noted that the cylindrical areas of the PVARA and run tank envelopes are approximately 220 and 900 ft^2, respectively. A radiator system capable of 250 to 500 kw would achieve most of the potential gain. Thus, the design integration external to the engine should not be formidable. However, the desirability of this means of performance improvement depends on integration of heat pipes with the critical portions of the NERVA core without inordinately upsetting the present design.

Table 3.13-5

COOLDOWN RADIATOR IMPLICATIONS

Power Level (kw)	Required Surface Area (ft^2)		Potential Payload Gain (lb) at 1 lb/kw
	1,000 °R	1,500 °R	
100	230	44	7,000
250	570	110	9,500
500	1,140	220	11,500
1,000	2,280	440	13,000

3.13.3.2 Trajectory Implications

NERVA aftercooling results in a prolonged injection phase relative to chemical propulsion. This impacts mission safety. Figure 3.13-6 shows the locus of instantaneous perigee altitude as a function of time from ignition in earth orbit. Should premature loss of thrust occur between about 0.8 and 3.3 hour from TLI ignition, lunar gravitation would perturb the resultant transfer trajectory so that earth impact would ultimately occur on the return leg.

Figure 3.13-7 illustrates the orbital spiral characteristic of the EOI maneuver for a NERVA steady-state run time of 600 seconds. The cooldown pulses are identified in the figure at their midpoints. The operational approach is to establish injection orbit parameters which result in the desired final circular orbit conditions (260 nmi at the earth and 60 mni at the moon) at the end of cooldown. These are shown in Table 3.13-6. Dispersions in cooldown performance during the EOI and LOI maneuvers will introduce dispersions in the terminal orbit at completion of cooldown if no countermeasures are taken.

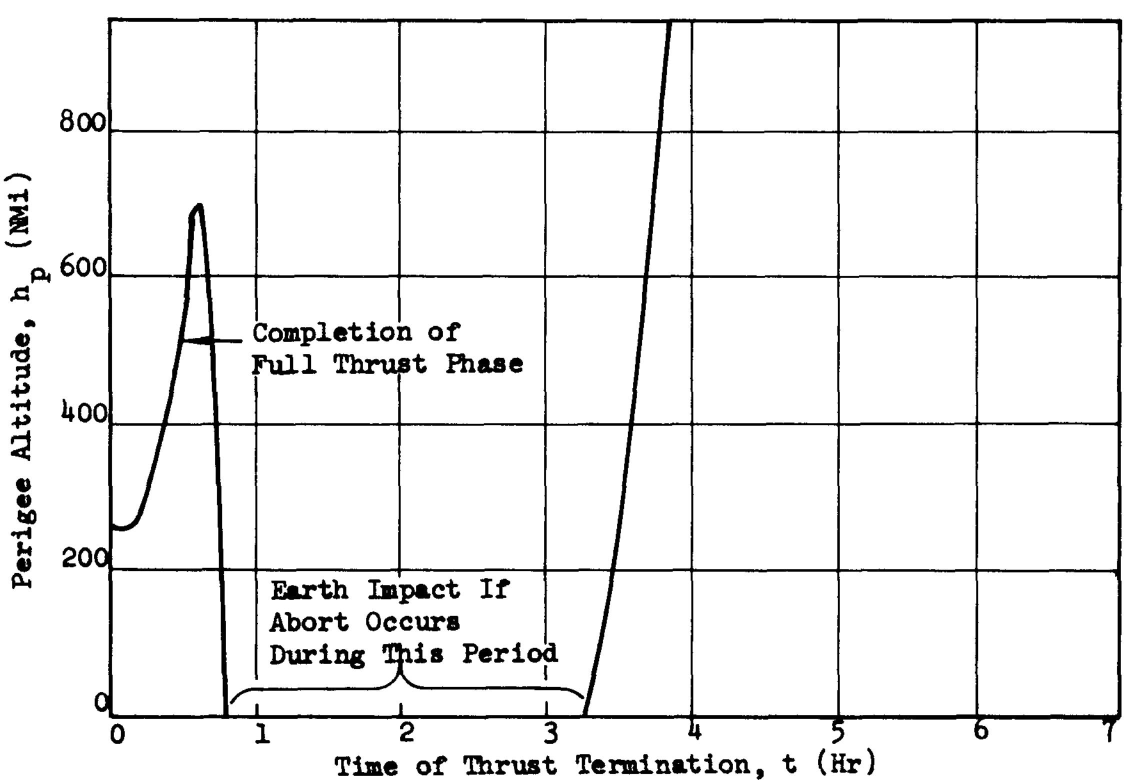

Figure 3.13-6 ABORT PERIGEE ALTITUDE (108-Hr Lunar Transfer)

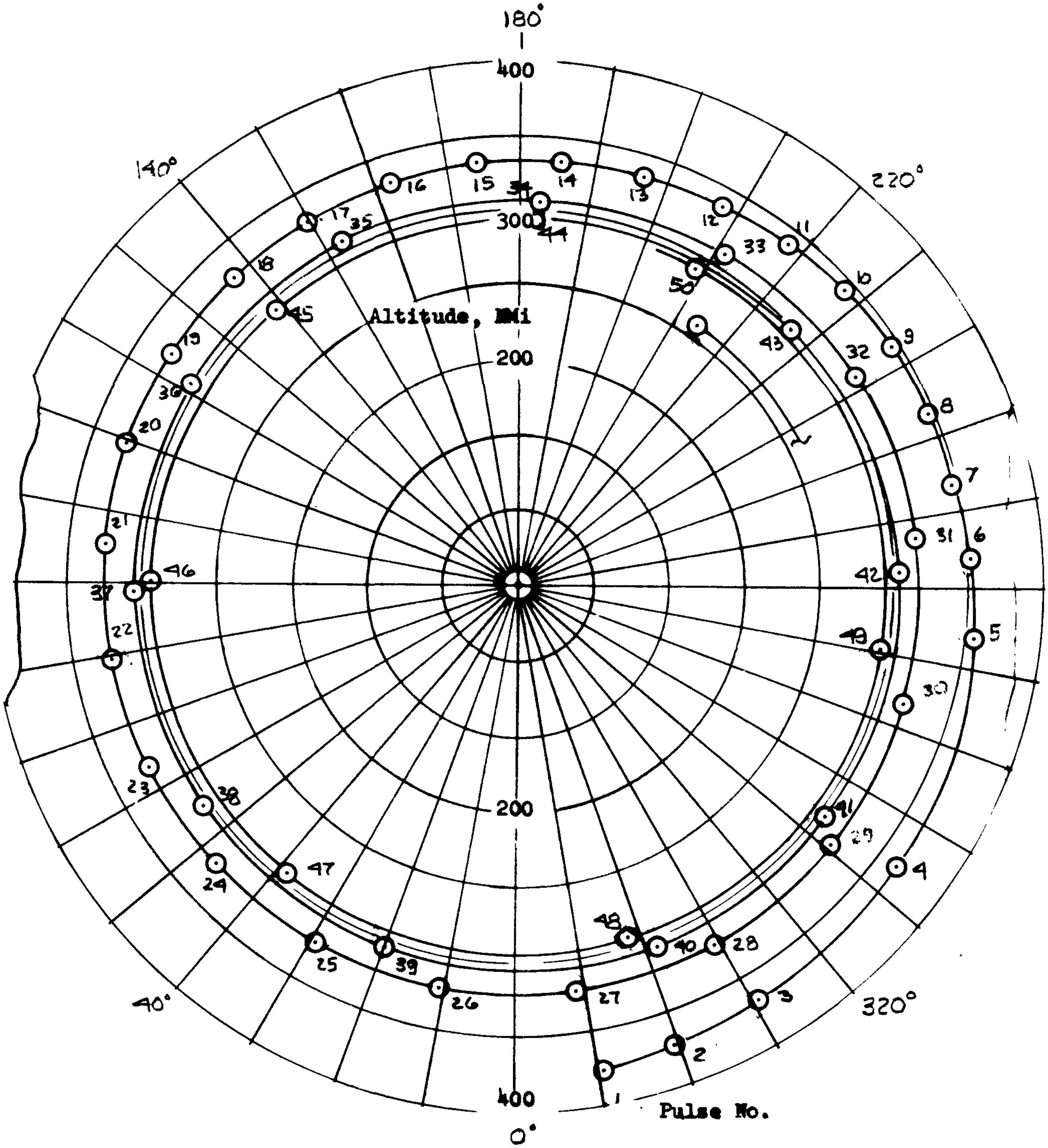

Figure 3.13-7 ORBIT GEOMETRY DURING COOLDOWN EARTH ORBIT INSERTION

Table 3.13-6

REQUIRED INJECTION ORBIT PARAMETERS

Maneuver	EOI	LOI (8-burn)	LOI (4-burn)
Steady-state time (sec)	465	160	287
Cooldown duration (hr)	45	21	33
Apoapsis altitude (nmi)	408	99	115
Periapsis altitude (nmi)	348	75	83

Specifically, the sensitivities of average terminal orbit altitude to total cooldown impulses are -1.38 nmi/percent for EOI, and -0.3 nmi/percent (8-burn), and -0.4 nmi/percent (4-burn) for LOI. Variations in impulse could be caused by either an extended pulse duration, variation in pulse thrust or weight flow. In the case of the total cooldown impulse being less than nominal, the resultant orbit at the end of the cooldown phase would be eccentric and above the target circle. Similarly, if the cooldown impulse is excessive or greater than nominal, an overshoot condition would result. The guidance function will provide up-to-date status of the cooldown phase as it progresses, so corrective action, such as attitude maneuvers can be taken prior to the termination of cooldown. The expected value of cooldown impulse will be skewed such that it will be more likely to require added impulse at the end of cooldown than to offset previous impulse with the APS.

3.13.4 Navigation and Guidance

Guidance cutoff for the main burn is predicated on assumptions about the magnitude and direction of the aftercooling impulse. If the aftercooling impulse were correctly modeled, the aftercooling impulse could be used to reduce the midcourse correction requirement to zero. Section 3.14.1 compares the approach of an impulsive midcourse correction at an optimum time (NERVA cutoff) for the TLI burn to the use of attitude control during aftercooling. The two approaches produce comparable results in terms of propellant penalties. Since the use of an impulsive correction is impractical at the end of burn due to the continuing impulse during aftercooling, the strategy of attitude control using the APS during aftercooling is recommended.

The uncertainty of ±20,000 lb-sec aftercooling impulse represents 0.6 percent of the TLI burn impulse. The sensitivity data to aftercooling and other error sources in Section 3.14.1 indicate this would correspond to a 14-nmi error at closest lunar approach if unaccounted for. Continuous correction of the stored aftercooling model using a heuristic algorithm, as suggested in Phase II (Section 2.3.4.2, Reference 3-1), could reduce this to almost zero.

Based on this analysis the use of the APS for attitude control during after-cooling and the updating of the aftercooling model will allow for the efficient utilization of the aftercooling impulse. This strategy has the potential of reducing the impulsive midcourse correction requirement to zero and providing relief to the present NERVA aftercooling impulse uncertainty requirement of ±20,000 lb-sec.

3.13.5 Attitude Control

The vehicle attitude disturbances resulting from thrust vector misalignment during pulsed aftercooling can be a very significant contribution to total coast attitude control propellant consumption. Three alternatives for thrust vectoring during cooldown are possible:

A. Not controlling the engine angular position

B. Positioning and maintaining the engine mechanically "centered"

C. Trimming the effective thrust vector through the vehicle center of gravity

The first alternative results in excessive attitude control propellant usage. The second is an improvement, but could still result in an excessive requirement. In the third alternative an active control system would be used to periodically retrim the thrust vector. In this adopted approach the disturbance resulting from aftercooling would be minimal. The weight saving in coast attitude control propellant and tankage will offset the added complexity of providing for active thrust vector control during coast.

However, even if the thrust vector is periodically retrimmed, there will be some small misalignment between the thrust vector and the line connecting the engine gimbal point with the vehicle center of mass, resulting in moments on the vehicle which must be cancelled by the APS. The cooldown impulse at an assumed specific impulse of 432 seconds, is shown for each burn in

Table 3.13-7. For this study a 0.1-degree thrust misalignment was assumed. The resulting control impulses for this misalignment are also listed in the table. These contribute about 8.5 percent to the total APS impulse requirement presented in Section 4.6.2.

Table 3.13-7
CLASS 1 IMPULSE REQUIREMENTS FOR
ATTITUDE CONTROL DURING COOLDOWN

Burn	Cooldown Impulse (lb-sec)	Misalignment Impulse (0.1 deg) (lb-sec)	Worst-Case Control Impulse (lb-sec)
TLI	3,140,000	5,500	25,700
LOI-1	332,000	580	2,700
LOI-2	123,000	220	1,080
LOI-3	582,000	1,020	5,990
TEI-1	366,000	640	590
TEI-2	86,000	150	160
TEI-3	258,000	450	430
EOI	1,205,000	2,100	2,150
Total	6,112,000	10,660	38,800

3.14 TRAJECTORY CORRECTIONS

3.14.1 Midcourse Corrections

The RNS presents an inherently complex trajectory correction problem due to the extended tailoff and long-duration cooldown phases. Normally, midcourse trajectory correction requirements would be determined from onboard or ground tracking data after the TLI burn is completed. Since the last cooldown pulse before LOI occurs 102 hours into the 108-hour translunar trajectory, the propellant expenditure for a midcourse maneuver at cessation of the cooldown pulses could be large compared to making corrections early in the trajectory. Flight path angle errors present at the beginning of tailoff will be amplified during the tailoff and cooldown phases if the thrust vector is nominally aligned along the velocity vector. However, if a midcourse correction is performed at the end of full-thrust NERVA operation, errors will still be induced during the tailoff and cooldown phases. The lunar arrival (LOI) and lunar plane change maneuvers and the TEI burn present similar, but far less severe, problems because their burn times and concomitant cooldown phases are much shorter.

Trajectory errors are identified by the differences between the state variables of the actual RNS trajectory and those of a nominal, or design, trajectory (ΔX, ΔY, ΔZ, $\Delta \dot{X}$, $\Delta \dot{Y}$, $\Delta \dot{Z}$). Consideration of errors incurred from such factors as differences in propellant weight loadings, atmospheric density fluctuations, guidance system errors and thrust level deviations are beyond the scope of the present study. However, the sensitivity of the end conditions to errors in the trajectory at the end of full thrust operation was investigated and is shown in Table 3.14-1. Initial errors of ±1 unit (fps or nmi) in each state vector at the end of full thrust were considered. The partial derivatives presented are based on the assumption that no corrective action was taken and no additional errors were introduced during either the tailoff or the cooldown phases. The region of applicability of these sensitivities is limited since the variation of the parameters is nonlinear. This indicates a requirement for either significant onboard computer capability or a ground command link so that the projected terminal errors and corrective maneuver(s) can accurately be determined.

Two approaches to midcourse trajectory corrections were considered for the RNS: (1) applying an impulsive correction or a series of impulsive corrections to minimize the end condition errors, and (2) utilizing vectored after-cooling thrust. Implementation of this second approach could range in sophistication from a continuously varying attitude control scheme that optimally minimizes errors, to a simple mode such as constant attitude throughout the cooldown phase. Both approaches were compared for a set of initial errors (not cooldown-induced errors) of a pluse one unit magnitude. For the cooldown approach, the control variables evaluated were the angle between the velocity vector and the projection of vehicle centerline on to the instantaneous orbit plane, ζ, the angle between the vehicle centerline and the orbit plane, δ, and the magnitude of the cooldown thrust vector impulse, I.

Table 3.14-1

DERIVATIVES OF LUNAR ARRIVAL PARAMETERS

TO STATE VECTOR AT FULL-THRUST TERMINATION

	Lunar Arrival Parameters					
	Perilune Altitude (nmi)	Lunar Inclination (deg)	Trip Time (hr)	Perilune Velocity (fps)	Latitude at Closest Approach (deg)	Longitude at Closest Approach (deg)
State vector components (1)						
X, (nmi)	$\partial h_p/\partial X = -176$ (2)	$\partial i/\partial X = 20.3$	$\partial T_t/\partial X = -0.267$	$\partial V_p/\partial X = 529$ (2)	$\partial \rho_p/\partial X = -2.74$ (2)	$\partial \mu_p/\partial X = 17.6$
Y, (nmi)	$\partial h_p/\partial Y = -77.4$	$\partial i/\partial Y = 4.85$	$\partial T_t/\partial Y = -0.081$	$\partial V_p/\partial Y = +260$	$\partial \rho_p/\partial Y = 1.0$	$\partial \mu_p/\partial Y = 4.25$
Z, (nmi)	$\partial h_p/\partial Z = 15.6$	$\partial i/\partial Z = -1.81$	$\partial T_t/\partial Z = 0.026$	$\partial V_p/\partial Z = -56.1$	$\partial \rho_p/\partial Z = 0.240$	$\partial \mu_p/\partial Z = -1.52$
$\dot{X}$, (fps)	$\partial h_p/\partial \dot{X} = 5.07$	$\partial i/\partial \dot{X} = -1.32$	$\partial T_t/\partial \dot{X} = 0.0087$	$\partial V_p/\partial \dot{X} = -18.3$	$\partial \rho_p/\partial \dot{X} = 0.077$	$\partial \mu_p/\partial \dot{X} = -1.10$
$\dot{Y}$ (fps)	$\partial h_p/\partial \dot{Y} = -57.0$ (2)	$\partial i/\partial \dot{Y} = 6.99$	$\partial T_t/\partial \dot{Y} = -0.093$	$\partial V_p/\partial \dot{Y} = 202$ (2)	$\partial \rho_p/\partial \dot{Y} = -0.87$	$\partial \mu_p/\partial \dot{Y} = 5.87$
$\dot{Z}$, (fps)	$\partial h_p/\partial \dot{Z} = 109$ (2)	$\partial i/\partial \dot{Z} = -6.40$	$T_t/\partial \dot{Z} = 0.086$	$\partial V_p/\partial \dot{Z} = 210$ (2)	$\partial \rho_p/\partial \dot{Z} = 0.918$	$\partial \mu_p/\partial \dot{Z} = -5.39$
Cooldown Disposal (3)						
Impulse, ΔI (percent)	$\partial h_p/\partial \Delta I = -21$	$\partial i/\partial \Delta I = 8$	$\partial T_t/\partial \Delta I = 0.10$	$\partial V_p/\partial \Delta I = 85$	$\partial \rho_p/\partial \Delta I = 9$	$\partial \mu_p/\partial \Delta I = 9$
In-plane misalignment, (deg)	$\partial h_p/\partial \zeta = -72$	$\partial i/\partial \zeta = 0.026$	$\partial T_t/\partial \zeta = 0.079$	$\partial V_p/\partial \zeta = 260$	$\partial \rho_p/\partial \zeta = -1.13$	$\partial \mu_p/\partial \zeta = 0.08$
Out-of-plane misalignment, (deg)	$\partial h_p/\partial \delta = 49$	$\partial i/\partial \delta = -0.3$	$\partial T_t/\partial \delta = -0.035$	$\partial V_p/\partial \delta = -170$	$\partial \rho_p/\partial \delta = 0.79$	$\partial \mu_p/\partial \delta = -0.23$

(1) Nonrotating ecliptic coordinate system
(2) Extremely nonlinear behavior
(3) Applied to 9th through 168th cooldown pulses only

Values of these control variables were selected to minimize the dispersion at lunar arrival and held constant for the 9th through 168th cooldown pulse. The sensitivities of the lunar parameters to these control variables are also shown in Table 3.14-1. These sensitivities are based on an error of ±1 unit (fps or nmi) in each cooldown parameter.

The propellant and residual arrival error required for each of these approaches is presented in Table 3.14-2.

Table 3.14-2
MIDCOURSE CORRECTION COMPARISON

Approach	Midcourse Propellant (lb)	Residual Error		
		Δr_p (nmi)	$\Delta \mu$ (deg)	Δi (deg)
1. Reference condition (no correction)	0	-68	+9.2	+8.2
2. Impulsive midcourse correction	85	-8	-1.6	-2.0
correct at end of full-thrust operation	85	-8	-1.6	-2.0
correct at end of cooldown	1,450	-10	-0.1	+1.1
3. Trajectory correction utilizing vectored cooldown thrust	153	+2.8	0	-0.1

It is concluded that multiple impulsive midcourse maneuvers or a single impulsive correction early in the trajectory are preferable to a single impulsive maneuver at the end of the cooldown phase. Manipulating the vehicle attitude during the cooldown thrusting appears viable. If impulsive midcourse maneuvers are adopted for the translunar trajectory leg, at least one correction should be applied early in the trajectory to counter the amplifying effect of tailoff and cooldown impulse. Impulsive trajectory correction maneuvers will be used in all mission phases other than the translunar leg due to the short-duration burns and their substantially reduced cooldown phases. The trajectory complexities introduced by the cooldown and tailoff phases negate attempts to linearize final error predictions and introduce the requirement for significant onboard computer capability or for a ground command link to initiate midcourse maneuvers. Currently, 50 fps is allocated for midcourse corrections on the translunar and transearth trajectories to determine RNS performance and propellant utilization. These preliminary results do not change this allocation. An error analysis is needed to determine expected trajectory dispersions, particularly during the tailoff and cooldown phases, before firm midcourse requirements can be established. The use of attitude and possibly thrust magnitude control during the cooldown phase to minimize terminal errors on the translunar leg deserves a more detailed analysis.

3.14.2 Rendezvous

In the event active rendezvous is required with a manned facility, either in earth or lunar orbit, it will be necessary to perform phase correction maneuvers beyond those performed during the normal course of cooldown (see Section 3.13.4.2). During the cooldown phase, corrections will be limited to NERVA idle mode operation or an APS maneuver to rotate the RNS to a retrograde orientation. Further refinements in orbital position will be accommodated through a combination of APS and idle mode operations. A procedure has been identified which is somewhat analogous to the pre-injection separation maneuver (Section 3.9.4) and does not unduly burden the APS. This approach is illustrated in Figure 3.14-1. For maximum flexibility, the cooldown phase of insertion is biased (as required) to assure that the RNS is ahead of the target facility at the same altitude. The first maneuver (idle mode) enlarges the RNS orbit to the extent required to result in closure to 7 nmi following one orbital revolution. At this time the RNS performs a retrograde maneuver in the idle mode (the target facility is within the shadow cone of the RNS), reducing its orbital eccentricity to the extent that apoapsis is 1.5 nmi above circular. On the subsequent revolution circularization is achieved with the APS operating in the retrograde orientation. This limits the APS contribution to 2.5 fps.

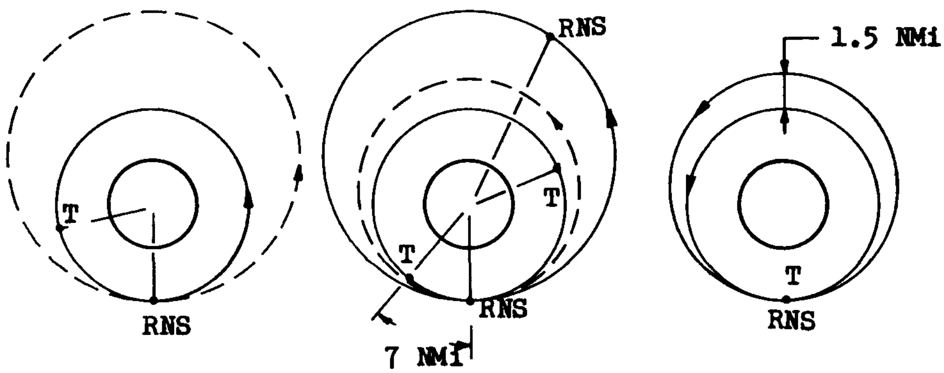

	ΔV_1	ΔV_2	ΔV_3
i	1	2	3
ΔV_i (fps)	As Req'd	ΔV_1-2.5*	2.5*
Time (Hr)	0	1.6	3.2
Separation (NMi)	-	7	0
Mode	NERVA Idle	NERVA Idle	APS

*1.1 fps in Lunar Orbit

Figure 3.14-1 MICRO-RENDEZVOUS PROFILE (Earth Orbit and Lunar Orbit Insertion)

3.15 MAINTENANCE AND REPLENISHMENT

The Phase II study concluded with selection of a maintenance level and replenishment concept for the Class 1-Hybrid RNS functional components which included replacement of multiple replacement modules in the forward skirt. This contrasted with the Phase II selection for the Class 3 RNS of replacement of the entire CCM and the low level of replacement using man or manipulators in other studies. The minimum requirement for orbital support and the operational simplicity of the Class 3 CCM concept stimulated a Phase III trade study on orbital maintenance for the Class 1-Hybrid, including consideration of the replacement of the entire CCM as in the Class 3 and the use of in-situ techniques as alternate candidates. In all cases the entire propulsion module is selected as the level of replacement for the engine and run tank based on the Phase II study results. The Phase III trade study then evaluated four candidate maintenance strategies for the Class 1-H propellant module: (1) disposal, (2) in-situ repair, (3) secondary or standby redundancy and (4) overdesign.

3.15.1 Maintenance Level Categories

The maintenance trade study considered three categories of concepts for the orbital maintenance level of the functional components: (1) multiple replacement modules, (2) single CCM, and (3) in-situ maintenance using the capabilities of man in orbit. These are broad categories containing multiple concepts. Their general characteristics are summarized as follows.

3.15.1.1 Multiple Replacement Modules

Various replacement module concepts were defined in Phase II on the principle of minimizing the number of fluid and electrical connections which must be broken to replace the module. All planned operations are accomplished without EVA using the space tug as an orbital support element. Maintenance consists of the replacement of a relatively large module at the forward end of the RNS. The RNS consumables will be replenished by replacement of a like module each round trip. Consumables include the APS and fuel cell reactants and pressurants. The onboard checkout system must be able to isolate faults only to the level of the candidate replacement module which substantially reduces the potential onboard checkout requirements compared to a low replacement level. The onboard checkout system, however, must still verify the operational readiness of the RNS prior to mission initiation.

3.15.1.2 Single Command and Control Module

All functional components and consumables are packaged in a single module which will be replaced each round trip using unmanned orbital support for both maintenance and replenishment. In order to minimize the system, subsystem, and component requirements, all operations that are required each round trip will be attributed to the ground recycle procedure. The entire replenished and qualified CCM would then be replaced on the RNS and the next mission initiated with an orbital checkout. Characteristically, this module has a simple interface with the balance of the RNS. A standard docking structure and procedure is used for all orbital operations, including payload attachment and refueling. No operational fluid connections are made or broken in orbit to recycle the module, and the electrical connections between subsystems in the CCM which must be broken are reduced to zero.

3.15.1.3 In-Situ Maintenance

This category is represented by manned (either direct or via manipulators) replacement of relatively small modules as required. All hardware, including fluid and electrical couplings, is mounted so that it is accessible for manned operations. Appropriate hand holds and restraining devices are used to help with connections or component removals and replacements. Manned orbital operations require that pressures are reduced to a safe level and hydrogen and oxygen mixtures are precluded. This implies a requirement for passivation of storable elements prior to manned maintenance operations. The use of manipulators would trade the requirements of life support and safety for the orbital support elements necessary to perform analogous functions. The onboard checkout system should be able to isolate faults to the line replaceable unit (LRU), however substitution of manned operations is possible for some subset of this requirement. Maintenance operations can then be performed by replacement of the LRU. Consistent with the in-situ concept of maintenance, replenishment in place will be considered for expendables. Hydrogen and oxygen would be tanked separately based on safety requirements. Fluid disconnects can be made either automatically or utilizing manual assistance.

3.15.2 Maintenance Level Evaluation Within Categories

Within each of the broad maintenance concept categories, multiple candidates have been identified. The trade study approach was to first select the most attractive candidate in each category based on minimum complexity, weight, reliability, and handling requirements, both in orbit and on the ground. The selected candidates for each category were then compared and a selection made based on technical feasibility, complexity of operations, support requirements, weight, and effectiveness. Effectiveness includes the portion of RNS unreliability covered, reliability of accomplishing repair and replenishment, and the impact on RNS reliability.

3.15.2.1 Multiple Module Candidate Evaluation

Three candidates were considered in this evaluation. These are depicted in Figure 3.15-1. The first is represented by the Phase II derivative approach which consists of eight discrete modules. The second candidate

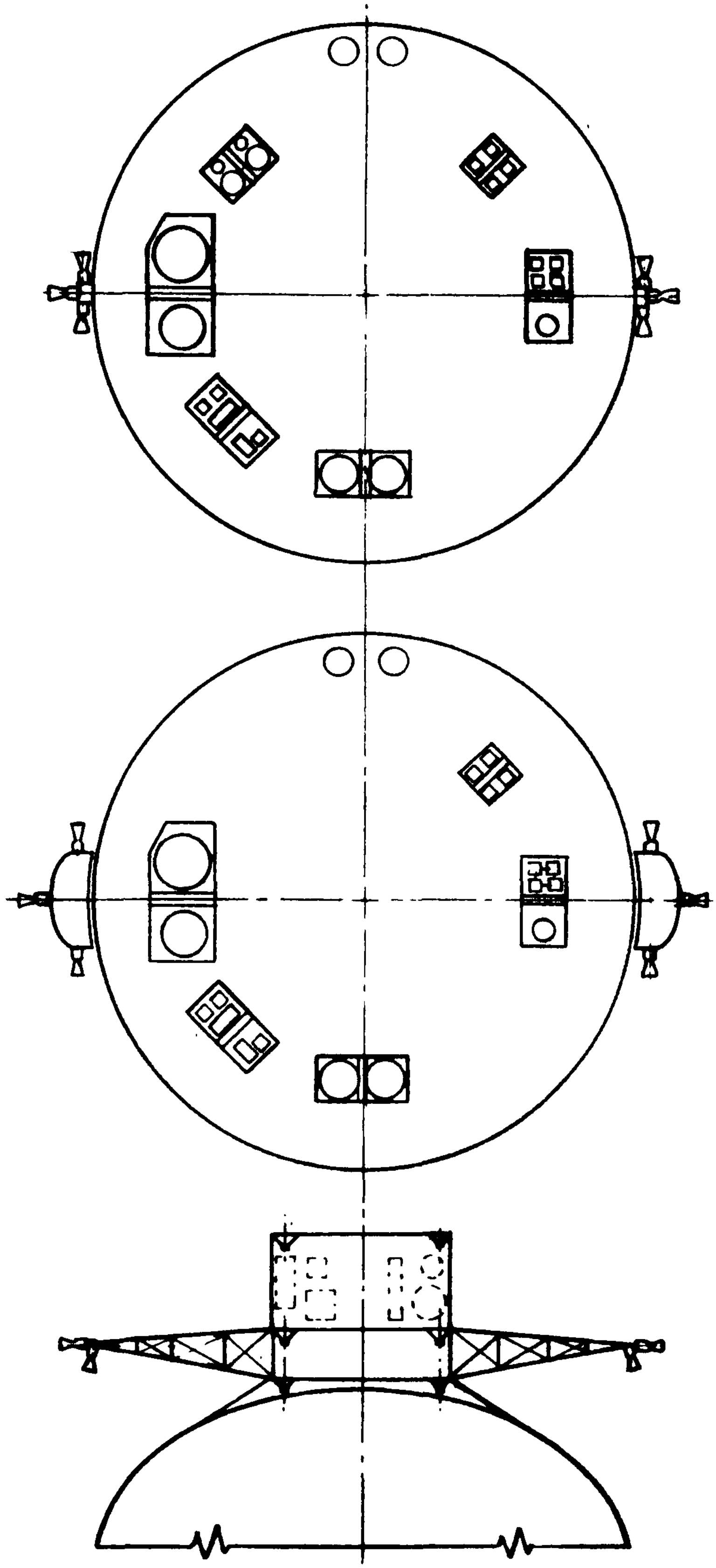

Figure 3.15-1 MULTIPLE REPLACEMENT MODULES

utilizes a similar concept but incorporates autonomous APS pods. The Phase II derivative requires a minimum of two module replacements per round trip based on replenishment requirements. Reconfiguration of the APS to autonomous pods would result in three module replacements and reduce the number of fluid disconnects to zero. Two autonomous pods 180 degrees apart, each containing functional redundancy, were selected as a representative subcandidate. Consideration of upward integration of nonconsuming equipment and integration of all consumables into a single replacement module (centralized replenishment) provides a continuous range of candidates between the Phase II derivative and the single command and control module. The third candidate, then, accumulates all modules that require replenishment into a single module, and the balance of the functional components into a second module. The module definition for these candidates is presented in Table 3.15-1.

Table 3.15-1

MULTIPLE MODULE CANDIDATES—DISCRETE MODULES

Phase II Derivative	Autonomous APS Pods	Centralized Replenishment
Power	X	Single module for replenishment
APS tankage Two APS engines	2 Pods (internally redundant)	
Propellant management	X	Single module for maintenance
Flight control	X	
Optical sensor	X	
Instrumentation	X	

These multiple maintenance module concepts were compared on the basis of: (1) the weight penalty incurred for packaging the various module approaches; (2) the number of functional disconnects required, both fluid and electrical, including the total required to be designed and the total number of disconnects to be made each round trip; (3) the number of operations required under both scheduled and unscheduled conditions and the number of replacement modules anticipated each round trip; and (4) orbital support requirements. Table 3.15-2 summarizes the results of the evaluation. Although considered a subcandidate of multiple maintenance modules, a centralized replenishment option approximates the concept of a single command and control module with respect to the operational considerations. Based largely upon the reduced number of fluid disconnects required and nominal weight penalty, the autonomous APS pod approach is selected to represent this category.

3.15.2.2 Single Command and Control Module Evaluation

For the Class 3 RNS, a configuration of the single CCM was established during the Phase II studies. This configuration is to be contained within a 15-ft maximum envelope dimension.

Two CCM candidates differing only in physical configurations are shown in Figure 3.15-2: (1) the wafer configuration, and (2) the outrigger configuration. The wafer configuration is compatible with the 15-ft-diameter constraint of the space shuttle and is mounted with the docking structure in plane with the forward bulkhead, utilizing the standard space shuttle payload deployment mechanism. The motivation for the outrigger configurations is to avoid the potential APS plume impingement on the RNS forward dome. In the wafer configuration the required thrust vector cant angle is 29 degrees. For the outrigger configuration, this angle can be reduced to zero.

An analysis was performed to determine the APS nozzle cant angle required for various outrigger configurations to reduce heating of structures due to impingement to an acceptable level. This was translated to an APS propellant and structural weight penalties for various lengths of outrigger arms. Based on 1,200 lb of APS aft nozzle propellant usage and 16 lb/ft of outrigger length, a relatively constant total weight penalty of between 133 and 150 lb occurs corresponding to the optimum range of 2 to 7 ft outrigger lengths. Three-foot outriggers with a structural weight of 69 lb were selected corresponding to a cant angle (θ) of 20 degrees. The APS propellant weight penalty is: $W_P = 1,200 (1-\cos\theta) = 72$ lb.

Table 3.15-2

MULTIPLE MAINTENANCE MODULE EVALUATION

	Phase II Derivative	Autonomous APS	Centralized Replenishment
Weight			
Structural racks	267 lb	317 lb	591 lb
Fluid disconnects	53 lb	33 lb	53 lb
Electrical panels	71 lb	65 lb	32 lb
Subsystem modifications (5% propellant residue)	--	90 lb	--
Docking structure	--	--	280
Total	391 lb	505 lb	956 lb
Number of disconnects			
Fluid:			
Each mission	4 (APS)	0	4
Total	8 (APS, vent, fill, 2 press.)	4	8
Electrical panels:			
Each mission	4	4	2
Total	11	10	5
Number of modules replaced:			
Each mission	2	3	1
Scheduled	2	0	1
Unscheduled	4	4	0
Orbital support	Tug + Maint. unit	Tug + Maint. unit	Tug only

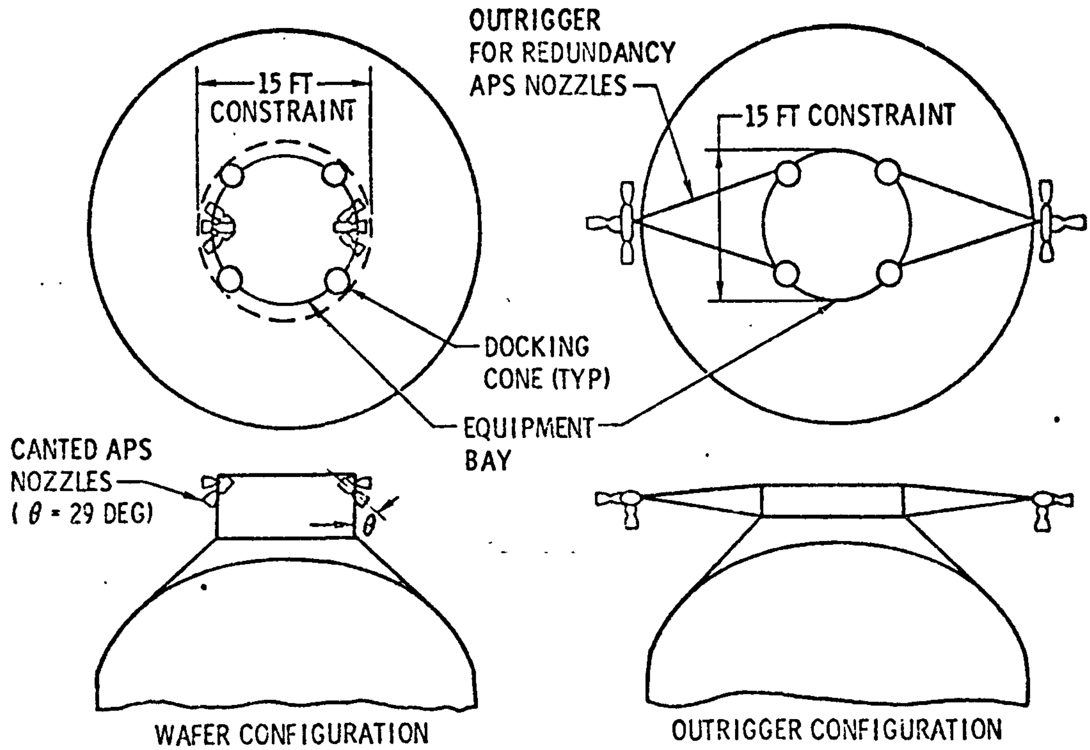

Figure 3.15-2 SINGLE COMMAND AND CONTROL MODULE CANDIDATES

3.15.2.3 In-Situ Maintenance Evaluation

The in-situ maintenance category using manned (either direct or via manipulators) replacement and inplace replenishment is represented by two candidates. The first candidate utilizes a pressurized forward skirt which would enable shirtsleeve maintenance operations when supported by an orbital workshop type airlock. Maintenance operations would be effected by a man at a low replacement level (black box or valve assembly). The second candidate would require backpack EVA or the use of manipulators and consist of accessible equipment in the forward portion of the RNS. These are shown in Figure 3.15-3. An estimated 80 line replaceable units (LRU) would be replaceable in either candidate.

Although a shirtsleeve environment provides substantially greater capability for diagnostics repair and calibration, it also has the highest passivation requirement and potentially offers some serious safety problems. Additionally, an air lock would be required as an orbital support element. Although backpack EVA offers somewhat less hazard than the shirtsleeve environment, it does require life support and generates maximum impact on the various

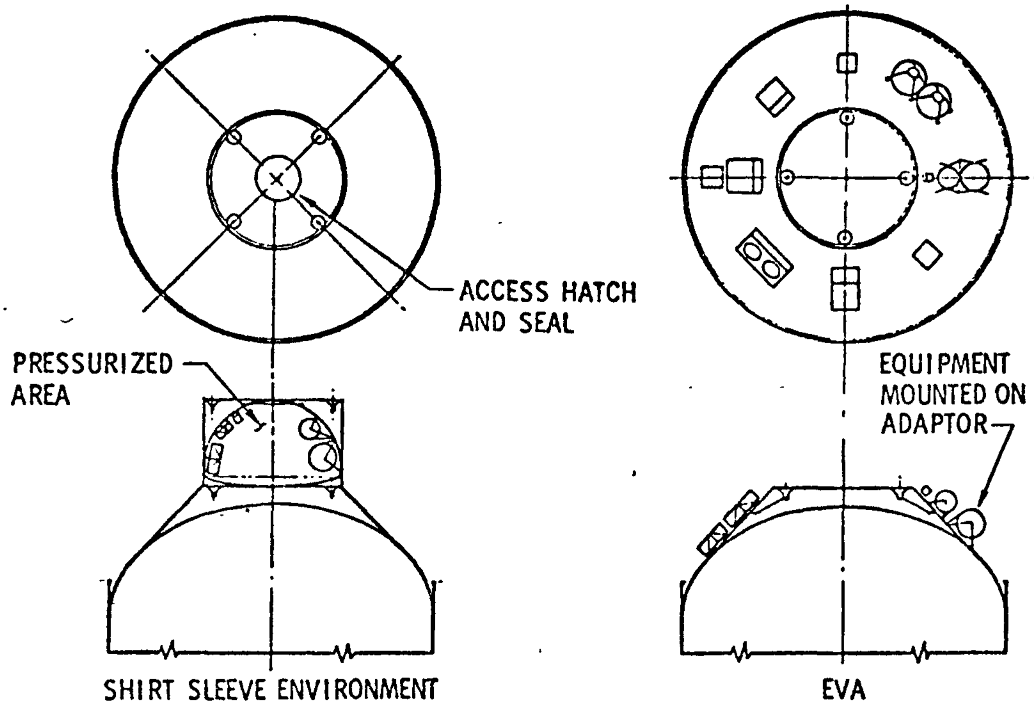

Figure 3.15-3 IN-SITU MAINTENANCE CANDIDATES

subsystem designs. Alternately manipulator systems would impose the requirement for an additional orbital support element. A minimum weight penalty for equipment mounting was assigned based on the RNS forward thrust structure being an accessible, free location. Nominal weights for astronaut aids, such as tether lines and handholds, were based on orbital workshop experience. Comparable weights would be required with manipulator systems. Instrumentation penalties are assigned based on the requirement to fault isolate to the LRU in orbit. Table 3.15-3 summarizes the relative weight penalties.

Backpack EVA was selected as the representative for this category based on the weight advantage and minimum requirement for orbital support.

3.15.3 Maintenance Level Evaluation

The representative candidates of the three categories were then compared to determine the maintenance level. Table 3.15-4 summarizes the evaluation results. The RNS offers essentially free mounting structure for in-situ maintenance conveniently located on the forward thrust structure. A weight

Table 3.15-3
WEIGHT COMPARISON
IN-SITU MAINTENANCE CANDIDATES

	Weight (lb)	
	Shirtsleeve Environment	Backpack EVA
Structure — equipment mounting	500	90
Pressurized structure	340	--
Astronaut aids	40	60
Disconnects	140	184
Instrumentation	240	380
Total	1,260	714

penalty for instrumentation was assessed to allow for fault isolation to the LRU. Additionally, a small weight penalty was assessed to provide for an estimated 60 electrical disconnects and 20 fluid disconnects to facilitate removal of anticipated LRU's. The relatively large number of LRU's accounts for a slight weight penalty for in-situ compared to the other two candidates.

Assuming the engine module is replaceable in all cases, all three candidates are able to maintain greater than 99 percent of the RNS unreliability. For the three candidates, the single CCM requires the minimum number of operations both each round trip and on an unscheduled basis.

With a minimum number of operations and a single repetitive operation each round trip, the single CCM was assessed to have the highest reliability of operations. Because of the extensive EVA and the relative unpredictability of successful manned or manipulator operations, the reliability of performing operations successfully with an in-situ maintenance policy was assessed to be somewhat lower. Because of the large number of disconnects that would have to be incorporated into the subsystem design, it is felt that an in-situ

Table 3.15-4

MAINTENANCE LEVEL EVALUATION

	Multiple Modules	Single Command and Control	In-Situ
Weight penalty	505	567	714
RNS unreliability covered	0.992	0.990	0.996 0.970 without engine modification replacements
Operations - each trip	Replace 3 modules (1 docking operation)	Replace 1 module	Replenish by tanking EVA expected for replacement
As required	Replace 4 modules	None	Extensive EVA (80 Units)
Reliability of operation	Nominal	Highest	Lowest
Impact on RNS reliability	Nominal	Minimum	Maximum
Support requirements	Tug + maintenance unit	None	Crew module or manipulator system

maintenance policy would impact the reliability of the RNS unfavorably. The ability to test the refurbished CCM on the ground with relatively unlimited support and the potential of using a minimum number of disconnects both fluid and electrical within an external to subsystems resulted in a minimum impact to RNS reliability for a single CCM concept. Also, minimum of orbital support is required for the single CCM.

Base on these considerations, the single CCM is selected for the orbital maintenance level.

3.15.4 Class 1-Hybrid Propellant Module Maintenance Strategy

Four candidate strategies have been identified for maintenance of the Class 1-Hybrid propellant module: (1) disposal, (2) in-situ repair, (3) secondary redundancy, and (4) overdesign.

Probable failures for the Class 1-Hybrid propellant module are summarized in Table 3.15-5. The functional components then are the first-order effect and should be considered in the maintenance strategy. Passive subsystems contribute such a small percentage of the unreliability that maintenance operations are considered unlikely for these subsystems.

Table 3.15-5

CLASS 1-HYBRID PROPELLANT MODULE FAILURES

Subsystem	Failures per 1,000 Round Trips
Structures	0.8
Meteoroid/thermal	2.4
Propellant management	116
Astrionics	72
Total	191.2

In the Phase II study, replacement of the Class 3 propellant module was selected as the maintenance strategy. This motivated the propellant module design to possess an absolute minimum of capability and components. The analogous strategy for the Class 1-Hybrid would be to dispose of the expended module since it is not space shuttle compatible, and replace it with a new module. Because this would require an INT-21 launch vehicle, the value of alternate maintenance concepts for the Class 1-Hybrid propellant module is relatively high.

Because of the high replacement cost of the Class 1-Hybrid propellant module, in-situ repair was considered. This would allow for orbital operations such as patching of insulation or replacement of failed components. The low value of failures expected in the passive subsystems (structures, meteoroid/thermal) focus the requirements for maintenance on the functional components. Some of the propellant management components are located in the tank, however, making them inaccessible. In most cases these could be mounted external to the tank, and accessible, at some penalty in weight and by accepting the associated heat short. In addition, those penalties associated with in-situ operations cited in Section 3.15.2.3 will be incurred.

The strategy of secondary redundancy would add additional or standby components to those with a relatively high expected value of failure. Secondary redundancy would allow mission initiation with a failed component and still maintain the required probability of mission success. The strategy of secondary redundancy yields approximately a factor of 50 to 1 reduction in the required maintenance operations for the baseline Class 1-Hybrid propellant module. To achieve this improvement in required maintenance operations the addition of specific components weighing an estimated 110 lb. Table 3.15-6 identifies these components, the associated weight penalty and illustrates the effects of secondary redundancy.

The overdesign of passive subsystems, such as structures or meteoroid protection, was considered as a viable alternative to substantially reduce the likelihood of required maintenance operations. Analysis early in the trade study indicated that the likely maintenance operations resided with the functional components, not the passive components, hence the weight penalties of overdesign were considered unattractive.

Table 3.15-6

SECONDARY REDUNDANCY EVALUATION

(Allowing Flight with One Component Inoperative)

Class 1-Hybrid—Propellant Module

Resulting Performance for Propellant Management

Component	Expected Failures/ 1,000 Round Trips Without Secondary Redundancy	No. of Components Added to Fly with One Inoperative	Weight Penalty (lb)	Failures That Need Repair — Frequency of Two Failures with Secondary Redundancy
Propellant feed valve (2)	12	1	45	0.107
GH_2 press. control valve (2)	20	1	10	0.27
Fill valve ground	(6)	--*		--
GH_2 Press. control S/O valve (Grd)	(14)	--*		--
Inflight fuel transfer valve	6	1	15	0.036
Vent and relief valve (Grd)	(10)	--*		--
Relief valve (Grd)	(8)			--
Flight vent (4)	24	5	50	1.22
	(100) 62	7	110	1.635

*Ground functions—Assume P (fail) ~ 0 after orbital checkout.

Table 3. 15-7 quantifies the values of maintenance for three candidate maintenance strategies: (1) disposal, (2) in-situ repair, and (3) secondary redundancy. Design compromises would be required with an in-situ repair strategy to make the components on the propellant module accessible and removable. These would also increase the likelihood of failures and penalize the RNS performance. Based on these considerations a secondary redundancy stategy is recommended as most economical for the propellant module of the Class 1-Hybrid RNS. The simple requirements of the propellant module allows for a minimum of capability and components, hence a relatively low likelihood of required maintenance. Enhancing this initially low likelihood of required maintenance by a factor of 50 appears to be the most attractive maintenance strategy.

The secondary redundancy approach could benefit both the propulsion and propellant modules, and deserves further consideration in future studies.

3. 16 END-OF-LIFE DISPOSAL

A trade study was conducted during Phase II which indicated that based on safety, simplicity, and economy the preferred mode for disposal of a complete RNS consisted of injection into a heliocenteric orbit, either with or without a payload (Reference 3-1). During Phase III the baseline RNS design was subdivided into three discrete modules: propulsion, propellant, and command and control. These modules will have different life cycles and disposal requirements. The command and control module is recycled to the ground for maintenance and replenishment, so space disposal is not required. An inoperative propellant module can be left unattended to permit orbit decay and burnup on reentry. Thus, the concern for end-of-life disposal is focused on the propulsion module. System economics evaluations during Phase II indicated that frequent replacement of the propulsion module could be warranted, on the basis that NERVA specific impulse has a greater impact on RNS transportation cost than NERVA lifetime. In the event of a failure, capability must be provided for disposal of it from either the operational orbit or lunar orbit.

Table 3.15-7

CLASS 1-HYBRID PROPELLANT MODULE

MAINTENANCE STRATEGY

EVALUATION

	Disposal ($ million)	In Situ Repair ($ million)	Secondary Redundancy ($ million)
Expected disposal cost at appropriate end-of-life point	47.5	4.75*	0.41
Operational penalty for added weight at $500/RT x 10 RT's	--	~0	0.55
Operations cost at $5 x 10^6/ expected operation	--	0.95	--
Total Cost per RNS	47.5	5.70	0.96

*10% of component unreliability inaccessable in tank

The velocity requirements and system performance for alternative disposal modes are identified and compared in Table 3. 16-1. Helicentric orbit injection is favored for safety. Whereas the full RNS can dispose of itself with a small fractional propellant loading from low earth orbit, the propulsion module capacity is not sufficient for that case and a space tug is required. Modest propellant requirements are identified for the tug options. A 63,000-lb propellant requirement for a reusable tug is indicated which would permit heliocentric disposal of the NERVA propulsion module from earth orbit at a propellant cost of about $10 million. If such a large tug system were not available, self-disposal or use of a CCM-derivative tug would permit injection of the propulsion module into a long-lived orbit.

Table 3. 16-1
COMPARISON OF PROPULSION MODULE DISPOSAL MODES

	Propellant Required for System Approach (lb)			
Disposal Maneuver	ΔV (fps)	Self-Disposal*	Expendable Space Tug**	Reusable Space Tug**
1. Operational earth orbit to heliocentric orbit	10,300	Exceeds capacity	33,000	~63,000
2. Operational earth orbit to 5-year lifetime orbit	440	1,300	Use reusable	~1,300
3. Operational earth orbit to ocean	362	>1,000	Use reusable	~1,100
4. Lunar orbit to helio-centric orbit	2,220	2,500	Use reusable	6,000
5. Lunar orbit to lunar surface	80	>1,000	Use reusable	>1,000

*Isp = 800 sec
**Isp = 450 sec

For disposal of NERVA from lunar orbit, the capacity of the run tank on the propulsion module is adequate for heliocentric disposal. However, additional navigation and guidance and control capability would be required on the propulsion module to accomplish such as operation. The propellant requirement for a reusable tug disposal of NERVA from lunar orbit is seen to be modest and would be easily provided by the lunar lander propulsion system. Thus, the reusable tug approach was adopted as a baseline for helicentric disposal of the propulsion module. Normal replacement would be accomplished in the earth assembly orbit, but emergency removal and disposal could be accomplished in lunar orbit or any other similar operational orbit with general procedures and interface employed. The functional requirements imposed on the propulsion module for this operation are fully analogous to those for normal assembly of the RNS, as defined in Section 3. 5.

3. 17 INTERFACE WITH OTHER PLANNED SYSTEM ELEMENTS

3. 17. 1 Summary

According to the MSFC guidelines and constraints document provided for the RNS study, the RNS may have an operational interface with a variety of system elements currently included in NASA planning. These system elements are summarized in Table 3. 17-1. A variety of operational interfaces of the RNS with these systems are shown, including rendezvous and docking, assembly and maintenance support, and functional interfaces. The space shuttle and space tug are the dominant systems effecting operational interfaces with the RNS. Therefore these will be discussed in greater detail in subsequent sections.

The selected mode of RNS operation is essentially independent of the various space station systems. However, some space station elements could become payloads for the RNS. Data management, power, and command and control interfaces with the space shuttle, space tug, and payloads are identified in Table 3. 17-1. A manned planetary mission spacecraft has a special relationship to the planetary RNS system. The increased data transmission and power requirements for such missions justify that the RNS configured for earth-centered applications should be parasitic and slaved to the mission spacecraft.

Table 3.17-1

RNS INTERFACE WITH OTHER PLANNED SYSTEM ELEMENTS—CLASS 1 HYBRID

System Element \ Operational Interface	Rendezvous and Docking	RNS Assembly and Maintenance Support	Propellant Resupply	Command and Control	Data Management	Power	NERVA Replacement and Disposal
Earth Orbital Space Station/Base	Optional operation RNS active	Not required	Not required	Baseline—not required but possible override if space station controls space tug	Optional RF link	Not required	Not required
Space Shuttle	RNS passive	1 RNS module delivery 2 Optional—assembly support	Space shuttle integral tanker	1 Shuttle C&C for launch and deploy 2 Shuttle override for assembly	Checkout and status monitoring	RNS parasitic during launch	RNS replacement module delivery
Propellant Depot	Not required	Not required	Not required	Not required	Not required	Not required	Not required
Space Tug	RNS passive	Payload handling	Not required	Space tug C&C for rendezvous docking and assembly of payload	Not required	Not required	Baseline disposal system
Lunar Orbital Space Station	Optional operation RNS active	Baseline—not required but possible safety and reliability impact	Baseline—not required but possible safety impact	Baseline—not required but possible safety impact	Optional	Not required	Not required
Lunar Surface Base	Not applicable	Not applicable	Not applicable	Not applicable	Not applicable	Not applicable	Not applicable
Manned and Unmanned Payloads	Autonomous or tug support RNS passive	Not applicable	Not applicable	1 RNS autonomous with ground override 2 Optional override by manned payload	1 Potentially parasitic on RNS 2 Optional override by manned payload	Potentially parasitic on RNS	Not applicable
Manned Planetary Mission Spacecraft	Autonomous or tug support RNS passive	Not applicable	Not applicable	RNS slaved to mission spacecraft	RNS parasitic on spacecraft	RNS parasitic on spacecraft	Not applicable
INT 21 Launch Vehicle	Not required	Class 1 Hybrid RNS propellant module delivery	Not required	Potential navigation update from launch IU at spacecraft	Not required	Not required	Not required

Although identified as a candidate system element for the RNS, the requirement for an orbital propellant depot has not been established. It is not required for either propellant resupply or support of assembly maintenance and repair.

The rendezvous mode shown for the interface with the various systems utilizes the RNS in a passive mode, where the space shuttle or space tug bring required payloads or services to the stationary RNS. However, it is required that the RNS should have a capability to assume an active role during rendezvous and docking with orbital facilities. This is indicated as an optional capability for interfacing with the earth orbital space station or lunar orbital space station. However, the baseline interface considered between those systems does not require a hard dock of the RNS to the space stations, but rather, the RNS would loiter at a specified exclusion distance from the facility, with either autonomous or space tug supported payload transfer.

3.17.2 Space Shuttle

The space shuttle is used to launch the RNS modules to orbit. The cargo bay has a clear volume 15 ft diameter by 60 ft long and provisions for deployment and boarding. The reference performance is shown in Figure 3.17-1, with a design point of 33,000 lb delivered to and returned from a 260 nmi 31.5-degree inclination operational orbit for the RNS. Increased performance is considered to be available for propellant delivery at a ratio of payload delivered to payload returned of -0.27.

The RNS modules are loaded into the space shuttle orbiter while it is in a horizontal attitude. The orbiter is subsequently erected on the booster on the launch pad. The general concept for launch support is defined in Section 3.3. Conventional orbital assembly docking interfaces are used for attachment to the space shuttle payload deployment mechanism at the forward end of the cargo bay. Since the propulsion module only has a docking interface at its forward end, additional provisions for lateral support are required. A concept for lateral restraint of NERVA with struts attached to the space shuttle cargo bay hard points was evaluated and is presented in Section 4.2.9. Load factors are defined in Section 4.2.2. It is required to locate a poison wire removal mechanism, consisting of an

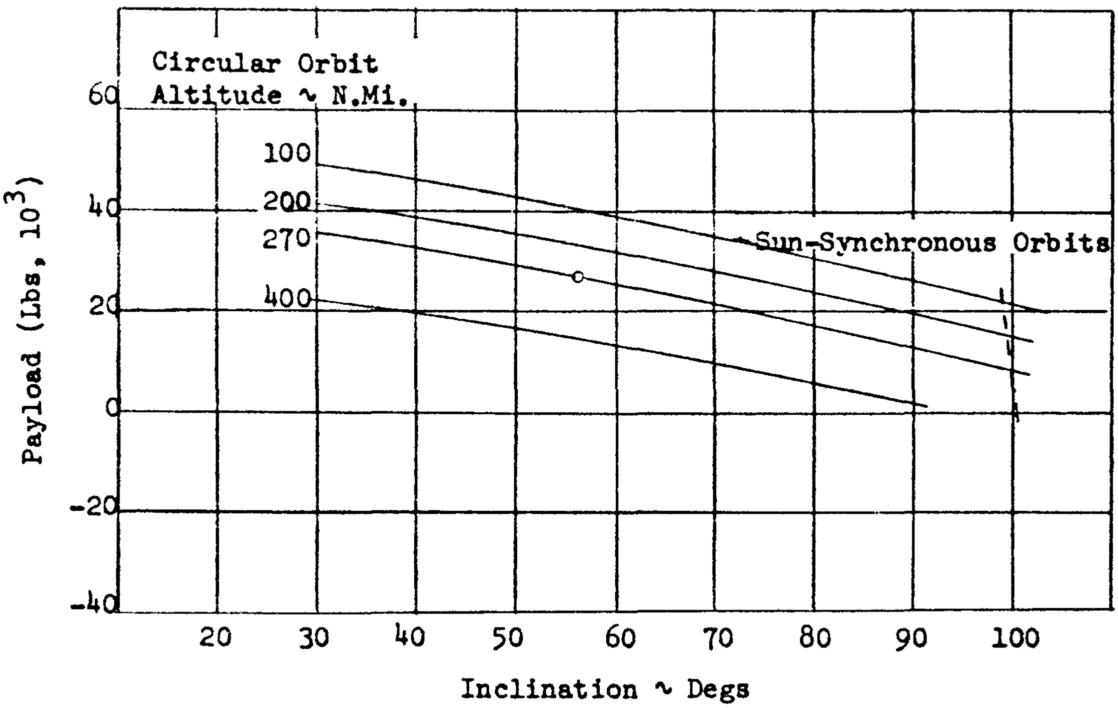

Figure 3.17-1 25K SPACE SHUTTLE PAYLOAD CAPABILITY

electric motor, reel and line, on the aft bulkhead of the cargo bay, to accomplish removal in orbit prior to propulsion module deployment.

The RNS modules are designed to use electric power from the shuttle while in the cargo bay in the form of 28 vdc and 400 Hz ac and to transmit and accept multiplex data and commands interfacing with the space shuttle data bus. Discrete display and control capability for crew override must be provided by the space shuttle. The RNS modules are designed to accept these services for all operational phases after installation in the cargo bay including propellant fill operations and launch. RNS modules will be checked out prior to installation in the space shuttle. Additional checkout requirements after LH_2 loading will utilize the space shuttle data bus and onboard checkout system. The electrical connections used for orbital assembly of the RNS modules will be used for establishing interfaces with the space shuttle.

As a baseline, the space shuttle is not required to dock with the RNS for assembly, maintenance, or payload handling, these services being nominally provided by the space tug. However, this could be a desirable optional approach for utilization of the space shuttle. It would be desirable, however, to provide a docking interface between the space shuttle and RNS for propellant transfer operations, permitting use of an integral tanker and not requiring deployment of propellant modules. The integral tanker version of the space shuttle orbiter is the baseline propellant resupply approach. This operation is discussed in Section 3. 6. 2. The rendezvous and docking criteria utilized in the RNS design are summarized in Section 4. 4.

A single probe/drogue docking mechanism could be utilized integrated with the orbital transfer lines. Fluid couplings could then be accomplished similar to the design approach for RNS assembly shown in Section 3. 5. The implications of the space shuttle orientation and location of the transfer line are discussed under Section 3. 6. 2. It would be desirable for the space shuttle tanker to provide linear acceleration along its axis for the propellant transfer operation. It is anticipated that the orbiter would deliver 1, 000-lb thrust in the forward direction for its normal operations. This acceleration level is higher than desirable for efficient propellant settling and transfer operations. At least an order of magnitude reduction in thrust level would be desirable.

3. 17. 3 Space Tug

The space tug is not utilized for assembly of the Class 1-Hybrid RNS, since the RNS command and control module is capable of performing the necessary operations autonomously. The space tug is utilized as the baseline support system for payload transfer operations. Table 3.17-2 summarizes the description of the baseline space tug provided for the RNS study by MSFC.

A kit is provided for the tug to operate as a lunar lander. The method of basing or sustaining the space tug is not defined. For example, it could operate autonomously, it could operate from the space shuttle for a particular set of RNS support operations, or it could be based at an earth orbit or lunar orbit space station. The latter approach would be more likely for RNS mission destinations.

Table 3.17-2

SPACE TUG CHARACTERISTICS

Propulsion Module:		
	Dry Weight	10,000 lb
	LO_2/LH_2 Capacity	60,000 lb
Kits:		
	Crew Module (3 to 6 men)	15,000 lb
	Cargo Module	4,000 lb
	Lunar Landing Legs	5,000 lb

The baseline MSFC tug is larger than required for efficient support of assembly and payload handling operations. Actually, a system the size of the RNS command and control module would be adequate. However, a space tug type propulsion system (probably a lunar lander) would be desirable for the propulsion module disposal operation. This is discussed in Section 3.16. A tug with a propellant capacity of approximately 63,000 lb would be desirable for a reusable disposal from each orbit and about 33,000 lb would be required for an expendable mode of operation.

Section 4
RNS ANALYSES

The RNS design concept was largely established during Phase II. The Phase I and Phase II trade studies resulted in selection of most of the major design features. The analyses are reported in References 4-1 and 4-2. These results were reviewed with the COR at the begining of the Phase III study to establish those features which required further analyses. Specific subsystem features are reviewed in the subsequent design sections.

Phase II studies concentrated on a reusable mode of operation based in a low earth orbit. Reusability imposed a requirement for maintenance and refurbishment in orbit, and a variety of orbital support concepts were considered. Provision of separate orbital support facilities was discarded after Phase II, and the basic support systems for the RNS were selected as the space shuttle and the space tug. Whereas the NFPM in Phase I was a single module concept, the reusable stage operation mode and the alternate launch vehicle concepts for Phase II resulted in definition of a variety of modular stage concepts, consisting of propulsion, propellant, and command and control modules. The single module concept evolved to the Class 1-Hybrid, which included a propulsion module for engine replacement. The Class 2 concept was based on a 22-ft-diameter launch vehicle, and the Class 3 concept was based on the 15-ft-diameter space shuttle cargo bay.

Economical performance of the range of reference missions favored a single propellant capacity. A 300,000-lb LH_2 capacity was selected for subsequent study phases, considering that interoribital shuttle missions or manned planetary missions, although imprecisely defined at that time, would require a stage of at least that capacity for an economical system.

The launch configuration was a major concern for the INT-21 launched RNS concept. As the designs evolved, it was found that a stiffened tank configuration approached the mission performance efficiency of a design utilizing an ascent shell, but had reduced development requirements. Accordingly, the stiffened tank launch configuration was retained for Phase III.

The Phase III study was focused on the Class 1-Hybrid and Class 3 concepts for which the launch vehicles were well defined. Investigation of the Class 2 concept was deferred pending further definition of the alternate second stages for the space shuttle, which would make that configuration attractive. During Phase III the manned Mars mission was deemphasized for design and an eight-burn lunar shuttle mission provided the basis for design requirements.

The objective of the Phase III study was to increase the definition of RNS operations and the assoicated design requirements. Results of these analyses are presented in Sections 2 and 3. The additional RNS design analyses reported in the subsequent sections represent trade studies and redefinition of design features responsive to the new design requirements. Also new subsystems have been defined to satisfy Phase III operational requirements.

A major consideration was the RNS configuration, considering the implications of launch on the INT-21 and orbital maintenance requirements. These affected the propellant tank geometry and stiffening requirements. Propulsion module launch support inside the space shuttle was defined. Also, the thermal and meteoroid protection system designs were revised to reflect the refinement of design criteria including environments, survival criteria, material properties, and mission timeline implications.

Functional subsystems were allocated to the individual modules of the Phase III RNS consistent with orbital maintenance requirements. A major consideration was the requirement to provide remote fluid line and electrical line deployment and coupling to accommodate orbital assembly/disassembly of the RNS modules. Stage startup and steady-state operations were evaluated, resulting in identification of additional propulsion functions and requirements. These include engine/stage feed system chilldown, run tank refill, and propellant management control. Intermodule propellant feed system interfaces were refined including consideration of orbital assembly requirements. The

APS system was re-evaluated in the context of new configuration and operational requirements, considering improved cryogenic APS concepts derived from the concurrent space shuttle program.

Navigation and guidance concepts were reviewed considering sensor requirements and the performance and data processing implications of relative autonomy on the RNS. Requirements for the data management system were defined including external and internal data flow, permitting synthesis of subsystem architecture. The primary power source tradeoff was carried forward considering revised engine power requirements and a refined mission profile. Radiation effects were evaluated for a range of component requirements. Engine/stage structural dynamics were evaluated for launch of NERVA integral with the RNS on the INT-21. These analyses and additional considerations are documented in this section.

The results of the RNS operations and design analysis have been accumulated into a baseline system description which is bound separately as Book 2 of this volume to facilitate its use as a reference document. Accordingly, only a summary of design criteria is included in Book 2. Complete documentation of design criteria applicable to both the Phase III design analyses and the system description is provided within Section 4.

4.1 CONFIGURATION

4.1.1 Phase II Configuration Evaluation

This section reviews the basis for the RNS configuration which was analyzed during Phase III. The Phase I expendable nuclear stage (NFPM) was a single module concept intended for launch as a third stage on Saturn V. Configuration issues during Phase I included load-carrying tank versus load-carrying shell launch configurations and aft bulkhead geometry. The launch configuration was carried forward to Phase II, where refinement of design weights resulted in a negligible operational weight difference between the load-carrying tank and load-carrying shell configurations. Since its development requirements are lower, the load-carrying tank was selected. Both conical and ellipsoidal aft bulkhead geometries were considered in Phase I, including strategies of telescoping the engine for greater separation and providing an internal tank. A 15-degree half-angle cone was recommended on the basis of available data, but the need for further optimization was identified. Subsequently, a 10-degree half-angle cone was selected in Phase II.

Major factors affecting the configuration during Phase II relate to modular reusable system concepts and emphasis was placed on combined optimization of radiation shielding and structural configuration to minimize system weight. Preliminary space shuttle characteristics were provided to the RNS study, including a baseline 15-ft-diameter by 60-ft-long cargo bay and a payload delivery to orbit of 50,000 lb. Availability of this system introduced the possibility of economical NERVA removal and replacement in orbit. Various engine stage interface concepts and support requirements were evaluated, which resulted in definition of a propulsion module consisting of NERVA and a run tank configured in a geometry compatible for launch inside the space shuttle.

Thus, two basic configuration candidates resulted for the 33-ft-diameter INT-21 launched RNS configuration. The single module, or Class 1 Standard, and the dual module, or Class 1-Hybrid, which was subdivided into a propellant module and the propulsion module. Upon completion of Phase II, the hybrid configuration was selected as a baseline for Phase III. The factors which entered into this selection will be reviewed in detail in the subsequent subsections. This configuration evolved further during Phase III as will be described in Section 4.1.2.

4.1.1.1 Candidate Configurations

Figure 4.1-1 shows a comparison of the two RNS Class 1 concepts which resulted during Phase II. Both versions have a tank diameter of 396 in. and were sized for a total propellant tank capacity of 300,000 lb LH_2 with a 5 percent ullage volume. Based on shield/configuration optimization the propellant tank aft bulkheads of both vehicles were designed to conform to a 10-degree half-angle cone which has the aft end of the reactor as an origin.

Table 4.1-1 presents a weight comparison between the standard and hybrid configurations representing the level of system definition achieved at the end of Phase II (Section 5.5 of Reference 4-1). The performance for the two configurations is comparable.

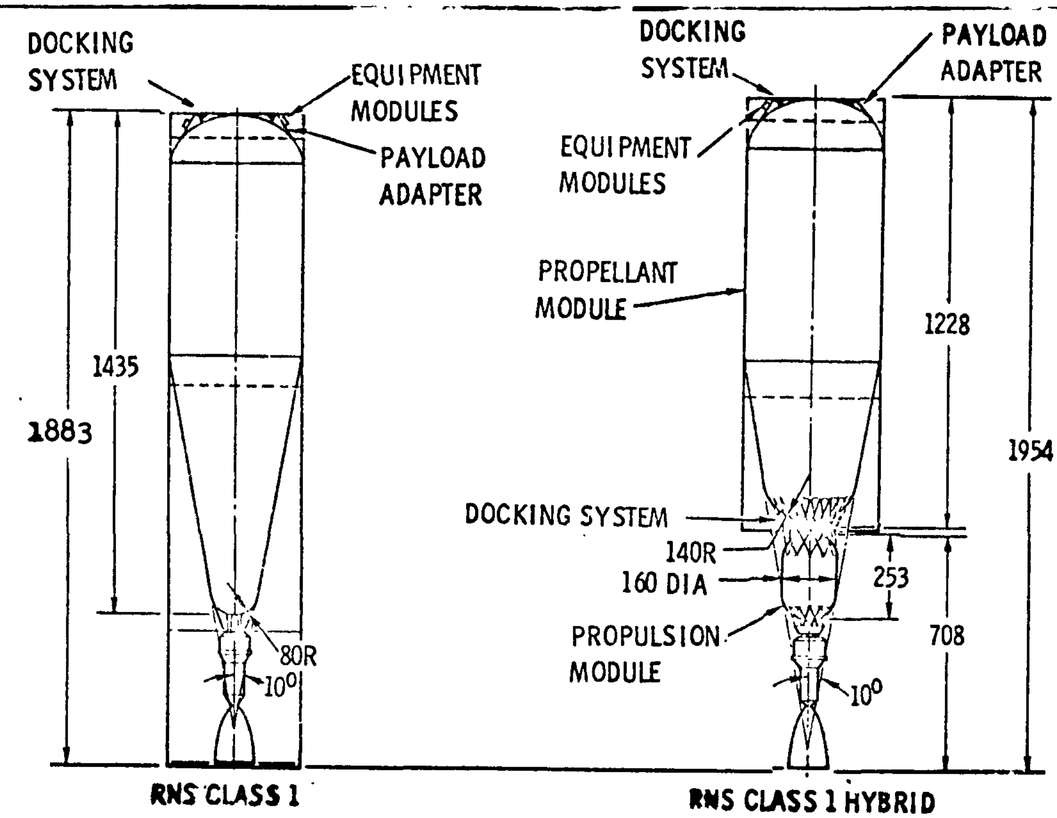

Figure 4.1-1 PHASE II RNS CLASS 1 CONFIGURATIONS (300,000 LB LH_2 PROPELLANT MODULE)

Table 4.1-1
CLASS 1 RNS WEIGHT COMPARISON

	Standard	Hybrid
Operational Weight (lb)	81,800	82,520
Total LH_2 Capacity (lb)	300,000	309,700
Propellant Mass Fraction	0.785	0.789

4.1.1.2 Launch Implications

The large envelope of a nuclear stage can increase the loading above the current design values for the INT-21. This question received considerable attention during Phases I and II, particularly to assess the implications of launching large manned payloads with the NFPM. Accordingly, an in-depth optimal control theory analysis was performed utilizing linear optimal control theory and Kalman's least-square state estimation theory to see whether an improved Saturn V autopilot design could obviate the requirement for structural modifications to the S-IC and S-II vehicles. These results, reported in Section 4. 1. 1 of Reference 4-2, indicated that this could be a promising approach.

The severity of the problem was reduced during Phase II, since the Class 1-H propellant module could be launched unmanned and by itself for the reusable shuttle mode of operation. This favored selection of the Class 1-H configuration.

4. 1. 1. 3 Radiation Implications

An extensive evaluation was conducted to reduce the stage inert weight penalty associated with minimizing the radiation dose to payloads located at the top of the stage. A large number of propellant tank geometries and NERVA external shield configurations were evaluated. Geometric considerations for the tankage included the cone angle of the aft bulkhead, separation from the engine, and provision of internal tanks.

The concept selected for the NFPM was the 15-degree half-angle cone with a 10-ft-diameter series flow internal tank, since excessive launch vehicle loading when used to launch manned payloads provided a strong motivation to keep the NFPM length as short as possible. In the Phase II reference program model all RNS launches to orbit were unmanned, so the length constraint was removed for the RNS. Therefore, the potential benefit of sharper cone angles for the aft bulkhead was investigated. Figure 4. 1-2 and 4. 1-3 show the results of this Phase II system optimization for both the Class 1 Standard and Hybrid configurations. The operational stage weight penalties included propellant tankage, skirts, heatblocks, tunnel, insulation, meteoroid protection, and intermodule structures.

There is a broad minimum in total system weight in the vicinity of 10-degrees for both the Class 1 standard and hybrid propellant tanks. In addition, the NERVA design was changed somewhat from that used during the NFPM study, primarily with the reconfiguration of external plumbing to reduce their scattering impact. This eliminated the advantage of the internal tank for the 15-degree half-angle aft bulkhead. Accordingly the 10-degree half-angle cone was selected for the propellant module in both the Class 1 and Class 1-Hybrid configurations. These results were substantiated by further investigation

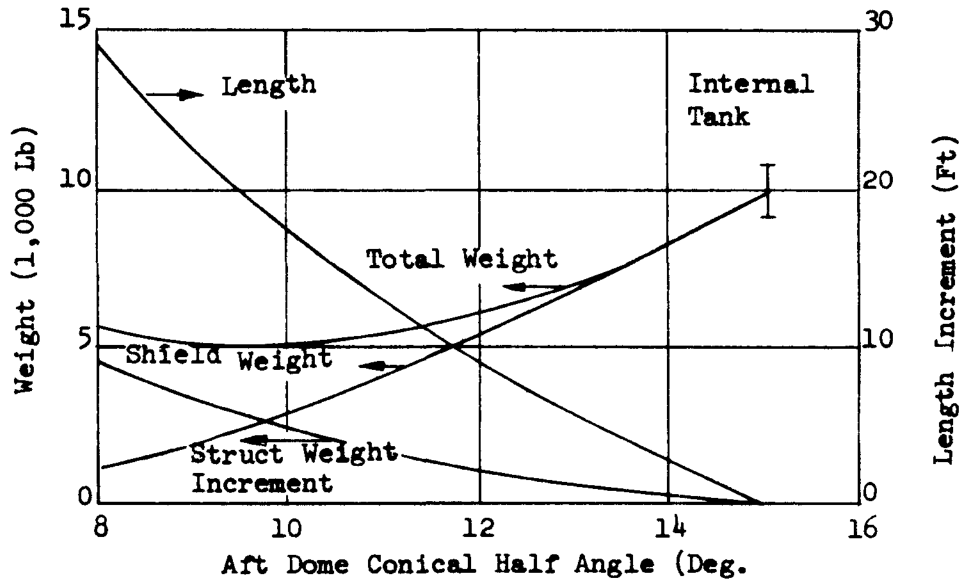

Figure 4.1-2 CLASS 1 STANDARD AFT DOME SHAPE TRADE-STRUCTURE & SHIELD WEIGHT

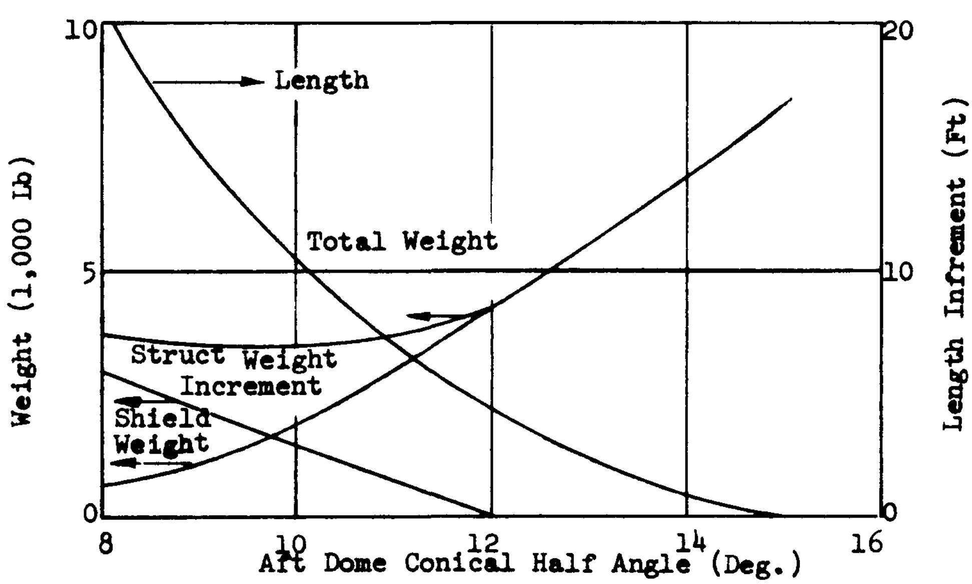

Figure 4.1-3 CLASS 1 HYBRID AFT DOME SHAPE TRADE-STRUCTURE & SHIELD WEIGHT

during Phase III. Inferior performance was found for sharper cone angles using a smaller aft dome radius because of scattering events which succeeded in bypassing the cone of LH_2.

4.1.1.4 Orbital Assembly Implications

Economical operation of the RNS for a large number of reuses over an extended period of time requires the capability to remove and replace the NERVA engine in orbit if either it is inoperative or its useful lifetime has been exceeded. A variety of concepts for NERVA replacement in orbit were investigated during Phase II. Orbital assembly interfaces considered were based on the standard engine/stage interface and the propulsion module/propellant module interface. Orbital support for these operations included consideration of large-scale, permanent, shielded maintenance facilities, portable shielding configurations, and unmanned automated operations. The complexity of the alternative orbital assembly interfaces is indicated in Table 4.1-2, which identifies the fluid lines and electrical lines that must be mated during the assembly operation. The fluid lines crossing the ANSC baseline engine/stage interface consist of two 10.5-in.-diameter feed ducts, an aftercooling bypass line, and a pressurant line. For the propulsion module/propellant module assembly interface, this is reduced to only a single 12-in.-diameter feed duct and a pressurant line. The electrical lines crossing the propulsion module/propellant module interface are reduced from the standard engine interface by having the capability to multiplex the engine data at the top of the run tank. Clearly, the propulsion module simplifies the orbital assembly of the stage functional systems and enhances the probability of success of the operation. Also, a standard module docking interface can be provided on the propulsion module, which can be mounted on the standard space shuttle payload support and deployment mechanism for launch to orbit.

The radiation dose levels at the engine/stage interface and the propulsion/propellant module interface are compared in Table 4.1-3 for a 3,300-lb NERVA internal shield and a 7,500-lb LH_2 average loading inside the run tank for a total of 10 missions. The resulting dose attenuation by a factor of 25 to 50 can be crucial and permits locating some engine control boxes at the top of the run tank without requiring additional component shielding.

Table 4.1-2

COMPARISON OF ORBITAL ASSEMBLY INTERFACE COMPLEXITY

Interface	Fluid Lines	Electrical Lines
NERVA/Stage (ANSC Baseline)	4	3,200 to 4,500
Propulsion Module/ Propellant Module	2	700 NERVA +126 Stage 826

Table 4.1-3

COMPARISON OF ORBITAL ASSEMBLY INTERFACE RADIATION DOSE LEVELS

(10 Missions)

Interface	Gamma (rad)	Neutron (n/cm^2)	Total (rad)
NERVA/Stage	10^7	6×10^{15}	2.4×10^7 hydrogenous 1.4×10^7 nonhydrogenous
Propulsion Module/ Propellant Module	5×10^5	10^{10}	5×10^5

Also, the propulsion module concept provides a cold-gas APS (supplied by NERVA tapoff) and minimal controls to stabilize the module for orbital assembly and disassembly. Combined with the remote assembly concepts defined in Section 3.5, this permits autonomous engine removal and replacement without large-scale shielded facilities.

4.1.1.5 Phase II Selection

In summary, the Hybrid configuration has a number of major advantages over the Standard configuration. The module docking interface facilitates NERVA replacement without large-scale orbital support facilities. Lower shield weight and improved propellant management offset the additional structural weight to result in an overall performance advantage. A zone of reduced radiation dose is available at the top of the run tank for stage and NERVA components. The propellant module can be launched to orbit separately, permitting use of existing S-IC and S-II structures. It has the potential of a significant reduction of launch cost by using the space shuttle booster and alternate second stages such as S-IVB to launch the propellant module to orbit while not requiring suborbit start. In addition, it has the potential for lower test program cost by simplifying test facility requirements.

Also, the propulsion module can operate autonomously to provide the propellant for short NERVA burns and aftercooling pulses, permitting more efficient propellant management. Propellant acquisition for NERVA after-cooling pulses is greatly simplified by the run tank because the LH_2 masses and distances of travel are greatly reduced compared to the large single module tank. If pressurization were required for aftercooling pulses, the single module concept would be severly penalized.

Considering all these factors, the Class 1 Hybrid configuration with a separate launch of the propellant module was selected at the end of Phase II as the baseline for an RNS concept utilizing an INT-21 launch. The selected configuration shown in Figure 4.1-1 has a 10-degree half-angle conical bulkhead on the propellant module and a $\sqrt{2}$ ellipsoidal forward bulkhead.

4.1.2 Phase III Configuration Evaluation

A major impact on the Phase II configuration was the desire to investigate the subdivision of the Class 1 Hybrid propellant module into a propellant module and a command and control module (CCM) to facilitate orbital maintenance. The merit of this approach was established for the Class 3 concept during Phase II. The evaluation of this concept is reported in Section 3.15. The reduced orbital support requirements associated with having a CCM led to its selection. Consideration of plume impingement resulted in an outrigger configuration for the CCM to provide sufficient clearance for the APS.

The launch configuration on the INT-21 is evaluated in Section 4.2.3, resulting in selection of a separate launch of the Class 1-H propellant module. The reduced payload envelope results in minimal impact on the launch vehicle. The propellant tank forward bulkhead shape was re-evaluated during Phase III, considering the reduced launch vehicle impact. A hemispherical forward bulkhead was selected in Section 4.2.6 for the Phase III baseline.

A revised NERVA interface permitted an increase in the run tank capacity from 9,500 to 10,850 lb of LH_2.

The resulting baseline configuration for Phase III is presented in Figure 4.1-4.

The Phase III analyses supported selection of the Hybrid configuration for the Class 1 RNS. The Phase II shielding results were confirmed. More favorable launch availability was established. Evaluation of engine/stage structural dynamics during launch indicated the desirability of developing a restraint and load attenuation concept for a single concept – space shuttle

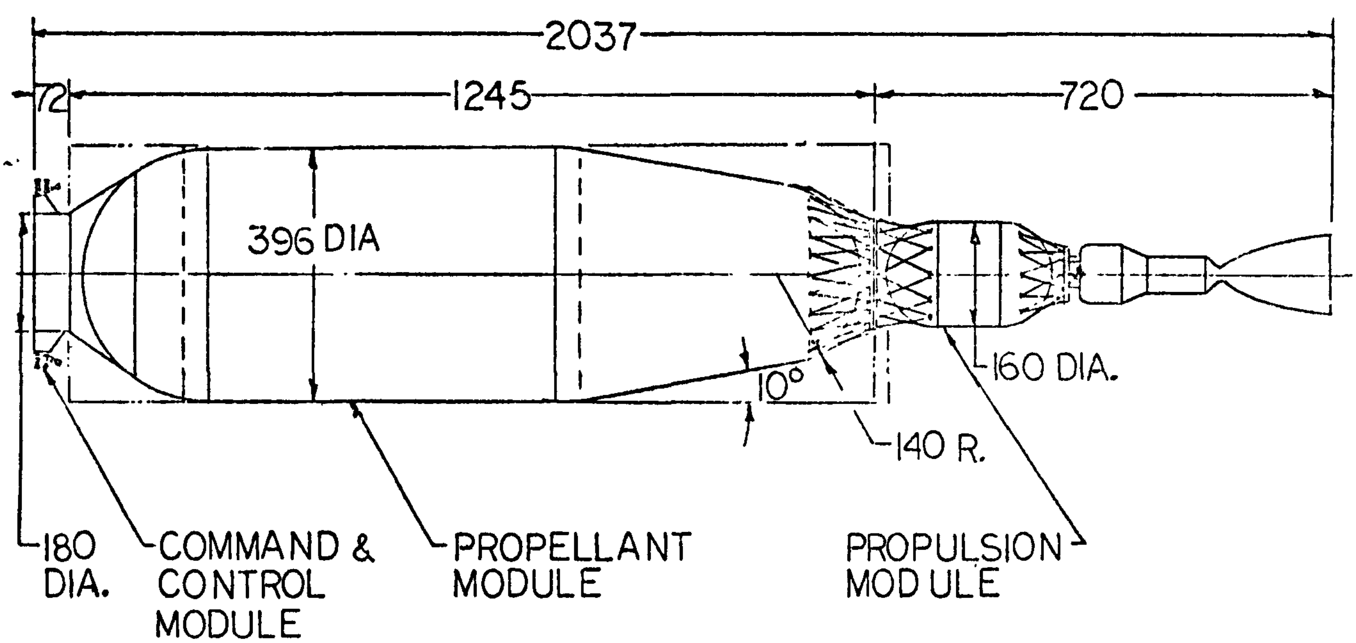

Figure 4.1-4 RNS CLASS 1 HYBRID

launch of the propulsion module. With further definition of RNS operations, additional advantages were identified for the propulsion module for autonomous startup operations by reducing pressurant demand on NERVA and permitting bootstrap propellant tank prepressurization at maximum pressurant temperature. Also, the run tank effectively isolates the nuclear heating of propellant and permits a design with complete mixing of the incoming propellant, which results in a minimal impact.

4.2 STRUCTURE

4.2.1 Phase II Concept

This section establishes the Phase II structures concept and the rationale for the additional analyses performed during Phase III. During Phases I and II, the materials and methods of construction for structural components were selected on the basis of weight, cost, and available technology (see Section 2 of Reference 4-2 for specific tradeoff data). The selected structural features, including the related thermal/meteoroid protection concept, will be reviewed. A load-carrying tank configuration was selected during Phase II. Issues related to the stage configuration are discussed separately in Section 4.1.

The propellant tank material selected was the aluminum alloy 2014-T6, based on performance compared to other aluminum alloys such as 2219, which exhibits superior manufacturing characteristics. The titanium alloy 6Al-4V was also evaluated, and a significant weight saving was identified for this material even without taking advantage of the increased biaxial stress characteristics which can be obtained with texture strengthening of titanium. However, titanium was not selected because it was considered that its technology was not sufficiently developed. Isotropic (60 degrees) waffle stiffening of the cylindrical sidewall was found to be the most efficient compared to alternate constructions. The forward skirt and interstage material selected was aluminum 7075-T73, based on stress corrosion data provided by MSFC. A corrugated construction was initially selected for these, but the alternative of an integrally stiffened forward skirt and interstage was carried forward to Phase II and selected, based on anticipated lower manufacturing cost. Heat blocks were provided at the forward and aft ends of the propellant tank. They were constructed of fiber glass honeycomb to minimize heat input to the propellant. Similarly, the thrust structure was a heat block in its entirety, and was also constructed of fiber glass honeycomb. An integral meteoroid bumper configuration was recommended with a layer of foam and a fiber glass outer shroud applied over the insulation system. This resulted in a lower operating weight and cost than the alternatives of deployable or fixed shrouds, particularly for earth-centered interorbital shuttle missions.

During Phase II, the multiple module RNS configurations were defined, as described in Section 4. 1, and selections made for the new components required. Specifically, fiber glass struts were selected for the intermodule structures and the propulsion module thrust structure when compared to alternate materials and constructions (Section 2. 2 of Reference 4-1). Also, a fiber glass honeycomb payload adapter was incorporated to facilitate equipment mounting. Otherwise, the bases for the inital feature selections remained unaffected by the configuration changes. Phase II was completed with a detailed definition of the design features, as documented in Section 5 of Reference 4-1.

Accordingly, the Phase I and II feature selections were retained, and the structural analyses during Phase III have dealt with refinement of the design criteria and the resulting design implications. The launch configuration of the INT-21 was reevaluated, resulting in changed tank geometry and stiffening requirements. Propulsion module launch support inside the space shuttle was defined. Also, Phase III thermal protection requirements were reviewed to evaluate the tank design pressure and the material and construction of the tank supports and intermodule structures. These analyses are presented in the subsequent sections, and the resulting definition of design features is contained in Book 2. In addition, engine/stage structural dynamics analyses were performed, which are documented in Section 4. 8.

4. 2. 2 Design Criteria

The RNS structural design was analyzed and developed using methods specified by NASA in Reference 4-4, which was provided for the Phase II study by the COR. Additional sources of structural design criteria were utilized which are applicable to space shuttle (Reference 4-5) and the Saturn orbital workshop (Reference 4-6).

4.2.2.1 General Criteria

The Class 1-H RNS reference propellant capacity is 300,000 lb LH_2, as provided by the propulsion module run tank volume plus the volume of the propellant module, including a 5 percent ullage volume (Reference 4-7).

In accordance with the RNS safety criteria specified in References 4-7 and 4-8, single failure points in structural parts are judged incredible if the part can be readily analyzed, i.e., if the geometry is simple, the material properties are known, and the load and strength distributions can be determined with accuracy and confidence.

All pressure vessels are designed so that pressure stabilization is not required for any ground, launch, or mission operation. This philosophy, which was applied for the S-IVB design, was recommended by MDAC for the RNS study. GSE must be designed so that structures will not be subjected to transportation and handling loads more severe than flight design condition.

The design limit values for regulated pressures are based on the upper limit of the relief valve setting, when pressure is detrimental to structural load-carrying capability (Reference 4-5). When pressure increases structural load-carrying capability, the lower limit of the operating pressure schedule is the design limit value. Propellant tanks will accept the design pressure for mission operations at the temperature of the expulsion pressurant.

Sufficient meteoroid protection will be provided for propellant tanks to ensure no penetration (Reference 4-7).

The design of the RNS accounts for dynamic loads (Reference 4-4), including thrust vector interaction, thrust transients, POGO, slosh, staging, docking, zero-elastic, and acoustic conditions. When a detailed dynamic response study cannot be performed within the scope of the study, an appropriate dynamic load factor is used in determining the limit condition. Analysis will account for rigid- and flexible-body dynamics and control-system dynamics of the vehicle.

Structural attachments to propellant tankage are designed to minimize heat input to the tank.

Structures are designed for normal operational loads, and loads arising from abort conditions will be limited to those of normal operations.

Material properties from References 4-9 through 4-12 are used for the RNS design.

The definitions of terminology, including limit load, design load, allowable load, factor of safety, margin of safety, operating pressure, limit pressure, proof pressure, combined stresses, etc., conform to Reference 4-4.

The RNS design employs manned vehicle factors of safety for all modules and all operational phases, with the exception that the propellant module launch on the INT-21 is unmanned. The following factors of safety are applied (Reference 4-4).

1. General Safety Factors:

   Manned Vehicle

Yield Factor of Safety	= 1.10
Ultimate Factor of Safety	= 1.40

   Unmanned Vehicle

Yield Factor of Safety	= 1.10
Ultimate Factor of Safety	= 1.25

2. Propellant Tanks:

   Manned Vehicle

Proof Pressure	= 1.05 x limit pressure
Yield Pressure	= 1.10 x limit pressure
Ultimate Pressure	= 1.40 x limit pressure

   Unmanned Vehicle

Proof Pressure	= 1.05 x limit pressure
Yield Pressure	= 1.10 x limit pressure
Ultimate Pressure	= 1.25 x limit pressure

In circumstances where certain loads have a relieving, stabilizing, or otherwise beneficial effect on structural load capability, the minimum expected value of such loads will be used and is not multiplied by the factor of safety in calculating the design yield or ultimate load (Reference 4-4). When a pressurized system or component is subjected to external loads, such as air loads, ground handling, transportation, in addition to pressure, factors of safety given above are used.

The following tolerances are provided by MDAC to account for manufacturing operations: chem-milling, +0.005 in.; machining, +0.005 in.; honeycomb face sheets, +0.003 in. The provision for weld lands is +15 percent of the component weight after addition of tolerances.

4.2.2.2 Interfaces

NERVA

The definition of the NERVA engine is contained in References 4-13 and 4-14. The following engine parameters apply:

Thrust	75,000 lb
Mass (without external shield)	27,800 lb
Overall length	408 in.
Gimbal point	23 in. (from interface)
Center of gravity	140 in. (from interface)
Thrust vector control	
Displacement	3 degrees
Velocity	0.75 degree/sec
Acceleration	0.5 degree/sec^2

The engine interface configuration utilized with the RNS is the baseline concept of the NERVA 75,000-lb flight-engine design shown on Aerojet drawing 1136339. The structural interface is a bolted connection and is defined in Section 7.3 of Book 2.

The RNS structure is physically and mechanically compatible with the NERVA engine. The design will withstand engine-induced loads (transient, acceleration, and gimbal hardover) and environments (mechanical, thermal, vibration, and radiation). If excessive gimbal actuator loading occurs during launch to orbit, stabilization will be provided.

Space Shuttle

RNS modules launched to orbit inside the cargo bay of the space shuttle orbiter must have external dimensions not exceeding 15-ft diameter by 60 ft long. The RNS modules are compatible with space shuttle provisions for cargo loading and deployment.

The space shuttle performance for launch to the RNS reference operational orbit is 33,000 lb up and down (Reference 4-4). The orbiter is capable of landing with a full payload.

RNS modules launched inside the cargo bay are designed to accommodate the preliminary acceleration load factors shown in Table 4.2-1 which are specified by Reference 4-15. The space shuttle launch is manned.

Table 4.2-1
PRELIMINARY ACCELERATION LOAD FACTORS
SPACE SHUTTLE PAYLOAD COMPARTMENT

(Based on payload at cg location. Sign conventions based on orbiter reference datum, level II requirements)

Mission Phase/Event	Longitudinal (X) Steady (g)	Longitudinal (X) Dynamic (g)	Lateral (Y/Z) Steady (g)	Lateral (Y/Z) Dynamic (g)
Launch Release Transient (within 2 sec of release)	+1.5	±2.0	0	±2.0 (Y & Z)
Lift-off +5 sec	+1.5	±0.25	0	±0.25 (Y & Z)
Max Q-Alpha Region (35 to 55 percent booster burn)	+2.0	±0.40	-0.75 (Z)	±1.5 (Y & Z)
Maximum Acceleration (80 to 100 percent booster burn)	+3.0	±0.25	-0.5 (Z)	±0.25 (Y & Z)
Cutoff/Separation (Within 2 sec of booster cutoff)	0	±3.0	0	±2.0 (Y & Z)
Separation +5 sec	+1.5	±0.25	0	±0.1 (Y & Z)
Maximum Acceleration (60 to 100 percent orbiter burn)	+3.0	±0.25	0	±0.1 (Y & Z)
Reentry	-1.0	0	-4.0 (Z)	±0.1 (Y & Z)
Landing/taxiing/braking	-1.0	0	-2.0 (Z) 0.5 (Y)	±2.0 (Z) ±0.5 (Y)

INT-21

The RNS propellant module will be designed to accommodate launch to orbit by the INT-21 launch vehicle, based on the Saturn V S-IC and S-II stages. Requirements for this vehicle are defined by Reference 4-16. The launch is unmanned. A launch vehicle operations policy is applied so that the existing Saturn V design loads are not exceeded. Launch vehicle allowables and wind criteria implications are identified in References 4-3 and 4-17.

Provisions for launch vehicle instrument unit equipment are made within the envelope of the RNS interstage. The existing forward attach pattern of the S-II is utilized. The propellant loading of the RNS module conforms to a gross weight above the S-II at launch of 249,000 lb.

Payloads

A maximum mission payload 15 ft diameter by 140 ft long of uniform density, weighing 118,000 lb, with a stiffness equal to the propellant tanks is considered for analysis of the structural design.

4.2.2.3 RNS Operational Requirements

Propulsion Module

Transportation and Handling — The propulsion module structure will be designed to accommodate transportation by slow-moving dolly and barge, or air (guppy). Limit load factors are defined in Table 4.2-2, based on Reference 4-18.

Prelaunch—The propulsion module is designed to permit loading (and removal, if required) in the space shuttle orbiter cargo bay with the orbiter in a horizontal position before booster mating. The design of the attachments and support structures will accommodate orbiter operations for erection and mating with the booster during launch preparation. Limit load factors will be 2.0 g vertical and 0.5 g in any horizontal direction.

Table 4.2-2
LOAD FACTORS FOR TRANSPORTATION MODES

Mode	Condition	Limit Load Factors (g) (Relative to the Transporter)			Description of Loading Condition
		Longitudinal	Lateral	Vertical	
Ground	(1)	±0.75	±0.5	-3.0	Road bumps
	(2)	0	±0.75	-3.0	Turning
	(3)	±1.0	±0.5	-2.0	Quick starts and stops
Water	(1)	±0.7	±0.8	-1.8 -0.2	Barge hull oscillations (6-10 Hz) during heavy sea conditions, 40 knot winds.
	(2)	±0.5	±1.0	-1.3 -0.7	Deep draft ship - 30 degree roll, 20 foot seas, 40 knot winds. (roll frequency 1/7 to 1/5 Hz)
	(3)	±0.5	±0.6	-2.5	Ship or barge - maximum vertical acceleration - 20 to 25 foot seas (pitch frequency 1/5 to 2/5 Hz)
Super Guppy	Emergency Landing:				(CAR 4b.260)
	(1)	-4.00	0	0	Max. Forward
	(2)	0	±1.00	0	Max. Sideward
	(3)	0	0	+1.33	Max. Upward
	(4)	0	0	-3.00	Max. Downward
	Landing:				
	(5)	0	±0.72	-1.00	40 knot cross wind
	(6)	-1.00	0	-1.00	Braking
	Flight:				
	(7)	-0.57	0	-2.00	Gust
	(8)	±0.33	±0.33	-2.50	Gust
	(9)	-0.22	0	±1.00	Gust

NOTES: (+) sign indicated aft, port, and up. (-) sign indicates forward, starboard, and down.
With each condition, include the effect of a 45 knot wind on the RNS.
In each condition include the effect of a 70 knot wind gust if the transporter (RNS) is not sheltered.

The run tank is dry, unpressurized, and purged with inert gas for launch operations.

Launch—The propulsion module is designed for launch to orbit in the space shuttle orbiter cargo bay. The launch loads are specified in Table 4.2-1. Vibration isolation and load attenuation will be provided by the propulsion module. Stabilization will be provided as required.

Assembly—The propulsion module will be deployed from the space shuttle in orbit. The standard space shuttle deployment mechanism is utilized. The design will accommodate the specified interface, mechanism operation, and poison wire removal in orbit. Docking loads are based on any combination of relative velocities and attitude misalignments at initial contact between this module and other modules. The structure will be designed for RNS assembly operations, including provisions for mounting of functional subsystems to simplify rendezvous, docking, mating and demating of lines, and checkout.

Mission Operations—The run tank will accept the design pressure at the temperature of the expulsion pressurant, as established by propulsion system requirements. The design will accommodate NERVA-induced loads and environments (mechanical, thermal, vibration, and radiation). The module design will satisfy vehicle stability and controllability requirements.

Propellant Module

Transportation and Handling—The launch interstage will be transported separate from the propellant module tankage. Both components are designed to be transported by slow-moving dolly or barge. Limit load factors are defined in Table 4.2-2. The interstage will be mated to the propellant tankage at KSC.

Prelaunch—The RNS propellant module will be designed to comply with the INT-21 prelaunch design load envelope. The RNS structure and protective measures will be limited to the exposure duration and risk level as established by the INT-21 design.

All ground wind environment is based on Reference 4-19. Definition of peak wind speed for exposure periods and percentiles of exceedance and its variation with altitude are given in Section 5.2.5 of that report. Definition of gust factors to be applied to peak wind to obtain mean wind and ground wind turbulence data are presented in Section 5.2.6 and 5.2.7 of Reference 4-19, respectively.

The following preliminary criteria for ground wind at KSC are applied: on-pad, unfueled, unpressurized, 30-day exposure, 5 percent risk; peak wind speed of 33.1 m/sec from any azimuth, measured at the 18.3 m reference level with the associated three sigma profile shape given in Table 5.2.15 of Reference 4-19. These wind velocities are presented in Table 4.2-3. It is noted that these criteria are conservative for the RNS design, since the analysis of the INT-21 with a payload envelope approximating the RNS propellant module contained in Reference 4-3, indicates that for the above criterion the INT-21 design loads are exceeded by a small margin.

Table 4.2-3
PEAK WIND PROFILE (KSC)

Height		Velocity	
(m)	(Ft)	(Knots)	(Ms^{-1})
10.0	33	60.1	30.9
18.2	60	64.4	33.1
30.5	100	68.3	35.1
61.0	200	74.0	38.1
91.4	300	77.6	40.0
121.9	400	80.2	41.3
152.4	500	82.3	42.3

Launch—The RNS propellant module is designed to comply with the INT-21 launch and ascent design load envelope, including maximum ($q\ \alpha$) and maximum longitudinal acceleration. The nominal, no-wind INT-21 launch trajectory (for injection into a 100 nmi by 260 nmi orbit) defined in Reference 4-3 yields a maximum dynamic pressure of 732 psf and maximum axial acceleration of 4.387 g.

The ascent wind environment is based on Reference 4-19. Definition of wind speeds for exceeding percentile and its variation with altitude are given in Section 5.3.6 of that report. Shear envelopes and gusts are defined in Sections 5.3.7 and 5.3.8, respectively. Synthetic wind profiles constructed according to Section 5.3.9 are used.

The preliminary RNS loading envelope is normalized to the current design loading at the S-II interface (2,540 lb/in.). A policy of utilizing a wind-biased launch trajectory and accepting a minimum seasonal launch availability of 84 percent for winter winds is applied.

The structural design includes provision for venting enclosed compartments and insulation.

Assembly—The structure will be designed for assembly operations, including provisions for mounting of functional subsystems to simplify rendezvous, docking, mating, and demating of lines, and checkout.

Mission Operations—Same as propulsion module run tank.

Command and Control Module

The operational requirements for the CCM are the same as for the propulsion module, except run tank and poison wire removal criteria are not applicable.

4.2.3 Launch Configuration

The large envelope for the RNS can increase structural loading above the current design value for the INT-21. Optimal control theory was investigated during

Phase II and found promising for minimizing structural modifications to the S-IC and S-II vehicles. Concurrent with the Phase III RNS study a comprehensive evaluation of the loading implications for a range of payload envelopes on the INT-21 vehicle was performed by Boeing (Reference 4-3). The payloads considered included Skylab, space station concepts, and RNS concepts. All are to be launched unmanned. The criteria used for the study included a 30-day exposure and 5 percent risk for ground winds at KSC and a 5 percent risk for launch release. The parametric results are summarized in Figure 4.2-1 in terms of launch availability vs. payload length. Several RNS launch configurations considered during Phase II are summarized in Table 4.2-4. The payload height including a 30-degree nose cone is indicated.

The Class 1 Hybrid, which permits launch of the propellant module by itself, provides the most favorable launch availability. Also, the Phase III concept of a separate CCM permits further reduction of the propellant module launch envelope. The propellant module could be launched inverted, as indicated in the table. However, this is undesirable because it would impose the require-

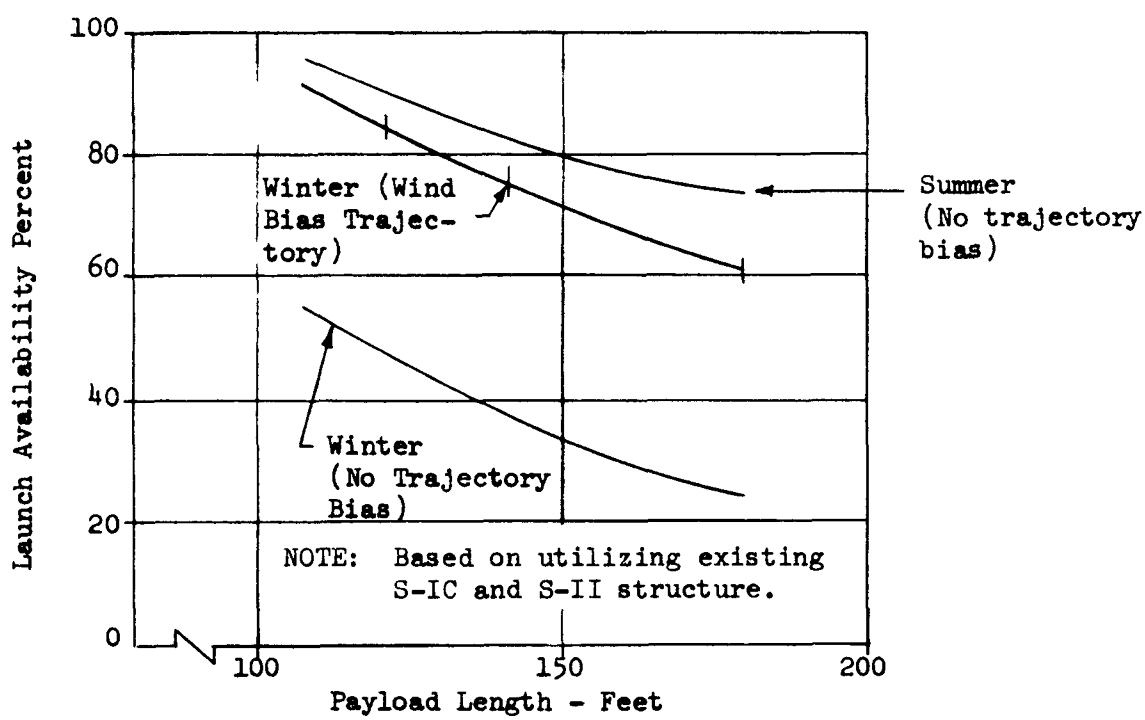

Figure 4.2-1 INT-21 LAUNCH AVAILABILITY WITH SA-511 CAPABILITY

Table 4.2-4

RNS LAUNCH CONFIGURATION COMPARISON

Payload Launched by INT-21	Bulkhead Geometry	Payload Height (ft)		Launch Availability (percent)*
		Without Nosecone	With 30 deg Nosecone	
<u>Phase II Concepts</u>				
1. NFPM	2 Ellipsoidal Forward and Aft	128.3	154.6	67
2. Class 1 Standard	10° Cone Aft $\sqrt{2}$ Ellipsoidal Forward	157.2	183.5	60
3. Class 1 Hybrid	10° Cone Aft $\sqrt{2}$ Ellipsoidal Forward			
a. Propellant Module		102.8	129.1	80
b. Propellant Module Inverted		85.9	112.2	87
<u>Phase III Concepts</u>				
4. Class 1 Hybrid	10° Cone Aft Hemispherical Forward			
a. Propellant Module + CCM		104.4	130.7	80
b. Propellant Module		92.2	118.5	84

* Winter winds, wind-biased trajectory

ment of a second flight vent system located at the tank aft bulkhead for launch to orbit and would complicate integration of a ground fill system interfacing with the conical aft bulkhead. Additional configurations considered during Phase III are also summarized in Table 4.1-2.

In the concept adopted as the Phase III baseline, the Class 1-H propellant module is launched upright by itself. Thus, the propulsion module and CCM are designed for launch inside the space shuttle for initial RNS assembly or normal replacement operations. The propellant module launch envelope is shortened by 12 ft when launched without a CCM. This results in a 84 percent launch availability for the worst winter winds. For summer winds, availability increases to 90 percent without wind biasing. Further improvements could be obtainted with the previously cited optimal control concept.

While the RNS envelope does require changes from current Saturn V launch practice, the use of wind-biased trajectories provides substantial increases in launch availability, while retaining existing S-IC and S-II structure. The restrictions on the Class 1 Standard or NFPM configurations are severe, but it is probably unwarranted to exclude them on this basis alone, considering that it is not necessary to meet precise launch windows for unmanned launches without payloads.

An evaluation of engine/stage structural dynamics was performed during Phase III (see Section 4.8) to evaluate launch of NERVA in both the Class 1 Standard and integral Class 1-H configurations on the INT-21 vehicle. Significant amplification of the launch lateral acceleration transient was obtained, which indicates a potentially serious impact on the NERVA core. Since a shuttle launch is required to accomplish NERVA replacement, it is probably most economical to develop a restraint and load attenuation concept for only a single launch concept. This further enhances the desirability of the hybrid configuration, with a normal separate launch of the propulsion module by the space shuttle.

4.2.4 Loading Analysis

Rigid-body analyses were performed to derive inertial loads on the propellant module for the following conditions: (1) transportation based on the load factors in Table 4.2-2, (2) prelaunch based on the wind profile presented in Table 4.2-3, (3) launch for both max q-α and maximum acceleration complying with the trajectory and ascent wind environment defined in the design criteria, and (4) mission operation with the engine gimbaled hardover at 5.7 degrees ($\sqrt{2}$ x 3 degrees for control plus 1.5 degrees for misalignment under full thrust, 75,000 lb).

The MDAC SA-33 ADMUS computer program, which consists of a series of interrelated subroutines within a mission analysis and vehicle design subprograms, was used to generate the loads for the launch conditions. Mach number, angle of attack, and dynamic pressure are inputs to the program. Axial and normal aero force distribution, total normal force, center of pressure, center of gravity, control force, and lateral and rotational accelerations are computed by the program and converted to shears and moments on the vehicle body. From these the loads are generated. The prelaunch and launch loading envelope, shown in Figure 4.2-2, was normalized to agree with the current design load at the S-II interface.

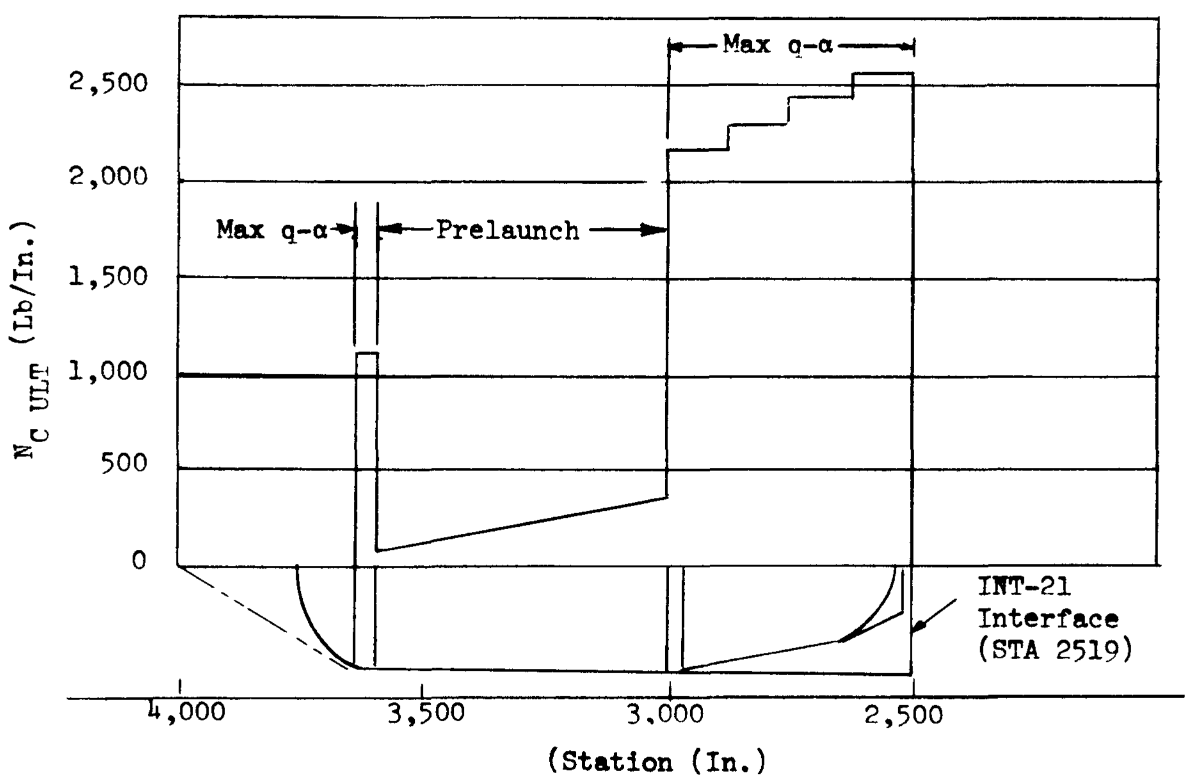

Figure 4.2-2 CLASS 1-H APPLIED LOAD DISTRIBUTION

The mass distribution for the Class 1-H was computed for five time points during the reference mission propellant depletion history. The condition of the engine gimbaled hardover at 5.7 degrees under 75,000 lb of thrust was input into the MDAC SB-15 "Structural Load Histories" program for the propellant depletion history to obtain moments, shears and axial loads during engine operation. The maximum load case occurred with both modules full and produced the limit loads shown in Table 4.2-5.

4.2.5 Propellant Tank Pressure

The tank weight sensitivity to design pressure is defined in Section 4.2.7. Thermal protection requirements (insulation and boiloff) are defined in Section 4.3. These are combined with the residual gas weight for the lunar shuttle mission profile to establish the total weight penalty for the tank design pressure. The pressure schedule defined in Section 3.12.2 was applied, which sets the tank design pressure at 3 psia over the required NERVA operating pressure, based on sensor tolerances, line losses, and propellant system operational requirements. Since the boiloff is vented

Table 4.2-5
COMPONENT LIMIT LOADS - MISSION OPERATION

Module	Component	Moment (in.-lb x 10^6)	Shear (lb)	Axial Load (lb)
Propulsion	Thrust Structure	0.74	5,750	69,750
	Intermodule Skirt	2.47	5,120	67,850
Propellant	Intermodule Thrust Structure	2.47	5,120	67,850
	Payload Adapter	3.42	2,680	16,820
CCM	Cylinder	3.42	2,680	16,820

during the mission, it has less impact on the performance than inert weight. The effective boiloff penalty is about half of the actual boiloff on the lunar shuttle mission.

The separate factors cited and total system weights are plotted in Figures 4.2-3 and 4.2-4 for two thermal protection system design strategies. The selected thermal protection design approach (Figure 4.2-3), entails venting of tank conditioning propellant and orbital coast heating to reduce the equivalent time and increase the propellant heat capacity for the mission. With this strategy, a reduction of the tank design pressure from the current baseline of 29 psia (imposed by the 26-psia NERVA requirement) to the vicinity of 24 psia is desirable. No vented boiloff would be incurred during the mission in this circumstance. The second approach (Figure 4.2-4), provides no venting for propellant conditioning before mission operation. This most severe thermal design requirement results in a negligible weight improvement by reduction of the tank design pressure.

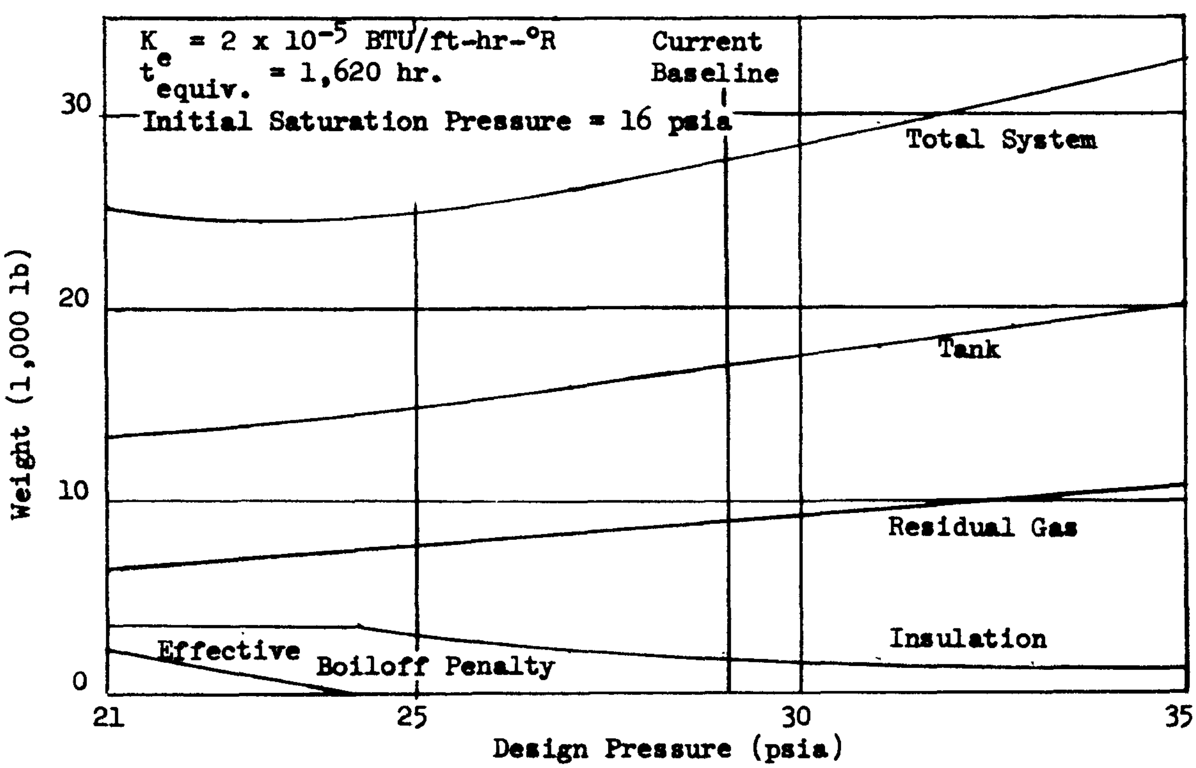

Figure 4.2-3 TANK PRESSURE OPTIMIZATION - CLASS 1-H PROPELLANT MODULE

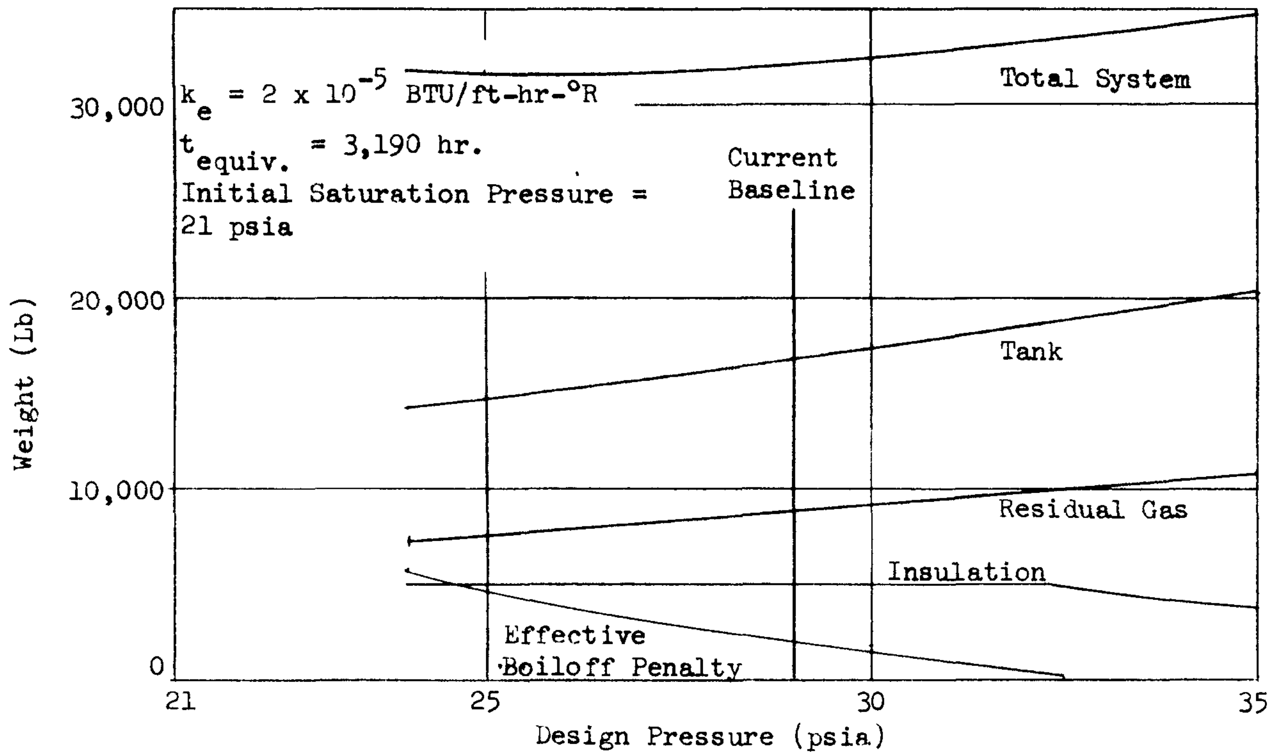

Figure 4.2-4 TANK PRESSURE OPTIMIZATION - CLASS 1-H PROPELLANT MODULE

The additional weights associated with the run tank and meteoroid protection were not included in the evaluation. These would slightly increase the bias toward a lower design pressure. Additional propellant subcooling would also increase this bias.

4.2.6 Forward Bulkhead Shape

An evaluation of the forward bulkhead shape was performed in which a hemispherical configuration was compared to an ellipsoidal configuration. The ellipsoidal shape had been selected as a baseline during Phase II, when module length had a major impact on launch vehicle loading for the RNS standard configuration. However, the current design criteria for launch of only a propellant module as a payload on the INT-21 alleviates this condition, and a more efficient design can be considered. For both configurations the tanks were sized to contain 290,500 lb of LH_2 with a 5 percent ullage volume and were designed for a pressure of 29 psi. The hemispherical dome weighed 90 lb more than the ellipsoidal, but because of increased volumetric efficiency, it reduced the integrally stiffened sidewall length by 29 in., which resulted in a weight savings of 690 lb. Also, the hemispherical configuration achieved a surface area reduction of approximately 1 percent. This resulted in an insulation and meteoroid protection weight reduction of 60 lb which combined with the tank weight savings for a total system weight savings of 660 lb. Thus, the hemispherical forward bulkhead shape was selected as the new baseline. Overall stage length with the hemispherical configuration is 19 in. longer than for the ellipsoidal.

4.2.7 Propellant Tank Stiffening

The propellant module tankage sidewalls, which are fabricated from 2014-T6 aluminum alloy, were analyzed to determine if integral reinforcement was required as a result of the various design loads. The conditions investigated were: (1) transportation with the load factors contained in Table 4.2-2 applied, (2) prelaunch using the peak wind profile contained in Table 4.2-3, (3) launch during max ($q\ \alpha$) based on the trajectory criteria contained in Section 4.2.2, and (4) RNS engine operation at full thrust with the engine gimbaled hardover at 5.7 degrees. The resulting ultimate loads for the design conditions are presented in Table 4.2-6.

These loads were used to determine the amount of stiffening required, if any, for the various design conditions. Reference 4-20 was employed to determine the buckling allowable for monocoque construction while the method described in References 4-21 through 4-24 based on Donnell-type buckling solutions applying a correlation factor of 0.65 was used to determine the buckling

Table 4.2-6
DESIGN CONDITION LINE LOADS

Condition	Nx_{ult} (lb/in.)
Transportation	170 compression
Prelaunch	335 compression
Launch (Max $q\ \alpha$)	1040 tension
Engine operation	95 compression

allowable for integrally stiffened cylinders. Only isotropic (60 degree) stiffening was considered based on the results of a trade study performed during Phase II of this study (Reference 4-1, page 2-18).

The analysis indicated that a monocoque tank designed for 29 psi was capable of resisting the buckling loads imposed during engine operation under zero ΔP and transportation. Zero ΔP may occur during engine operation as a result of a vent valve malfunction or a meteoroid penetration. For the transportation condition, the module was assumed to be supported at the forward end of the forward skirt and the aft end of the intermodular thrust structure. The max q α condition was investigated because the tank is launched off-loaded under saturated LH_2 pressure (16 psi), rather than being pressurized to the design pressure during flight through the sensible atmosphere. However, even though the tank experiences essentially a zero ΔP on the ground, it will be exposed to an internal pressure of 13.3 psi when max qα occurs. This pressure differential is sufficient to overcome the compressive forces resulting from bending and axial loads and to ensure a tension load in the tank sidewalls.

In the case of the prelaunch condition, the 335-lb/in. compressive line load produced buckling in an unpressurized monocoque tank. For this condition additional stiffening must be provided or the tank must be pressure stabilized. Pressure stabilization is undesirable from a safety standpoint; therefore, the tank cylinder was integrally reinforced. This is in accordance with the S-IVB design philosophy. The weight penalty for the additional stiffening is minimal (590 lb). Figure 4.2-5 depicts the weight of an integrally stiffened tank for a range of design pressures and was used for the propellant tank pressure study in Subsection 4.2.5.

The propulsion module tankage was also analyzed for the same conditions as the propellant module with resulting ultimate compressive line loads of 20, 90, and 340 lb/in. for transportation, launch, and engine operation, respectively. For the transportation condition the loads were computed based on transporter support points at the aft end of the thrust structure and the forward end of the skirt. In addition the NERVA was not attached to the module. In the case of the space shuttle launch, the NERVA was assumed

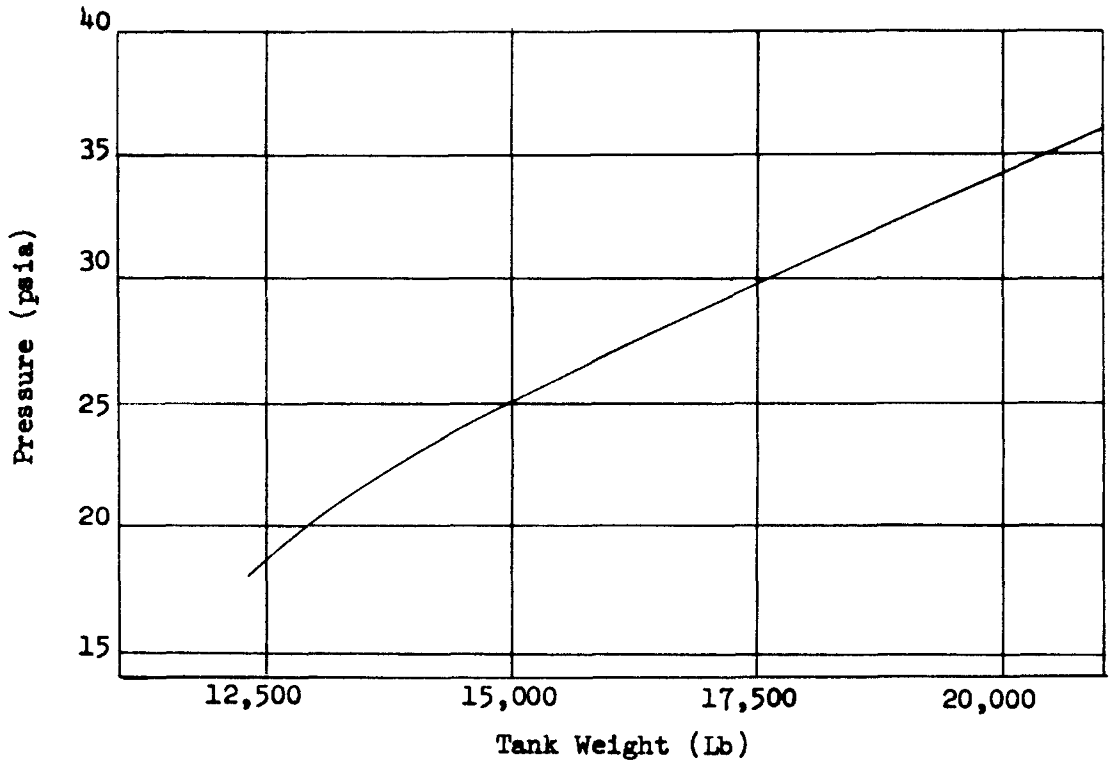

Figure 4.2-5 CLASS 1 HYBRID PROPELLANT TANK PRESSURE SENSITIVITY (INTEGRALLY STIFFENED)

to be stabilized at its center of gravity by supports within the shuttle. As noted above, engine operation produced the greatest loads. At the design pressure of 30 psi, an integrally stiffened tank designed to resist engine operation loads only suffers a 20-lb weight penalty over one of all monocoque construction.

4.2.8 Tank Supports and Attachments

A trade study was conducted to evaluate the materials and method of construction for structural components which attach to the propellant tankage and therefore result in a heat short. These include the intermodule structure, thrust structure, and payload adapter.

Based on the results of a similar trade study for the Class 3 (Volume II, Part B), only the three most efficient candidates from an overall cost were analyzed. These were: (1) fiber glass struts, (2) fiber glass honeycomb sandwich, and (3) titanium (Ti 6Al-4V) struts.

Component limit loads are defined in Table 4.2-5. All configurations were analyzed for general instability and local buckling. References 4-20 and 4-25 were employed for honeycomb sandwich construction. General instability for the strut designs was analyzed using the Euler column formula. The strut thickness was determined by the modified Euler equation of Von Karman and Tsien. A summary of the loads, weights, and selected designs is presented in Table 4.2-7 (closing frame weights are not included).

The tubular fiber glass struts are wrapped with the titanium end fittings in place. A precision casting is used to make the central X-section splice and threads are machined onto the fitting employing a boring mill to ensure a close tolerance on the angle subtended by the legs of the X-fitting.

Parallelism of dome and interface ring attach points and their centerlines is established by tool masters. Master tooling is used to locate and drill the holes in the strut end fittings, interface ring, and dome lugs. Attach points are machined perpendicular to the plane of the strut subassemblies with the clevis slot oversize. After the subassemblies are positioned in the clevises, washers are installed to ensure a tight fit.

The cost of manufacturing each candidate material and construction was estimated using current MDAC CER's. Considered in the manufacturing cost was the subassembly, and installation of the strut subassemblies. The manufacturing cost for all structural attachments is cumulated in Table 4.2-8.

The heat input to the tank was a major factor in comparing the candidates. Thermal performance of the components insulated with HPI was analyzed in detail, and is discussed separately in Section 4.3.6. Using DAM/Dacron net spacer HPI, a 3-ft insulated length was obtained for the fiber glass components compared to 6 ft for titanium. The thickness was optimized for system performance. The resulting HPI weight and equivalent boiloff weight are shown in Table 4.2-8.

Table 4.2-7
SUPPORT STRUCTURE CONFIGURATION COMPARISON

		Propellant Module		Propulsion Module	
		Intermodule Thrust Structure	Payload Adapter	Forward Skirt	Thrust Structure
Construction	Forward Diameter (in.)	246	180	160	140
	Aft Diameter (in.)	160	310	160	60
	Length (in.)	87	92	70	70
Fiber Glass Struts	Number	48	32	24	24
	Diameter (in.)	5.25	6.0	4.125	4.625
	Wall Thickness (in.)	0.065	0.070	0.055	0.065
	Length (in.)	100.4	121.7	81.3	84.0
	Load (lb/strut)	14,360	16,430	9,000	12,710
	Weight (lb)	563	501	185	205
Fiber Glass Honeycomb	Face Thickness (in.)	0.015	0.015	0.015	0.015
	Core Height (in.)	0.875	0.686	0.50	0.625
	Load (lb/in.)	Nxc - 190 Nxb - 120	Nxc - 40 Nxb - 190	Nxc - 190 Nxb - 140	Nxc - 520 Nxb - 370
	Weight (lb)	402	523	221	173
Titanium Struts	Number	48	32	24	24
	Diameter (in.)	4.75	5.5	3.875	4.125
	Wall thickness (in.)	0.022	0.25	0.018	0.022
	Length (in.)	100.4	121.7	81.3	84.0
	Load (lb/strut)	14,360	16,430	9,000	12,710
	Weight (lb)	363	344	118	138

Table 4.2-8
STRUCTURAL ATTACHMENT COST COMPUTATION (OPTIMIZED HPI THICKNESS)
(Reference Lunar Shuttle Mission)

	(1) Material and Configuration (HPI Layup in Parentheses)	(2) Total Structural Weight (lb)	(3) Total Mfg Cost ($)	(4) Total HPI Weight (lb)	(5) Total Inert Weight (lb)	(6) Inert Weight Transportation Cost Per Mission ($)	(7) Total RNS Boiloff on Mission (lb LH_2)	(8) Cost of Boiloff per Mission ($)	(9) Total Cost per Mission ($)
		*	**	***	(2) + (4)		***		$\frac{(3)}{10}$ ÷ (6) + (8)
Fiber Glass Strut	Propellant Module (0.387 in., 0.396 in. x 3 ft)	1,064	546 K	44	1,108		45		
	Propulsion Module (0.48 in. x 3 ft)	390	213 K	33	423		51		
	Total	1,454	759 K	77	1,531	766 K	96	27 K	849 K
Fiber Glass Honeycomb	Propellant Module (0.30 in. x 3 ft)	925	694 K	45	970		42		
	Propulsion Module (0 392 in x 3 ft)	394	307 K	35	329		62		
	Total	1,319	1,001 K	80	1,299	650 K	104	29 K	779 K
Titanium Strut	Propellant Module (0.742 in., 0.775 in. x 6 ft)	707	177 K	164	871		376		
	Propulsion Module (1.26 in. x 6 ft)	256	65 K	141	397		772		
	Total	963	242 K	305	1,268	634 K	1,148	298 K	956 K

* Based upon strength requirement

** To be amortized over 10 missions for RNS

*** $K_c = 2.0 \times 10^{-5}$ Btu/hr-ft-°R

The total system cost per mission is compared in Table 4.2-8, consisting of the manufacturing cost (amortized over 10 missions), the transportation cost of the inert weight, and the transportation cost of the boiloff, which can be vented en route. The fiber glass honeycomb construction is found to be most cost effective. However, the weights are idealized and can be increased by design factors not included here. Also, insulation layup has subtleties which could increase the thermal protection penalty for the honeycomb construction. It was decided to retain the fiber glass struts as a baseline to obtain greater visibility of its design and manufacturing implications.

Upon completion of the above study an improved method of analysis was developed for the truss structure struts which took into account the consistency of the applied loads and reactions at the truss support. The resulting strut loads decreased for all of the structural components. The pertinent data are presented in Table 4.2-9 with closing frame weights included. The payload adapter is not included because a fiber glass honeycomb sandwich construction was selected for it based on propulsion component and equipment mounting considerations. In order to have a common propulsion module for both the Class 1-H and the Class 3, the struts were sized for the Class 3 loads. This resulted in a forward skirt that weighed 250 lb and a thrust structure that weighed 170 lb.

Table 4.2-9
FIBER GLASS STRUT CONSTRUCTION

	Propellant Module	Propulsion Module	
	Intermodular Thrust Structure	Forward Skirt	Thrust Structure
Forward Diameter (in.)	246	174	120
Aft Diameter (in.)	174	160	60
Separation (in.)	87	70	45
Number of Struts	48	24	24
Diameter (in.)	5.0	4.0	3.5
Wall Thickness (in.)	0.045	0.055	0.065
Length (in.)	100.4	81.3	58.8
Load (lb/strut)	6,330	8,070	10,630
Weight (lb)	470	230	160

4.2.9 Propulsion Module Launch Support

A concept for propulsion module support in the shuttle cargo bay is illustrated in Figure 4.2-6. In this baseline scheme the module with the engine mated to it is loaded into the space shuttle while both are in a horizontal attitude with the propulsion module tank empty and unpressurized. Loading pickup points for the module are compatible with those for the transportation mode (i.e., forward end of the intermodular skirt and aft ring of the thrust structure). An additional pickup is provided at the engine support plane.

After the module is loaded in the cargo bay, it is latched to the shuttle payload adapter attach points. Longitudinal and vertical loads are transmitted to the shuttle by this support. In addition two other supports are provided, one at the aft ring of the thrust structure and the other at the engine support plane. These transmit lateral and vertical loads to the shuttle and are mounted on rails to compensate for relative longitudinal motion between the shuttle and the propulsion module. Lateral loads are transmitted to the payload bay door sills while vertical loads are transmitted to the payload bay keel. Engine support is required because the launch and boost loads associated with a shuttle launch impose requirements on the propulsion module and NERVA which exceed those anticipated for nuclear engine operation in space. The tankage loads associated with this support scheme were determined for launch and are denoted in Section 4.2.7.

Module stabilization at the thrust structure aft ring is required to minimize the launch loads induced into the propulsion module tankage, thrust structure and forward skirt. Engine support is shown at the bell throat because this was the location selected by the engine contractor (Reference 4-26) for the RNS Class 1 standard configuration.

It would be possible to reduce loads on the gimbal and the gimbal actuators if this support location was relocated at the engine center of gravity. An alternative is to provide additional stabilizing members at the forward end of the engine.

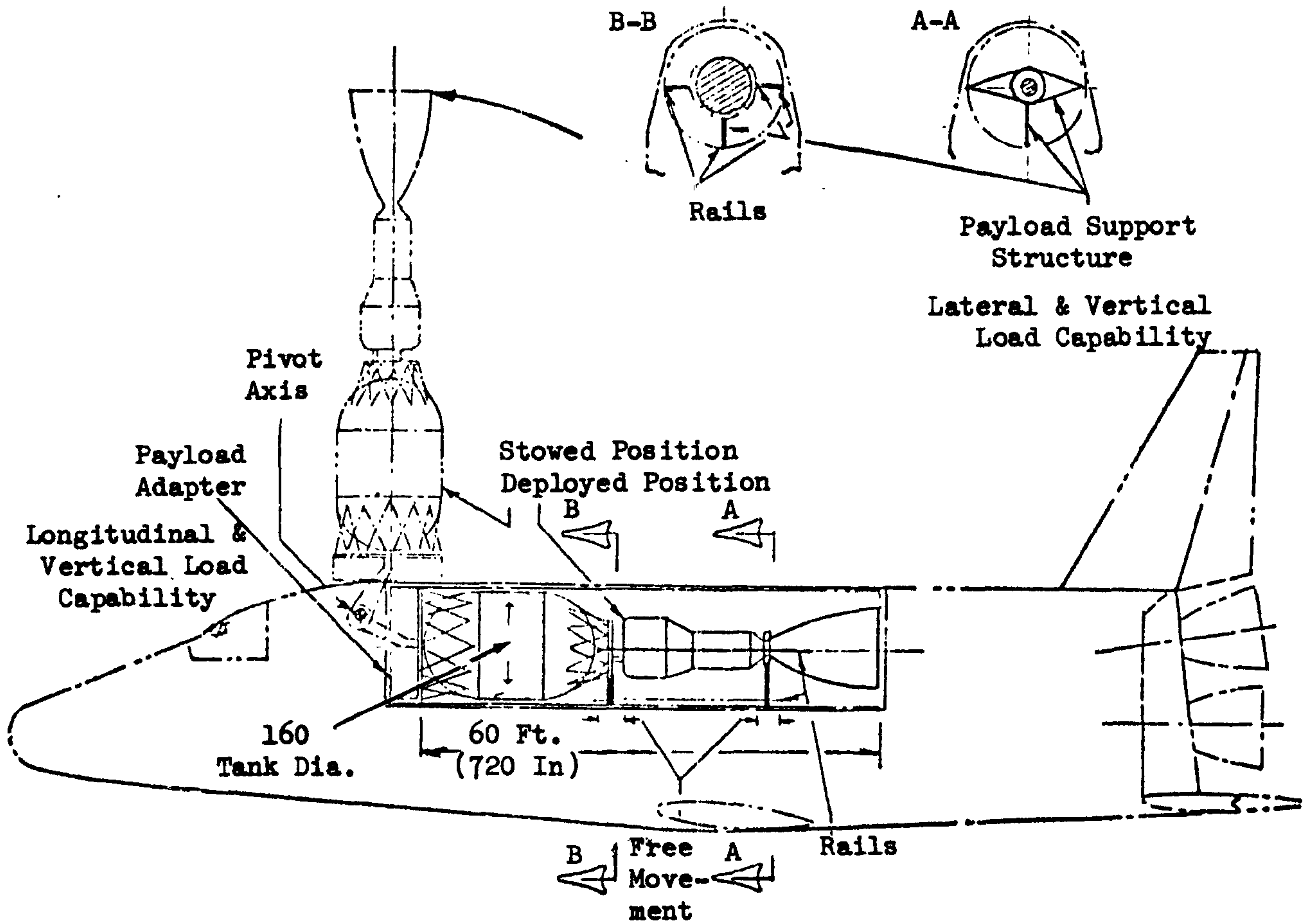

Figure 4.2-6 PROPULSION MODULE LAUNCH SUPPORT

Module deployment is effected by first releasing and retracting the thrust structure and engine supports and then actuating the payload adapter to rotate the module out of the cargo bay. After the module is deployed, the payload-adapter latches are released and the propulsion module draws away from the shuttle employing its auxiliary propulsion system.

A preliminary static analysis was performed on the thrust structure and engine supports to ascertain the weight penalty incurred by the orbiter for this structure. The launch acceleration load factors are contained in Table 4.2-1. The most severe vertical and longitudinal loads occurred during reentry and launch release transient respectively. Results of the analysis produced a total support system weight of 80 lb.

The two methods of engine support recommended by Aerojet-General Corporation for the integral launch configuration have been analyzed and are discussed in Section 4.8 which covers structural dynamics for the hybrid. Because of unresolved questions concerning the excitation transient a satisfactory support system cannot be selected at this time.

4.2.10 Radiation Effects

A literature search was performed to assess the effects of nuclear radiation on fiber glass structural components and adhesives. Fiber glass structures are used extensively in the RNS as tank supports and attachments to reduce heat input to the propellant. Adhesives are used primarily to bond plastic stand-off insulators and clips to the tankage and for bonding fiber glass face sheets to fiber glass honeycomb.

The gamma dose rate and fast neutron flux are defined in Section 4.5.11. The critical location is the propulsion module aft zone, with a dose criterion for 10 round trips of 10^8 rads, which includes a factor of 10 safety margin.

All types of laminated fiber glass are relatively invulnerable to radiation, since most of the strength is contributed by the glass. Glass impregnated by phenolic is the most radiation-resistant, showing only slight mechanical damage (slight embrittlement of the phenolic) at a dose of 10^{10} rads. Fiber glass impregnated with polyester or silicone resin shows significant deterioration (embrittlement) beginning at a dose of 3×10^9 rads (Reference 4-27). Fiber glass impregnated with epoxy as is envisioned for use on the RNS has a radiation damage threshold of 10^9 rads and significant damage does not occur until 10^{10} rads (Reference 4-28).

The shear strength for two adhesives was measured at LH_2 temperature at a total dose of 1.7×10^8 rads (Reference 4-29); an epoxy-Polyamide would degrade 40 percent, and a polyurethane only about 25 percent. Additional radiation tests of adhesives at cryogenic temperatures are recommended.

4.3 METEOROID/THERMAL PROTECTION

4.3.1 Phase II Concept

This section establishes the Phase II meteoroid/thermal protection concept and the rationale for the further analyses performed during Phase III.

During Phase I of the NFPM study meteoroid/thermal protection system, concepts were evaluated for a set of study mission applications including expendable injection stage missions, interorbital shuttle missions, and expendable manned Mars missions (see Section 2.4 of Reference 4-2 for specific tradeoff data). Three candidate insulations, foam, doubly aluminized Mylar (DAM)/foam, and DAM/Nylon net, were considered compressible and were evaluated for the load-carrying tank configuration, for which the insulation would be compressed during launch. Three other candidate insulations, DAM/tissuglas, Superfloc, and NRC-2, were considered unsuitable under compression and were considered only for the load-carrying shell NFPM configuration, which was a candidate at that time.

The alternatives considered for meteoroid protection included a load-carrying ascent shell, a deployable shroud, and an integral foam bumper with a fiber glass protective shroud. Considering the mission performance implications of the combined requirements for thermal and meteoroid protection as well as the implications of compressibility for HPI conductivity, the system selected during Phase I was the DAM/Nylon net insulation system together with an integral foam meteoroid bumper and fiber glass protective shroud. As test data indicated outgassing probelms for the Nylon net spacer, a Dacron net spacer was substituted.

During the Phase II a design of the meteoroid/thermal protection system was made (see Section 2.5.3 of Reference 4-2). A major concern was the integration of the foam bumper external to the HPI blankets. The reference design was based on the lunar shuttle mission and consisted of an armor surface density of 0.75 psf including 54 layers of DAM/Dacron net insulation. Dimensional changes were evaluated for the thermal cycling of the system. The insulation was installed as three blankets supported by tension straps attached to studs at the top of the vehicle. Each blanket is held together by small Nylon studs and buttons located 12 in. on center in both directions. The foam is held in place by the fiber glass shell, which contains expansion loops serving as a tensioning device. The foam is compressed to 0.15 psi by the fiber glass skin. A manifolded purge system is integrated with the blanket design with the evacuation passages located at the interface between the foam and HPI blankets. The design concept is similar in detail to those shown in Section 3.3.2 of Part B.

Having developed a basic concept for installation of the HPI blankets, the major consideration for the Phase III study has been to refine the design criteria applied to the design: environments, survival criteria, thermal environments, vehicle orientation, material properties, heat short effects, mission timeline, venting requirements, and propellant utilization effects. These criteria and the associated analyses are reported in the subsequent sections.

4.3.2 Meteoroid Protection Design Criteria

Design of the meteoroid protection subsystem requires specification of: the meteoroid flux level, the meteoroid penetration model for the structural configuration of interest, and the meteoroid survival probability for the prescribed mission timeline. These items will be treated in the following subsections.

4.3.2.1 Meteoroid Environment

The space meteoroid environment is defined in Reference 4-30. The meteoroid flux-mass model for the mass range of interest is described mathematically as follows:

$$\log N_t = -14.37 - 1.213 \log m$$

where N_t = number of particles/meter^2 -sec of mass m or greater, and m = meteoroid mass in grams. The mass density is 0.5 g/cm^3 and the average meteoroid velocity is 20 km/sec.

The gravitationally focused, unshielded flux, N_t, must be multiplied by an appropriate defocusing factor for earth, G_E, and, if applicable, by the planetary shielding factor, ξ. These factors are to be obtained from:

$$G_E = 0.565 + \frac{0.435}{r}$$

$$\xi = \frac{1 + \cos \theta}{2}$$

$$\sin \theta = \frac{1}{r}$$

$$r = \frac{R + h}{R}$$

where R = planet's radius and h = altitude above surface. Gravitational focusing due to the moon is low (about 3 percent) and will not be treated explicitly. No advantage is taken of the apparent directionality of stream meteoroids.

The baseline mission for RNS design purposes is a lunar shuttle based in a 260-nmi altitude earth orbit. Three meteoroid flux levels will be used to represent the environment for this mission. These are: earth orbit at a 260-nmi altitude, one value during transfer from earth orbit to lunar orbit, and a 60-nmi lunar orbit. For computational ease, the meteoroid flux in the operational earth orbit will be computed and plotted; then, operations away from earth orbit will be related to this flux by definition of an effective exposure time. This is possible since all meteoroid exposures are represented by a product of the meteoroid flux and the exposure time. The effective exposure time for mission phases away from earth orbit will be defined as the actual time multiplied by the ratio of meteoroid flux at that location to the flux level in the operational earth orbit.

In the operational Earth orbit the altitude, h, is 260 nmi, while R = 3,440-nmi. This yields: r = 1.0755, G_E = 0.970, and ξ = 0.683. Applying these values, the meteoroid flux in earth orbit at 260 nmi is equal to 0.652 times the focused, unshielded flux, N_t. That is N = 0.652 N_t, where N will be the reference flux in earth orbit. Since log 0.652 = -0.19 the reference flux is:

$$\log N = -14.46 - 1.213 \log M$$

The relationship is shown in Figure 4.3-1 for the range of interest in the RNS design.

During translunar flight r will be taken at its mean value of 30 R. This yields G_E = 0.579 and $\xi \approx 1$. Then, the meteoroid flux equals 0.579 N_t = 0.888 N. Thus, the effective exposure time during transfer operations will be 0.888 times the actual time.

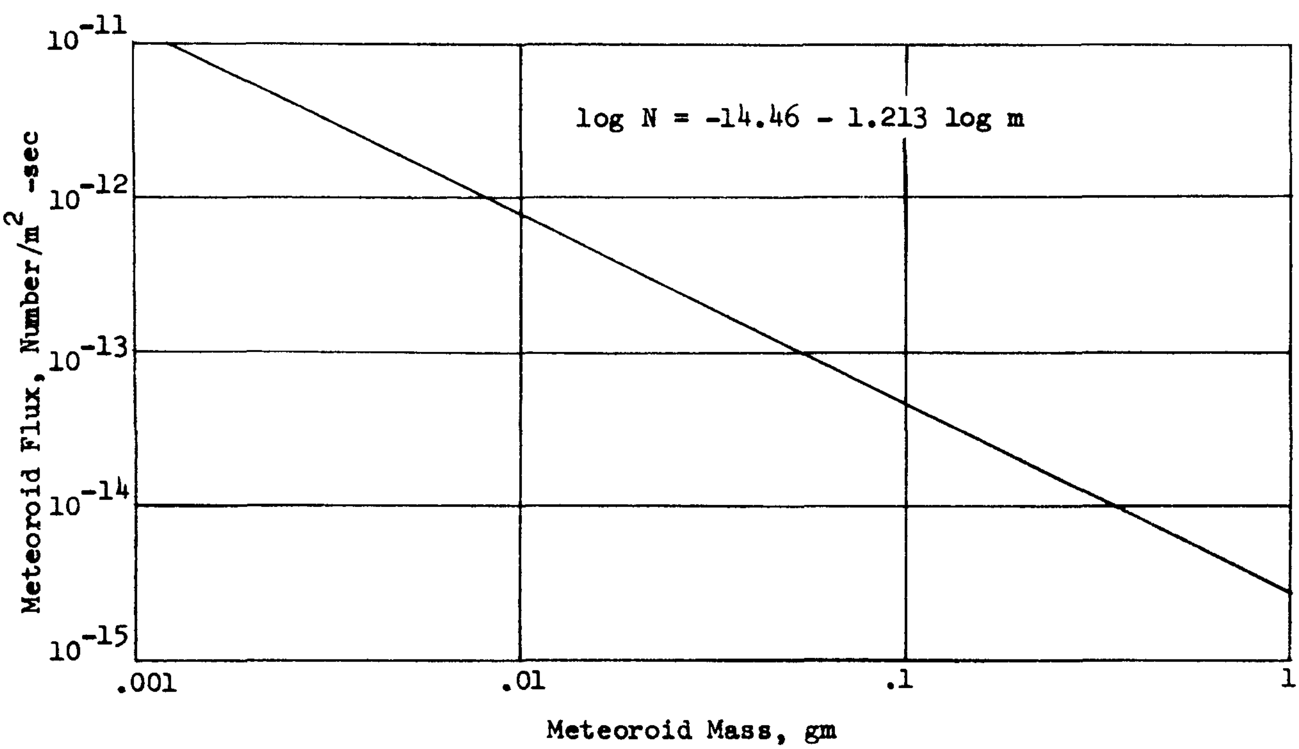

Figure 4.3-1 METEOROID FLUX (260 N.MI. EARTH ORBIT)

In lunar orbit, $r = 60$ R from earth so that $G_E = 0.572$ and $\xi_{Earth} \approx 1$. Relative to the moon $h = 60$ nmi with $R = 932$ nmi. This yields $\xi_{Moon} = 0.670$. Since lunar gravitational focusing was ignored, no defocusing factor is utilized. Then, the meteoroid flux in the operational lunar orbit, including earth's gravitation defocusing and the moon's shielding, is equal to $0.384\ N_t = 0.589$ N. This yields a multiplier of 0.589 to define effective exposure times in lunar orbit.

4.3.2.2 Meteoroid Penetration

Results of light gas gun hypervelocity impact tests are used to establish the penetration resistance of meteoroid armor. For the complex configuration considered, HPI, foam, and shroud, these tests must closely reproduce the actual materials and spatial distribution. Test results for the armor configuration of interest are documented in Section 2.5.2 of Reference 4-1. These results are scaled to represent meteoroid conditions of velocity and density by the following relationship:

$$m = m_{test} \left(\frac{V_{test}}{20}\right)^{2.48} \left(\frac{\rho_{test}}{0.5}\right)^{0.4}$$

where m = meteoroid mass, m_{test} = test mass (same units as m), V_{test} = impact velocity of test (km/sec), and ρ_{test} = test projectile density (g/cm^3).

The damage criterion for tankage is no penetration of the tank wall (Reference 4-7). Applying this criterion, test results for the integral shroud meteoroid protection concept, with a total thickness around 3 inches, yield the following relationship for the armor effectiveness:

$$W_A = 0.75 \left(\frac{m}{0.0104}\right)^{0.352}$$

where W_A = armor weight in lb/ft^2 to defeat meteoroid of mass m and m = meteoroid mass in grams.

4.3.2.3 Survival Criteria

The meteoroid protection system of the RNS will provide at least a 0.995 probability of no tank penetration in one lunar mission (Reference 4-7). The baseline lunar shuttle mission is used for the meteoroid design criteria. Its mission duration is 27.5 days, embedded within a 54.6-day repeating cycle. This duration is measured from initial RNS startup in earth orbit to completion of aftercooling upon return to earth orbit, and consists of the mission phase times shown in Table 4.3-1. The meteoroid flux level varies over the mission according to location as described in Section 4.3.2.1. Since meteoroid exposure is the product of flux and time, an effective exposure time is defined for mission phases away from earth orbit to relate the meteoroid exposure to the flux is earth orbit, N. This multiplier is also shown in the table.

The survival probability of 0.995 for the total round trip mission is equivalent to a probability of 0.9975 for survival through the operational and transit phases of the missions (excluding only the lunar orbit coast phase from the table).

No vehicle orientation requirements shall be imposed on the RNS during any mission or coast phase for meteoroid protection purposes (Reference 4-7).

Table 4.3-1
MISSION TIMELINE FOR METEOROID PROTECTION

Mission Phase	Duration	Multiplier for Effective Exposure Time	Exposure Times
Translunar coast	108 hours	0.888	96 hours
Lunar orbit injection	24 hours	0.888	21 hours
Lunar orbit coast	16.1 days	0.589	9.5 days
Transearth injection	24 hours	0.888	21 hours
Transearth coast	72 hours	0.888	64 hours
EOI cooldown	45 hours	1	45 hours
	659 hours, or 27.5 days total		475 hours

4.3.3 Meteoroid Protection Analysis

The meteoroid protection subsystem is integrated with the thermal insulation subsystem and with the aerodynamic shroud covering the tank during launch. Consequently all three functions must be considered in sizing the subsystem. This subsection will summarize the analyses performed to support this sizing. It is found that the protection afforded by the minimum thickness compatible with these other requirements and with the penetration test results described in Section 4.3.2.2 provides protection exceeding the minimum survival criterion supplied in the study guidelines and the economic optimization based upon replacement of a penetrated propellant module.

The survival probability P(O) is the probability of not encountering a meteoroid with a mass greater than the design mass of the meteoroid protection subsystem during the mission. Assigning this survival probability to the RNS with a known vulnerable area for the specified mission (location and duration) and employing the reference meteoroid flux relationship allows definition of the design mass, m. Then, employing the armor effectiveness relationship derived from test results, Subsection 4.3.2.2, allows specification of the meteoroid protection requirements.

The survival probability is:

$$P(O) = e^{-NAT}$$

where P(O) = probability of no puncture with protection for mass m, N = reference meteoroid flux having mass greater than m (number/meter^2-sec), A = surface area subject to meteoroid puncture (meter^2), and T = effective exposure time (sec).

Figure 4.3-2 shows the meteoroid design mass for a range of values of P(O) as a function of the product AT. The baseline design value at AT = 1.57×10^9 m^2-sec is shown on the figure. This corresponds to a vulnerable area of 916 m^2 and the effective exposure time of 475 hours. At the specified survival probability of 0.995, the meteoroid design mass

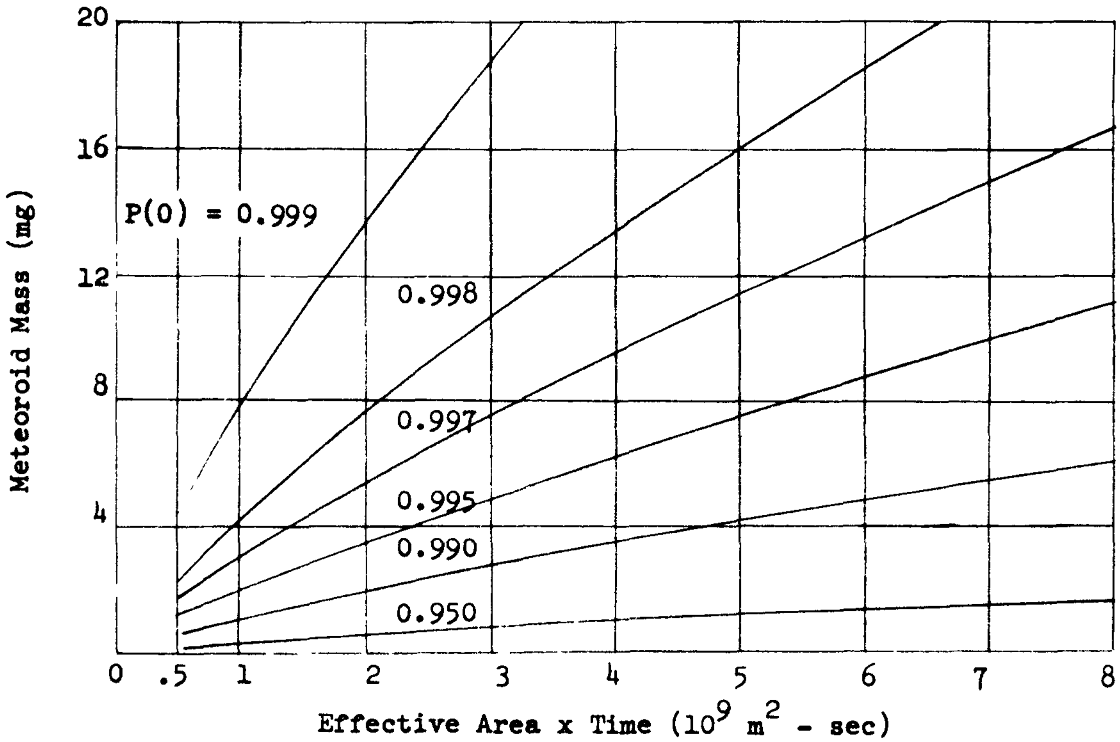

Figure 4.3-2 METEOROID MASS VS. EXPOSURE

is 2.9 mg. Applying the armor effectiveness from Section 4.3.2.2, the armor weight per unit area is $0.75\ (\frac{2.9}{10.4})^{0.352} = 0.48$ psf. The total minimum armor weight then is 4,700 lb.

While this represents the armor weight required to provide the minimum survival probability called for in the study guidelines, a further investigation was made to assess any possible economic advantage of providing greater meteoroid protection. To aid the overall evaluation of meteoroid protection, the armor weight as a function of survival probability was tabulated for several survival criteria. These criteria are defined below together with corresponding value of the product of vulnerable area and effective exposure time.

A. Survival for full mission period of 54.6 days. This is an economic criterion. Adding 651 hours of additional exposure in earth orbit increases the effective exposure time to 1,126 hours and the product AT to $3.72 \times 10^9\ m^2$-sec.

B. The baseline criterion of survival during the lunar mission after injection out of earth orbit. $AT = 1.57 \times 10^9 \ m^2$-sec.

C. Survival during transfer phases between earth orbit and lunar orbit. This criterion represents the case where a "safe haven" for the crew exists in lunar orbit. Clearly, the abort actions required are greater if a penetration occurs during transfer than during lunar orbit coast. This criteria imposes an effective exposure time of 247 hours which produces $AT = 0.82 \times 10^9 \ m^2$-sec.

A parametric display of armor weight according to these criteria is shown in Figure 4.3-3.

An economic optimization was performed by comparing the incremental transportation cost due to carrying additional meteoroid armor on the round trip mission with the savings due to the corresponding reduction in the probability of penetration of the propellant tank. The incremental transportation cost is $770/lb of stage weight based on the maximum launch cost for LH_2 of $167/lb to earth orbit. The costs assessed to a meteoroid penetration of the propellant tank are $65 million for losing the mission (transportation costs to earth orbit of $50 million for the propellant and $15 million for the payload) and $60 million for the average value of the propellant module in earth's orbit (module cost of $13 million, launch cost of $107 million, and half amortized at time of penetration). Charging the full cost of one mission is considered to be conservative relative to the average effect of the penetration and to fully cover the costs for those events where an overt rescue operation is required. This optimization uses the armor weight versus survival probability shown in Figure 4.3-3 for criterion A. The armor weight above the minimum found above (4,700 lb) is multiplied by $770/lb to represent the total penalty for a single mission. The corresponding survival probability is used to determine the probability of penetration, 1-P(O), over one full mission cycle, which is multiplied by $125 million to establish the economic impact of penetration. These results are shown in Figure 4.3-4. It can be seen that the optimum occurs at a survival probability of 0.992 for criterion A (0.9965 for criterion B). Since the result of this economic optimization is close to the minimum armor required to meet the study guidelines, and since the curve shows a shallow minimum, further economic analysis is not warranted.

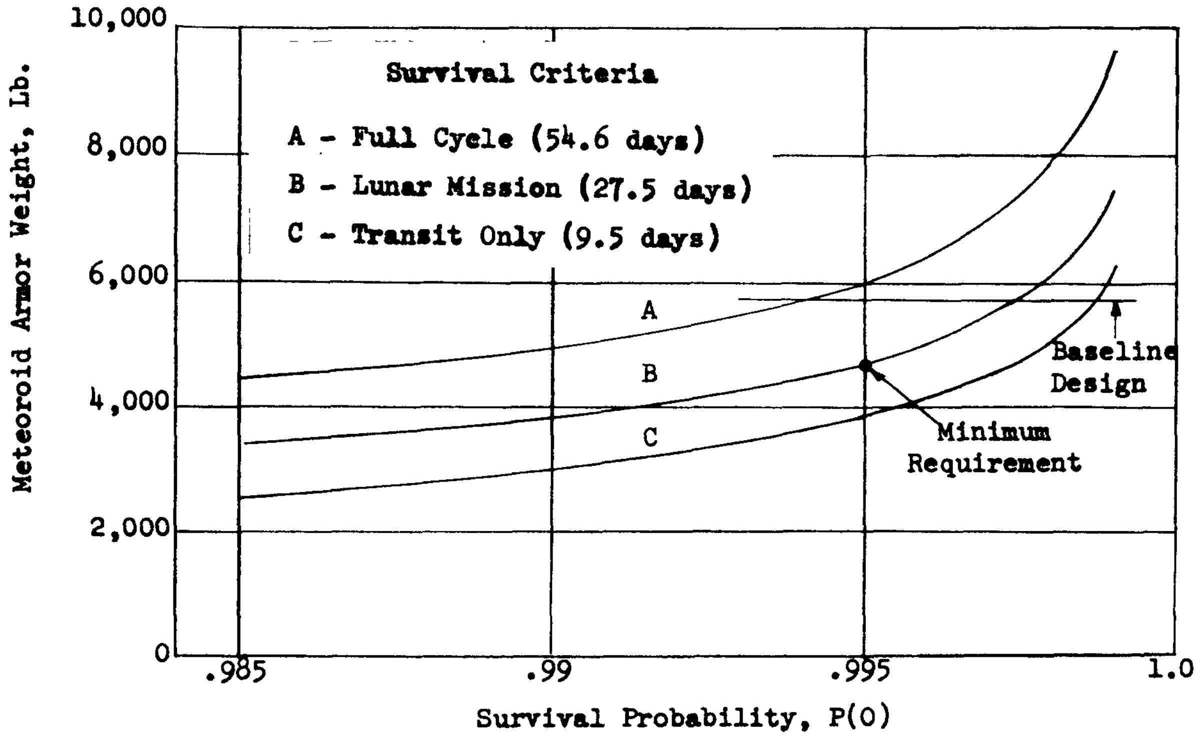

Figure 4.3-3 PARAMETRIC ARMOR WEIGHT

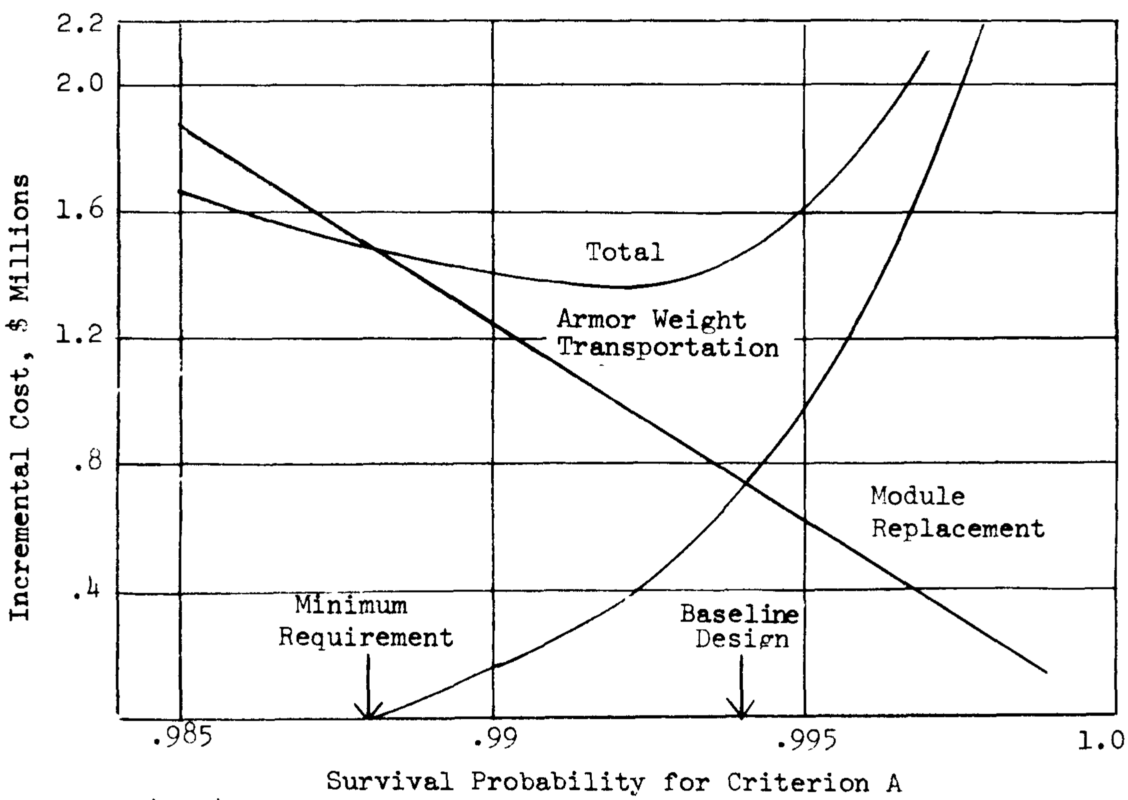

Figure 4.3-4 METEOROID ARMOR ECONOMIC OPTIMIZATION

While the analyses described above established the minimum meteoroid armor requirements, final subsystem specification must consider the other requirements imposed on the combined thermal/meteoroid protection subsystem. Thermal protection requirements, established in the following subsections, utilize 0.54 in. of high-performance insulation having a density of 4.1 lb/ft^3. This yields an area density of 0.184 psf and a total weight of about 1,800 lb. This excludes the weight of attachments and other components which do not contribute to meteoroid protection.

A 0.020-in. fiber glass cloth outer shell is used as an aerodynamic shroud during launch of the propellant module. This is considered to be the minimum thickness for this function and provides a 0.20 psf or 1,960 lb total for meteoroid protection.

A flexible polyurethane foam with a density of 1.2 lb/ft^3 is used to space the shroud away from the high-performance insulation which is attached directly to the propellant tank. A thickness of 1 in. which is consistent with ground-hold insulation requirements, would be required to meet the 0.995 survival criterion given in the study guidelines. The economic optimization would increase this thickness to about 1-1/2 in. However, decreased total armor thickness results in substantially reduced effectiveness and extrapolation of the hypervelocity test results from Section 4.3.2.2 to a total thickness of less than about 2-1/2 in. is not considered warranted. Applying this constraint established 2 in. for the foam thickness which adds 0.20 psf or 1,960 lb to the meteoroid protection subsystem.

These three components provide 0.58 psf or 5,720 lb total of meteoroid armor. This is noted as the baseline design on Figures 4.3-3 and 4.3-4. The subsystem provides the following survival probabilities:

Criterion	P(O)
Full cycle (54.6 days)	0.994
Lunar mission (27.5 days)	0.9974
Lunar mission during transit (9.5 days)	0.9987

It should be noted that Criterion B corresponds to the study guideline requiring a minimum survival probability of 0.995 which is exceeded in the baseline design.

4.3.4 Thermal Protection Design Criteria

4.3.4.1 Thermal Environment

The thermal environment is defined here for prelaunch, launch, and space operations.

Prelaunch

The RNS modules shall be protected from temperature extremes during ground handling and transportation. The extremes for potential RNS program locations and operations are defined in Table 4.3-2.

Launch

The Class 1-H propellant module design will accommodate aerodynamic heating during launch. Preliminary design will be based on RNS launch heating data generated during Phase II for the Class 1 RNS, utilizing a Saturn V launch trajectory and the Patrick AFB 1963 Reference Atmosphere. The following temperature limits are applied: aluminum forward skirt, 190°F; fiber glass shroud, 350°F; and fiber glass H.C. aft skirt, 290°F.

Modules launched inside the space shuttle cargo bay shall be designed to accommodate a temperature limit of 200°F max during launch to orbit.

Table 4.3-2

PRELAUNCH TEMPERATURE EXTREMES

Condition	Location	Temperature (°F) Maximum	Minimum
Ground handling	Sacramento	115	
River transportation	Michoud		-23
Aircraft compartment	Ground	190	
Aircraft compartment	20,000 ft		-49
Ground storage	ETR	99	
Space shuttle cargo bay		80	

Orbital and Mission Operations

The on-orbit temperature limits of -150°F to + 200°F will be used for all modules that are launched inside of the space shuttle cargo bay. The RNS will be designed for the orbital and mission thermal environment defined by Reference 4-32 consisting of the following values of environmental parameters:

Sun	Mean Solar Constant at 1.0 A.U.		
	Thermal Radiation 1,353 ± 20 watts/m^2		
	(variation with distance from sun to follow $\frac{1}{R^2}$ relationship)		
Earth	Average Total Albedo 0.3		
	Thermal Radiation (mean value) 238 watts/m^2		
Lunar	Average Total Albedo =	Front side	0.110
		Back side	0.217
	Thermal radiation	324.35 watts/m^2	

4.3.4.2 Material Properties

Surface Coatings

The surface coating will adhere and maintain integrity throughout the full RNS lifetime of 10 round trips and 3 years in space. The design will take into account the performance degradation of absorptivity and emissivity after extended exposure in space. Z-93 (SP500 ZNO-pigmented potassium silicate paint) and S-13G (silicate treated - ZNO in methyl silicone base) are surface coating candidates. The following properties are applied for design:

	α_s/ϵ			
Material	Nominal	Degraded	Exposure Time (ESH)	References
Z-93	0.20	0.21	1580	4-33, 4-34
S-13G	0.22	0.32	1600	4-35, 4-36

High-Performance Insulation

The technology of high-performance insulation is in a rapid state of development. The RNS design incorporates HPI performance data accounting for the effects of blanket design and installation (including perforations, joints, studs, and tank attachment) and effects of environments (including compression, decompression, evacuation, and degradation from meteoroid damage) as it becomes available from Contract NAS8-21400 or related studies approved by NASA. The RNS baseline design utilizes doubly aluminized Mylar with a Dacron net spacer. The following properties are applied for design:

Conductivity - space	2.0×10^{-5} Btu/hr ft °R
- ground	0.025 Btu/hr ft °R
Density	4.1 lb/ft^3
Layer Density	96 pairs/in.
Mylar Sheet Thickness	0.00015 in.
Manufacturing Acceptance Rate	75 percent
Evacuation Time	1 hour

The approach to thermodynamic analyses will treat HPI performance in parametric fashion. Unpublished MSFC and MDAC test data were evaluated to select a realistic value of DAM/net performance to complete system definition for a point design.

The MDAC test data utilized are based on a 15-in.-diameter calorimeter, 24 in. long. The test temperature range was 520/40°R. The insulation test specimen consisted of 70 sheets of DAM/net (B-2A). This net has a weight of 0.0024 psf and a mesh count of 198 meshes/in.^{2}. The insulation was applied to the calorimeter at a natural layup density of 96 layers per inch. The conductivity selection rationale is summarized briefly in Table 4.3-3. The natural layer density (96 layers/inch) will be utilized for space performance until compression tests in progress justify an alternative criterion. Even while the DAM/net system is retained as a baseline, it should be anticipated that further work evaluating compressibility effects could lead to identification of other spacer concepts as more attractive.

Foam

Spray foam properties are obtained from page 75 of Reference 4-37. The design value for thermal conductivity is 0.01 Btu/hr-ft °F.

Table 4.3-3

DAM/NET CONDUCTIVITY SELECTION RATIONALE

		Conductivity (Btu/ft hr °R)
MDAC Test Data at 520/40°R (96 layers per inch)		1.37×10^{-5}
Experimental error	+ 3.4%	
Lateral conduction, estimated	+ 2.7%	
Adjustment to eliminate technique	+ 6.1%	1.46×10^{-5}
Provision for perforations, joints, and studs (experimental)	+62 %	
Provision for straps (estimated)	+13 %	
Adjustment for	+75 %	2.56×10^{-5}
Adjustment for mission temperature range at 400/40°R (calculated)		2.01×10^{-5}

4.3.4.3 Orientation

The thermal protection system will impose no requirements for vehicle orientation during any operations or mission phases. The thermal protection system design will accommodate all operational requirements for orientation, including thrust vector orientation, rendezvous and docking, and station keeping.

4.3.5 Surface Temperature Evaluation

The surface temperature implications of surface coating properties, material thicknesses, and vehicle orientation have been investigated with MDAC orbital heating codes for the RNS lunar orbit and in transit. The surface properties have the greatest impact, while the sensitivity to vehicle attitude in earth orbit is small, and the influence of the fiber glass external meteoroid bumper thickness is negligible.

Three RNS orientations in earth orbit were considered: (1) planetary oriented, longitudinal axis pointed toward earth center (gravity-gradient stabilized); (2) planetary oriented, longitudinal axis parallel to velocity vector; and

(3) inertial orientation. The vehicle orientation geometry for the first case is defined by Figure 4.3-5. It is the same for Case 2, but with the RNS axis rotated 90 degrees. However, to obtain a worst case for the inertial orientation, the sun position was rotated 90 degrees, normal to the plane of the figure, while the vehicle axis orientation remained in the plane of the figure. Temperature distributions were calculated around the vehicle circumference. The resulting maximum, minimum and average surface temperatures for several anamolies, and average orbital surface temperatures are tabulated in Table 4.3-4.

Two cases were considered for the RNS in 60-mni polar lunar orbit: for the first the sun was at a 90 degree angle to the orbital plane, and the second had a sun angle of 0 degrees. Both cases have the vehicle in a vertical orientation (parallel to the radius vector). Maximum, minimum, and average surface temperatures for several anomalies, and average orbital temperatures are tabulated in Table 4.3-5. With the angle 90 degrees, the vehicle presents a constant position with respect to the sun and thus surface temperatures are independent of anomaly.

The impact of vehicle attitude during translunar or transearth coast is shown in Table 4.3-6.

The impact of surface absorptivity on the surface temperature history in earth orbit is shown in Table 4.3-7.

Considering these factors, and a space degraded absorptivity of 0.32, a reference surface temperature of -90°F or 370°R was adopted for preliminary thermal protection system design.

4.3.6 Heat Short Definition

The heat shorts include the tank support and intermodule structures, propellant feed, pressurization, and vent lines. These are defined for the RNS Class 1-H modules in Table 4.3-8. The fiber glass honeycomb skirts at each end of the propellant module will contribute 300 to 600 ft^2 to the heat short insulated area for the current baseline design. However, these are not included in the subsequent analyses on the basis that if the Class 1-H is of sufficient interest to

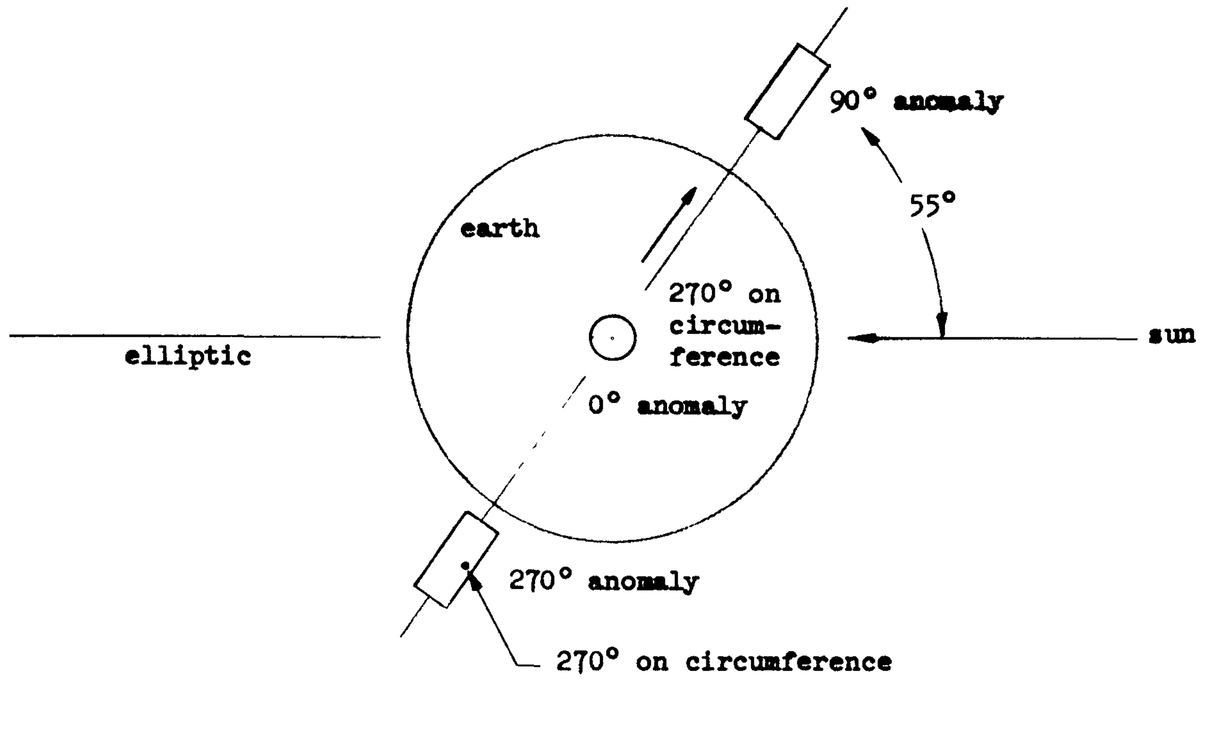

Figure 4.3-5 VEHICLE ORIENTATION GEOMETRY

Table 4.3-4

TEMPERATURE HISTORY FOR RNS IN EARTH ORBIT

(α = 0.32, ϵ = 0.96)

Orientation	Vertical			Horizontal			Inertial			
Anomaly	0°	90°	270°	0°	90°	270°	0°	90°	270°	180°
T_{max} °F	+84	+80	-113	+80	+82	-20	+80	+95	+95	-25
T_{min} °F	-130	-112	-130	-325	-293	-288	-70	-108	-202	-236
T_{avg} °F	-52	-38	-127	-74	-47	-117	-25	-65	-58	-130
T_{avg} (orbit) °F	-73			-73			-70			

Table 4.3-5

TEMPERATURE HISTORY FOR RNS IN LUNAR ORBIT

($\alpha = 0.32$, $\epsilon = 0.96$)

Vertical Attitude

Sun Angle	0°				90°
Anomaly	0°	90°	180°	270°	All
T_{max} °F	-32	+100	-105	+104	+102
T_{min}	-92	-101	-105	-105	-105
T_{avg}	-56	-52	-105	-53	-53
T_{avg} (orbit)	-67				-53

Table 4.3-6

TEMPERATURE HISTORY FOR RNS IN TRANSLUNAR COAST

($\alpha = 0.32$, $\epsilon = 0.96$)

Sun Angle (to normal)	0°	30°	60°
T_{max} °F	76	58	-9
T_{min}	-415	-415	-415
T_{avg}	-178	-187	-199

Table 4.3-7

IMPACT OF SURFACE ABSORPTIVITY
ON RNS SURFACE TEMPERATURE HISTORY

(Vertically Oriented RNS)

Absorptivity		0.1			0.2			0.32 (Nominal)			0.4		
Anomaly	Deg	0	90	270	0	90	270	0	90	270	0	90	270
T_{max}	°F	-24	-28	-118	+40	+30	-113	+84	+80	-113	+136	+105	-105
T_{min}	°F	-130	-125	-130	-130	-118	-130	-130	-112	-130	-130	-108	-130
T_{avg}	°F	-97	-100	-128	-78	-80	-127	-52	-62	-127	-42	-49	-125
T_{avg} (Orbit)	°F		-106			-91			-73			-65	

receive further definition, design concepts will be developed to cover the stub ends with HPI in orbit after jettison of the interstage and nosecone.

An accurate thermal analysis model was used to account for partial insulation coverage over a cylindrical component. The heat input through the ith heat short is

$$Q_{H_i} = \frac{\beta_i K_i A_i}{\tanh (\beta_i l_i)} \Delta T$$

where

$$\beta_i = K_e^{1/2} (K_i h_i d)^{-1/2}$$

Table 4.3-8

HEAT SHORT SUMMARY
RNS CLASS 1-H

Item	K_i (Btu/ft^2 hr °R)	h_i (in.)	A_i (ft^2)	A_{H_i} (ft^2)
PROPULSION MODULE				
Thrust structure	0.12	0.060	0.11	66
Forward skirt	0.12	0.060	0.141	84.8
NERVA feed system				
Inconel lines	4.5	0.035	0.0305	28.9
CRES lines	7.1	0.035	0.0290	4.14
Al lines	38.0	0.25	0.0545	2.18
Intermediate feed system	7.1	0.035	0.00915	22.54
Pressurization line	7.1	0.035	0.00153	3.98
Vent	7.1	0.035	0.00458	7.85
			Total	220.39
PROPELLANT MODULE				
Thrust structure	0.12	0.065	0.357	198
Payload adapter	0.12	0.070	0.293	151
Aft feed system	7.1	0.035	0.00915	17.77
Fwd feed system	7.1	0.035	0.00915	23.09
Pressurization line	7.1	0.035	0.00153	3.89
Vent	7.1	0.035	0.00458	7.85
			Total	401.6

K_i = Thermal conductivity

h_i = Tube wall thickness

A_i = Cross-sectional area

A_{H_i} = HPI coverage area

and the following nomenclature is used: K_e, equivalent thermal conductivity of HPI; K_i, thermal conductivity of heat short; A_i, heat short cross-sectional area; h_i, thickness of (tubular) heat short, l_i, insulated length of heat short; d_{Hi}, heat short HPI thickness. Typically for RNS applications the heat input through the component is several times that predicted by the linear conduction law, even with HPI.

Heat inputs calculated for the candidate materials and construction for the Class 1-H propellant module interface structures are shown in Figure 4.3-6 as a function of the length and thickness of HPI coverage. The coverage for most tank attachments should be longer than 2 ft and performance is not improved appreciably when the coverage is extended beyond 4 or 5 ft. The insulated areas in Table 4.3-8 are based on a 3-ft length for struts and ducts. The insulation thickness on the heat shorts will be considered equal to the tank blanket thickness.

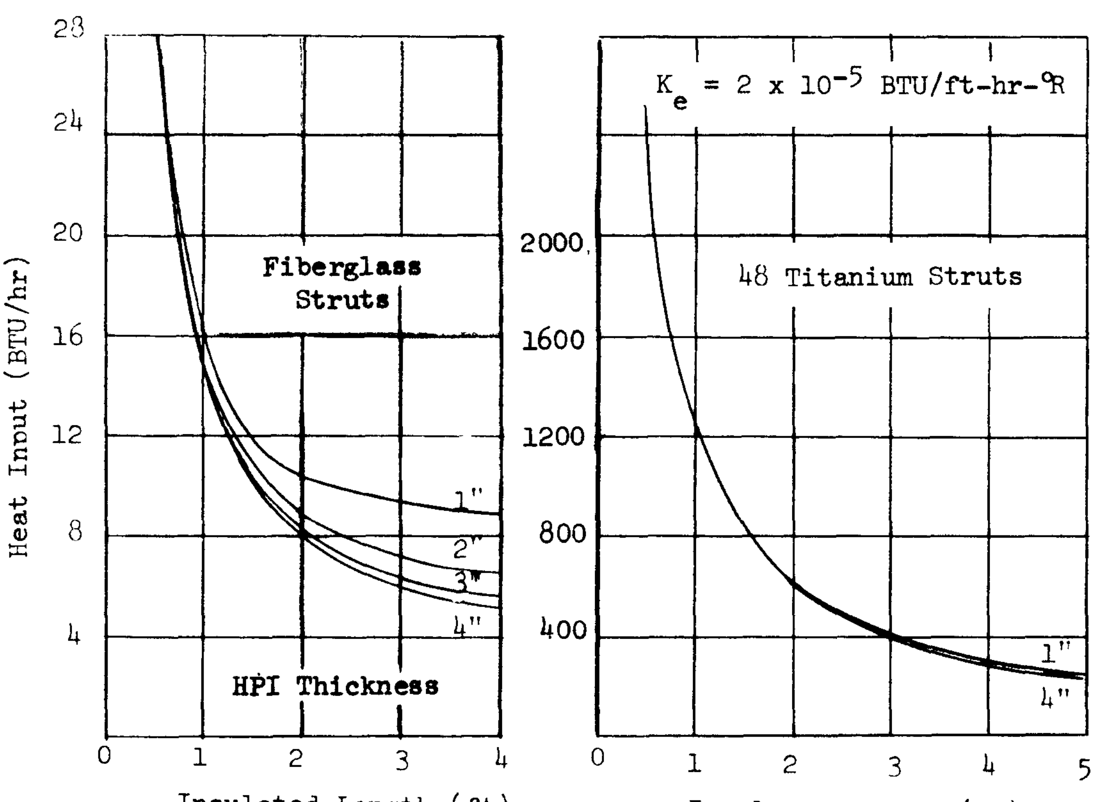

Figure 4.3-6 EFFECT OF INSULATION LAYUP ON CANDIDATE THRUST STRUCTURE PERFORMANCE CLASS 1-H PROPELLANT MODULE

4.3.7 Equivalent Time Analysis for Mission Phases

The analysis of propellant heating for the RNS lunar shuttle mission is complicated by multiple burns and multiple tankage. The various propellant tanks spend prolonged periods of time in various degrees of off-loading. An off-loaded tank has a more severe thermal protection requirement than a full tank because the heat flux entering through the sidewalls must be absorbed by a smaller amount of fluid which has a lower heat capacity than for a full tank. This effect is conveniently defined by converting the actual mission time as an offloaded tank, $t_{act.}$, into an equivalent full tank time, $t_{equiv.}$ The relationship is approximated by

$$t_{equiv.} = \frac{(W_L + W_G)\text{ full}}{(W_L + W_G)} C \; t_{act.}$$

where $(W_L + W_G)$ is the mass of liquid and gas in the tank and C is a correction factor, obtained from a detailed energy, mass, and volume balance, which accounts for vaporization as the tank is depleted. Complete mixing within the system is assumed.

The lunar shuttle mission timeline defined in Section 2.3 and the associated propellant utilization history which defines the propellant tank loadings in Section 3.10 were used to establish the equivalent time history for the propellant module and the run tank. Figure 4.3-7 displays accumulated equivalent times vs. actual phase times for both the propellant and propulsion modules, assuming they start at the same saturation pressure. The run tank starts out slightly warmer than the propellant tank but after being refilled, and after completing the LOI-3 burn, is less severely off-loaded and therefore stays cooler for the remainder of the mission.

The RNS propellant is resupplied over a prolonged orbital coast period prior to the mission. The associated propellant logistics history is defined in Section 3.6.3. A baseline of 4 days per space shuttle tanker flight was adopted for thermal protection, with delivery of 30,000 lb LH_2 per flight. Propellant resupply is initiated 53 days before the start of the mission and the stage is fully loaded for the last 18 days before TLI while CCM replacement in payload

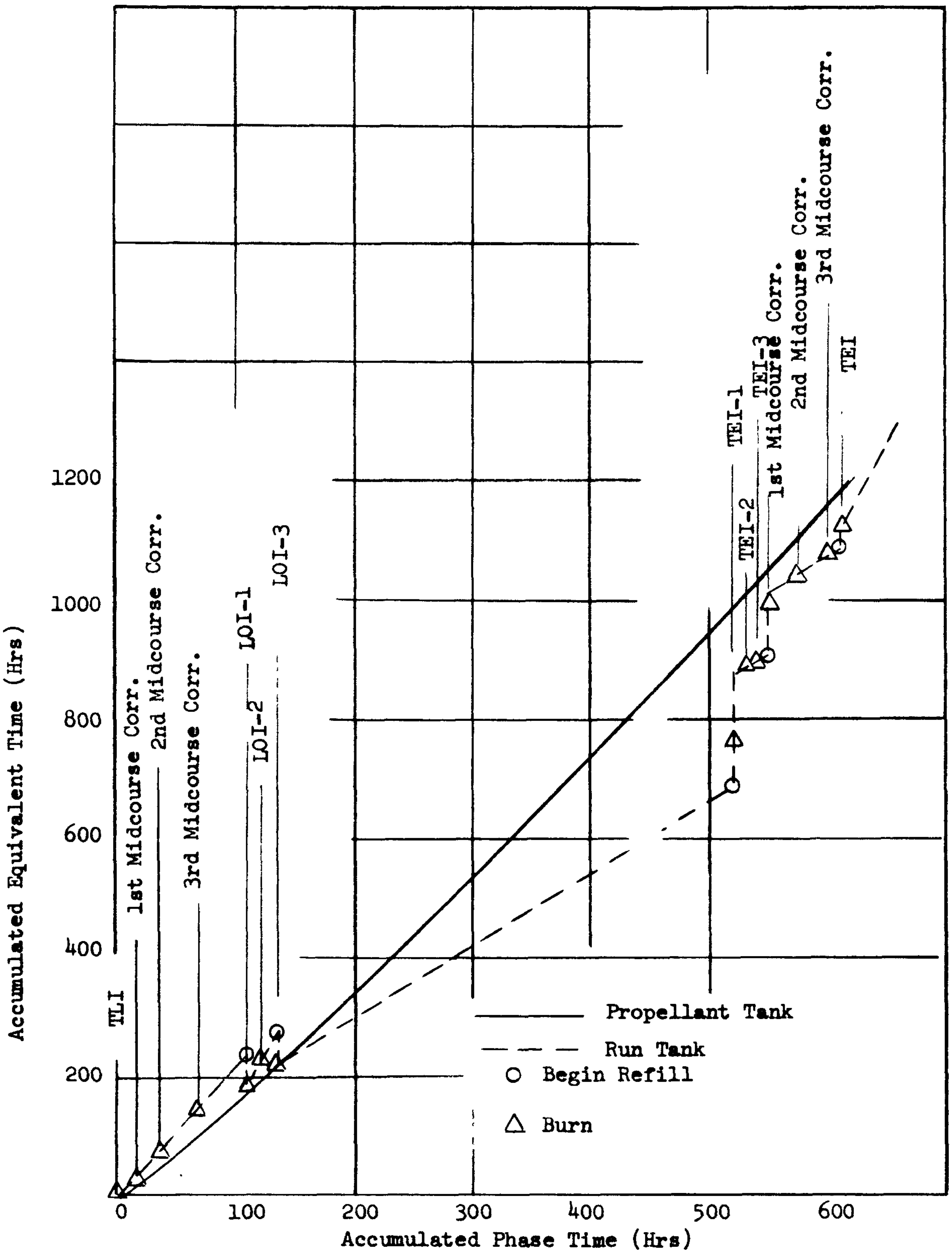

Figure 4.3-7 PROPELLANT HEATING EQUIVALENT TIMES

assembly are in progress. The resulting orbital heating is actually more severe than imposed by the operational portion of the mission away from earth orbit. The resultant equivalent times for the baseline mission are summarized in Table 4.3-9. These are used for selection of a point design in the thermal protection system optimization.

4.3.8 Insulation Optimization

The optimum insulation system is one that causes a minimum penalty on the delivered payload. The system weight penalty consists of the insulation weight on tankage and heat shorts combined with the boiloff incurred on the mission, weighted according to the location where it is vented. The total system weight penalty was optimized as a function of the insulation thickness. The method of analysis is summarized in Tables 4.3-10 and 4.3-11. The analyses were programmed to facilitate handling the complications introduced by inclusion of exact heat shorts in the optimization.

Table 4.3-9
EQUIVALENT TIME PHASE SUMMARY (HR)
(CLASS 1-H)

	Propellant Module	Run Tank
Before Mission		
During loading	1,570	1,570
After loading	430	430
Subtotal	2,000	2,000
During Mission	1,190	1,298
Total	3,190	3,298
Total After Loading	1,620	1,728

Table 4.3-10

THERMAL PROTECTION SYSTEM WEIGHT PENALTY SUMMARY

1 Total system penalty

$$W_P = W_T + W_H + \frac{1}{\gamma} W_{BO}$$

2 Breakdown of elements

Tank HPI $\quad W_T = \rho A d$

Heat Short HPI $\quad W_H = \rho \sum A_{Hi} d_{Hi} = \rho d \sum A_{Hi}$

LH_2 Boiloff $\quad W_{BO} = \frac{1}{\lambda} \left[(Q_T + Q_H) t - C_p W \Delta T_{LH_2} \right]$

Where

Heat Input Through Tank $\quad Q_T = \frac{1}{d} K_e A \Delta T$

Heat Input Through Heat Short $\quad Q_H = \sum \frac{\beta_i K_i A_i}{\tanh (\beta_i l_i)} \Delta T \simeq \sum \beta_i K_i A_i \Delta T$

and

$$\beta_i = K_e^{1/2} (K_i h_i d)^{1/2}$$

3 Nomenclature

A	Tank surface area
A_{Hi}	Heat short HPI coverage area
A_i	Heat short cross-sectional area
C_p	Heat capacity of LH_2
d	Tank HPI thickness
d_{Hi}	Heat short HPI thickness
h_i	Thickness of (tubular) heat short
K_e	Equivalent thermal conductivity of HPI
K_i	Thermal conductivity of heat short
Q_H	Heat leak rate through heat shorts
Q_T	Heat leak rate of tank HPI
T	Temperature
t	Time
W	Bulk weight of LH_2
W_{BO}	Boiloff LH_2 weight
W_H	Weight of heat short insulation
W_P	Total weight penalty
W_I	Weight of tank insulation
γ	Effective growth factor for performance
λ	Heat of evaporation of LH_2
ρ	Weight density of HPI

Table 4.3-11
OPTIMUM INSULATION THICKNESS SUMMARY

1. HPI thickness for minimum thermal protection system weight penalty:
   1.1 For systems with no boiloff
      1.1.1 Tank only:

$$d_o = \frac{K_e A \Delta T t}{C_p W \Delta T_{LH_2}}$$

      1.1.2 Tank with effect of heat shorts

$$d = 1/2 \left\{ (D^2 d_o + 2) + D(D^2 d_o{}^2 + 4D_o)^{1/2} \right\} d_o$$

where

$$D = \frac{1}{A} \sum \left(\frac{K_i}{K_e} \frac{1}{h_i} \right)^{1/2} A_i$$

   1.2 For systems with boiloff
      1.2.1 Tank only

$$d_o = \left(\frac{K_e \Delta T t}{\rho \lambda Y} \right)^{1/2}$$

      1.2.2 Tank with effect of heat shorts

$$d \quad d_o + \epsilon$$

with

$$\epsilon = \frac{1}{2} \left\{ \frac{1}{2} K_e{}^{1/2} \frac{\sum A_{H_i} \left(\frac{K_i}{h_i} \right)^{1/2}}{A + A_{H_i}} d_o + \frac{A}{A + A_{H_i}} - 1 \right\} d_o$$

   1.3 Transition time from no boiloff to LH_2 boiloff
      1.3.1 Tank only

$$t = \frac{1}{K_e \Delta T \rho \lambda Y} \left(\frac{C_p W \Delta T_{LH_2}}{A} \right)^2$$

      1.3.2 Tank with effect of heat shorts
      Solutions may be obtained from graphs plotting

d_{NBO} and d_{BO}

The payload delivery partials in Table 2.2-1 indicate that for the typical case of venting after completion of translunar coast, the performance penalty for vented boiloff is obtained by reducing the actual boiloff by an effective growth factor $\gamma = \partial$ (vented propellant)/∂ (RNS inert) PLD = 1.5. This idealized weighting must be increased to account for the incremental weight of increased propellant tankage and a bias toward venting before the mission. A value of γ = 2.0 is used as an approximation for the reduced weighting of boiloff in subsequent data.

The insulation thickness for no boiloff or the amount of boiloff incurred when it is required depends on the initial and final propellant state conditions. The LH_2 enthalpy rise is indicated in Table 4.3-12 for a range of initial saturation pressures and NERVA operating pressures which are typical of the system optimization cases.

The amount of equivalent time elapsed before it is favorable to vent boiloff is indicated in Figure 4.3-8 as a function of propellant enthalpy rise permitted for a range of thermal conductivities. The anticipated conductivity is adequate to avoid venting during the mission if the full tank equivalent time is not much greater than that incurred after TLI and if the availably enthalpy rise is not severely limited by prior orbital heating or tank chilldown.

Figure 4.3-9 shows the thermal protection system weight penalty for the propellant module as a function of the full tank equivalent time and LH_2 enthalpy rise. The parametric values of insulation plus boiloff indicated above the curve for insulation only show the penalties associated with boiloff (as reduced by γ = 2) for a range of propellant enthalpy rises. The curves for insulation only in the no boiloff regime indicate the additional performance gains which can be obtained by propellant subcooling. This system performance map provides the basis for defining and evaluating alternative thermal protection system point designs. These will be discussed further in Section 4.3.11. Figure 4.3-10 indicates the comparable system performance map for the propulsion module run tank. Heat shorts are a severe penalty on the run tank thermal protection.

Table 4.3-12

LH_2 ENTHALPY RISE MATRIX (BTU/LB)

Initial Saturation Pressure (psia)	NERVA Pressure (psia) 26	30	
1	32.4	35.2	Subcool to triple point
10	14.3	17.2	Typical subcool
16	8.2	10.8	Baseline delivery to orbit
21	4.0	6.7	Includes childown of warm tank
	Design Goal	Old Specification	

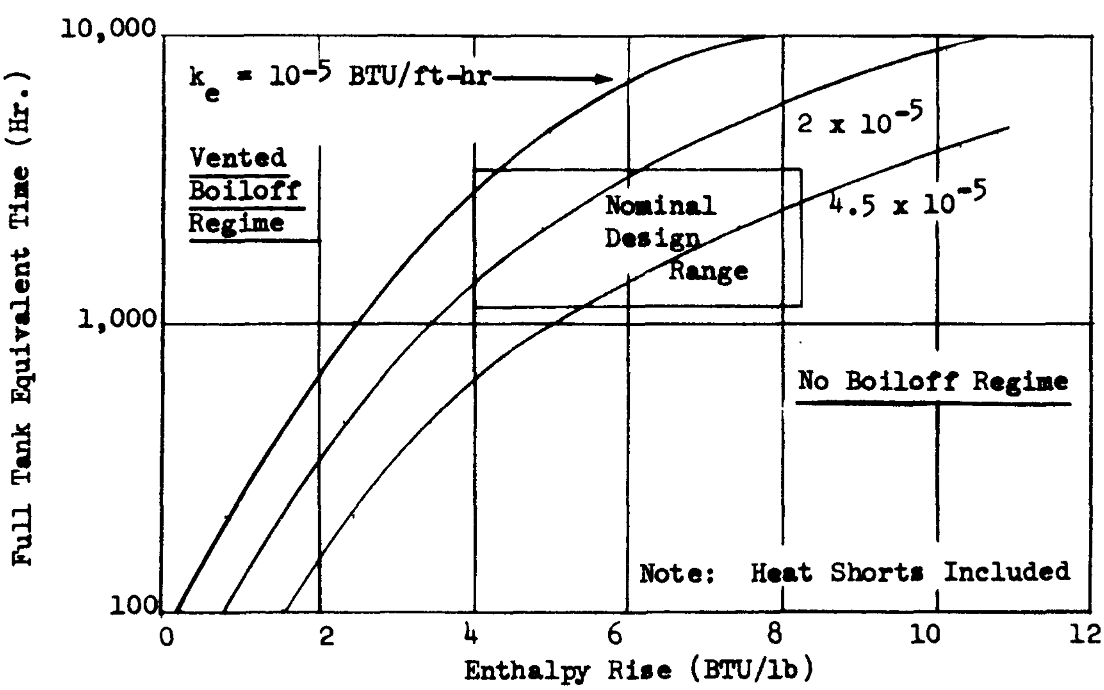

Figure 4.3-8 VENTING AND NO BOILOFF DESIGN REGIMES
CLASS 1-H PROPELLANT MODULE

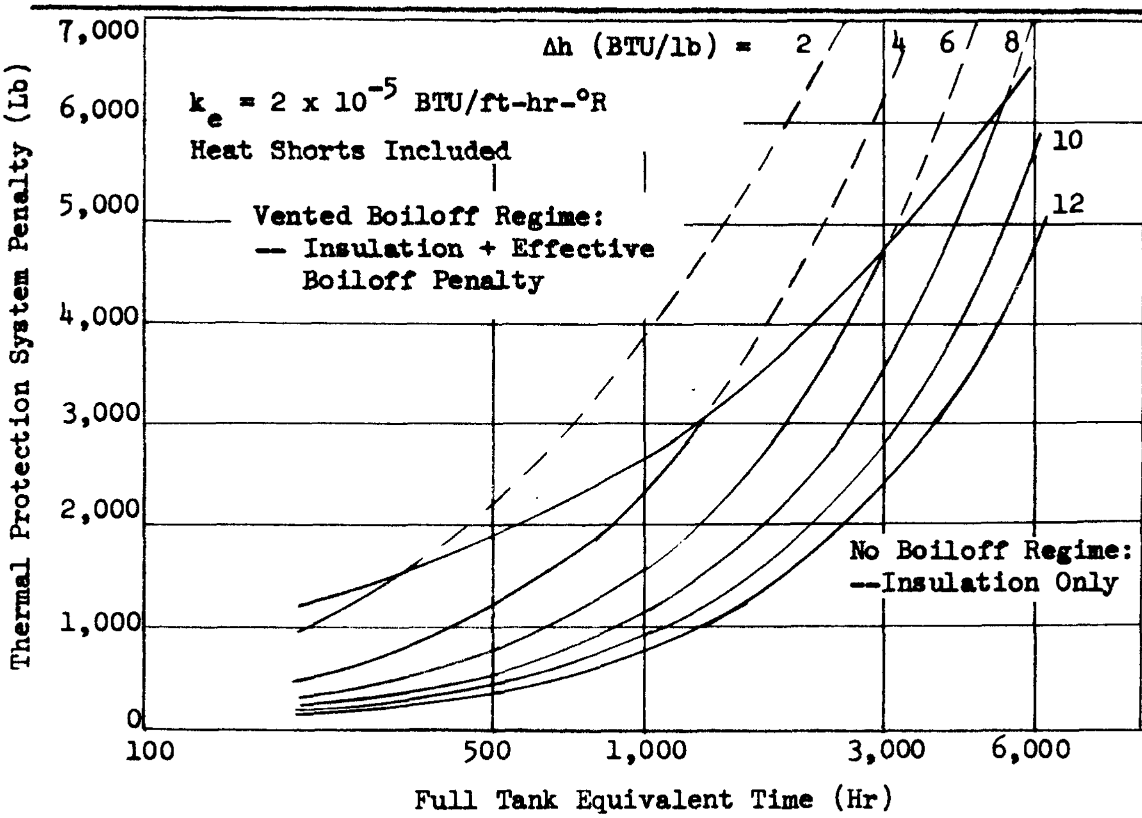

Figure 4.3-9 THERMAL PROTECTION SYSTEM DESIGN PARAMETERS -- CLASS 1-H PROPELLANT MODULE

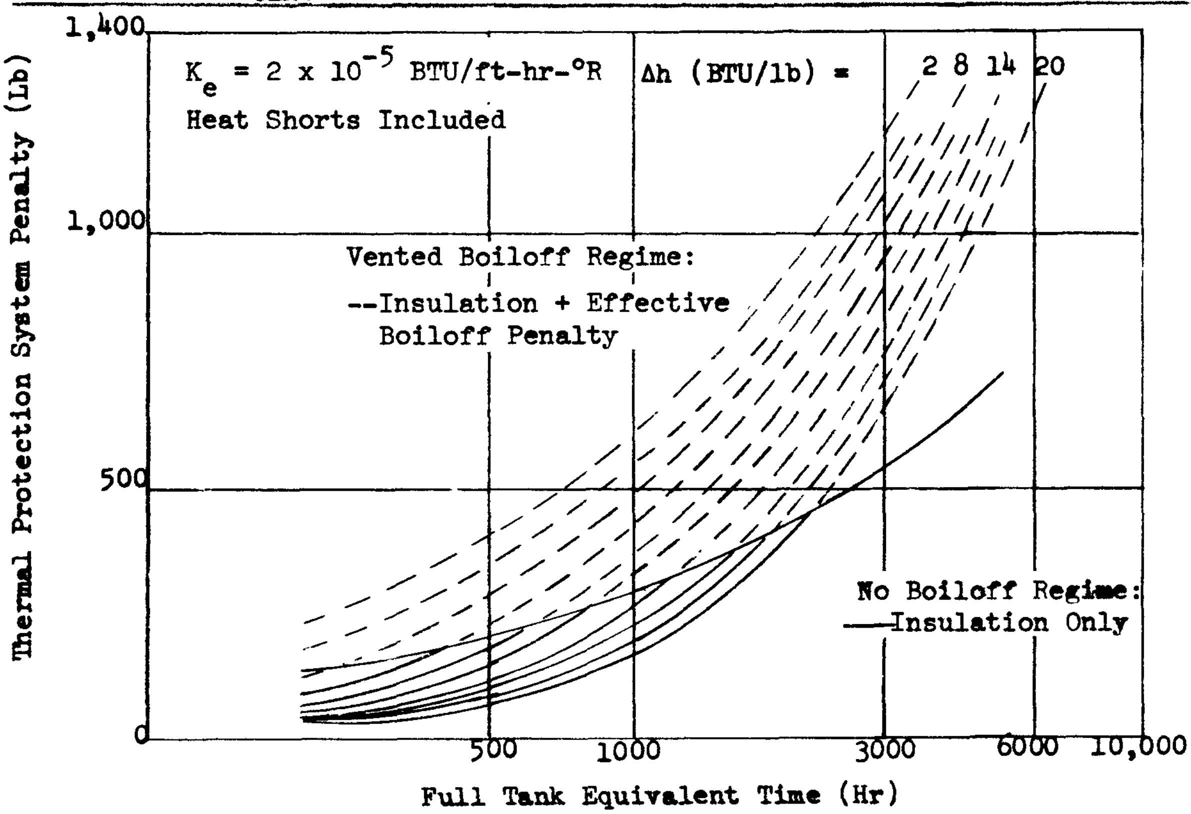

Figure 4.3-10 THERMAL PROTECTION SYSTEM DESIGN PARAMETERS-- PROPULSION MODULE

Figure 4.3-11 shows the sensitivity of the propellant module thermal protection system weight penalty to the insulation performance for two point design alternatives which are discussed in Section 4.3.11. A degradation of the design value from 2×10^{-5} up to the range of 4×10^{-5} would impose a major penalty on the design of the RNS system.

The thermal protection system weight sensitivity to subcooling is shown in Figure 4.3-12. Major performance gains could be achieved by reducing the hydrogen saturation pressure to the triple point (1 psia) or even using slush. The RNS structural design criteria require that propellant tankage shall not be pressure stabilized for any operations. However, if subcooling were utilized, pressure stabilization would be required for ground fill and launch operations unless supporting structures were incorporated into the tank design. A detailed analysis of this tank buckling problem is beyond the scope of the present study. However, a cursory investigation indicated that provision of ring frames to stabilize the tank against crushing pressure would result in structural weight which exceeds the potential savings in the thermal protection system. Accordingly, delivery of subcooled or slush hydrogen to orbit is not considered applicable for the RNS without further investigation of the structural design implications.

4.3.9 Nuclear Heating of Propellant

An evaluation was made of nuclear heating of propellant in the propulsion module run tank. A map of the energy deposition in the tank is shown in Figure 4.3-13 depicting isoheating lines. The total energy deposition rate at full power corresponds to 13 kw. This divides into 4 kw from gammas and 9 kw from neutrons. These were based on PATCH point kernel calculations with the following assumptions: (1) 1,574-Mw NERVA operating power; (2) no external shielding; (3) 80-in.-diameter run tank; (4) total-to-fast neutron flux ratio of 3; and (5) leakage fraction of 0.65 for LH_2 capture gammas in run tank.

The implications of nuclear heating were evaluated for several models and operational alternatives which are summarized in Table 4.3-13. There is a

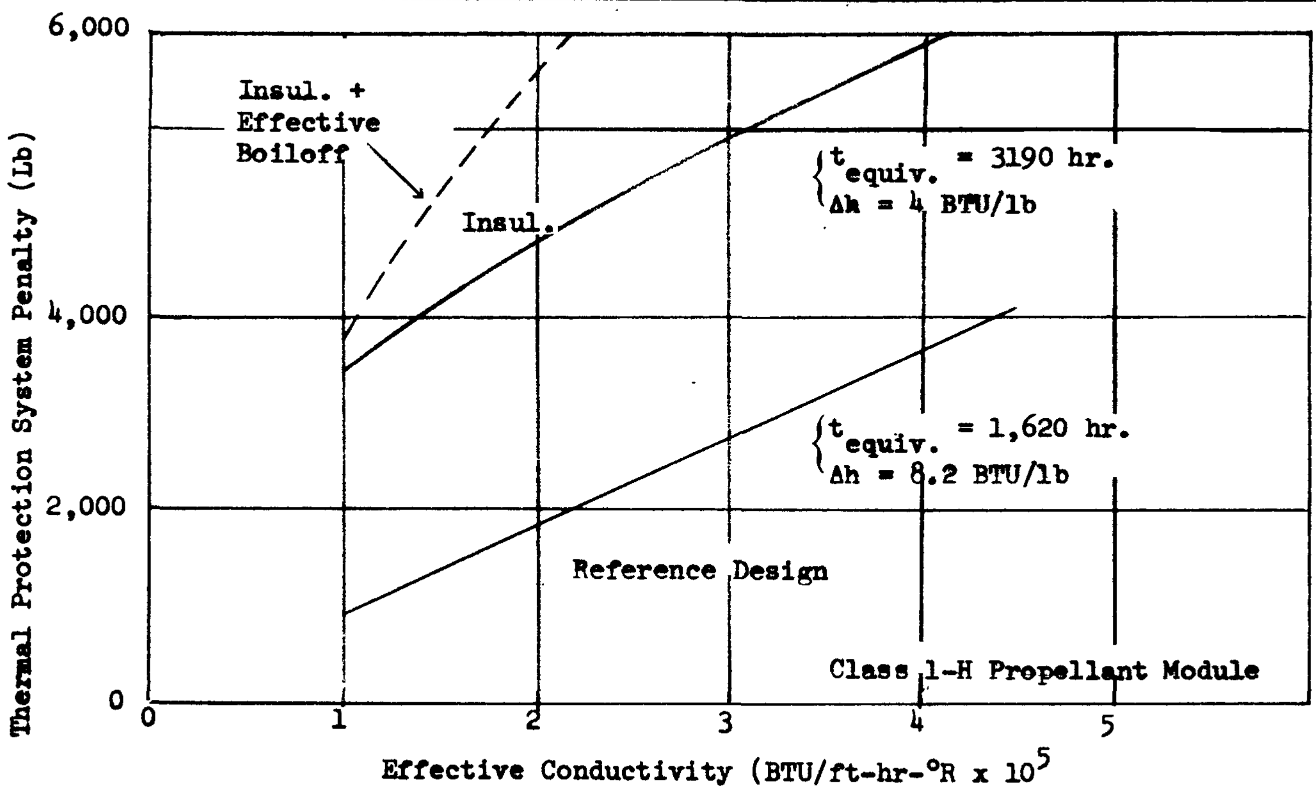

Figure 4.3-11 HPI PERFORMANCE SENSITIVITY

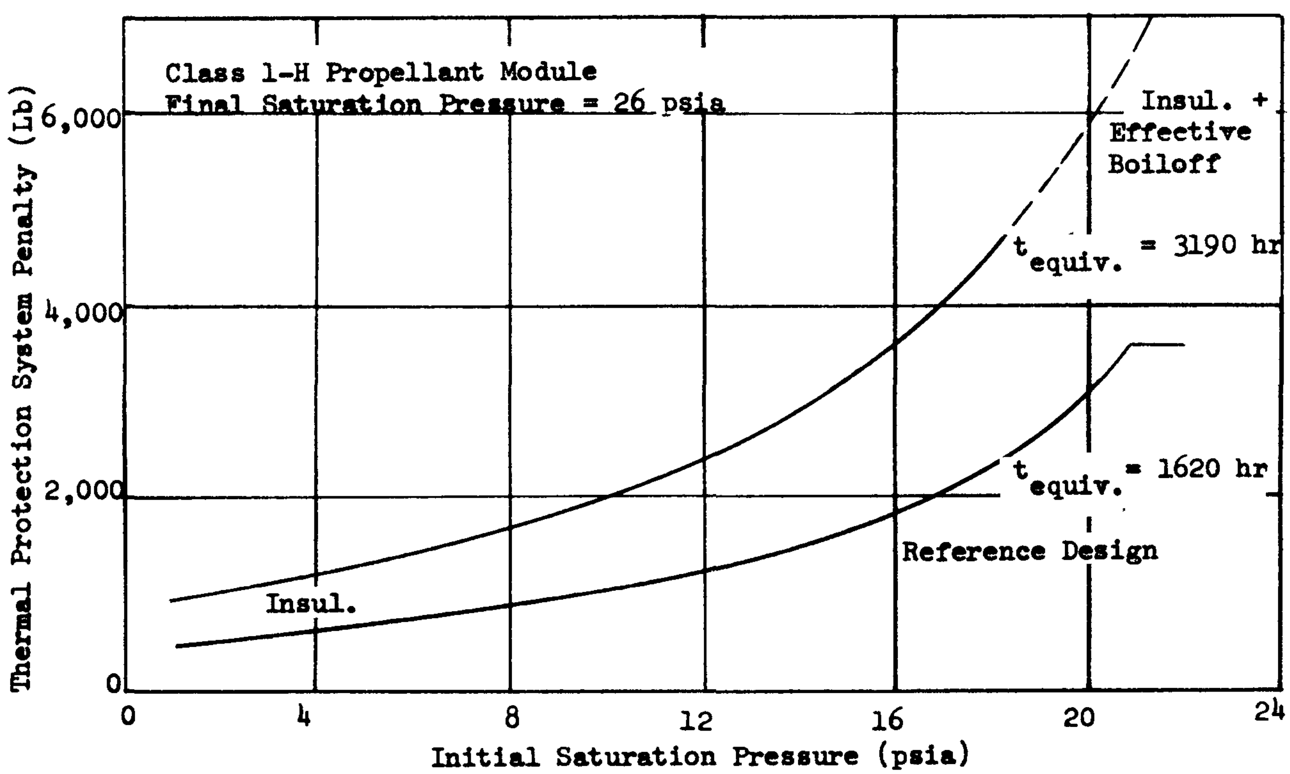

Figure 4.3-12 PROPELLANT CONDITION SENSITIVITY

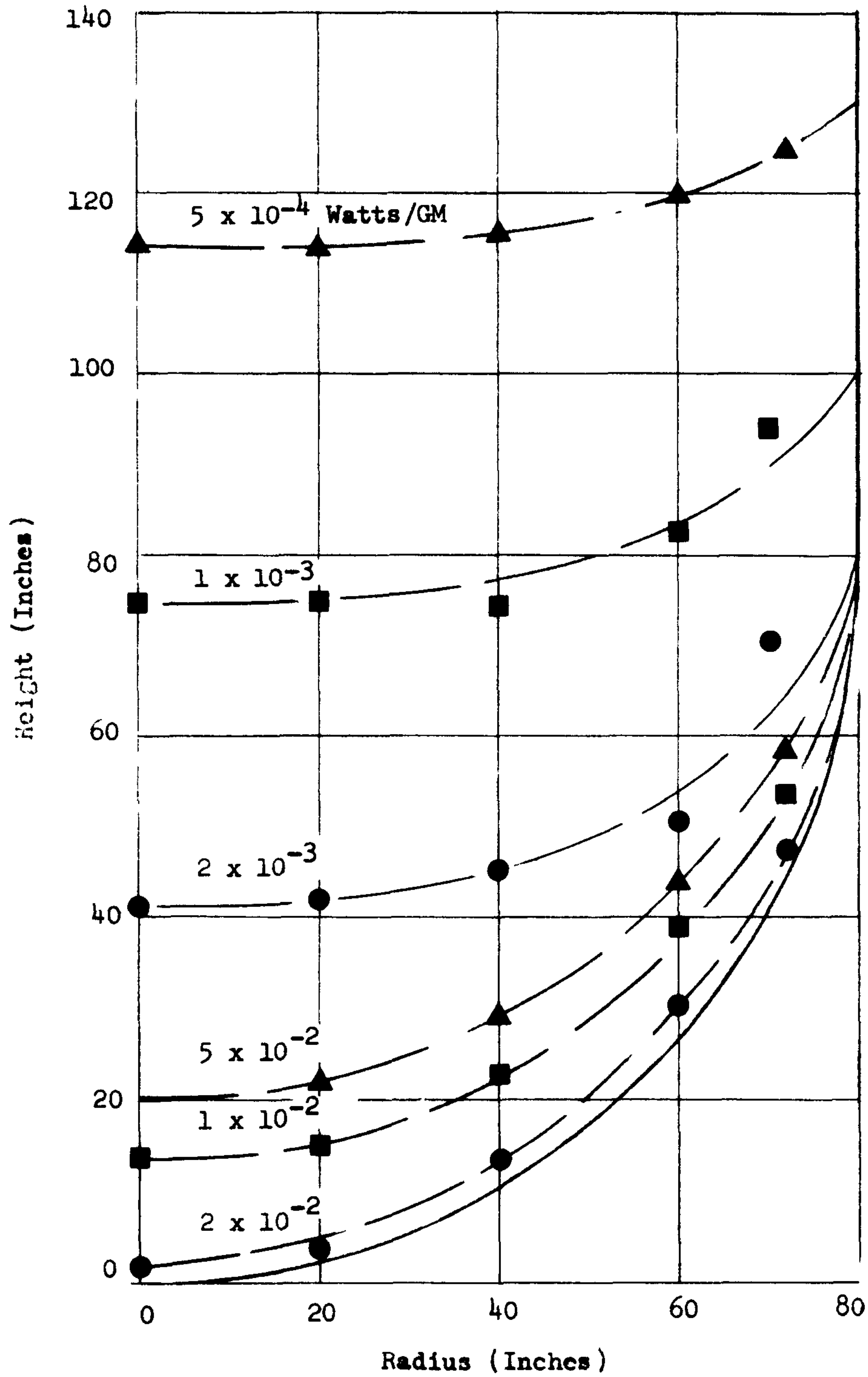

Figure 4.3-13 NUCLEAR HEATING IN RUN TANK

Table 4.3-13
NUCLEAR HEATING MODEL COMPARISON

Energy Distribution	Run Tank Status	Temperature Rise (°R)
Complete mixing	Steady state	0.054
Stratification	Steady state	8.8*
Complete mixing	Depletion for startup ramp	0.034
Complete mixing	Depletion for LOI-2 burn	0.094

*Alternative: 216 lb boiloff per mission.

minimal impact by nuclear heating if complete mixing occurs. Stratification would impose a severe pressure penalty without venting but can be accommodated with venting with a minimal boiloff penalty.

The criterion for determining when the complete mixing mode would dominate or when stratification would occur is not as yet established. Experiments by Anderson and Kolar (Reference 4-38) indicate that with bottom heating alone complete mixing is obtained. However the combination of bottom and sidewall heating results in an interaction between the modes in which the bottom heated fluid is unable to penetrate through the stable stratified layer resulting from sidewall heating. The shape of the energy deposition profile shown in Figure 4.3-13 suggests that a major portion of the heating would enter the tank as bottom heating. The feed system inlet from the propellant tank can be configured so that the incoming fluid jet would be directed upward to break up any stratified layer. Thus, nuclear heating should have a minimal impact on the RNS propulsion module design and operation.

4.3.10 Stratification

The implications of propellant stratification in the RNS were investigated for the lunar shuttle mission. Stratification can occur when a heat transfer mechanism (conduction or convection from boundary layers) permits the buildup of a layer of warm fluid near the surface of the liquid. The pressure in the tank will closely follow the surface temperature. The principal configuration of concern for evaluation of the RNS is a tank with the liquid oriented at one end with the heat flux through the sidewall being carried through the boundary layer on the sidewalls into a stratified layer at the surface. Such a configuration permits the bulk of the fluid to be unaffected by the sidewall heat input until the stratified layer has grown sufficiently to fill the entire height of the fluid volume. Use of an oriented fluid model with a sidewall boundary layer would require that the acceleration level be sufficiently large to provide a Bond number of unity. For very low acceleration levels, the liquid would assume a minimum energy configuration with wet walls and a central ullage bubble. The implications of stratification for this unoriented configuration are not well defined, but its impact is considered negligible.

The effects of acceleration from aerodynamic drag, solar pressure, limit cycling, attitude maneuvers, and orbital rates were evaluated. The critical acceleration levels for stratification assessment associated with various mission coast phases, the source of acceleration, tank Bond number, and liquid orientation are defined in Table 4.3-14. For orbit coast phases, the rotational rate associated with the gravity-gradient-stabilized mode tends to keep the liquid oriented at one end of the tank. However, at the aft end of the inboard propellant module the values in the table are reduced by a factor of 6, so the oriented model tends to break down.

Stratification was analyzed for the oriented liquid cases using the boundary layer model in References 4-39 and 4-40. The effects of bottom heating and ullage heating were neglected at this level of analysis. The difference between the surface temperature and the bulk temperature developed across the stratified layer is shown in Table 4.3-15, together with the time to fully develop the stratified layer.

Table 4.3-14

ACCELERATION CRITERIA FOR STRATIFICATION EVALUATION (CLASS 1-H)

Mission Phase	Duration (hr)	Source of Acceleration	Propellant Module		Run Tank		Liquid Orientation
			Acceleration* (g)	Bond No.	Acceleration* (g)	Bond No.	
Earth orbit (fully loaded)	904** 408	Orbit rate	2.7×10^{-6}	25	4.0×10^{-6}	6.0	Bottom
Lunar transit	108	Limit cycle	4.2×10^{-12}	3.9×10^{-5}	5.7×10^{-12}	8.5×10^{-6}	Wet walls
Lunar orbit (with payload)	24	Orbit rate	1.7×10^{-6}	16	2.3×10^{-6}	3.5	Bottom
Lunar orbit (without payload)	410	Orbit rate	5.3×10^{-7}	4.9	1.1×10^{-6}	1.7	Bottom
Earth transit	72	Limit cycle	1.1×10^{-10}	1.1×10^{-3}	2.3×10^{-10}	3.5×10^{-4}	Wet walls
Earth orbit (empty)	697	Orbit rate	1.0×10^{-6}	9.3	2.1×10^{-6}	3.2	Bottom

*Axial acceleration at aft end of module

**Propellant loading time

Table 4.3-15

POTENTIAL STRATIFICATION IMPACT
(CLASS 1-H)

	Propellant Module		Run Tank	
	Maximum Temperature Difference (°R)	Time to Fully Develop (hr)	Maximum Temperature Difference (°R)	Time to Fully Develop (hr)
Earth orbit (fully loaded)	1.3* 1.6	800* 1,000	1.4	500
Lunar orbit (with payload)	1.2	800	1.5	600
Lunar orbit (without payload)	1.1	1,000	1.8	900
Earth orbit (empty)	-	-	1.6	700
Sidewall Heat Flux (Btu/ft^2 Hr)	0.06		0.06	

*Half propellant loading

In LH_2 the stratified layer builds up very rapidly at first so that almost the entire temperature difference is developed in about half of this time. Once the temperature difference has developed across the stratified layer the base temperature of the fluid will grow with further heat input and the temperature difference will be maintained across the liquid. Comparing the estimated stratification times to the mission phase durations on this basis, it is evident that stratification is likely for the prolonged orbit coast phases of the lunar shuttle mission profile, if no mitigating factors are incorporated into the RNS design or operations.

The APS could be used without additional hardware to introduce slosh disturbances and geysering to mix the liquid. Alternatively, a pump mixer could be located inside the tank. While this approach would impose a small weight and power requirement, it does entail additional hardware. Thus, use of the APS is more compatible with the RNS design approach for maintenance. Several types of disturbance can be used to mix the liquid: continuous rotation about the tank axis, rotational slosh (about the tank axis), axial acceleration to induce geysering, and lateral acceleration. The lateral acceleration approach is adopted here as a representative baseline. According to the slosh wave criteria in Reference 4-41, a lateral impulse of about 10^{-2} fps can induce a breaking wave (amplitude of about 1/3 tank radius) on the quiescent surface. This would require less than 0.25 lb APS propellant for each disturbance. If such a disturbance were imposed each 48 hours, up to 50 pulses, or 12 lb of APS propellant would be required. Thus, use of the APS is considered to provide a practical approach to alleviation of stratification, but refinement of the technique will not be considered.

4.3.11 Thermal Protection System Definition

The various factors involved in definition of the RNS thermal protection system for the lunar shuttle mission have been defined in the preceding sections. Based on the considerations cited, nuclear heating of the propellant and stratification effects during coast will be neglected. Consequently, the principal considerations are the propellant initial and final conditions, the basis for the full tank equivalent time, and the strategy applied for propellant venting.

The evaluation of propellant tank design pressure in Section 4.2.4 indicates that there is no motivation for increasing the NERVA operating pressure from 26 psia. Chilldown of a warm tank can be taken alternatively as an increase in the initial saturation of pressure (5 psia) or as vented boiloff (7,000 lb). The full tank equivalent time for the mission, as broken down in Table 4.3-9, can include the period during which the propellant tank is being filled, or if the orbital heating is vented before the mission, it extends only from the time the propellant tank is topped off. Accordingly, four thermal protection system design strategies have been considered, defined in Table 4.3-16. Subcooling by venting in orbit is considered, but this would not be attractive if a space shuttle launch of subcooled propellant were feasible.

Evaluation of these strategies focused on the transportation cost for payload delivered to lunar orbit, considering that the reference RNS design has a fixed propellant capacity of 300,000 lb of LH_2. The payload delivery partial in Table 2.2-1 is $\partial PL_D/\partial$ inert weight = 2.7 lb/lb, which is applied to the total thermal protection system weight penalty. The reference payload

Table 4.3-16

CANDIDATE THERMAL PROTECTION SYSTEM DESIGN STRATEGIES (CLASS 1-H)

Description of Strategy	$t_{equiv.}$ (hr)	Δh (BTU/lb)
Non-vented chilldown; venting as required during the mission on demand.	3,190	4.0
Venting of initial tank conditioning propellant at the time of chilldown with subsequent venting as required during the mission.	3,190	8.2
Venting of tank conditioning propellant and orbital heating to reduce the propellant initial condition after topping off down to and including the propelland delivery condition of 16 psia.	1,620	≤8.2
Same as last paragraph but with additional venting prior to topping off to chill the LH_2 in orbit, resulting in an initial condition below 16 psia.	1,620	>8.2

delivered to lunar orbit is 110, 000 lb when the thermal protection system performance penalty is zero. The payload delivery to lunar orbit is plotted as a function of the propellant enthalpy rise in Figure 4. 3-14 for the cited system design strategies, indicating a continuous payload gain with increased heat capacity.

The cost of payload delivery to earth orbit was held fixed at $15 million (considering palletized cargo) while the value of the RNS was taken as $14 million per mission. Thus, the major economic factors are the payload weight delivery, which is reduced by the thermal protection system performance penalty, and the propellant delivery cost to orbit, which includes additional propellant delivery requirements if venting occurs prior to the mission. Propellant delivery was assessed $167/lb (30, 000 lb LH_2 at a cost of $5 million), which is considered high, but accentuates the optimization. This charge was applied uniformly to all propellant delivered to orbit on the basis that leftover propellant in the tanker would be delivered to a second RNS so that space shuttle flights would not be wasted.

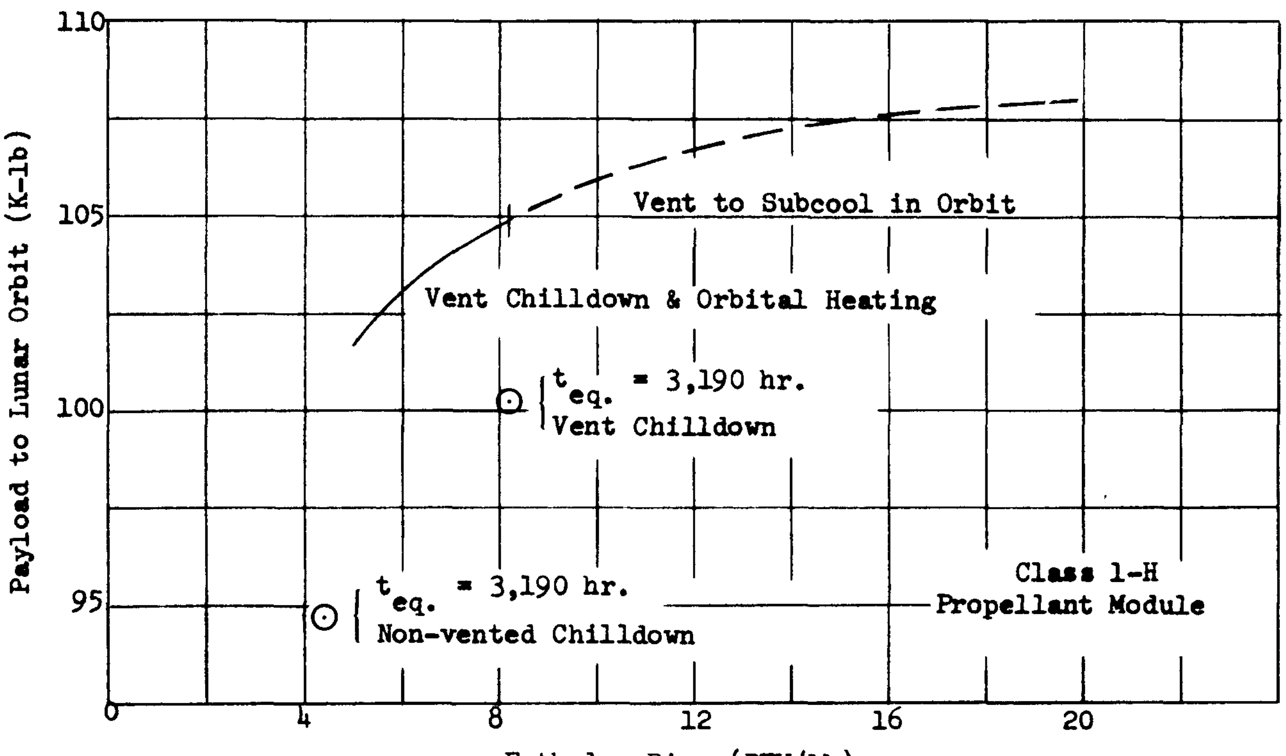

Figure 4.3-14 THERMAL PROTECTION PAYLOAD IMPACT

The economic implications of the various design strategies considered is shown in Figure 4.3-15 according to the indicated ground rules. It is most favorable to vent the tank conditioning propellant and the orbital heating incurred prior to TLI. The tank must then be topped off, with the optimum resulting initial condition being approximately 16 psia, which is the condition of the delivered propellant. There is no further performance benefit by venting to subcool the propellant module. The resulting thermal protection system design is summarized in Table 4.3-17. The run tank is filled initially at the time of topping off, so only tank conditioning propellant is vented from it.

Heat shorts severely impact the run tank, and pre-TLI venting and topping off to subcool to 7 psia is indicated to avoid venting during the mission. This would require venting an additional 600 lb LH_2 prior to topping off. If NERVA after-cooling utilized gas instead of liquid from the run tank, venting during the mission could be accomplished without a performance penalty. While not explicitly provided for in the reference design, gas or mixed phase cooldown could be accomplished. Accordingly, the run tank initial condition is set equal to that of the propellant module and the required vented boiloff during the mission is not charged against the design weight.

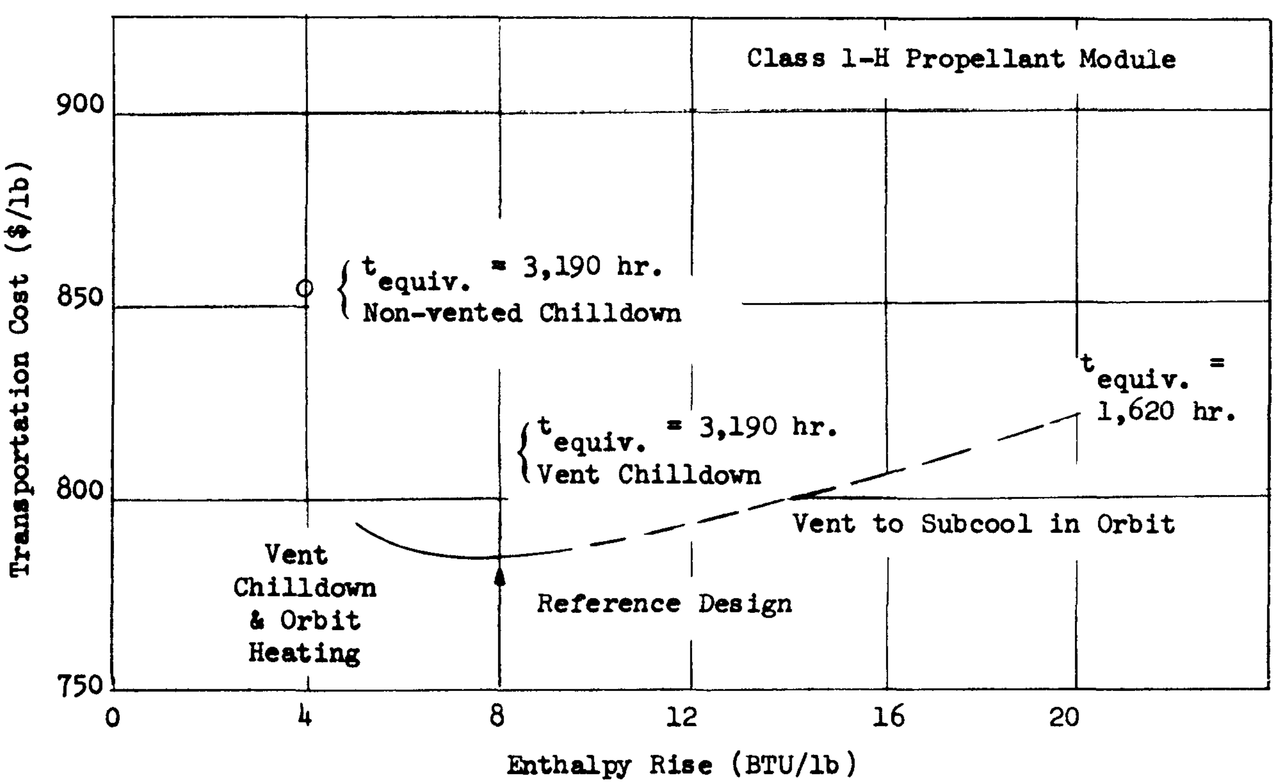

Figure 4.3-15 THERMAL PROTECTION SYSTEM ECONOMICS

Table 4.3-17.

THERMAL PROTECTION SYSTEM DESIGN SUMMARY

Class 1-H

	Propellant Module	Run Tank	Total System
Tank surface area (ft^2)	9,706	964	
Heat short insulated area (ft^2)	402	230	
Propellant loading (lb LH_2)	289,150	10,850	
LH_2 saturation pressure after topping off (psia)	16.0	16.0	
Full tank equivalent time (hr)			
Before mission	430	430	
During mission	1,190	1,298	
Total	1,620	1,728	
Insulation thickness (in.)	0.53	1.0	
Number of sheets	51	96	
Insulation mass (lb)	1,820	410	2,230
LH_2 boiloff (lb)			
Vented during mission	0	0*	0
Vented prior to topping off	12,800	220	13,020

*Not charged, considering use as aftercooling.

The transportation cost minimum covers a broad range of initial conditions, so the amount of premission venting is not critical. When less than maximum payload delivery were required on a mission, the amount of premission venting could be reduced accordingly.

Lower propellant delivery costs could be considered. The value applied here takes no credit for improved space shuttle payload delivery to orbit when it is not required to return with equal payload. The $167/lb value could be reduced to about $137/lb by this consideration (see Vol. II, Part B, Section 3.6.2), and potential increased space shuttle performance could reduce the cost further. Availability of cheaper LH_2 would increase the bias toward premission venting and propellant subcooling.

It should be emphasized that the coast time in orbit prior to initiating TLI becomes a major factor in this system optimization. The 18-day coast time as a full tank provided herein is conservative, and further optimization is available, as indicated by Figure 4.3-16, by arranging the propellant delivery and the payload delivery and CCM replacement operations. There is a 35 percent insulation weight margin compared to a zero coast time after topping off. Since all of that weight reduction could not be achieved in practice, the inherent design margin is reasonable.

4.3.12 Propellant State History

The propellant state conditions for the reference thermal protection system design in Table 4.3-17 are based on the mission equivalent time history presented in Figure 4.3-7. No venting occurs after propellant has been topped off at 16 psia. The primary consideration is the propellant saturation pressure at startup in Table 4.3-18, which establishes the tank pressurization requirements.

4.3.13 Radiation Effects

A literature search was performed to assess the effects of nuclear radiation on the components of the meteoroid/thermal protection system: Mylar, Dacron, Nylon, and polyurethane foam.

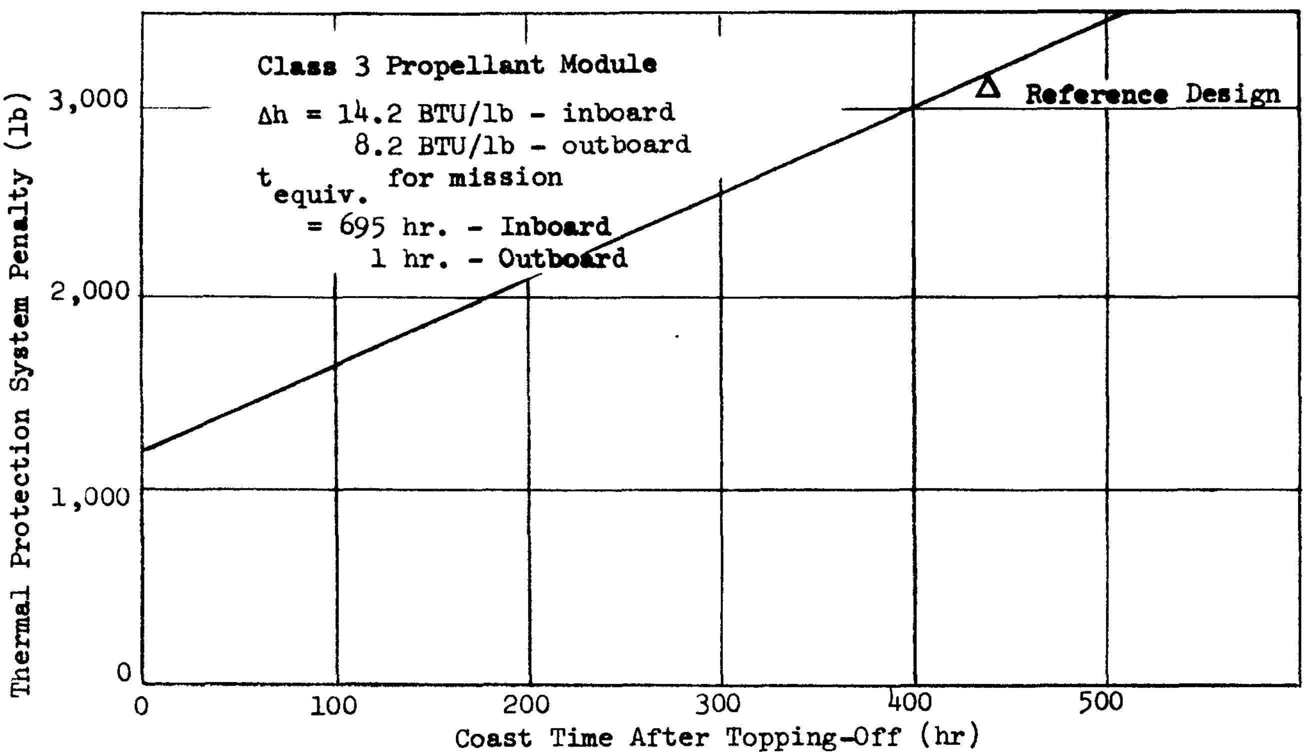

Figure 4.3-16 ORBITAL COAST TIME SENSITIVITY

Table 4.3-18

PROPELLANT SATURATION PRESSURE AT STARTUP (PSIA)

CLASS 1-H

Burn	Propellant Module	Run Tank
TLI	18.6	18.4
LOI-1	19.6	19.4
LOI-2	-	19.5
LOI-3	19.8	19.6
TEI-1	24.6	22.5
TEI-2	-	23.5
TEI-3	25.0	24.0
EOI	26.0	24.9

The gamma dose rate and fast neutron flux are defined in Section 4.5.11. The critical location is the propulsion module aft zone, with a dose criterion for 10 round trips of 10^8 rads, which includes a factor of 10 safety margin.

Although there is considerable spread in the radiation data on Mylar, it seems likely that at the temperature at which it will operate (near that of the liquid hydrogen) and in a vacuum, it could withstand at least 3×10^8 rads (Reference 4.42 through 4-45) before there was any danger that it would buckle or crumble spontaneously, since almost no lateral stress is applied.

Gassing of the Mylar, Dacron, and Nylon is not a serious problem, since the blanket layers contain perforations and gas passages which will allow the gas to escape. No blistering of the alumunim coating on the Mylar is expected, since the aluminum is only 13 Angstroms thick; it is expected that the gas will escape through gaps and perforations. However, there is a slight possibility that some of the aluminum would flake off at the expected dose.

There are no data on how radiation affects the thermal conductivity of Mylar and Dacron; however, since in plastics in general radiation does not cause a permanent change in electrical conductivity (Reference 4-27), and since electrical and thermal conductivity would be expected to behave similarly, no change is anticipated.

Since Dacron, which is a type of polyethylene terephthalate, like Mylar, is considered very radiation-stable, and is under only a slight stress in this application, it is expected to withstand at least as much radiation dose as the Mylar.

For the foam, the main radiation effects are gassing, a change in compressive strength and a possible increase in thermal conductivity. Gassing is not a problem as long as the gas which forms in the individual cells is able to escape, along with the gas formed by the Mylar. To allow the gas to vent, the fiber glass shroud has blowout patches. Changes in compressive strength are not important, since the foam will not be compressed after it reaches earth orbit. Only limited data are available on changes in thermal conductivity, but it shows that at cold temperatures some types of rigid foam may increase significantly (30 percent) while other types increase only a few percent, at the radiation dose expected at the aft end of the propulsion module (Reference 4-46). Results may be different in a vacuum, however, since the absence of oxygen would decrease the radiation damage.

No radiation problems are foreseen for the laminated fiber glass, as discussed in Section 4.2.9.

There are no available data on the combined effects of nuclear radiation and long term exposure to the space environment on the performance of thermal protective coatings.

4.4 DOCKING

4.4.1 Phase II Concept

During Phase II the four docking systems depicted in Figure 4.4-1 were evaluated considering 42,000-lb, 15-ft diameter by 60-ft long modules. The preliminary system weights compared as follows: cone/ring, 520 lb; fork/ring segment, 280 lb; ramp/ring, 280 lb; and multiple probe/drogue, 280 lb. The cone/ring system was considered most complex, based on number of components, while the others had a complexity factor equal to one-half that of the cone/ring. The fork/ring segment concept was rated somewhat less favorable for capture compliance, which is related to the inherent margin for operation of the acquisition or capture latching mechanism. Good indexing in roll is inherent for the ramp/ring and multiple probe/drogue systems, but is difficult for the cone/ring. Axial length is also significant for volumetric efficiency of modules launched in the space shuttle. The multiple probe/drogue arrangement was selected on the basis of minimum weight and space, and probable best performance. In addition it is adaptable to the "retractor" docking concept wherein the modules instead of impacting at low velocity, are stationed within range of the probe mechanisms. The probes are then deployed, latched and retracted to draw the modules together. This selection of this system was not considered crucial, however, and could be revised to be compatible with other space program elements.

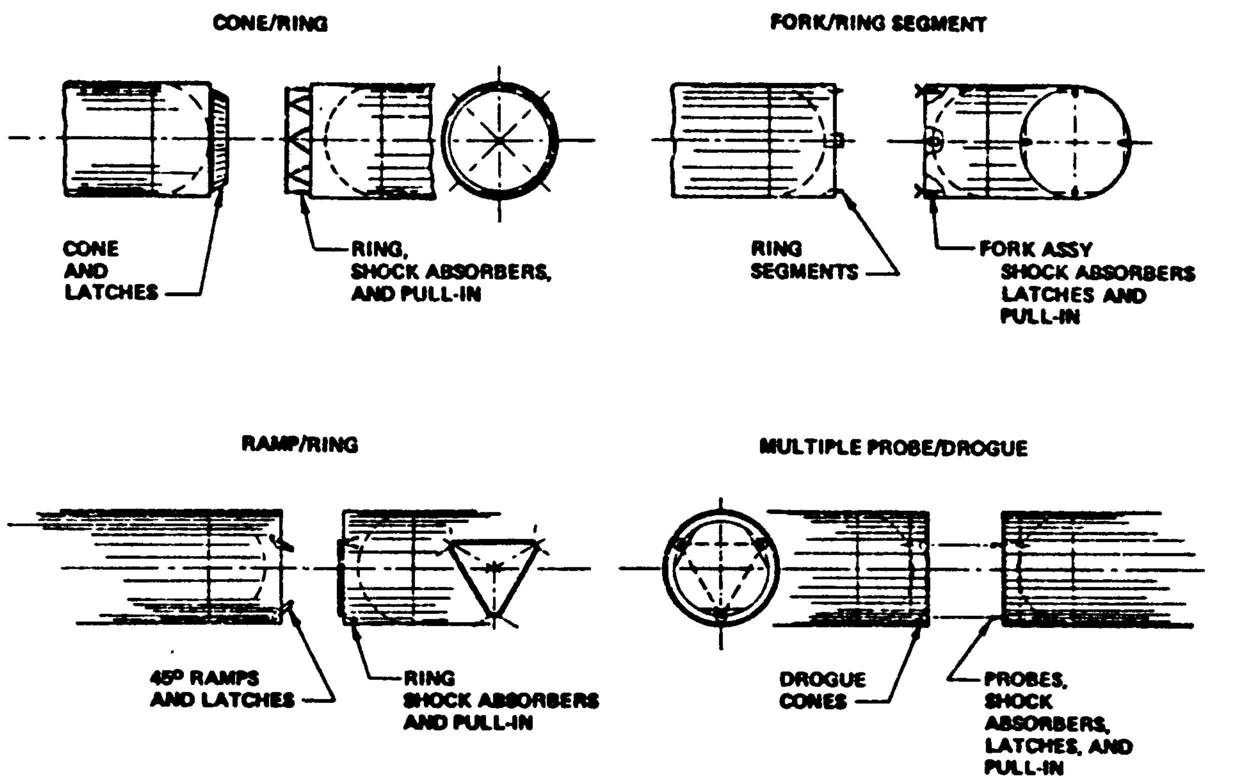

Figure 4.4-1 CANDIDATE DOCKING STRUCTURES SCHEMATIC

Figure 4.4-2 shows an inboard profile at the docking interface. The four probes and their supports are shown in View A-A, the cones in View B-B. The cone diameter is 28 in. to provide for a maximum axial misalignment of 10 to 12 in. In the deployed position, the probe tips extend 20 in. axially beyond the module interface.

4.4.2 Design Criteria

The RNS system design is based on multiple modules which can be assembled and disassembled in orbit. This will be accomplished under automatic or remote control.

The RNS module designs will incorporate end-to-end docking. The docking interfaces between RNS modules, space tug, payloads, and space shuttle are considered to be common and reusable. The docking mechanism provides for mechanical latching (capture or acquisition) within a prescribed misalignment tolerance at initial contact or before large forces are developed. Impact

BLANK

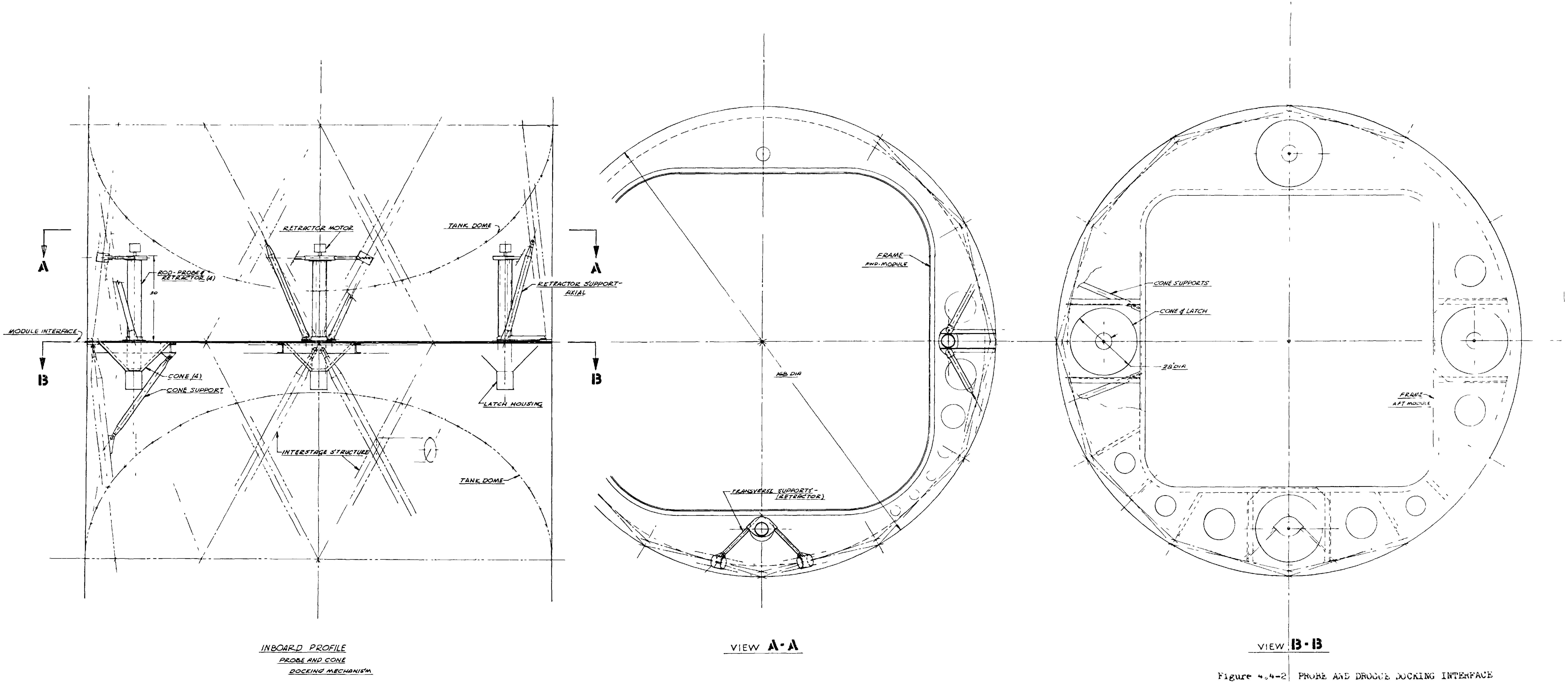

Figure 4.4-2 PROBE AND DROGUE DOCKING INTERFACE

energy will be dissipated without imposing excessive loads on the vehicle structure. Docking forces will not be used to actuate or lock latching mechanisms. The system design will align the modules, lock them rigidly together, and transmit all subsequent operational loads. Provision is made for unlatching and demating. The docking and clustering mechanism designs will incorporate provisions for status monitoring and external control during assembly or docking operations.

The docking mechanism designs will satisfy all structural design criteria in Section 4.2.2 to assure incredibility of failure of structural components. The docking mechanism design accommodates tolerances, established with reference to nominal laser radar performance characteristics (Reference 4-47) for a corner cube pattern on the modulus, considering the resultant of a 10 lb-sec impulse for maneuvering an empty propellant module, as denoted in Table 4.4-1.

Table 4.4-1
DOCKING MECHANISM DESIGN CRITERIA

Parameter Accuracy	Design Value
Longitudinal position (in.)	± 5
Lateral position (in.)	± 5
Angle, pitch, or roll (deg)	± 3
Longitudinal velocity* (ft/sec)	± 0.1
Lateral velocity (ft/sec)	± 0.1
Pitch angular velocity (deg/sec)	± 0.2
Roll angular velocity (deg/sec)	± 0.02

*The design will accept a relative impact velocity of up to 0.2 ft/sec

4.4.3 Probe/Drogue Mechanism

The probe/drogue assembly is shown in Figure 4.4-3. The upper half of the sectional view depicts the system in the latched position and the lower half shows the retracted or launch position. The probe assembly (including shock absorbers and pull-in mechanisms) is attached to one module and a mating drogue cone is mounted to the other module. The probe, which has a flexible tip, is actuated by a motor-driven screw jack. The flexible tip is deflected along the cone surface and enters a latch pocket at the vertex. Capture is accomplished by the probe riding up the inclined plane latching cams, which are spring loaded closed and probe deflected open to accomplish the catch. Probe release is effected by actuating the four pull-solenoids to retract the cams. The flexible sections are then retracted, pulling the rigid sections of the probes into the cones, to align the modules. Marring of the cone is prevented by installation of a soft wire mesh on the rigid probe. Further retraction of the probe draws the aligned modules into contact. A flange is incorporated on the probe housing to provide a better draw up load path and to improve stability and tolerance absorption capability. A solenoid operated deactuating ratchet to prevent recoil of the hard probe is mounted on the probe housing. The cone diameter was reduced to 14 in. as a result of a 50 percent reduction in axial misalignment criteria.

4.4.4 Latching

The tension load on the docking structure was determined based on the data generated from the tank support and structural attachment study delineated in Section 4.2.7. In this investigation the engine was gimbaled hardover at 5.7 degrees under 75,000 lb of thrust and produced a moment of 2.5×10^6 in-lb, a shear of 5,130 lb, and an axial load of 67,800 lb at the interface of intermodular thrust structure. These loads in turn induced a tension load of 8,950 lb into the docking structure, which exceeds the tension-carrying capability of the system. Therefore, additional latches are required to ensure the structural integrity of the assembled vehicle. The system must also be capable of unlatching in order to separate the modules if replacement is necessary.

Two concepts were investigated. The first system utilized a rotating turnbuckle which extended open-end latches to engage shoulder studs in the mating module.

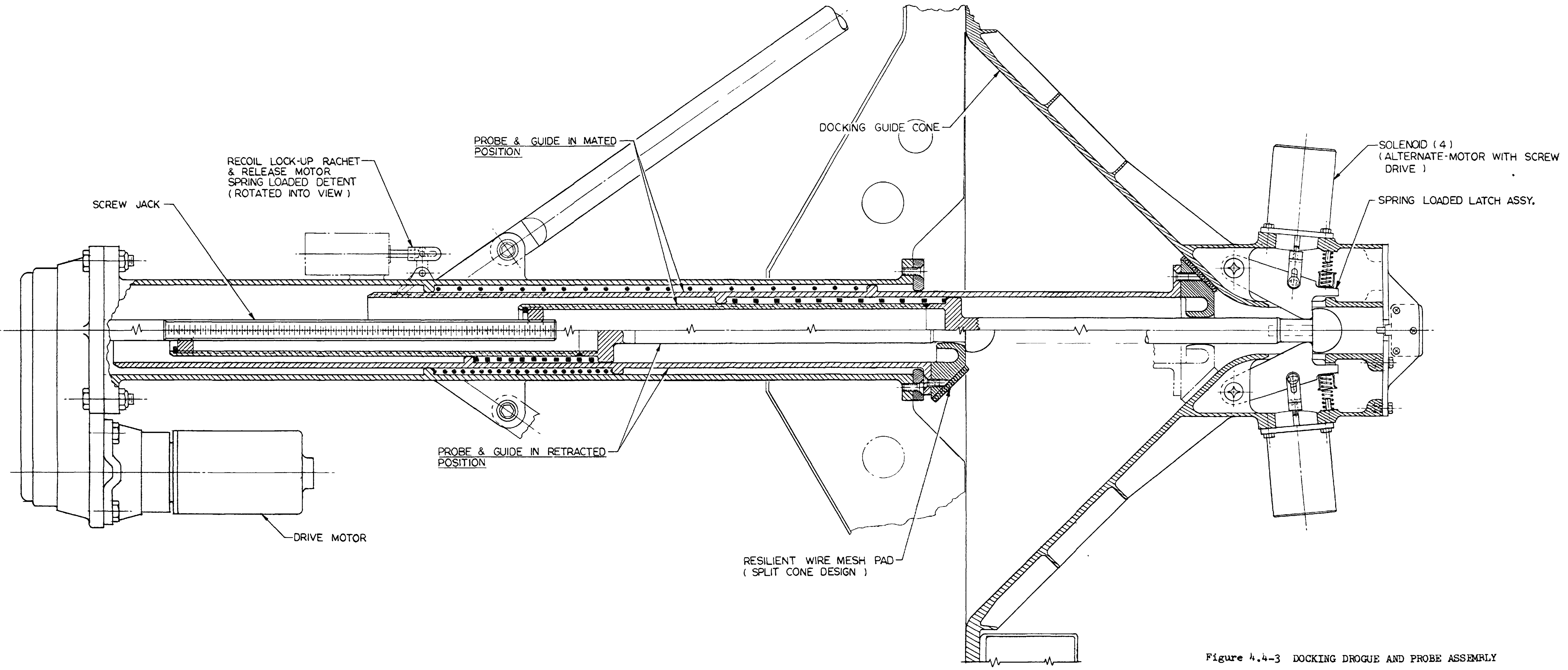

Figure 4.4-3 DOCKING DROGUE AND PROBE ASSEMBLY

The second system employed hook-type latches to engage striker plates in the mating module. Both systems were designed to withstand a tension load of 4, 280 lb acting normal to the interface plane at the intersection of each pair of skirt structure struts. These intersections are spaced 30 degrees apart on a 174-in. diameter circle, resulting in an approximate spacing of 46 in.

The hook system was selected based on simplicity and reliability. Twelve motors, one at each latch point, were required for the turnbuckle concept while only one is needed to operate all 12 latches in the hook concept. Another disadvantage of the turnbuckle system is the possibility of the open-end latch binding under the shoulder stud and not being able to bottom.

The hook system shown in Figure 4.4-4 is actuated after the docking system has aligned and joined the two modules. The hook-type latches located at 12 points around the interface frame are activated simultaneously by a single cable driven by a reversible drum and motor assembly. A braking system incorporated in the motor holds the latches in both the closed over-center or open positions.

The latch and link assemblies are attached to machined supports in the aft module interface frame with the axes lying in a radial plane of the frame. Each assembly consists of a hook and four links. Motion of the hook is controlled by a pin riding in a machined slot in the frame. Upon actuation, the hook travels through clearance holes in the mating frames and engages an adjustable striker plate mounted on the opposite frame. The frames are locked as the links are rotated to their over-center position. Unlatching is accomplished by reversing the direction of cable travel which returns the hook to its normal unlocked position. A shear pin is provided at each latch for alignment and transfer of shear loads between modules.

4.5 MAIN PROPULSION

4.4.5 Phase II Concept

This section establishes the Phase II propulsion systems concept and the rationale for the additional analyses performed during Phase III. During

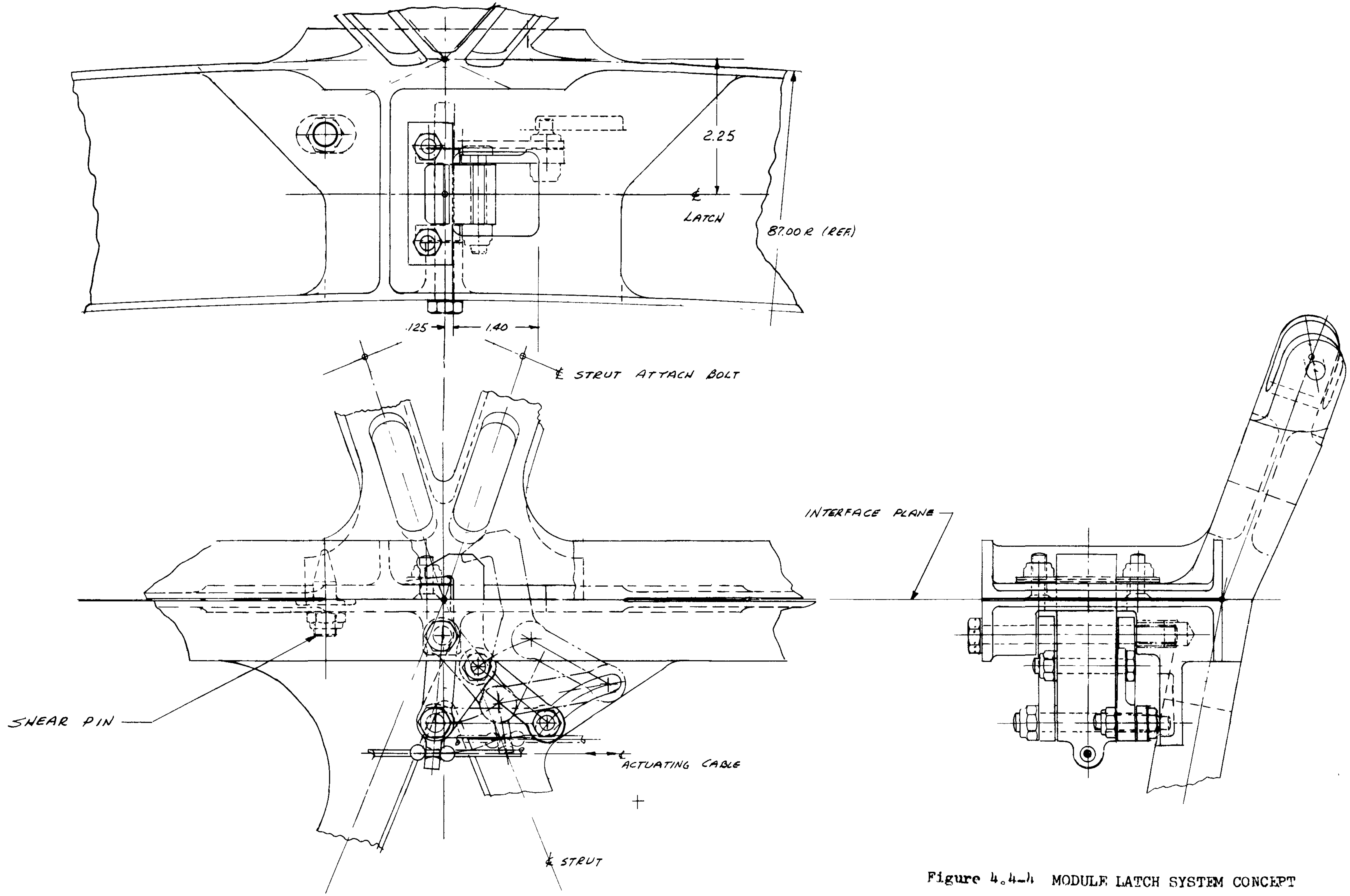

Figure 4.4-4 MODULE LATCH SYSTEM CONCEPT

Phases I and II, most basic propulsion system design features were selected on the basis of weight, cost, and reliability (see Section 2 of Reference 4-2 for specific tradeoff data). These included valve sizes and types, valve actuation, valve normality, seals, ducting, remote coupling, functional checkout and leak check provisions, and the type of prepressurization system. Saturn-derivative and advanced system configurations were defined, including evolutionary requirements, for the reference mission/program model. Reduced development requirements led to selection of the advanced stage concept.

Phase II concentrated on a reusable mode of operation requiring advanced propulsion systems. Multiple module RNS configurations were defined, as described in Section 4.1, and the propulsion functions were allocated to the individual modules consistent with orbital maintenance requirements. Selections were made for the new components required. A major consideration was the requirement to provide remote fluid line deployment and coupling to accommodate orbital assembly/disassembly of the RNS modules. Electric-motor-driven ball screw jacks were selected for these functions. The engine/stage interface selected was a ground assembly interface within the RNS propulsion module. Reduced prepressurization requirements associated with the propulsion module run tank permitted selection of a prepressurization system concept of ambient GH_2 bottles, rechargeable by the engine tap-off gas, located on the propulsion module. This system was integrated with a cold-gas APS system for stabilization of the module during assembly operations. The propulsion schematic was revised for the multiple module approach, but except for the considerations indicated, the bases for the applicable Phase I advanced stage feature selections remained unaffected by the configuration changes. Phase II was completed with a detailed definition of design features, as documented in Section 5 of Reference 4-1.

The philosophy utilized in the Phase II study was to position all of the major valving in the forward area of the vehicles, thereby reducing radiation dose levels to where state-of-the-art organic lip seals could be used as main gate seals. This philosophy was continued in the Phase III with the following exception: instead of adhering to existing valve main gate organic seal configurations solely, seal development will proceed with the evolutionary requirement of metal-to-metal seals considered.

The NERVA engine configuration utilized in the Phase II study had both of the main turbopumps mounted inside a shrouded upper thrust structure (UTS). The updated NERVA configuration for Phase III is an outboard mounted pump configuration with an internal thrust structure, which affords the ability for remote access to equipment. This is contrary to the baseline Phase II MDAC philosophy of maintenance at the orbital assembly level, which was carried over to Phase III, and results in a number of engine design compromises with respect to configuration and location of components.

NERVA requirements changed for Phase III, including its configuration, required propellant conditions and autogenous start capability. The latter consideration eliminated the rechargeable, ambient GH_2 prepressurization system. Stage startup and steady-state operations were evaluated during Phase III, resulting in identification of additional propulsion functions and requirements. These include engine/stage feed system chilldown, run tank refill, and propellant management control, which are covered in Section 3 of this report. The subsystem designs for these functions are generated and analyzed in the subsequent sections. Intermodule propellant feed system interfaces were refined. Feed system pressure drops were established to permit definition of propellant management control operations and tank design pressures. Orbital assembly requirements were also evaluated in depth to establish deflections of ducting. Radiation effects on organic seals were reviewed. These analyses are presented in subsequent sections, and the resulting definition of design features is contained in Book 2.

4.5.2 Design Criteria

4.5.2.1 NERVA Requirements

The definition of the NERVA engine and its requirements are contained principally in References 4-8, 4-13, and 4-14. These are supplemented by additional data submitted by ANSC and MSFC.

The ANSC fluid line interface with the RNS consists of: (1) feed duct, two required, 10.5-in. diameter; (2) aftercooling bypass line, 3-in. diameter; and (3) pressurant line, 1.25-in. diameter. The isolation valves for these lines are currently located on the engine side of the engine/stage interface.

NERVA LH_2 flow rate requirements for nominal performance are: (1) full power, 91.9 lb/sec; and (2) aftercooling pulse, 0.7 lb/sec. NERVA bootstrap startup and shutdown ramps are defined by References 4-13 and 4-14 and the aftercooling pulse parameters defined parametrically in Reference 4-13. The propellant conditioning requirements for steady-state full-power operation conform to Figure 4.5-1, derived from Reference 4-48, which includes a steady-state operating pressure of 26 psia, saturated liquid, with 0 NPSP. Reduced flow rates are permitted at 0 NPSP and saturated liquid for saturation pressure below 26 psia, according to Figure 4.5-2, to provide autogenous start capability.

The RNS must provide propellant conditions for a NERVA malfunction mode. However, the total pressure (saturation pressure plus NPSP) will not exceed 26 psia for such a mode. During pulsed aftercooling, the RNS will provide saturated liquid to the bypass line at a pressure exceeding 16 psia.

The NERVA engine will provide pressurant flow as required for all RNS operations except during pulsed aftercooling. GH_2 is supplied at 225°R.

4.5.2.2 Stage Design Principles and Philosophy

The RNS propulsion systems are designed to fail-safe criteria on all credible features to prevent loss of crew and supporting personnel or unacceptable risk to the general population. They are designed to permit remote assembly and disassembly of RNS modules in orbit, consistent with the policy for initial assembly, maintenance and repair. Fault detection and isolation is consistent with this policy. All components are designed for the full system lifetime.

NERVA removal and replacement in orbit will be accomplished by removal and replacement of the complete propulsion module. The propulsion module will be launched to orbit in the cargo bay of the space shuttle in a dry, unpressurized condition. An engine purge function is not provided by the RNS for launch.

The RNS propulsions systems will contain provisions for automated functional and leak checks. All static connections shall contain dual seal flanges with an integrated leak check port. Welded joints are used wherever possible.

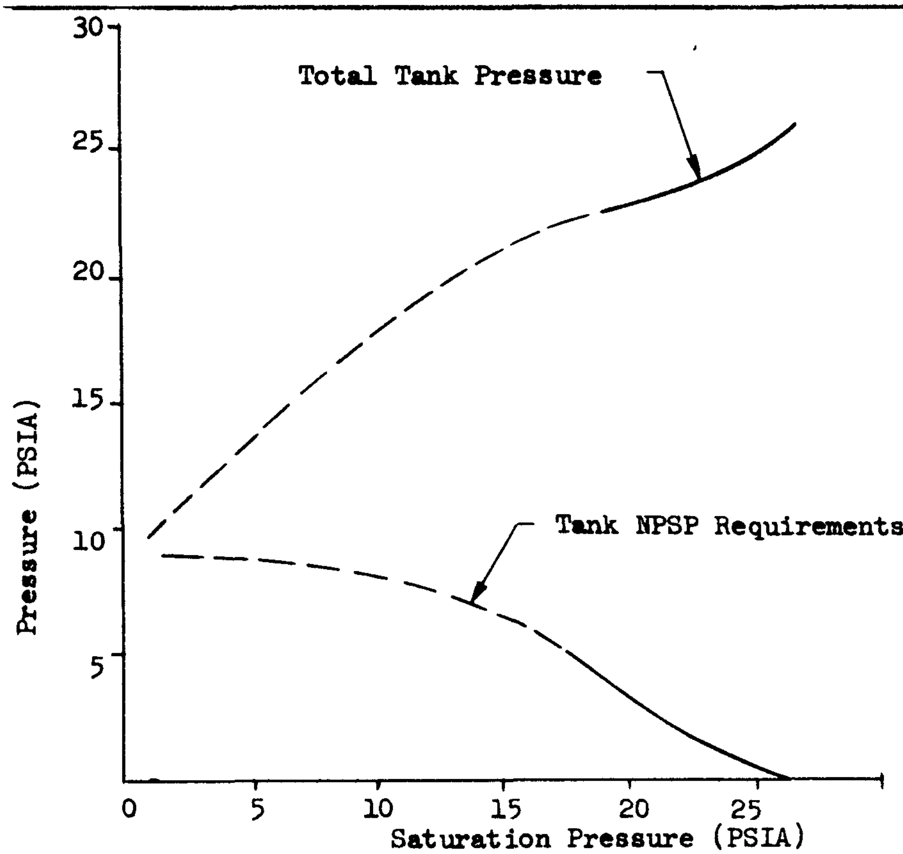

Figure 4.5-1 RNS PRESSURE REQUIREMENTS

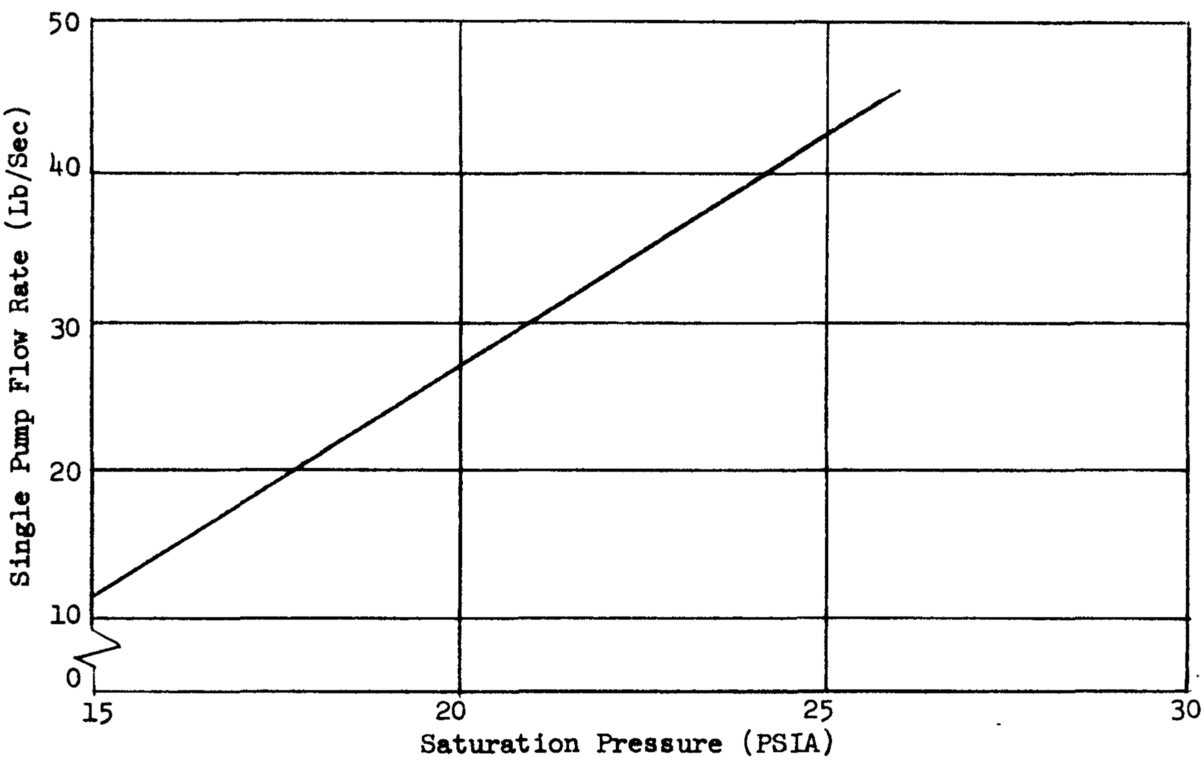

Figure 4.5-2 NERVA PUMP PERFORMANCE FOR SATURATED LIQUID AND ZERO NPSP

All discrete LH_2 tanks are designed to permit isolation, independent checkout, and independent pressure control.

Fluid line interfaces between propellant and propulsion modules are limited to LH_2 feed ducting and pressurization lines. Disconnects are provided for coupling these in orbit. All ducting will be designed to minimize the heat input into LH_2 tankage. Bellows shall be multi-ply, gimbaled, and have mechanical stops to preclude excessive loading. No unrestrained bellows are used. In all LH_2 ducting where fluid can be trapped between series valves, closed loop pressure relief provisions will be incorporated. All RNS valves operated during orbital and flight operations will be electrically actuated. Valve sequencing system operations will consider minimizing liquid entrapment in ducting.

Pressure stabilization of LH_2 tankage is not employed for transportation, handling, prelaunch, or launch operations. Interfaces with existing facilities and GSE will be accommodated to the maximum extent feasible, without performance degradation.

All equipment will be located and mounted so as to prevent degradation of their performance by natural or induced environments.

4.5.2.3 RNS Operational Requirements

Prelaunch

A low-pressure inert gas purge is provided in all tankage before filling. Confined areas external to the LH_2 tank are purged by GSE or space shuttle support services. LH_2 tanks are filled in the as-launched position, with provision for topping off. Ground pressurization for rapid expulsion of LH_2 is provided by GSE.

Launch

Umbilical interfaces are provided to the space shuttle for status monitoring and power to support emergency operations during launch.

Orbital Assembly and Disassembly

Fluid line coupling and decoupling in orbit will be accomplished under automatic or remote control. Docking forces are not used for coupling. Flexible ducting elements will be used to accommodate and assembly and operational deflections and tolerances. Progressive checkout will be utilized during the assembly operations.

Flight Operations

The active portion of the LH_2 feed system must be chilled down prior to NERVA bootstrap start. Prepressurization and expulsion pressurization utilizes NERVA bleed hydrogen gas. The propulsion module run tank will be refilled and maintained at a specified level during full-power operation to minimize the radiation impact on equipment. Propellant for pulsed after-cooling will be provided by the propulsion module. Provision is made to vent propellant tanks prior to or during the mission. Propellants will be maintained oriented at the bottom of the tanks during venting operations.

Propellant Resupply

LH_2 is resupplied by orbital transfer. The propellant will be in a settled condition during transfer operations. Equilibrium of liquid and gas conditions will be maintained to obviate venting during transfer. The RNS will control liquid levels and pressures inside the propellant modules during transfer. Chilldown of tanks for propellant transfer will be accomplished in a manner compatible with the normal operational tank pressure schedule.

4.5.3 Basic Propellant Management Functions

The simplified propellant management schematic in Figure 4.5-3 shows the propulsion module propellant module with functions provided for ground, launch, and minimum mission operations. This essentially represents the Phase II concept as modified for Phase III requirements. The stage/engine interface is a ground assembly interface. The stage intermodule interfaces are flight remote couplings. Stage operational requirements discussed in the preceding section concerning design criteria apply to this schematic, and since the complete propellant management schematic is discussed in depth in Section 3.4 of Book 2, these functions will not be described further here.

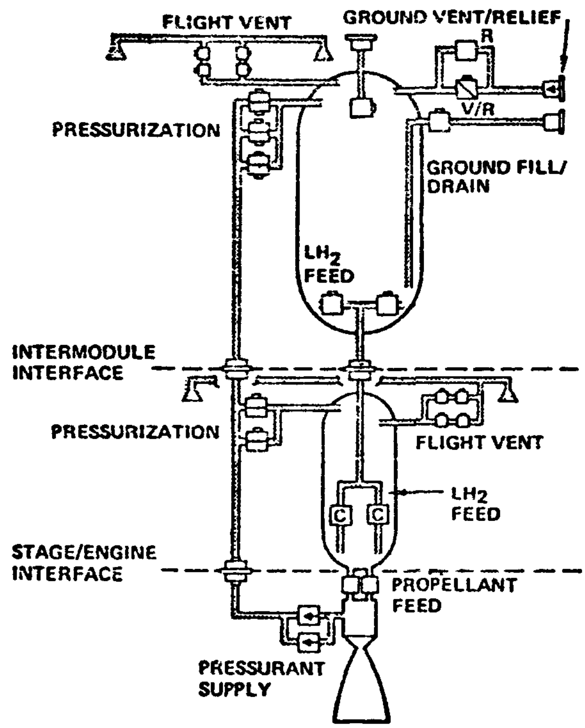

Figure 4.5-3 BASIC PROPELLANT MANAGEMENT SCHEMATIC

The subsequent sections will address the design and analysis of new subsystems which have been defined during Phase III to satisfy RNS operational requirements and consequently must be added to this simplified schematic to establish the Phase III baseline design. These functions are: propellant resupply, feed system chilldown, run tank refill, and pressure control for all operations.

4.5.4 Propellant Resupply

The schematic of the design concept for orbital propellant resupply is depicted in Figure 4.5-4. This concept is used for orbital fill on both propellant and propulsion modules. An objective of the design is to fill a propellant tank in orbit without venting or an excessive pressure rise. This is accomplished by using spray-nozzle injection to accomplish ullage collapse (i.e., avoiding compression), maintaining propellant orientation during the propellant transfer operation with axial acceleration provided by the tanker vehicle.

It is also necessary to minimize pressure surges during chilldown of a warm tank. This requirement is imposed on modules which have been depleted

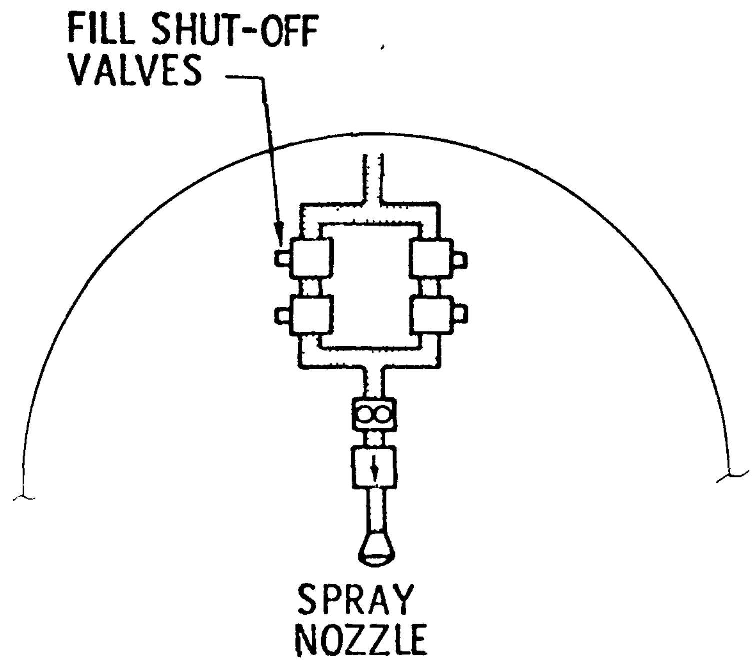

Figure 4.5-4 PROPELLANT RESUPPLY METHOD

early in the mission or have sustained a long coast in orbit before refill. A check valve and a flow meter are located in the fill line to control the propellant in-flow rate. The flow meter permits injecting only small quantities of propellant during the initial portion of the chilldown, when large pressure surges can occur. This approach gives the system time to move toward equilibrium. The check valve prevents backflow surges. Quad-redundant fill shut off valves are provided to ensure a capability to transfer propellant between tanks during the mission.

4.5.5 Feed System Chilldown

Chilldown is required under three circumstances: (1) NERVA feed system prestart, (2) stage propellant feed system prestart, and (3) warm propellant tanks for propellant resupply in orbit. The feed system prestart operations requirements are defined in Section 3.11.4, including component masses and chilldown times. A trade study was conducted to establish a chilldown system concept for the RNS. Although propellant settling is required to orient LH_2 at feed duct inlets, economical settling acceleration levels are not adequate to fill the ducts with LH_2, and forced convection chilldown systems are required. The evaluation of chilldown thermodynamics has resulted in formulation of chilldown system concepts with flow control features which accommodate the expected surge effects when LH_2 is introduced into warm lines.

4.5.5.1 Chilldown Concepts Evaluation

Schematics for several chilldown system concepts considered will be described here. A concept for NERVA feed system prestart chilldown is shown in Figure 4.5-5. It is a closed-loop recirculation system located in the propulsion module run tank with separate feed and return lines configured to precondition the pump inlet ducting, pump shutoff valves, and turbopump. The system contains a submerged motor-driven centrifugal pump, an antibackflow check valve, and an on-off isolation valve. Flow from the pump discharge is directed into the main feed duct downstream of the PSOV. Flow proceeds in a forward direction through the pump inlet ducting and the turbopump down to the pump discharge shutoff valve. Upstream of the pump discharge valve a tap-off is made for the return line. This duct terminates in the run tank via a check and a shutoff valve. The system utilizes a dual pump for each feed system. A common return line completes the loop.

Several concepts were considered to precondition the feed system between two adjacent modules. The design approach avoided adding any additional fluid line connections between modules. Figure 4.5-6 shows two closed-loop pump chilldown systems. The same tank return system consists of a submerged motor-driven pump, pump discharge valve, antibackflow check valve, and a return line with a check valve. Pump discharge flow is introduced into the main feed duct downstream of the tank isolation valves. The isolation valves are closed and chilldown flow is provided down to the blocking valve of the adjacent module. An upper line provides the return flow path to the tank via a check valve. The check valve and return line prevent tank surges and geysering. The pump discharge check valve provides the same function in the pump discharge line. A feedthrough chilldown system is also shown, identical to the same tank return system for the supply position of the pump loop, but utilizing the baseline spray nozzle refueling system of the adjacent module for discharge into the ullage of the lower module.

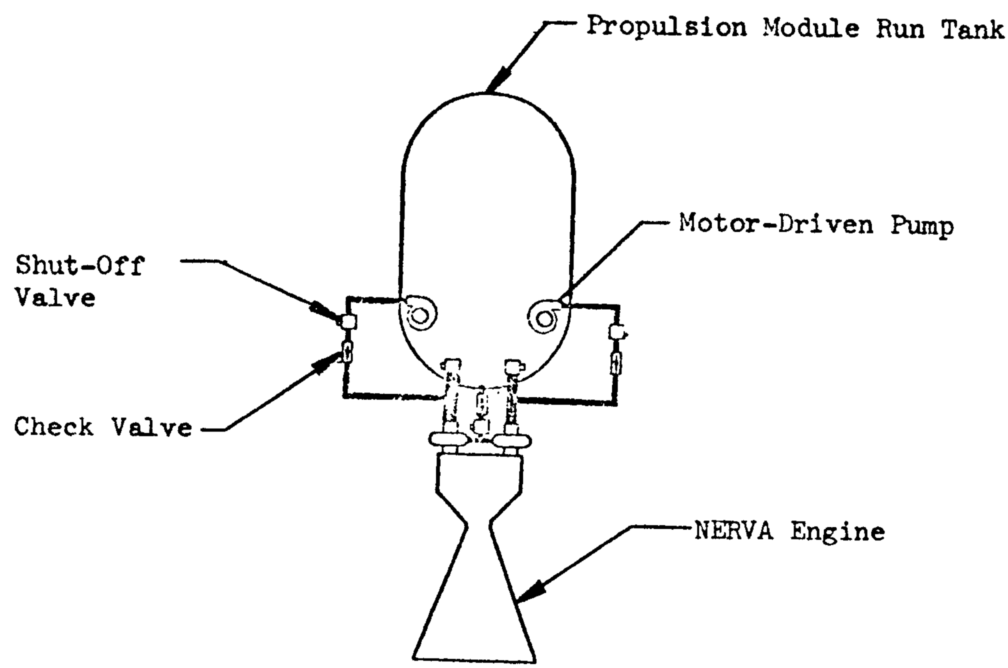

Figure 4.5-5 NERVA FEED SYSTEM CHILLDOWN SYSTEM

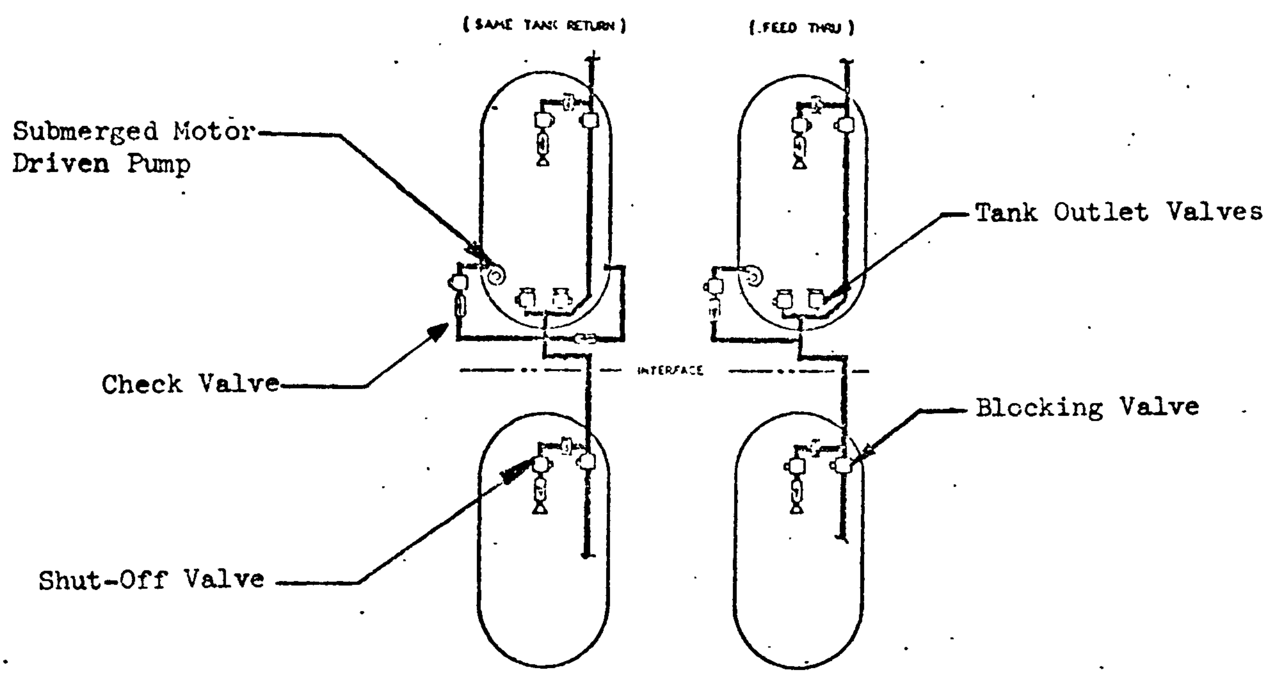

Figure 4.5-6 INDIVIDUAL MODULE PRESTART CHILLDOWN PUMP RECIRCULATION SYSTEMS

An open-loop overboard dump intermodule chilldown concept was considered. The pump is eliminated from the bypass supply line and the return line is also eliminated. Instead, the lower duct tap-off line and shutoff valve direct the flow to two overboard dump nozzles located 180 degrees apart on the module outer structure, permitting tank head to provide the chilldown hydrogen. The nozzle discharge flow aids in providing propellant settling thrust during chilldown.

Another closed-loop convection chilldown concept considered operates on the principle of an ejector. Helium is injected into a return line that eminates from a low point tap-off on the feed duct. The high-velocity low static pressure at this point causes the gas or liquid from the feed duct to be sucked into the return line and returned to the tank. Liquid is supplied to the feed duct from the tank downstream of the tank isolation valve via a bypass line and check valve.

Since engine and stage feed system chilldown requirements are similar, an integrated chilldown system concept in which the run tank located submerged motor driven pumps are sized for the complete stage chilldown was also evaluated. All of these concepts are compared on the basis of hardware weight, boiloff, and reliability in Table 4.5-1. Clearly, redundant systems are required to achieve satisfactory performance.

The tank weight is penalized for the closed-loop systems to accommodate a saturation pressure rise from heated propellant. This can amount to 5 psia for the run tank from the NERVA feed system. The overboard dump and helium bubble ejector concepts incur prohibitive weight penalties without a significant reliability improvement compared to the pump recirculation concepts. An integrated NERVA/stage pump driven system is both lighter and more reliable than providing separate pump recirculation systems at each module interface, and maintains propellant module simplicity.

4.5.5.2 Integrated Chilldown System Definition

Figure 4.5-7 shows a schematic of the selected integrated system concept compatible with the current NERVA interface. The propulsion module run

Table 4.5-1

CHILLDOWN SYSTEM COMPARISON

(Class 1-H)

Chilldown System Concept	Boiloff (lb)	Tank Weight (lb)	Non-Redundant System			Redundant System		
			Chilldown Hardware (lb)	Total Weight (lb)	Failures per 1,000 Missions	Chilldown Hardware (lb)	Total Weight (lb)	Failures per 1,000 Missions
Individual module — Pump recirculation	0	100	150	250	345	300	400	21
Individual module — Overboard dump	1,470	0	80	1,550	54	150	1,620	~1
Individual module — He injector	0	100	1,290	1,390	360	--	--	--
Integrated RNS— Pump recirculation	0	120	50	170	115	100	220	7

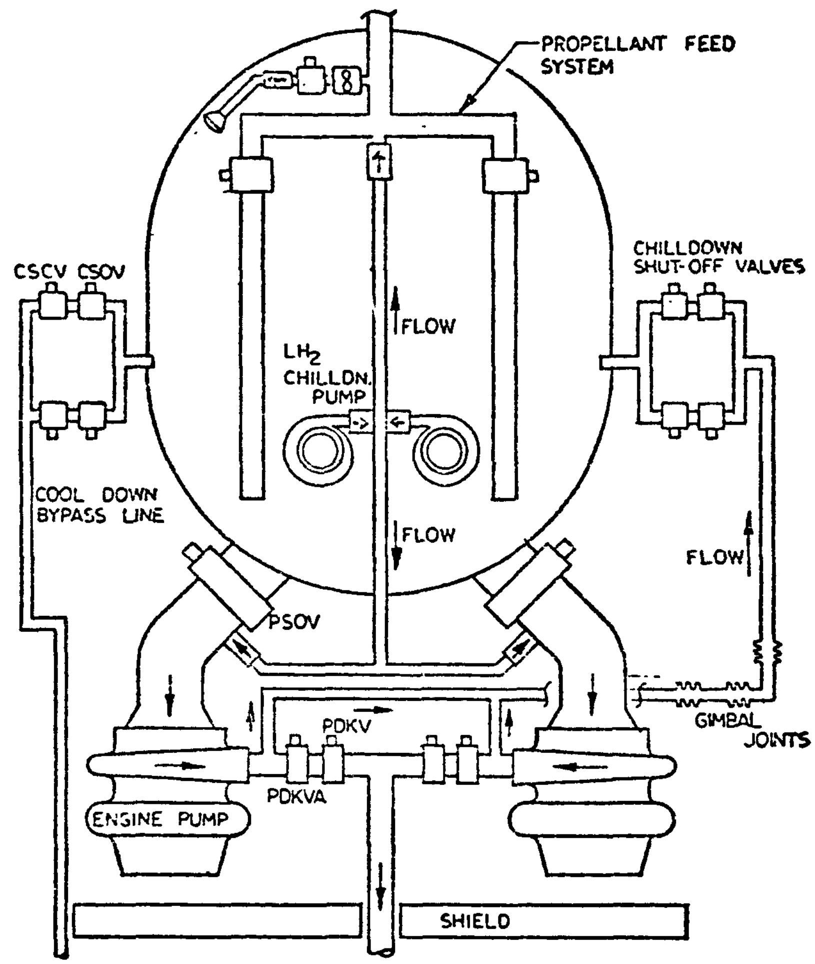

Figure 4.5-7 INTEGRATED CHILLDOWN SYSTEM CURRENT INTERFACE

tank contains redundant submerged ac-motor-driven centrifugal pumps. An inverter is provided for each motor to utilize the dc power bus. Each pump is sized for full system chilldown capacity. In normal operation at reduced flow the pumps will operate at a higher head. The parallel manifolded pumps discharge via two antibackflow check valves into a header that directs flow forward to the stage main propellant feed ducting and aft to the engine. Return for stage feed duct chilldown is accomplished with the refueling spray nozzle bypass system on the run tank.

NERVA feed system chilldown concerns the conditioning of the inlet ducting to the NERVA turbopump, the pump, and pump discharge ducting to the location of the pump discharge valve (PDKVA). There are two such sections for the dual turbopump configuration. The pump shutoff valve (PSOV) and pump discharge valve are closed during chilldown. Conditioning is accomplished by directing the chilldown pump discharge flow to two lines that tee from the chilldown pump discharge manifold. Each line injects flow forward into the NERVA pump inlet duct down stream of the closed PSOV. Check valving located at the injection points prevent surges and disturbances from being transmitted to the adjacent system. This chilldown ducting does not cross the gimbal plane. The present consideration is to inject the supply flow through a boss that is an integral part of the PSOV valve body casting. Chill flow proceeds through the NERVA pump inlet ducting, turbopump, and down to the pump discharge valves. Upstream of these valves a tap-off takes the return flow manifolded from both engine pumps to a common return line. This return line crosses the gimbal plane and contains three gimbal joints to provide for the required deflection. Return flow is introduced back into the tank via a set of quad-redundant shutoff valves at a location well removed from chilldown pump location to prevent degrading fluid inlet condition.

Chilldown system sizing was based on the minimum permissible time for chilldown of each interface, considering film boiling heat transfer for a duct initially at ambient temperature, and providing a margin of safety for flow surges. These were defined in Table 3.11-4.

total time

34 stage

43 NERVA

77 sec

The stage feed system is chilled first, followed by both legs of the NERVA feed system in parallel. The nominal capacity of each pump is 2 lb/sec of LH_2. The dominant pressure drop in the system is at the NERVA turbopump, estimated as 3.5 psia. This sizes the chill pumps at 0.84 HP, which represents a negligible power drain for the short chill duration, 0.1 kwh per chill. The system weight is summarized in Table 4.5-2.

If further definition of NERVA leads to a requirement for a pressure feed during aftercooling, the baseline chilldown system could be integrated with the bypass line used for aftercooling pulses.

4.5.6 Run Tank Refill

NERVA engine restart for full-thrust operation requires that the propulsion module run tank be refilled and topped off before or as a part of the start sequence (see Sections 3.10 and 3.11). This is required for five burns, and up to 8,500 lb of LH_2 must be transferred. Run tank pressures at this time can be in excess of propellant module pressures due to coast heating, as shown in Section 4.3.12. A preliminary estimate of the largest differential pressure occurring is on the order of 0.6 psi.

Table 4.5-2

INTEGRATED CHILLDOWN SYSTEM WEIGHT SUMMARY (lb)

Pumps (2 required)	26
Check Valves (5)	3
Shutoff Valves (4)	12
Lines	25
Total	66

The preferred method for refilling the run tank without incurring the loss of propellant required in a blowdown scheme is a pump-fed system. Such a system is shown schematically in Figure 4. 5-8. The system modifies the feed duct configuration in the run tank by extending the 12-in. -diameter feed duct to the tank bottom. At this location a closing fitting provides the housing for the two 8-in. -diameter main control valves and a base inlet sump. The base sump will contain two parallel redundant transfer pumps. The pumps are submerged, centrifugal type driven by ac motors. These pumps intake from the main feed system which has been conditioned and is open to the propellant module which will supply the refill. Pump discharge is directed through two antibackflow check valves and then manifolded into a quad-redundant set of shutoff valves. A single riser then runs up to the tank ullage. The riser discharges into the ullage via a flow meter and spray nozzle. This is the baseline nonvented transfer system modified to permit locating the motor pumps in a submerged position. Submergence of the motor pump is desirable to provide reliable bearing cooling and lubrication. This refill system is compatible with the integrated stage/engine chilldown system and various configurations, such as a single motor, double-ended pump could be used to integrate these systems.

The refill system sizing criteria was based on a maximum refill requirement of 8, 500 lb. The time required to accomplish feed system chilldown and subsequent run tank refill transfer was selected as half the inviscid settling time. Accomplishing the transfer within this time frame does not incur any additional penalty for settling for the refill operations and establishes a nominal total pump flow rate of 10 lb/sec. System reliability considerations warrant the selection of two parallel mounted pumps, each delivering 5 lb/sec. In case of failure, extended transfer times would incur modest settling propellant penalties. System impedances and tank pressure differences are estimated at 3 psi. The above parameters and the use of a 70 percent efficiency factor for both the pump and motor result in each motor being sized at 1. 3 HP and a power consumption of 0. 975 kw. Total refill time for five burns on the lunar shuttle mission is 2600 sec. The system weight is summarized in Table 4. 5-3.

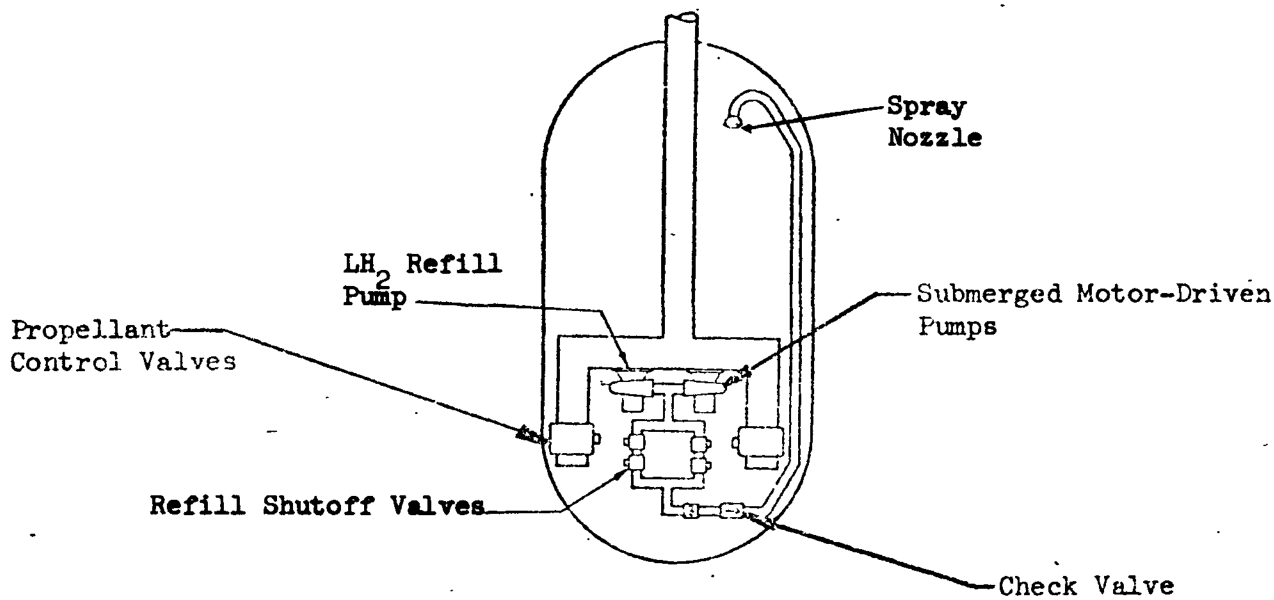

Figure 4.5-8 PRESTART RUN TANK REFILL SYSTEM

Table 4.5-3

REFILL SYSTEM WEIGHT SUMMARY (lb)

Motor-Driven Pumps (two required)	26
Check Valves (three required)	1.5
Flowmeters (one required)	2
Shutoff Valves (four required)	12
Ducts	18
Fuel Cell Reactant and Tankage	2
Total	62

4.5.7 Pressurization System Definition

4.5.7.1 Schematic and Operation

A pressure schedule and pressure control functions are established in Section 3.12. Prepressurization requirements are defined in Section 3.11.5. These are satisfied by a two function pressurization system on the propulsion module consisting of expulsion and pressure control. An additional prepressurization function is provided on the propellant module. The functions and flow rates provided (at 225°R) are defined schematically in Figure 4.5-9. These are operated together for various module pressurization requirements according to the prescription in Table 4.5-4. The flow rate requirements are based on a collapse factor of 1.1. The system is a bang-bang type controlled by pressure sensing strain gage sensors located in the respective tankage. Each function contains quad-redundant, normally closed valves, with the flow rate controlled by a choked orifice. When the required flow rate is exceeded, the functions operate automatically in an intermittent mode.

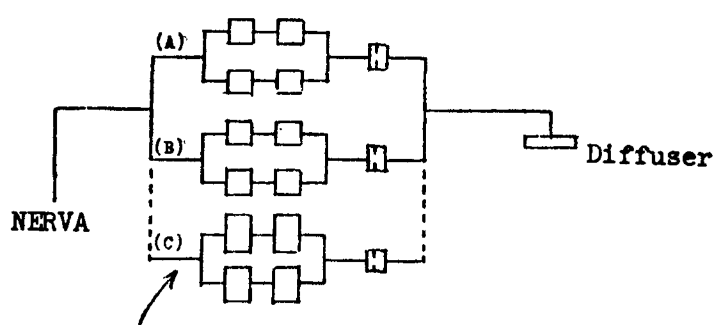

	Function	Flow Rate (Lb/Sec)
(A)	Expulsion	0.6
(B)	Pressure Control	0.4
(C)	Prepressurization	4.0

Figure 4.5-9 MODULE PRESSURIZATION SYSTEM SCHEMATIC

Table 4.5-4

PRESSURIZATION SYSTEM OPERATION

(Class 1-H)

Pressurization Requirement	Flow Rate (lb/sec)	Functions Utilized
Propellant Module		
Expulsion (normal)	0.58	A
Pressure control	0.06	B
Prepressurization	5.0	A + B + C
Run Tank Refill	0.81	A + B
Malfunction mode	0.35	B
Propulsion Module		
Expulsion (normal	0.58	A
Idle mode	0.39	B
Pressure control	0.06	B
Steady state	0	-

4.5.7.2 Pressurant Supply Pressure Level

Pressurant is available from NERVA at pressures ranging from 978 psia at the turbine inlet to 704 psia at the turbine discharge. An intermediate turbine tap-off has also been considered. Thus, two approaches were considered for pressurant supply to the stage: a low-pressure system operating at 30 psia, and a high-pressure system operating at a nominal engine tap-off pressure of 850 psia.

Pressurization duct sizes and weights are compared at these pressures in Table 4.5-5 for a range of flow rates, based on a limiting Mach number of 0.3. It has been found that velocities higher than M = 0.3 cause vibration in the metal bellows, resulting in fatigue failures. Duct gages in Table 4.5-5 are indicated based on pressure alone, and based on the safe

Table 4.5-5

PRESSURIZATION DUCTS WEIGHTS

Pressure	30 psia			850 psia		
Weight flow (lb/sec)	4	0.6	0.4	4	0.6	0.4
Diameter (in.)	6.00	2.50	2.00	1.25	0.500	0.500
$\bar{t}$ (in.)	0.0029	0.00120	0.00096	0.0170	0.00680	0.00680
Weight - 60 ft (lb)	12.1	2.1	1.35	15	2.4	2.4
$\bar{t}$ Minimum (in.)	0.020	0.012	0.012	0.012	0.010	0.010
Weight - 60 ft (lb)	81	21	16.2	15	3.42	3.42

handling and manufacturing minimum gages defined by SAE ARD-735, Aerospace Vehicle Cryogenic Ducting Systems. This specification is accepted for manned vehicles and is current in-house practice. Due to the minimum handling gages needed to insure reliable installation and to prevent damage, it is clear that the low-pressure system affords no advantage in weight.

The high-pressure system permits using light braided metallic hose or small gimbals for flexible elements, whereas, heavy tied gimbals would be required for the low-presure system. Metallic bellows are considered suitable for either system. The high-pressure system would be expected to incur less leakage, because of less seal perimeter and the use of pressure-actuated seals.

The low-pressure valve sizing is larger, and for the 6-in. nominal diameter size a motor-driven control valve is required. This valve required intermediate gearing between the motor drive and the gate. Large valves of this type could present response problems for opening and closing, and furthermore, are exceedingly heavy (about 30 lb). If the high-pressure, low-diameter systems are used, this will permit the use of pilot-operated solenoid valving. These are basically lighter valves, approximately 12 lb, and do not incur excessive weight penalties when quad redundancy and other reliability constraints are imposed on the system. Although the force requirements in an 850-psi system and the sizes shown do not exceed that of direct-acting solenoids, a pilot-operated solenoid system can be used. Solenoid valves of this type will provide the fast response required for system control.

Preliminary considerations indicate that a wide-tolerance, single-stage regulator system located on the propulsion module would suffice to provide low-pressure gas to all the propellant modules. In the case of the high-pressure system, no such regulation would be required. Single failure mode considerations might require that even in a low-pressure system the full ducting run would have to be designed for the high pressure should a single failure occur in the regulation system. Large pressure drops may be incurred in the high-pressure system on the order of 30 to 40 psi per 60 ft of run, although the available head of 850 psi is sufficient to provide for system losses of this type.

In view of these considerations the high-pressure duct system was selected.

4.5.7.3 Valve Type and Actuation

The valving recommended for the high-pressure pressurization system shown schematically in Figure 4.5-9 is presented in Table 4.5-6. Normally closed quad-redundant on-off valving powered by a 28-vdc supply is used for each pressurization function. Identical valving is used for the expulsion and control functions with the flow rates established by orificing. A direct acting solenoid poppet valve, shown in Figure 4.5-10, is the simplest type applicable to these functions. No external dynamic seals are required. Good leakage control is provided. Life expectancy exceeds 10,000 cycles. This valve provides the shortest available response times, in the range of 5 to 50 msec, which is ideal for the bang-bang control function. The larger valve size requirement of prepressurization function combined with the high-pressure closing force exceed the practical capabilities of a direct acting solenoid, so a pilot-operated design is utilized. This would result in a slightly longer response time of about 200 msec.

Table 4.5-6

PRESSURIZATION SYSTEM VALVE TYPE AND ACTUATION

Function	Flow Rate (lb/sec)	Line Size (in.)	Valve Type	Actuation
Expulsion	0.6	0.5	Poppet	Direct-acting solenoid
Control	0.4	0.5	Poppet	Direct-acting solenoid
Prepressurization	4.0	1.25	Poppet	Pilot-operated solenoid

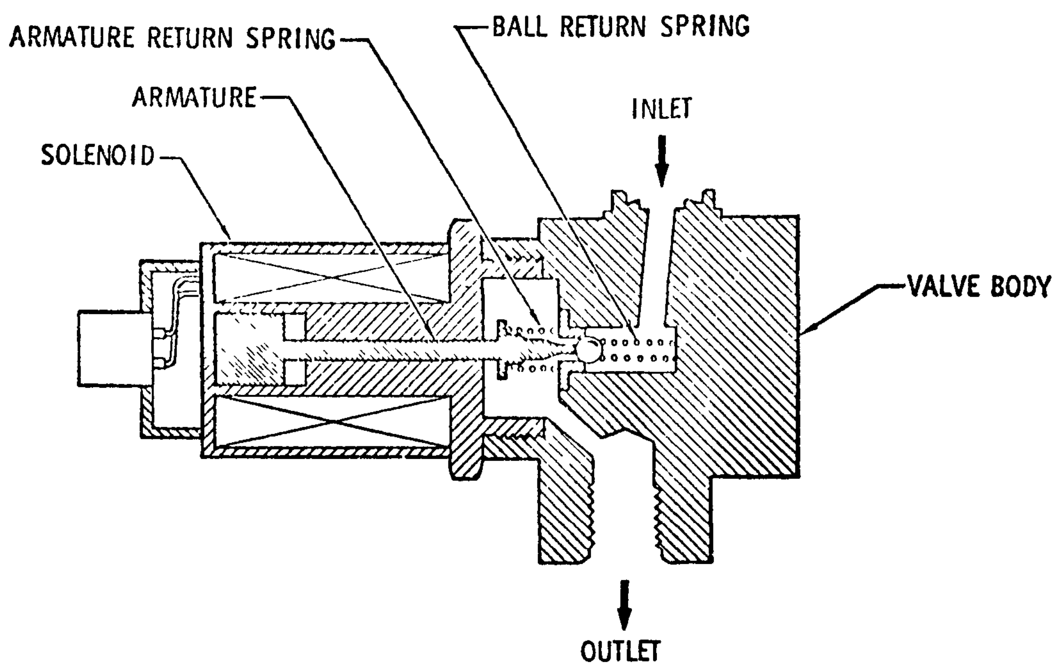

Figure 4.5-10 DIRECT ACTING SOLENOID

4.5.8 Vent System Definition

The thermal protection system concept selected in Section 4.3.11 does not require venting of boiloff during the mission, i.e., subsequent to TLI. Propellant transfer operations can be performed without venting. However, venting is required in earth orbit prior to initiating the mission to reject the propellant heating from tank chilldown and orbital coast. The tanks are subsequently topped off without venting. According to Section 4.3.10, the propellant will remain oriented at the bottom of the tank during the prolonged orbital coast storage phases. Also, the propellant transfer operations employ acceleration provided by the tanker vehicle. During the translunar and transearth portions of the mission, the propellant will be in a randomly oriented configuration. Venting would not be possible for the latter situation without either utilizing a vent system configuration with a liquid-vapor separator or incorporating a propellant orientation operation. However, these portions of the mission are relatively short compared to the prolonged orbital coast phases. It is possible to perform any required venting operation either while in a gravity-gradient-stabilized mode or while settled in preparation for propellant transfer. Since prolonged propellant settling periods are also incorporated as a part of the normal RNS startup ramp, a vent operation can be incorporated in that portion of the mission. Thus, a zero-g liquid-vapor separator is not required. Also, separate propellant settling operations are required for venting. A propulsive vent concept such as used on the S-IVB appears to be adequate for the RNS mission requirements.

The flight ground vent functions were indicated schematically in Figure 4.5-3. The systems utilized are summarized in Table 4.5-7.

The flight vent system on each module consists of four normally closed quad-redundant on-off valves that are actuated by a strain gage, pressure-sensing system located in the tank ullage. Its size is determined by the pressurization expulsion flow rate of 0.6 lb/sec at approximately 30 psi. A pilot-operated solenoid was selected for this application because a direct-acting solenoid valve in sizes in excess of 1/2 in. in diameter generally is excessive in weight due to the large stroke required. In the selected design, the solenoid controls a very small flow of fluid which permits the line pressure to actuate the main poppet. Figure 4.5-11 illustrates a normally

Table 4.5-7

VENT SYSTEM VALVE TYPE AND ACTUATION

Function	Flow Rate (lb/sec)	Line Size (in.)	Valve Type	Actuation
Flight Vent	0.6	2.25	Poppet	Pilot-operated solenoid
Ground Vent and Relief*				
Vent Mode	10	6.0	Poppet	Pneumatic
Relief Mode	1.8	2.5	Poppet	Pilot sensor
Ground Relief*	1.5	2.5	Poppet	Pilot sensor

*Propellant module only

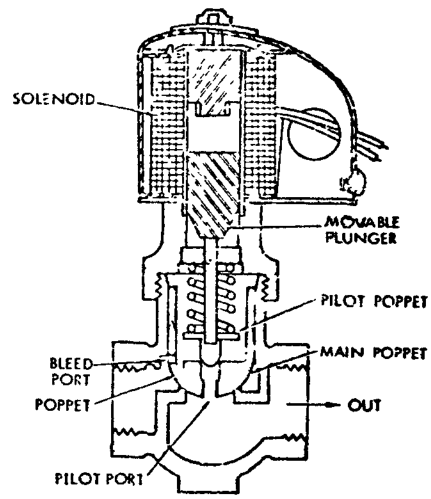

Figure 4.5-11 PILOT OPERATED SOLENOID

closed pilot-operated solenoid of this design. The solenoid opens the pilot valve which dumps fluid from behind the main poppet through the pilot port. Since pilot port is sized larger than the bleed port, the resulting pressure unbalance forces the main poppet open. Note that a differential pressure must be available to operate this type of valve. In the vent system the differential pressure is supplied by venting the back side of the poppet to a downstream pressure.

Ground venting of the propulsion module run tank is restricted to ground test only, so field connections are provided to both of the flight vent propulsive nozzles. In addition, ground test fill rates will be governed by the flight vent valve flow capabilities. This eliminates the addition of a ground vent system as part of the baseline flight module.

The propellant module requires a separate vent and relief system for both ground and prelaunch operations. The ground vent and relief system is sized for the ground fill flow rate of 3, 000 gpm. A 6-in. nominal diameter vent and relief valve is provided, and it is backed up by a 2-1/2-in. nominal diameter relief valve. These valves are mounted in parallel and both discharge to an umbilical coupling that is located on the umbilical panel in the forward skirt regions of the propellant module. They are sized for $40^{o}R$ gaseous hydrogen.

The 6-in. vent and relief valve shown in Figure 4.5-12 is a combination pneumatically controlled vent valve and an absolute pressure relief valve utilizing a single flow path. The pneumatic control capability is a ground only control. The main poppet is connected via a guided shaft to a pilot piston and a single-acting pneumatic piston. Normal command operation is accomplished via the pneumatic actuator with a spring return to the normally closed position. The relief function is controlled by pilot valve sensing absolute fluid pressure which directs fluid to the pilot piston in the event of pressure buildup. The pilot piston has a larger surface area than the main poppet and a differential force will open the valve until the pressure has decayed to a safe level. The valve is used to permit venting of the hydrogen tank and to provide a primary safety device in the event of inadvertent pressure buildup.

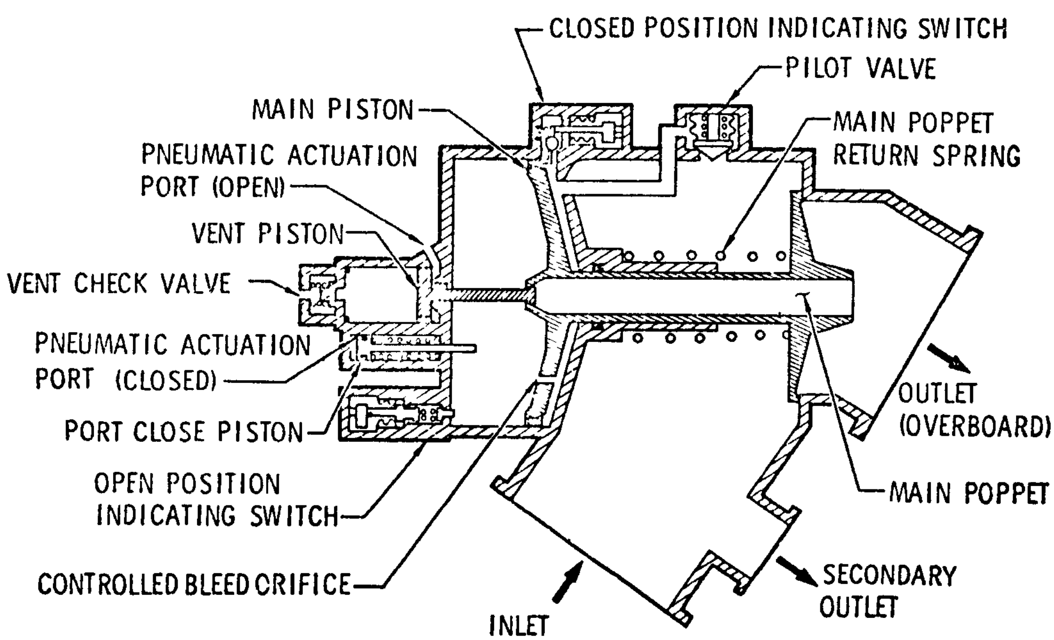

Figure 4.5-12 VENT AND RELIEF VALVE

The 2-1/2-in. relief valve shown in Figure 4.5-13 automatically maintains LH_2 tank pressure within specified limits in case the vent and relief valve fails to open. It has a spring-loaded poppet controlled by an absolute pressure sensing pilot. The cracking pressure is set high enough to prevent actuation if the vent and relief valve functions properly.

4.5.9 Module Interface Definition

Figure 4.5-14 shows the propellant feed system interface between the propulsion module and the propellant module. Provision is made for remote orbital assembly. A linear deployment mechanism is located on the feed duct for the propulsion module, and a coupling mechanism is located on the propellant module. Figure 3.5-3 and 3.5-4 show detailed views of these mechanisms and their operation is described in Section 3.5.

In order to meet the motion requirements of this automatic coupling interface, various flexible elements were considered for the feed system. The approach for flexible element selection and criteria is summarized below. Three concepts were considered. The first would allow the flexibility of the pipe to absorb the motion as internal stress. The use of bends can reduce the induced stress in the duct for a given deflection, but bending moments are incurred. The duct will see combined longitudinal, transverse, and to a small extent radial stresses. This system contains no bellows section and is therefore highly reliable. The second concept utilizes angular bellows assemblies (such as gimbal joints). These can be used to absorb axial motion only if they are placed in sets of three in complementary sections of the duct assembly. This requires the duct routing to have bends in it to enable proper joint placement. Squirm or stability limits the length of bellows used in each joint and therefore the maximum angular motion of the joint. A representative allowable angle of 10 degrees per joint is characteristic of hydraulically formed omega bellows for the operating pressures. This could be increased if close-pitch low-convolution-height special formed bellows are to be considered. This type of system is applicable for mid-range deflection requirements which are characteristics of the in-line interfaces where docking and latching accomplishes major duct alignment. The system is load predictable and a reliable method of tying metal bellows.

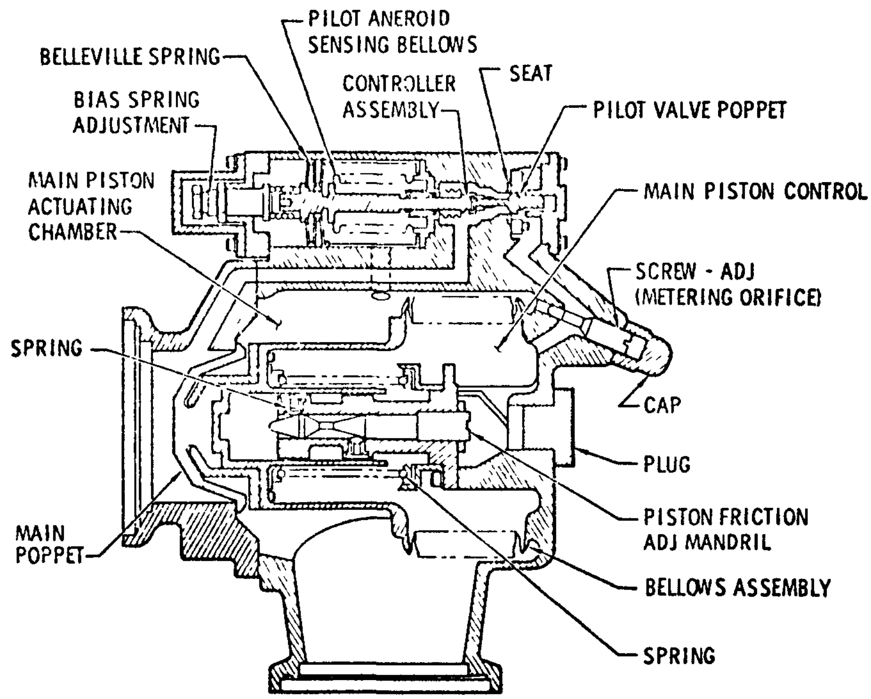

Figure 4.5-13 RELIEF VALVE

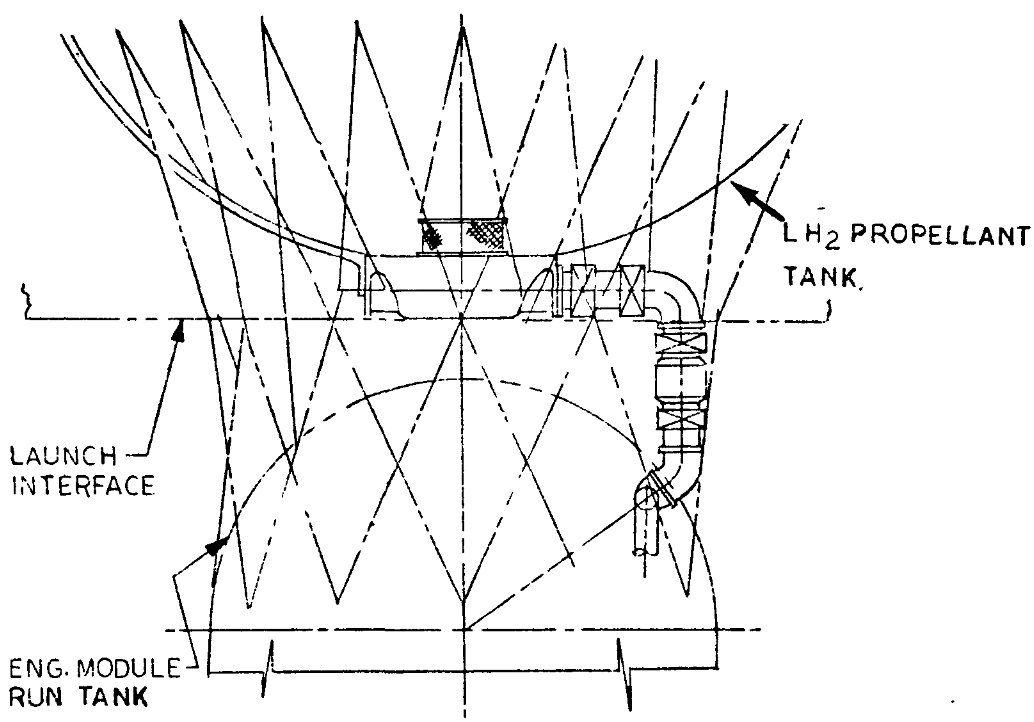

Figure 4.5-14 CLASS 1 HYBRID PROPELLANT FEED SYSTEM INTERFACE

The third concept utilizes a linear compensator. The compensator bellows are interconnected so that pressures are balanced and, therefore, the end loads are balanced. The three sections of bellows within the compensator are also constrained by the squirm limitation. The system meets the requirements for high axial motion.

The propellant module section of ducting shown in Figure 4.5-14 is a straight run starting from the propellant module sump exit and running to the intermodule structure. This 12-in.-diameter straight section of ducting contains two gimbal joints and is soft mounted at the interface flange end. The section feed ducting on the propulsion module is a straight line duct containing two gimbal joints and a pressure volume compensator.

The intermodule feed ducting will require thermal protection for both ground operations and flight operations. A separate ground fill system is incorporated. Various types of thermal protection were considered. The baseline tank system which is essentially high-performance insulation covered by a foam blanket and then a fiber glass shroud. Although adequate for the tank, it presents a problem when applied to this type of feed duct, which must have both linear and lateral motion-capability. A representative design concept is shown in Figure 4.5-15. This configuration utilizes high-performance insulation wrapped around the parent duct in the manner shown. The insulation blanket runs over the gimbals, over the pressure volume, compensator, bellows, and finally takes a U-configuration enclosed in a U-manifold welded to the end of the duct. The U-overlap will provide for the linear deployment motion required of this duct. Integration of vacuum jacketing or foam for ground hold and fill is necessary and requires further evaluation.

4.5.10 Feed System Definition

The propellant module must supply 91.9 lb/sec of hydrogen at the tank design pressure. The propellant module feed system contains two parallel redundant 8-in.-diameter, normally closed, ball-type valves located in the sump of the propellant tank. These valves will utilize ac electric motors as drivers. Vehicle 120 vac power input is used for the ac induction motor actuator. The motor actuator drives a compound planetary transmission system which in

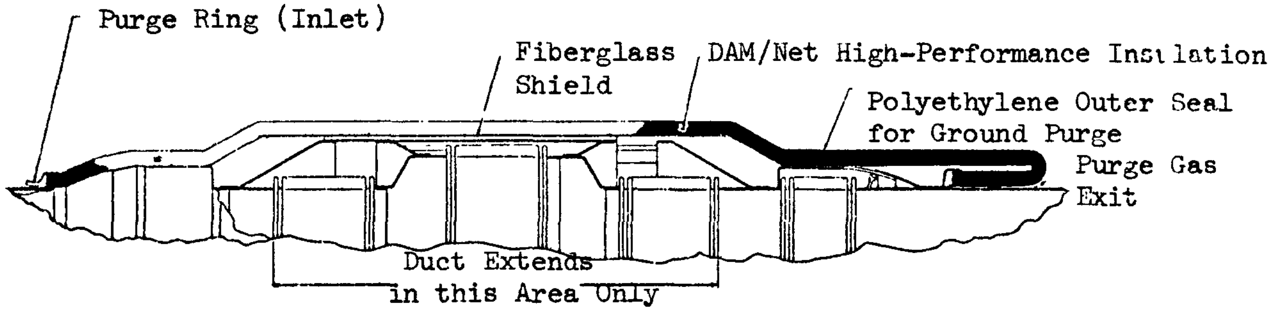

Figure 4.5-15 INSULATION OF COMPENSATED BELLOWS SECTIONS

turn operates the valve. Adjustable overload provisions are provided for by a slip clutch that is incorporated in the planetary transmission assembly. This type of electric actuator will be used to drive all feed system valving. Each 8-in. nominal diameter shutoff valve is an on-off valve utilizing a ball-configured main gate. The 90-degree rotation of the main gate opens the valve to a full-flow condition. Full open diameter is duct diameter. The main gate seal for this ball-type valve will be a conventional cryogenic Teflon lip seal. To support the evolution to a pure metal-to-metal gate seal, the pure rotational opening motion of this valve is modified so that the initial opening command will first withdraw the ball from the lip seal and then rotate the full open 90 degrees. Closing is achieved by the use of a disconnect solenoid which releases the actuator from the ball drive and permits mechanical spring force to return the valve to the closed position.

The propulsion module feed system consists of two 8-in. nominal diameter, ball-type, motor-driven control valves. These valves are located inside to the propulsion module run tank in a parallel configuration similar to the outflow valves on the propellant modules. These valves utilize the baseline motor drive as an actuator and contain a main gate seal configuration identical to the valves described above. For use in the propulsion module, these valves do not contain any bias failure mode and are not utilized as on-off type valves. Instead, they will be utilized in a throttle mode to control liquid level in the run tank. These flow-type control valves will respond to a liquid level sensing element located in the propulsion module run tank.

The feed system pressure drop was evaluated to establish module pressure schedules. The pressure schedule is defined in Section 3.12.2. At the steady-state flow rate of 91 lb/sec, the 12-in.-diameter ducting has velocity of 28 ft/sec, resulting in Reynolds numbers in the order of 10^6, which is in the turbulent flow regime. The friction factor used for the straight ducting was 0.015. An equivalent factor of 0.08 was used for convoluted metal bellows derived from empirical data. Straight sections of bellows will be internally lined. The pressure drop is defined in Table 4.5-8, and is combined with the hydrostatic head to establish the net loss plotted in Figure 4.5-16.

Table 4.5-8
FEED SYSTEM PRESSURE DROP (psia)

Propellant Module		
Screen	0.07	
Isolation valve	0.27	
90-degree bend (2 required)	0.14	
Bellows (2 ft)	0.06	
Duct (10 ft)	0.05	
	0.59	
Propulsion Module		
Bellows (3 ft)	0.09	
Duct (23 ft)	0.13	
90-degree bend (2 required)	0.14	
Control valve	0.27	
	0.63	
Total Stage Feed System		1.22 psia

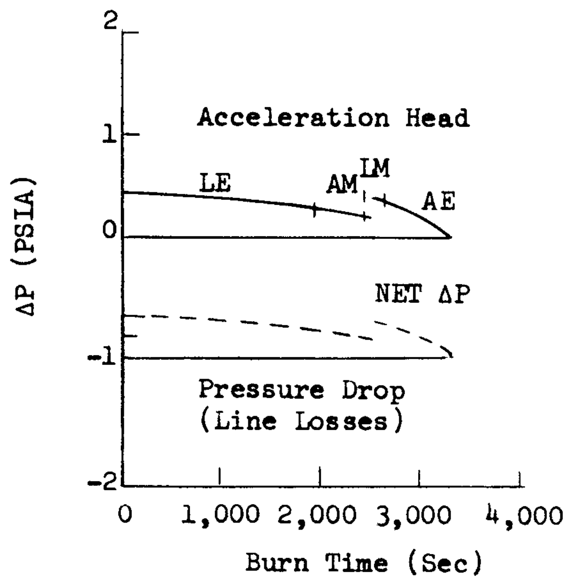

Figure 4.5-16 FEED SYSTEM PRESSURE DROP AND ACCELERATION HEAD HISTORY

4.5.11 NERVA Shield Evaluation

The objective of shielding analysis during Phase III was to confirm the shield weight requirements of the current Class 1 Hybrid RNS design. The basic shield optimization studies were performed in Phase II and resulted in selection of a configuration having a 10-degree half-angle aft dome for the propellant tank with the run tank contained within this cone.

The fundamental radiation criterion was a dose of 10 rem per mission to a manned capsule located 11 ft ahead of the RNS. The dose attenuation factor of the crew compartment was taken to be 3, yielding an ambient design level of 30 rem for the baseline RNS design. Parametric shield weights will be shown to meet a new criterion, imposed near the conclusion of the study, which eliminates the attenuation factor of 3.

Data on the engine and its radiation sources were based on the May 1969 Common Radiation Analysis Model (Reference 4-49) subsequent modifications (Reference 4-50). Together with input relating to the propellant tank design, these data were used with the PATCH point kernel code. Selection of this method was based on (1) the general utility of this technique for survey work, and (2) the general accord shown between such point kernel calculations and experimental data on simulated nuclear engine/propellant tank configurations (Reference 4-51). The PATCH code embodied these techniques and offered two features uniquely applicable to this study: (1) direct evaluation of single scatter and secondary production events in the propellant tank, as well as the usual line-of-sight contributors, and (2) tallying of detector response by source and by the specific shield zone transmitting the radiation. Multiple scattering in the tank was approximated by applying a buildup factor to the calculated value of the singly scattered contribution.

The output of the PATCH code was dose rate by shield zone as a function of propellant level in the tank. These data were integrated over engine operation, after equating propellant level to drain time. The resultant dose by shield zone was then coupled with data on shield geometry and shield material attenuation and fed into the ZONER code. This code, a formulation of the Lagrangian multiplier method, was then used to distribute a given weight of shield material so as to yield the minimum crew dose.

Figure 4.5-17 shows the variation of the gamma dose rate with LH_2 drainage time. (The neutron dose rate is now shown as it is appreciable only when the propellant is nearly exhausted and it is not a significant contributor to the overall dose.) The data in this figure correspond to the following conditions:

A. Propellant flow rate of 90.7 lb/sec (327,000 lb/hr).
B. Maintenance of 7,500 lb of LH_2 in the run tank during draining of the main propellant tank.
C. 160-in.-diameter run tank.
D. 3,300-lb internal shield and no external shield.

Figure 4.5-18 presents the minimum shield weight requirements as a function of radiation level 11 ft forward of the main tank. These data reflect no significant secondary gamma radiation due to neutron capture in the disk shield located between engine and run tank.

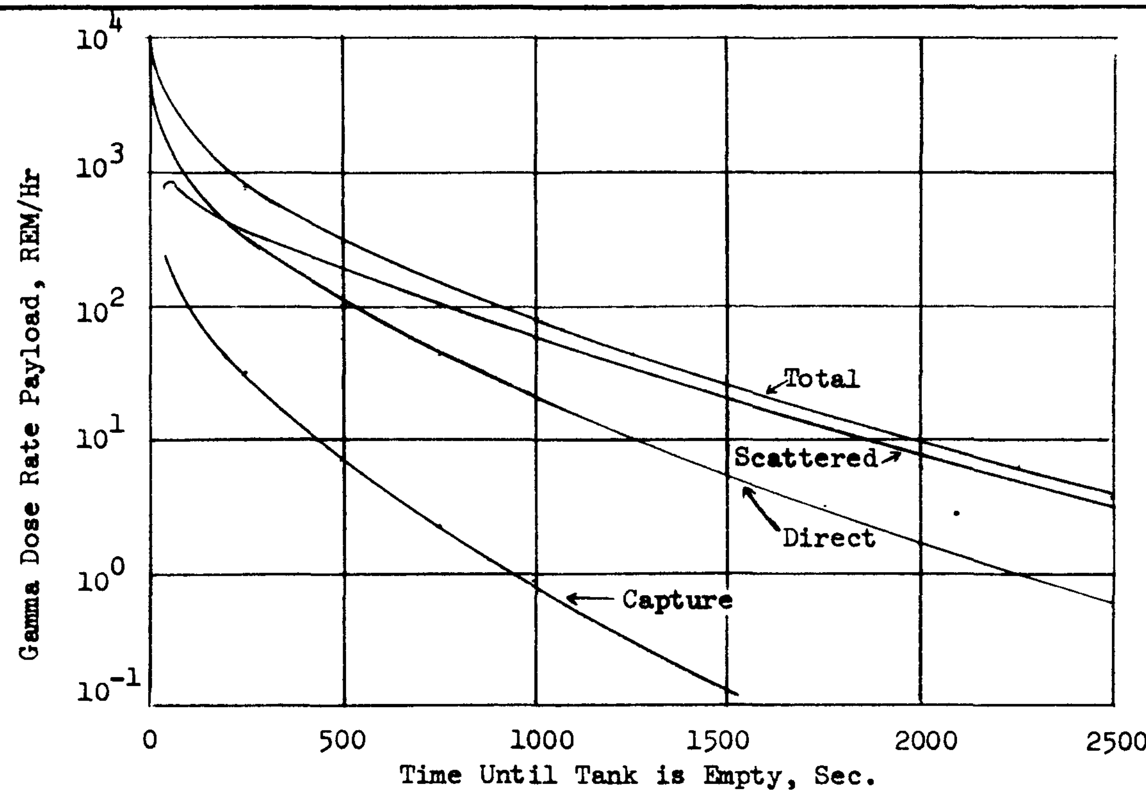

Figure 4.5-17 DOSE RATE DURING TANK DRAIN

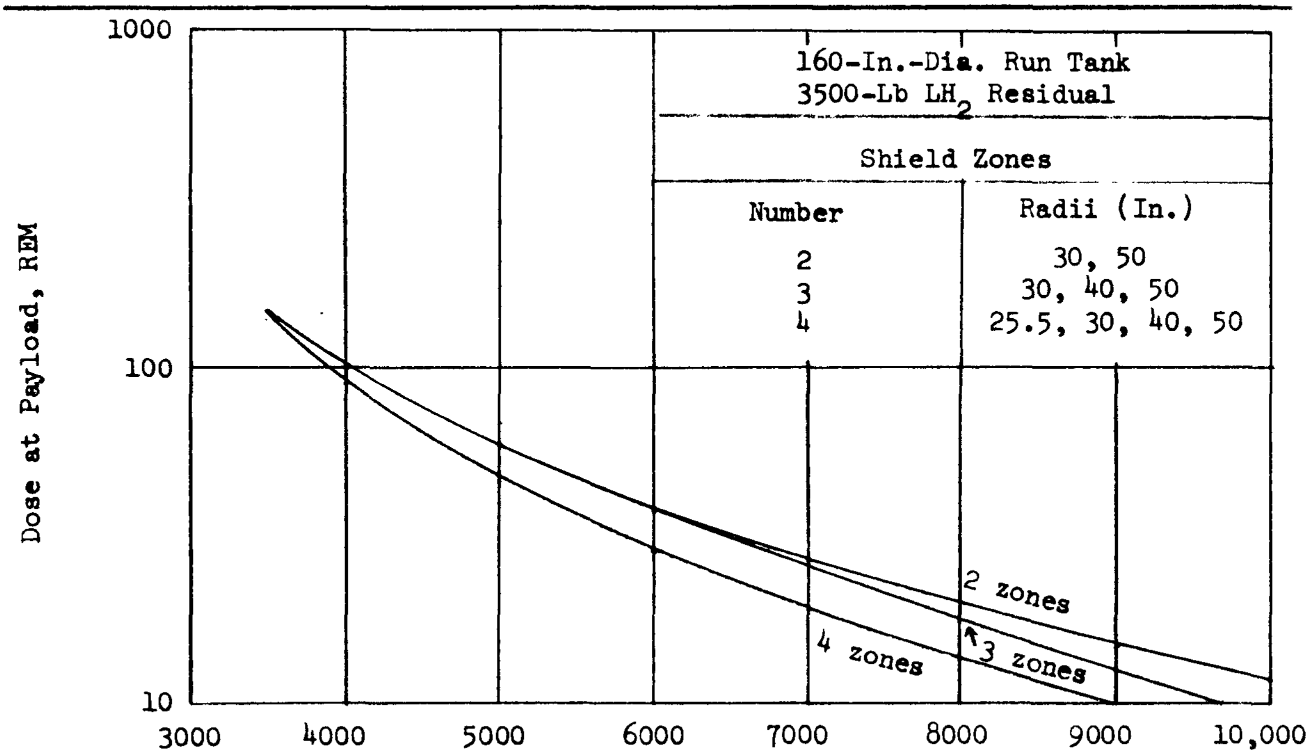

Figure 4.5-18 SHIELD WEIGHT REQUIREMENTS

Allowing for a 10 percent uncertainty in the calculated dose and using a crew compartment attenuation factor of 3.0, the disk shield weight needed to reduce the crew dose to 10 rem per mission is 2,900 lb. This result is based on (1) a 3,500 lb LH_2 residual; (2) a three-zone disk shield with radii of 25.5, 40 and 50 in.; and (3) a 160-in.-diameter run tank. Table 4.5-9 compares the required shield's weight for other values of propellant residual and run tank diameter for the same dose criterion and a three-zone shield.

Application of the 10-rem dose criterion without the payload attenuation factor would warrant use of a four-zone shield. Reference to Figure 4.5-18 shows that a total shield weight of about 9,000 lb would be required. With a 3,300-lb internal shield, this requires a 5,700-lb disk shield. This represents an increase of 2,800 lb compared with the baseline design.

A schematic representation of radiation exposure for RNS equipment in different zones on the stage is shown in Figure 4.5-19. Total accumulated doses for 10 missions are given. The three zones of interest are: (1) the CCM/payload region, (2) forward on the propulsion module and aft on the propellant module, and (3) aft on the propulsion module. The exposures given are the maximum accruing in the specified zones, and all equipment is to be evaluated for these levels without regard to the detailed layout in the zone. Where this imposes a serious constraint on equipment selection, subsequent specifications can be established and used.

Table 4.5-9

CLASS 1 HYBRID SHIELD WEIGHTS

Run Tank Diameter (in.)	LH_2 Residual (lb)	Disk Shield Weight (lb)
112	0	2,900
	3,500	2,400
	7,500	2,200
160	3,500	2,900
	7,500	2,400

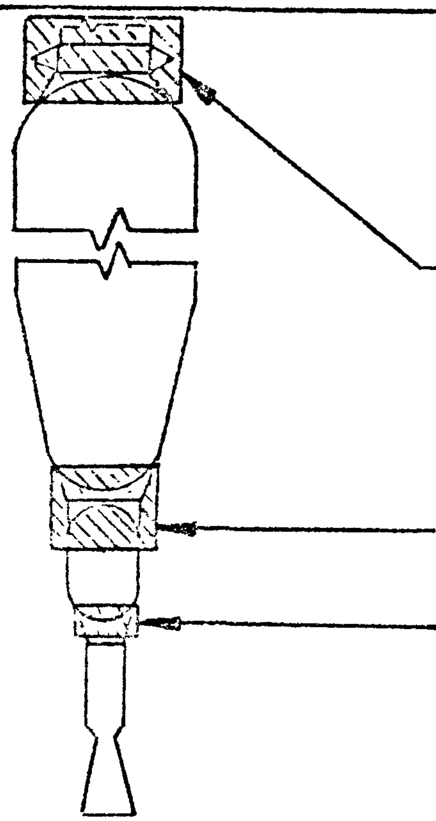

Region	Irradiation: Gamma, Rad (c)	Irradiation: Neutron, n/cm^2
CCM and Payload	500	10^8
Propulsion Module:		
Forward	5×10^5	10^{10}
Aft	10^7	10^{16}

Figure 4.5-19 RADIATION EXPOSURE TO RNS EQUIPMENT (10 MISSIONS)

4.5.12 Radiation Effects

A literature search was performed to assess the effects of nuclear radiation on organic seals. The selection of a seal material is a major concern for both valve gate seal and shaft seal applications as well as static flange connections. Current cryogenic technology is to utilize Teflon and Kel-F type organic seals. A soft seal material of this type affords good sealing characteristics and extended cycle life.

The gamma dose rate and fast neutron flux are defined in Section 4.5.11. The critical location is the propulsion module aft zone, with a dose criterion for 10 round trips of 10^8 rads, which includes a factor of 10 safety margin. This is reduced to 5×10^6 rads at the top of the propulsion module.

A compilation of radiation effects data on various seal materials is shown in Table 4.5-10. Additional data (reference 4-45) on TFE-teflon indicates that its tensile strength remains good in a vacuum even at a dose of 8×10^8 rads, but it crumbles if irradiated to this does in air, and shows some crazing and spall at 4.4×10^6 rads and powdered at 4×10^9 rads in air. Other tests in air

Table 4.5-10

RADIATION EFFECTS ON ORGANIC SEAL MATERIALS

Material	Dose (rads)	Environment	Property Change (%) Tensile Strength	Property Change (%) Elongation	Reference
TFE Teflon	10^5	Air/Ambient	-20	-40	4-52
	10^6		-50	-95	
	9×10^5	Vacuum/Ambient	-45	-75	4-43
	10^7		-45	-88	
FEP Teflon	4×10^6	Vacuum/Ambient	-18	-18	4-43
Kel-F	8×10^7	Air/Ambient	-15	-60	4-52
	1.2×10^8		-45	-90	
	5×10^6	Vacuum/Ambient	0	0	4-43
	1.5×10^8		-100	-100	
Nylon	3×10^8	Air/Ambient	+5	-75	4-52
Kynar	1.3×10^8	Vacuum/Ambient	-34	-20	4-43
	10^8	Cryogenic	0	0	4-27
Mylar C	1.3×10^7	Vacuum/Ambient	-25	-10	4-43
	5×10^8	Vacuum/Ambient	25	25	4-42
Tedlar	10^7	Vacuum/Ambient	-5	-7	4-43
Kapton	10^8	Air or Vacuum/Ambient	-3	-20	4-43

(Reference 4-27) show that TFE Teflon crumbles and/or powders and becomes very brittle at 10^7 rads and its flexibility decreased somewhat at 10^3 rads. In a vacuum FEP Teflon withstands about 10 times the dose that TFE does for an equal amount of damage and 16 times as much when irradiated in air (Reference 4-43).

It is concluded that Teflon is unsuitable for use in the aft region of the propulsion module and questionable elsewhere. Kel-F is also unsatisfactory in the aft region of the propulsion module, but it could probably be used in the rest of the vehicle. Nylon, Kynar, Kapton, and Tedlar may be adequate in all regions of the RNS. Mylar may be applicable above the run tank. Additional test data are necessary.

The use of metallic seals in small valving such as direct-acting solenoids can be considered current technology, but application to gate seals for 8- and 12-in. diameter valves would represent an advancement in technology.

Metallic seals used in such applications would influence the basic valve configuration. A conventional butterfly type valve utilizing a Teflon or Kel-F main gate seal would not lend itself to a metallic seal because the wiping type motion required would not permit low leakage and long cycle life. Instead utilization of metallic seals for large valving favors a poppet type configuration which would permit linear motion for sealing. Various ball or visor type valves could also be adapted to a linear sealing motion by camming devices that would first withdraw the valve seal from its seat and then a normal rotary opening to a closing motion be used.

These considerations have led to the design philosophy that all RNS propulsion system valving will utilize metallic seals where size constraints do not incur a large penalty. For large valve sizes located in the aft region of the propulsion module the baseline design will be a valve concept that can use soft seals but is equally compatible with a metallic seal. In other regions, the same basic design configuration will be utilized with current cryogenic or soft seal configurations. This philosophy permits an evolutionary technology development in the areas of metallic sealing for both low leakage and extended cycle life without tying the valve basic design to this type of an advancement.

4.6 AUXILIARY PROPULSION

4.6.1 Phase II Concept

This section establishes the the Phase II APS concept and the rationale for the additional analyses performed during Phase III. During Phase II preliminary impulse levels were established and the APS locations and subsystem features were selected. The definition of multiple module RNS concepts resulted in two APS subsystems: (1) a cold GH_2 system located on the propulsion module and recharged by NERVA tap-off gas to provide module stabilization for orbital assembly, and (2) a low-pressure cryogenic APS with radiation-cooled nozzled configured with two pods located on the forward skirt. For the Class 1 RNS configurations, main tank LH_2 was utilized and LO_2 was located in a replacement module for orbital replenishment.

The cold-gas APS concept on the propulsion module was retained for Phase III. However, the APS system located in the forward skirt was subjected to a complete re-evaluation based on the following considerations: (1) extensive definition of RNS orbital and mission operations during Phase III (see Section 3); (2) a focus on improved cryogenic APS concepts within the concurrent space shuttle program; and (3) reconfiguration of the Class 1-H RNS during Phase III with a CCM for orbital maintenance and replenishment.

4.6.2 Design Criteria

The auxiliary propulsion system (APS) located in the CCM will provide thrust for: (1) attitude control during coast phases, (2) attitude maneuvers, (3) attitude control during cooldown thrusting, (4) separation maneuvers, (5) roll control during main engine burns, (6) rendezvous maneuvers, and (7) propellant settling.

Long-term storage of the RNS will be in the local vertical to minimize attitude control impulse requirements. Altitude losses resulting from aerodynamic drag in earth orbit will be made up by the orbital support system to minimize RNS requirements. The design will make maximum practical use of external support for orbital operations, including assembly and payload handling. A policy of minimizing APS use before initial mission injection is implemented. The design of APS has been based on normal mission and orbital operations, without regard to main propulsion system failure considerations. If contingency maneuvers associated with main propulsion system failures were defined, they could impact the APS design.

Each of the functions that the APS will perform are summarized as follows, based on the operations defined in Section 3:

A. Coast Attitude Control (Limit Cycling) - The APS has been sized to provide stablization capability for all operations performed during orbit coast, and for translunar and transearth coast phases, as defined in Section 3.9.2. A coast deadband of ±1.0 degrees is applied. The coast attitude rate is between 0.9×10^{-4} and 7.0×10^{-4} degrees/sec. A minimum bit pulse of 3 lb-sec is utilized.

B. Attitude Maneuvers - The APS total impulse requirement depends on the number of orbital attitude maneuvers and maneuver rates. These are discussed in Section 3.9.3. An attitude rate of 0.1 degree/sec is utilized. Maneuvers occur prior to and following: (1) each RNS burn, (2) exclusion distance separation maneuvers, (3) each midcourse trajectory correction, and (4) macro-rendezvous orbit phasing corrections. The maneuvers that are used to establish the APS impulse requirements are shown in Table 3.9-3.

C. Attitude Control for Aftercooling - Vehicle attitude disturbances during aftercooling can result from the misalignment of the thrust vector and the center of mass. Section 3.13.5 discusses these disturbances and their effect on the APS impulse requirements. In sizing the impulse requirements to counteract these disturbances an alignment of the thrust vector within 0.1 degree was assumed. This alignment would be activated by periodically retrimming the NERVA by the use of an active control system.

D. Separation Maneuver - The APS will be used to provide $\Delta V = 2.5$ fps to ensure a safe separation between the RNS and the space facility prior to NERVA operation for each transfer burn. Section 3.9.4 discussed these maneuvers and established the ΔV requirements.

E. Roll Control - The APS will null out roll disturbances during each burn. Section 3.12.4 defines the impulse requirements.

F. Rendezvous ΔV - The rendezvous ΔV requirements have been defined in Section 3.14.2. A capability of providing 10 fps for each rendezvous maneuver has been assigned to the APS.

G. Propellant Settling Acceleration - The impulse and thrust level requirements for propellant settling have been discussed in Section 3.11.2. An impulse of 40,000 lb-sec and an axial thrust level of 3.2 lb have been established as the requirement for this function.

The impulse budget derived from these requirements is shown in Table 4.6-1. The design moments of inertia and moment arms are presented in Section 3.2.3 of Book 2. The associated thrust level requirements (derived for attitude maneuvers in Section 3.9.2) are 100 lb for pitch, roll and yaw, 200 lb axially for longitudinal maneuvers, and 3.2 lb for propellant settling. The 100-lb thrust level requirement, combined with a minimum valve operating time of 30 msec, yields a 3 lb-sec minimum impulse bit.

Table 4.6-1

APS IMPULSE BUDGET

Maneuver	Impulse (lb/sec)
Coast attitude control	1,800
Attitude maneuvers	145,000
Attitude control for aftercooling	38,800
Separation	49,400
Roll control	11,300
Rendezvous	108,000
Propellant settling	40,000
Subtotal	394,000
Contingency (15%)	58,700
Total	453,000

The APS could be mounted either forward or aft of the center of mass. In the Phase II study it was determined that while the aft location reduced the total impulse requirements, the radiation levels were considerably higher, making component design and development difficult. Based on these findings and on the need for recycling the APS to the ground after each mission for replenishment and refurbishment, the CCM was selected as the APS location.

The APS will be designed to provide autonomous auxiliary propulsion capability for all normal mission operations. The system will be designed to fail operational for all credible failures. However, single failures of the structural components will be judged incredible. Subsystems will be designed for the full RNS lifetime of 10 round trips over 3 years. Refurbishment will be provided between each mission to allow use of component lifetimes which optimize cost and performance.

4.6.3 APS Engine Configuration

The rationale for the APS engine configuration selection is partially explained by Table 4.6-2, which indicates the pod locations, the engines utilized, the design thrust level, and the impact of engine failure for the various maneuvers required. The first consideration is the number of APS pods. Candidates with two and four pods were evaluated. The Class 1-H RNS the command and control module envelope constraints required locating the APS motors on outriggers to avoid plume impingement. Thus, two pods are provided for that case. The space shuttle launch configuration for this CCM is described in Section 3.3. In addition, utilizing only two pods simplifies the hardware installation requirements, thereby tending to minimize system weight.

Table 4.6-2 indicates which APS engines are operational for the design thrust level in the various RNS maneuvers. Economical system development favors utilization of a single motor size and consequently results in multiple motors for some operations. A major consideration is the RNS design requirement to fail operational. The impact of engine failure is reviewed in Table 4.6-2, showing how this reliability philosophy is implemented. The

Table 4. 6-2

APS ENGINE CONFIGURATION

Maneuver	Total Design Thrust (lb)	PODS/Engine Configuration (View)	Impact of Engine Failure
Pitch	100	(End) (Side) 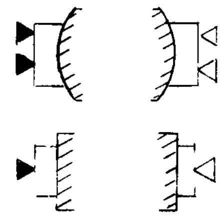	Perform maneuver at 1/2 rate
Yaw	100	(End) (Side) 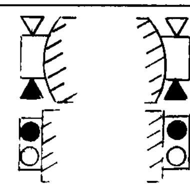	Redundant - normally operate 1 engine in each pod
Roll	100	(End) (Side) 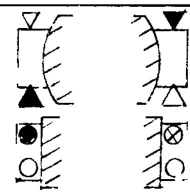	Redundant - normally operate 1 engine in each pod
Aft Thrust	200	(End) Looking Forward (Side) 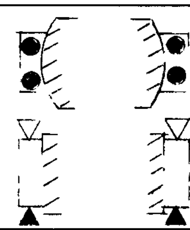	Perform at (a) 75% thrust (b) or 50% one engine in each pod
Forward Thrust	200	(End) Looking Aft (Side) 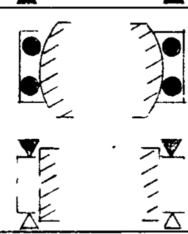	Perform at (a) 75% thrust (b) or 50% one engine in each pod
Settling	3. 2	(End) (Side) 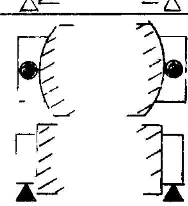	(a) Perform at 1/2 thrust (b) Utilize 100 lb thrust
Resultant Design Configuration		(End) (Side) 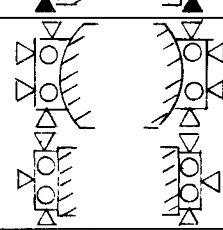	

approach for most maneuvers is to accept a lower maneuver rate in case of a single engine failure. Full redundancy is available only for the yaw and roll maneuvers. This approach is considered adequate for the present RNS design requirements, since the maneuver rates are not critical. If the RNS were required to hard dock with a manned facility, the maneuver rates could be critical, requiring a revision of this philosophy.

The selected configuration shown at the end of the table contains a total of twenty 50-lb thrust motors divided among the two pods. In addition two 1.6-lb thrust propellant settling motors are provided, one in each pod. Because the motor configuration is confined to two pods, it would be necessary to provide deflectors between adjacent motors to protect against burnthrough.

4.6.4 <u>APS Propellants, Storage, and Conditioning</u>

An analysis of APS propellants and the approach for their storage and conditioning was performed to select the type of system most suitable to the RNS. Both earth storable and cryogenic APS systems were considered. The design basis used for the comparison is reviewed as follows.

4.6.4.1 Earth-Storable APS

Two types of systems using earth-storable propellants were considered: (1) monopropellant hydrazine, and (2) the bipropellant combination of nitrogen tetroxide (N_2O_4) and monomethylhydrazine (MMH). These are representative of current technology. While earth-storable systems do not provide the high specific impulses attainable with cryogenic systems, their higher bulk density is attractive for the low total impulse of the RNS. Surface tension or bellows type positive propellant expulsion devices are most favorable for reusability. Other devices were assumed as a baseline. Expulsion pressurization is accomplished with ambient stored helium, which is simple and lends itself to reusability. Although other types of storable propellant pressurization systems (such as gas generators) are usually lighter than the selected approach, they are also more complex.

4.6.4.2 Cryogenic APS

Cryogenic auxiliary propulsion systems (LO_2/LH_2) have received considerable attention for the space shuttle, which requires both high thrust and high total impulse. Since the propellants are not hypergolic, either a catalyst or ignition system is required. Liquid/liquid injection of O_2 and H_2 results in unpredictable and inefficient combustion, so gas/gas injection or at least GH_2/LO_2 injection is required to achieve satisfactory performance. Gas/gas injection is considered most favorable. Since gaseous storage of propellants is inefficient, a propellant conditioning system consisting of gas generators, heat exchangers, and accumulators is required, which degrades the overall system performance. For a low total impulse attitude control system, the resulting hardware weight can offset the high specific impulse.

Simplified schematics for three candidate cryogenic APS systems are shown in Figure 4.6-1. The first concept is a low chamber pressure system. Both propellants are vaporized before entering their respective accumulators. The gaseous propellants in the accumulators are then routed to the various

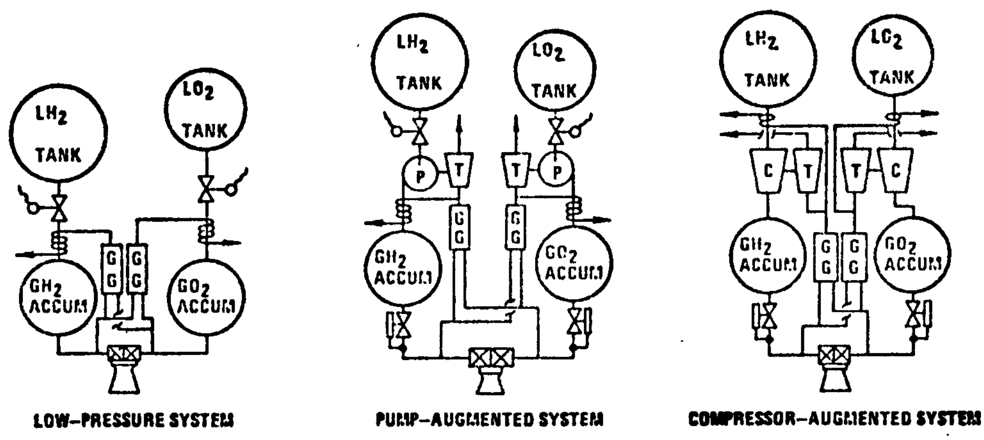

Figure 4.6-1 CANDIDATE CRYOGENIC APS SYSTEMS

thrusters as well as the gas generators which provide the heat source for propellants vaporization. Although this system is the simplest cryogenic APS concept, it suffers from low specific impulse due to the limited thruster expansion ratio at low chamber pressures.

Higher thruster chamber pressure operation may be realized by using either a pump or compressor to raise the pressure in the respective accumulators. Concepts for these systems are also shown in Figure 4. 6-1. In the pump-augmented system, the liquid is vaporized after it leaves the pump and before entering the accumulator. In the compressor-augmented system the liquid is vaporized prior to entering the compressor where its pressure is raised en route to the accumulator. Both the turbo-compressor and turbo-pump systems use the gas generator efflux to drive the turbines.

4. 6. 4. 3 System Comparison

Preliminary design system weight curves were generated over a range of total-impulse requirements for the concepts described above. Table 4.6-3 summarizes the values of the major parameters which were used. Thrust chamber assembly weights were based on radiation-cooled thrust chamber assemblies.

The weight of the five candidate APS systems is compared to Figure 4. 6-2. The system weights include all inert hardware, pressurants, and propellants, using the cited design assumptions for a total impulse of 455, 000 lb-sec. The compressor augmented cryogenic APS concepts offer the lightest system for this total impulse level by a small (~100 lb) margin over the pump-augmented cryogenic APS. However, this slight weight advantage is probably not sufficient to warrant the recommendation of the compressor system. O_2/H_2 turbopump technology is well developed, so except for long-life and reusability considerations, the advance development requirements for the turbopump system should be minimal. However, turbocompressors have not been developed for cold gas applications of O_2 and H_2, so the uncertainties in the development requirements preclude the recommendation of that system. Thus, the turbopump-augmented cryogenic APS is selected. However, the bipropellant storable system, requiring minimum development may be viewed as a backup to the recommended pump-augmented O_2/H_2 system, at the cost of about a 200-lb weight penalty.

Table 4.6-3
SUMMARY OF AUXILIARY PROPULSION SYSTEM PROPULSION CHARACTERISTICS

Category	Cryogenic System			Storable Systems	
Propellants	O_2/H_2	O_2/H_2	O_2/H_2	N_2H_4	N_2O_4/MMH
Feed Concept	Pressure	Pump	Compressor	Pressure	Pressure
Thrust (lb)	50	50	50	50	50
Chamber Pressure (psia)	10	100	100	100	100
Expansion Ratio	40	60	60	60	60
Mixture Ratio	3.0	4.0	4.0	-	2.3
Steady State Vacuum I_{sp} (sec)	330	365	394	230	298

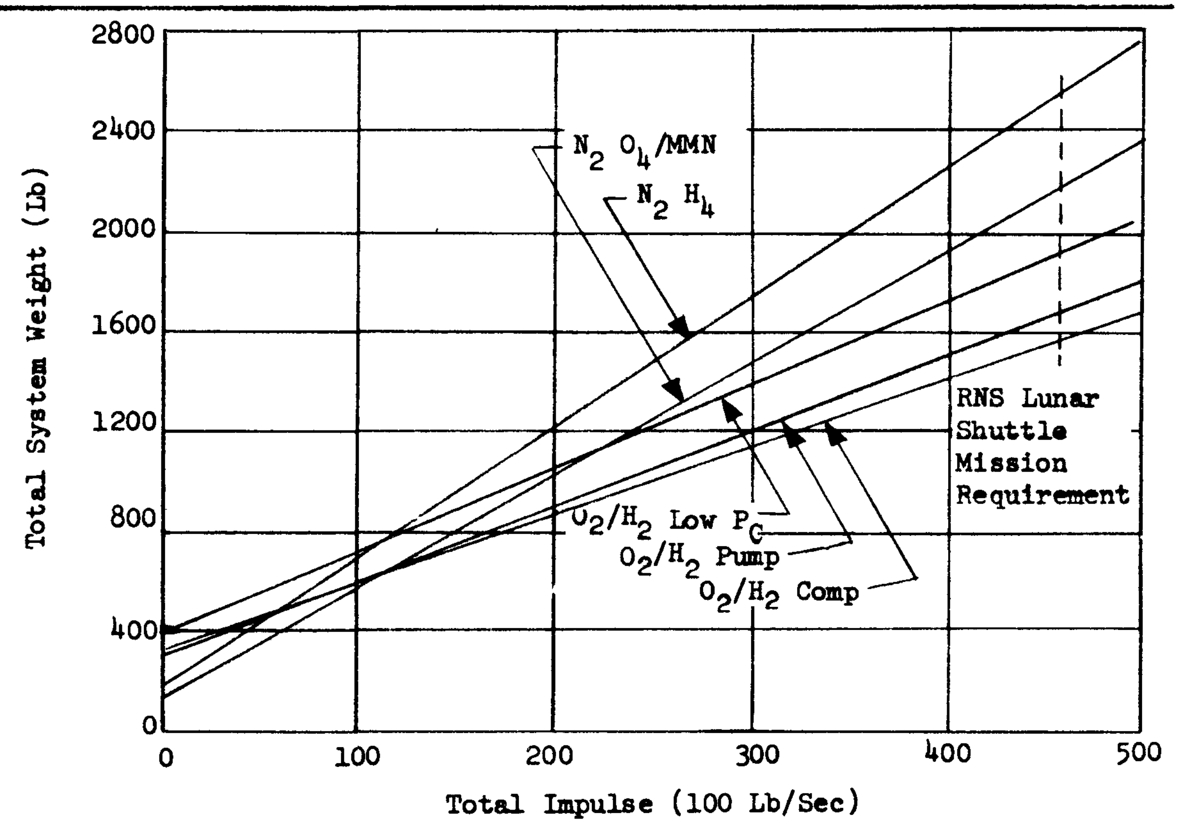

Figure 4.6-2 AUXILIARY PROPULSION SYSTEM COMPARISON

4.7 ASTRIONICS

4.7.1 Phase II Concept

This section establishes the Phase II astrionics concept and the rationale for the additional analyses performed during Phase III. During Phases I and II several astrionics concept selections were made on the basis of weight, cost, and reliability (see Section 2 of Reference 4-2 for specific tradeoff data). Saturn-derivative and advanced system configurations were defined, including evolutionary requirements, for the reference mission/program model. Reduced development requirements led to selection of the advanced stage concept.

Phase II concentrated on a reusable mode of operation requiring advanced astrionics systems. Multiple module RNS configurations were defined, as described in Section 4.1, and the astrionics functions were allocated to the individual modules consistent with orbital maintenance requirements. Accordingly, most astrionics subsystems were located on the CCM, which would be recycled to the ground after each mission for maintenance, calibration, and replenishment. This module provided a forward location for ease of replacement which also reduced the radiation environment on equipment. Selections were made for new design features as required. Remote coupling panels with screw jack drives were provided for orbital assembly/disassembly of modules. A data bus concept (plus emergency backup) with distributed multiplexing was adopted to minimize interconnections. Phase II was completed with a detailed definition of design features, as documented in Section 5 of Reference 4-1.

The Phase II study defined the navigation and guidance (N&G) functional requirements by mission phase. An autonomous N&G approach was selected based on minimum support requirements. However, satellite and ground-assisted approaches were carried in the Phase III study to evaluate sensor requirements and the performance and data processing implications of relative autonomy on the RNS. The Phase II study identified the measurement requirements and controllable function requirements for the RNS. From these requirements the Phase III study derived the external system communications requirements (see Section 3.8), internal data flow, and the requirements for the data management system. A representative subsystem was then synthesized and the requisite architecture defined. The primary power source selection of fuel cells from Phase II was reviewed compared to an alternative of solar cells, considering revised engine power requirements and a refined mission profile. Also, radiation effects on solar cells, semiconductors, and insulators were reviewed. These analyses are presented in subsequent sections, and the resulting definition of design features is contained in Book 2.

Phase II study results that were carried forward into Phase III include the use of internal electric heaters for thermal conditioning, use of secondary AgZn rechargeable batteries for emergency and peaking power, decentralized multiplexing of instrumentation, and the use of a data bus concept, PCM encoding of RF transmission external to the RNS, an independent hardwire emergency detection system, the use of RNS stored procedures for onboard checkout, and provision of an inertial stabilization package on the propulsion module for assembly operations.

4.7.2 Design Criteria

The RNS astrionics design was analyzed and developed in accordance with study guidelines provided by NASA in Reference 4-7. Navigation and guidance, data management, command and control, and power functions are independent of payload and the capability for orbital checkout, fault isolation and detection, and emergency detection is provided. Uplink and downlink capability for data and control between the RNS, ground and necessary support system elements are required. The design must provide for status monitoring of each module during all operations and phases of its lifetime. The RNS navigation and guidance policy will provide for maximum practical utilization of aftercooling pulses for final velocity attainment, midcourse correction, and/or rendezvous maneuvers. The RNS will have automated rendezvous and docking capability.

The RNS astrionics systems are designed to fail-safe criteria on all credible failures to prevent loss of crew and supporting personnel or unacceptable risk to the general population. They are designed to permit remote assembly and disassembly of RNS modules in orbit, consistent with the policy for initial assembly, maintenance and replenishment. The design will locate astrionics components on the CCM to the maximum practical extent to facilitate maintenance.

Electronic technology expected in the 1974 time period will be utilized (Reference 4-7). This implies that the technology should be presently under development with a high expected value of success, and no breakthroughs should be required. For areas where extrapolation beyond demonstrable technology is employed, current technology should be carried as an alternate/backup. The approach for selection of components and subsystems will consider commonality and applicability to other planned space program system elements and support facilities.

4.7.2.1 Navigation, Guidance and Control

A summary of the functional requirements for the NG&C subsystem for the lunar shuttle mission are shown in Table 4.7-1, derived in Phase II (Section 2.3.4 of Reference 4-1). The mission requirements include navigation in low earth orbit, navigation and guidance for interorbital flight, and guidance and command generation for rendezvous and docking with other space vehicles. The NG&C subsystem provides control for the engine actuators and the APS.

The RNS will have the capability to be the active element in terminal rendezvous and docking with orbital elements. It will also have the capability to be the passive element by provision of reflecting corner cube patterns to allow for electro-optical docking and will remain oriented and stable for that operation.

4.7.2.2 Instrumentation

The instrumentation subsystem includes the appropriate transducers, signal conditioning, multiplexers and analog-to-digital converters. The preliminary measurements list derived in the Phase II study (Section 2.3.3.1 of Reference 4-1 is shown in Table 4.7-2. For the early vehicles, an additional 420 parameters are required. The number of channels of signal conditioning is assessed as 60 percent of the total number of analog channels. Transducers are required for 80 percent of the analog channels and not required for event channels.

Table 4.7-1

NAVIGATION AND GUIDANCE FUNCTIONAL REQUIREMENTS

Mission Phase	N&G Functions	Performance Requirements
Earth orbit	Perform navigation during active (nondormant) periods.	±1.8 nmi: and 2 fps (radial) required at TLI
Translunar and coast	Provide guidance and navigation during boost; periodic navigation during coast; guidance for midcourse corrections.	±15 nmi: and 2 fps (radial) (±0.004 degree sensor angle accuracy for autonomous)
Lunar arrival and orbit	Determine braking velocity vectors required and time of application for capture and subsequent orbit shaping; navigate in orbit; rendezvous and dock with lunar tug for payload transfer.	±2 fps for ±10 nmi, perilune accuracy
Transearth coast	Perform guidance and navigation during boost; periodic navigation during coast; guidance for midcourse corrections.	Approximately 3 to 5 times TLI requirements
Earth arrival and orbit	Determine braking velocity vectors required and time of application; rendezvous and dock with space tug; navigate in earth orbit.	±6 fps for ±10 nmi: perigee accuracy

Table 4.7-2
SUMMARY MEASUREMENT LIST BY FUNCTION
FOR OPERATIONAL RNS

Function	Number of Parameters
Acceleration	13
Temperature	220
Pressure	120
Flow	6
Position	54
Guidance and Control	46
RF and Telemetry	11
Event	141
Level	5
Voltage, Current, and Frequency	37
Miscellaneous	24
Angular Velocity	24
Speed	4
Neutronics	9
Torque	18
Total	732

The frequency response requirements for this data set is distributed as shown in Table 4.7-3. For early vehicles the addition of vibration, acoustic and other high-frequency response parameters causes a bit rate requirement that is about five times as great as for operational vehicles.

4.7.2.3 Command and Control (Communications)

The command and control (communications) subsystem accepts all communication from ground and external space program elements, onboard vehicle sensors and the payload. This information is processed to a usable form and transmitted as required to ground or external space program elements. The projected capabilities of the Deep Space Information Facility (DSIF/MSFN) are assumed. The availability of ground tracking stations and satellites was considered but not assumed.

4.7.2.4 Electric Power

The electric power subsystem delivers primary and secondary 28-vdc power to all vehicle subsystems. Inverters are provided in each module to supply

Table 4.7-3

DISTRIBUTION OF FREQUENCY RESPONSE REQUIREMENT FOR OPERATIONAL RNS

Frequency Response Requirement (Hz)	Number of Parameters
1-3	457
10-14	168
20-120	82
200-1,000	25
Total	732

120 VRMS, 400 Hz to motor driven functions. The power requirement for the RNS is defined in Table 4.7-4. Figure 4.7-1 shows the power profile for a typical engine burn and the physical location where the power will be utilized. The majority of steady state power is consumed in the CCM, shown by the cross-hatched area. The energy required for one lunar shuttle mission is 317 kwh.

Table 4.7-4

RNS POWER REQUIREMENTS

	Power (watts)					
	Engine Operation		After-cooling		Coast	
	Nominal	Peak	Nominal	Peak	Nominal	Peak
NERVA Engine	2,300	3,500	200	1,000	60	60
Guidance, Navigation and Control	500	2,000	400	400	50	50
Instrumentation	300	300	200	200	50	50
Command and Control	50	300	50	300	20	300
Environmental Control	-	200	-	200	-	50
Onboard Checkout	50	50	50	50	50	200
Data Management	300	350	300	350	100	100
Total	3,500	6,700	1,200	2,500	330	810

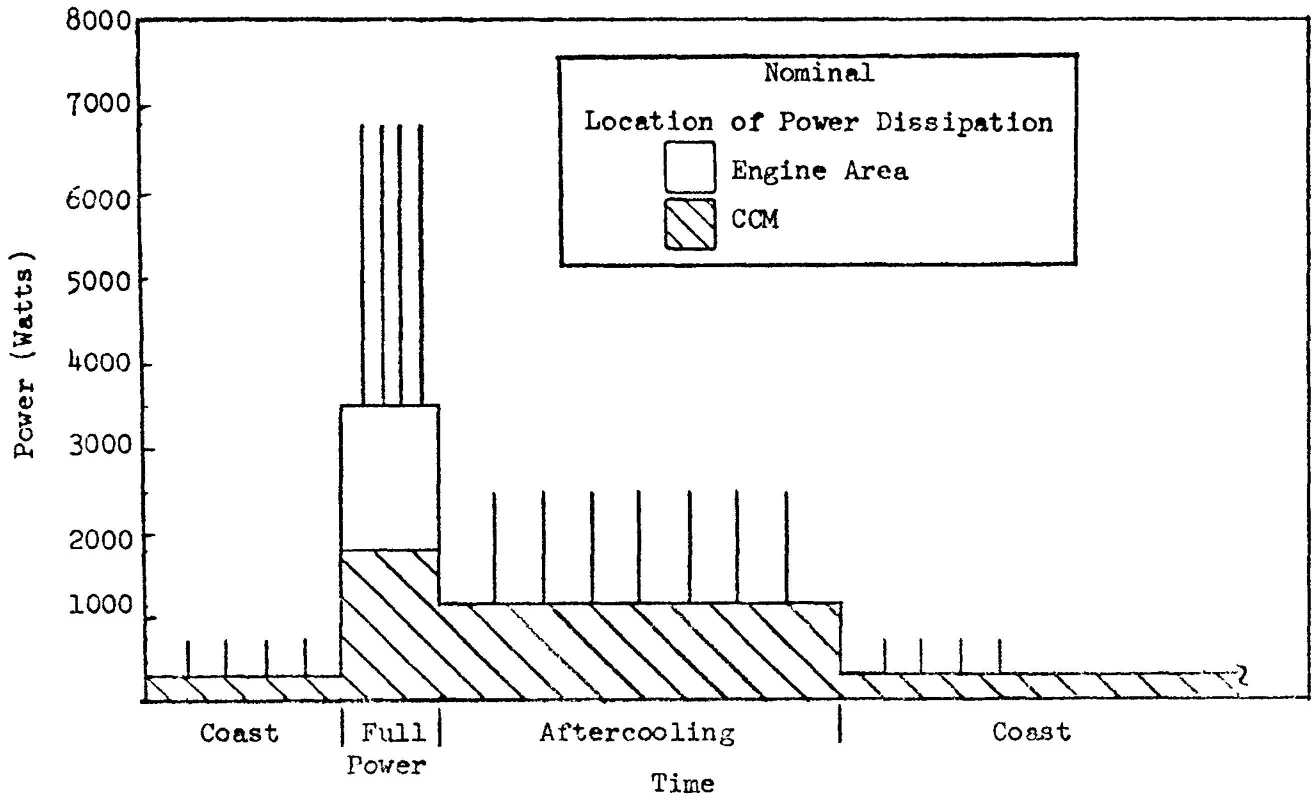

Figure 4.7-1 RNS POWER PROFILE FOR A TYPICAL ENGINE BURN

4.7.2.5 Onboard Checkout

The RNS is capable of determining its operational readiness for a mission in orbit with no external assistance. The results of the checkout is communicated to ground, and capability of receiving override and procedure modification via uplink is provided. The checkout system is also capable of fault isolation to the replaceable module as defined in the maintenance policy.

An emergency detection system (EDS) is continuously operational with capability for monitoring and control of potentially hazardous conditions independent of the balance of the astrionics system.

4.7.2.6 Data Management

The data management subsystem stores the RNS procedures, processes the data, and issues the required commands for control of the RNS. A serial transmission (data bus) approach is utilized to communicate between subsystems and modules.

4.7.3 <u>Navigation, Guidance and Control</u>

A study was made of the relative autonomy of the RNS for NG&C functions. A selection was made for the type of sensor that would fulfill each of the sensing requirements identified.

4.7.3.1 RNS Autonomy

The candidate N&G concepts include ground tracking, navigation satellite and beacon ranging approaches, and onboard autonomous navigation. Detailed descriptions of these are presented in Reference 4-53. Ground tracking uses the present MSFN tracking network and an onboard transponder. The autonomous navigation approach considered here requires no ground equipment. Table 4.7-5 shows the performance of candidate ground assisted approaches and Figure 4.7-2 shows the performance characteristics of autonomous configurations with various sensor complements. The accuracy of each concept meets the requirements specified in Table 4.7-1.

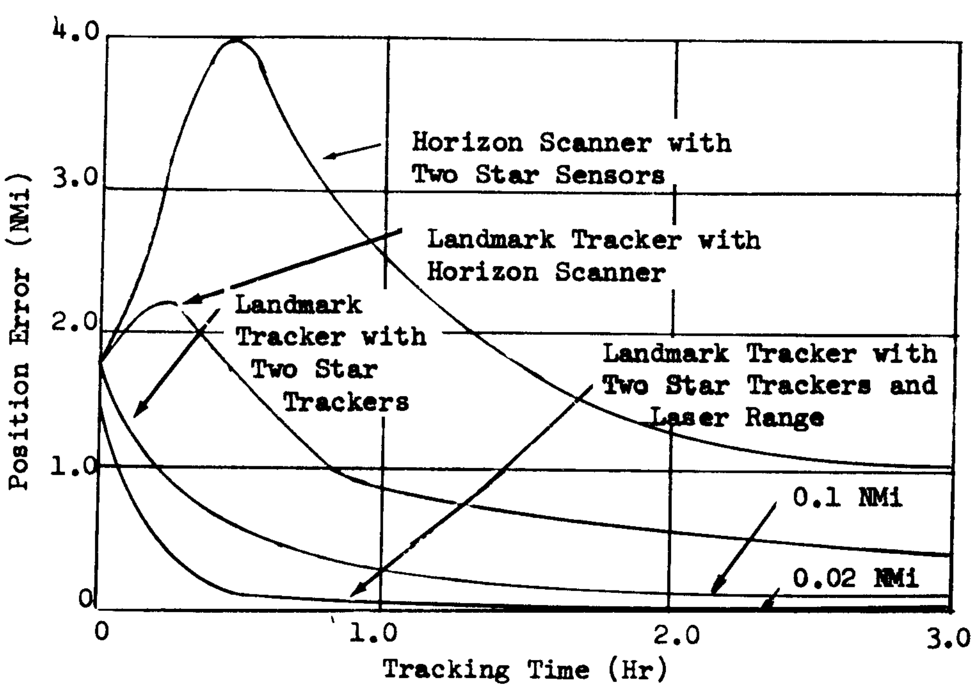

Figure 4.7-2 PERFORMANCE OF AUTONOMOUS NAVIGATION CONFIGURATIONS

Table 4.7-5

PERFORMANCE CHARACTERISTICS OF NONAUTONOMOUS N&G CONCEPTS

Concept	Position Error Earth Orbit (ft)	Velocity Error After TLI[2] (ft/sec)	Position Error First Midcourse (ft)	Velocity Error Lunar Injection (ft/sec)	Position Error Lunar Orbit (ft)
Ground Tracking (MSFN)					
5 Stations	678	16	---	--	---
3 Stations	1, 188	16	1, 200	0. 2	2, 000
1 Track/Day	1, 881	20	2, 400	0. 4	4, 000
Ground Beacons	1, 000	20	---[3]	0. 2[1]	2, 200[1]
Navigation Satellites					
Ranging to Satellite	1, 000	20	---[3]	0. 2[1]	2, 200[1]
Satellite as Relay to Ground	1, 700	16	1, 200	0. 2	2, 200

(1) With lunar orbit satellite or lunar surface transponder.

(2) A significant portion of this error is due to the just completed burn.

(3) Ranging from these distances require appreciable power on-board, or very large antennas.

The processing and storage requirements for the candidate concepts are shown in Table 4.7-6. The processing requirements are expressed in equivalent adds per second (ops). Although all processing requirements may not occur coincident in time (at peak), they are summed to provide a first-order approximation of the processing requirement differences between concepts. The storage requirements makes no distinction between high-speed and bulk storage requirements. The storage requirement is a gross representation of the software complexity required for each alternative. About 15 percent of the storage requirement is data, the balance being instructions.

Table 4.7-7 summarizes the hardware and software characteristics for each concept. The autonomous approach utilizes the greatest computer capacity. Slightly greater weight and power and lower reliability is attributed to the ground assisted approaches.

The primary operational constraints associated with the candidate approaches are related to the attitude restrictions and the supporting requirements. The autonomous approach requires the optical sensor to be oriented toward the planet to within about 20 degrees. A similar requirement exists for the antenna system for the navigation satellite alternative. The ground tracking candidate requires the associated ground tracking network. Outside of the attitude restriction, there is little major distinction between candidates insofar as vehicle constraints are concerned. The cloud cover degradation of accuracy has been shown by past studies to be of minimal effect on stated accuracies.

An autonomous system approach was selected. There are only modest increases in hardware and software requirements for the autonomous approach because of the common attitude reference requirements for all candidates. The operational flexibility achieved with this concept is consistent with the high anticipated usage of the RNS and the variety of manned and unmanned payloads that must be accommodated. Additionally, the cost of any additional equipment is amortized over the many reuses of the RNS. This approach also allows for an independent backup capability to be provided by the ground tracking network. The difficulty with lunar orbit requirements for both navigation satellites and ground beacons makes these approaches less desirable

Table 4.7-6
PROCESSING AND STORAGE REQUIREMENTS
FOR THE RNS N&G SUBSYSTEM

Function	Autonomous + Ground Update		Ground Track		Nav. Satellite or Ground Beacons	
	Processing (ops/sec)	Storage (Words)	Processing (ops/sec)	Storage (Words)	Processing (ops/sec)	Storage (Words)
Attitude Determination	(19,700)	(2,300)	(19,700)	(2,300)	(19,700)	(2,300)
Gyros	5,000	500	5,000	500	5,000	500
Star Tracker	9,450	1,280	9,450	1,280	9,450	1,280
Horizon Sensor	4,000	400	4,000	400	4,000	400
Control Logic	1,250	120	1,250	120	1,250	120
Position Determination	(59,500)	(13,700)	(30,000)	(4,400)	(57,000)	(11,400)
Landmark Tracker	30,000	10,000	---	---	---	---
Pointing and Control	4,000	4,000	4,000	400	4,000	400
Data Mixing (Space & Ground)	500	300	---	---	---	---
Orbit Keeping	5,000	1,000	5,000	1,000	5,000	1,000
Orbit Change	20,000	2,000	20,000	2,000	20,000	2,000
Ranging Navigation	---	---	1,000	1,000	28,000	8,000
Total	79,200	16,000	19,700	6,700	76,700	13,700

Table 4.7-7

NG&C TRADE STUDY SYSTEM CHARACTERISTICS

Concept	Sensor Types Required	System Weight (lb)	Processor Requirement	Memory	Communications Requirements	Extended System MTBF	Power Requirements (watts)
Autonomous	Landmark tracker IMU 2 Star trackers Horizon Sensor	310	59,500 ops/sec	13,700 words	None	12,400 hr.	110
Navigation Satellites or Ground Beacons	Ranging radar IMU 2 Star trackers Horizon Sensor	380 + antenna	50,000 ops/sec	11,400 words	Ku-band ranging channel	10,000 hr.	185
Ground Tracking	Transponder & Receiver 2 Star trackers Horizon sensor IMU	295	30,000 ops/sec	4,400 words	S-band ranging channel	15,000 hr.	100

than groundtracking. The potential of saturation of the ground tracking network in a dynamic space program makes it less desirable than an autonomous approach. An autonomous selection is also consistent with the other NASA leading programs including space shuttle and space station.

4.7.3.2 Sensor Candidates

Alternate sensors were evaluated for the determination of attitude and position. Reference 4-53 provides a detailed description of each of the sensors and an explanation of their operation. Regardless of the approach selected for navigation, the determination of attitude would require the selection of some combination of the following sensors.

Celestial (Optical) Sensors

Star trackers and horizon sensors may both be used for attitude determination of the RNS. Three types of star trackers are candidates for the RNS: gimbal, pattern recognition, and strapdown. Tables 4.7-8 and 4.7-9 summarize the performance and other characteristics of these sensors. The gimbaled star

Table 4.7-8

STAR SENSORS

	Pattern Recognition Star Sensor	Strapped-Down Star Sensor	Gimbaled Star Sensor
Accuracy	~10 sec (exact number Classified)	10 sec	10 sec
Field of View	10 deg	8-10 deg	1.0 deg
MTBF	35,000 hr	60,000 to 90,000 hr	21,000 hr
Power	9 watts	8 watts	39 watts
Weight	16 lb	8-10 lb	40 lb
Development	Presently undergoing environmental test	---	Operational
Star Magnitude	---	3.0-4.0	2.0
Comments	Operates on transit of star signal between slits on detector, requires vehicle attitude motion to operate	Strapped down to vehicle, senses star patterns	Gimbal limits ±60 deg

Table 4.7-9

EARTH VERTICAL SENSORS

	Horizon Sensor - Edge Tracker	Monopulse Radar System
Operating Range	70 to 100,000 nmi	Up to 300 nmi
Accuracy	0.10 deg, ±3 mi altitude	0.1 to 0.01 deg, ±13 ft in altitude
MTBF	150,000 hr	15,000 - 20,000 hr
Weight	10 lb	15 lb
Power	5 watts	35 watts
Volume	250 in^3.	500 $in.^3$
Special Notes	Operates 14 to 16 μ-band	Requires 15-in.-diameter antenna Operates at 10×10^9 Hz (X-band) early models have not met specifications

sensor is preferred based on the minimum constraint imposed on RNS attitude. A horizon sensor is also used to allow for initialization of attitude and as a backup for both attitude and position determination.

Inertial Systems

Short-term inertial attitude reference is generally obtained from gyros. Several alternate gyro concepts merit consideration for RNS including gas bearing, ball bearing, laser, and electrostatic gyros. Gyros can be used in either a platform or strapdown configuration. Table 4.7-10 compares the performance of four classes of gyros. Ball bearing gyros were selected because of the restart difficulties presently associated with gas bearing, the catostrophic failure mode of electrostatic gyros with a momentary loss of power and the relative insensitivity of laser gyros to the slow rates experienced with the RNS. The strapdown gyro in a redundant dodecahedron configuration is preferred at this point; however, the space shuttle preference for a gimbaled system would favor taking advantage of future development work. Two ranges of accelerometers, 1 to 10^{-3}g and 10^{-3} to 10^{-6}g, are included to allow for accurate measurement of the thrusting and aftercooling impulse respectively.

Table 4.7-10

GYRO COMPARISON

	Ball Bearing	Gas Bearing	Laser	Electrostatic
Bias Drift	---	---	0.1 to .01 deg/hr	---
Random Drift	0.4 deg/hr	0.005 deg/hr	0.01 deg/hr	0.00001 deg/hr
Scale Factor Linearity	100 ppm	100 ppm	20 ppm	10 ppm
Input Rate Limit	30 deg/sec	30 deg/sec	30 deg/sec	---
MTBF	30,000 hr	50,000 hr	33,000 hr	TBD
Life	2,000 hr	>45,000 hr	>18,000 hr	20,000 hr
Weight	1.6 lb	1.0 lb	5 lb	6.16 lb
Power	6 watts	3 watts	2-4 watts	TBD
Size	2.3 x 6.7 x 1.6	2.0 x 3.5 x 1.0	5.7 in equilateral triangle	60 cu in.
Comments	Poor reliability	Limited restarts to 10,000 sometimes sticks	Requires biasing away from dead zone around null, needs development	Not operational much development cost

4.7.2.3 Guidance Policy

The RNS has a slow response time, primarily limited by vehicle dynamics, so that for short burn times guidance errors potentially would not be nulled out before main engine cutoff. This is most severe for the Class 3 RNS, for which an evaluation of the effects of a simple guidance policy on control system stability and response was performed (Section 4.7.3.3 of Part B, Book 1). Thrust vector misalignment is the most severe disturbance the system must cope with during the flight. Initial angular position and angular rates upon the vehicle have a smaller influence upon the lateral velocity penalty at end of burn. Improvement in system response to thrust misalignment may be further improved via an optimal guidance/control approach with position and gain changes between and during burns. Thrust misalignment may also be minimized by the use of a heuristic algorithm. These approaches offer about a factor of 10 improvement in the control system response. In addition, response requirements can be reduced somewhat by operation in the throttle mode (45,000-lb thrust) for short burns, which may be required for separate propellant management considerations.

4.7.4 Power

The Phase II selection of fuel cells as the power source was reviewed based on current power requirements. The primary change was a substantially lower NERVA engine power requirement. A breakdown of RNS power requirements by function is contained in Table 4.7-4. These result in the power profile shown in Figure 4.7-1. Table 4.7-11 details the resulting power requirements for each of the 8 burns. The total mission integrated power requirement is 317 kwh.

Sizing of the power source was based on the concept of using secondary batteries on the run tank to supply peak NERVA engine demands and a main power source located on the CCM to recharge these batteries and satisfy other power requirements during the long aftercooling periods. This concept offers a considerable weight advantage, since the main power source is not sized for the large peak demand level of 6.7 kw required for mainstage, but instead at the 1.2 kw level required during aftercooling. The peaking energy required to be delivered during NERVA full power operation is then 1.15 kwh,

Table 4.7-11

POWER REQUIREMENTS

Burn	Maneuver	Mainstage			Peak			Aftercool			Coast		
		Power Level (kw)	Time (min)	Energy (kwh)	Power Level (kw)	Time (min)	Energy (kwh)	Power Level (kw)	Time (min)	Energy (kwh)	Power Level (kw)	Time (min)	Energy (kwh)
1	Translunar Injection Midcourse Correction	3.5	29	1.69	6.7	6	0.01	1.2	120	144			
2	Lunar Orbit Injection - I	3.5	1.2	0.07	6.7	6	0.01	1.2	12.5	15.0			
3	Apolune Plane Change	3.5	0.4	0.02	6.7	6	0.01	1.2	11.9	14.3			
4	Lunar Orbit Injection - II	3.5	2.7	0.16	6.7	6	0.01	1.2	18.9	22.7			
	Lunar Orbit Operations										0.33	367.3	122.4
5	Transearth Injection - I	3.5	1.4	0.8	6.7	6	0.01	1.2	14.0	16.8			
6	Apolune Plane Change	3.5	-	-	6.7	6	0.01	1.2	5.0	6.0			
	Pre-TEI Coast										0.33	7.9	2.64
7	Transearth Injection - II	3.5	0.7	0.04	6.7	6	0.01	1.2	10.1	12.1			
	Midcourse Correction												
	Earthbound Coast										0.33	61.7	20.58
8	Earth Orbit Injection	3.5	7.8	0.46	6.7	6	0.01	1.2	45	54.0			

based on a 30 minute TLI burn. The power distribution cables from the main power source, located in the CCM, to the peaking batteries, located forward of the run tank, are sized for current levels of 20 amps, compared to the 120 amps that would be required to provide only the peak engine demands of 3.5 kw. The weight reduction in cabling is approximately 400 lbs.

Two types of power source were analyzed: solar cells and fuel cells. Radioisotope sources were eliminated in Phase II based on increased operational complexity and cost.

A typical solar cell power system as on the MDAC Skylab or proposed space station is composed of deployable solar cell panels, a deployment and panel orientation mechanism and power isolation and distribution modules. The panels would need to be rolled in during NERVA thrusting. The Skylab design incurs a weight of 3.3 lb/ft^2 with a 6-mil cover glass. The radiation effects study presented in Section 4.7.7 indicates the potential requirement for up to a 30 mil cover glass which could add another 0.5 lb/ft^2. Based on an MDAC space station proposal for a free-flying module of comparable power levels, which promises slightly greater than 2 lb/ft^2 with a 6-mil cover glass, and some optimism on improvement in current technology, 2 lb/ft^2 is used in the present trade study. Figure 4.7-3 is a design curve developed in the MDAC Phase B space station study, which is used to determine the amount of solar cell area required to obtain a predetermined level of power when the orbit plane inclination is known (Reference 4-54). Using the one-axis gimbaling curve to minimize deployment mechanism weight penalty, the solar panel area requirement for the 30-degree orbit of the RNS is 310 ft^2/kw of average power. The average power usage during aftercooling, the determining factor in main power source sizing, is 1.2 kw.

A typical fuel cell power system as on the MDAC proposed space shuttle is composed of multiple hydrogen/oxygen fuel cells with switching control circuitry for load sharing and fault recovery. The fuel cell system weight was determined using previously established sizing laws of 200 lb per fuel cell. This is representative of the Allis Chalmers 5-kw fuel cell proposed for the Manned Orbiting Laboratory (MOL). Both reactant and tankage weight are included in the weight tradeoff. Reactant, including both hydrogen and oxygen, is assumed at 0.8 lb/kwh and aluminum tankage of 0.4 lb/lb reactant.

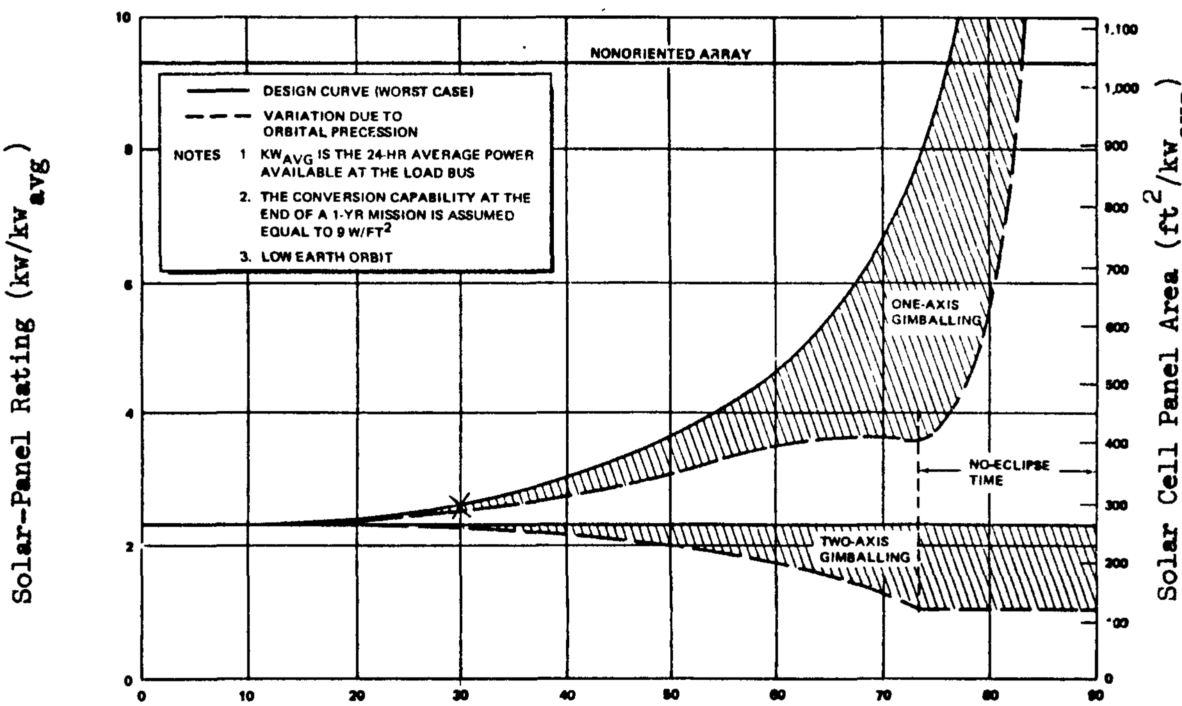

Figure 4.7-3 DESIGN CURVE FOR SOLAR CELL SYSTEMS

Figure 4.7-4 shows comparative system weights for the solar cell and the fuel cell systems as a function of average aftercooling power requirements.

Table 4.7-12 summarizes the information used to evaluate both power source systems. The models used to establish the estimated reliability of the candidate power sources are shown in Reference 4-1. The weight difference for the candidate power sources are negligible for the anticipated power profile. The power source is essentially sized for the aftercooling requirement. As this increases, the weight advantage is shifted to fuel cells. For lower power requirements, a weight criterion favors solar cells. The fuel cell system was chosen on the basis of initial system cost, relative insensitivity to changes in requirements, and technology status. The uncertainty of Li-doped solar cell development, the potential requirement for heavy cover glasses to provide radiation protection, and the operational complexity of panel deployment after each burn further favor the selection of fuel cells. The selection and anticipated development of a 2-kw fuel cell system for the space shuttle matches the RNS requirement of 1.2 kw and offers a potential weight advantage when compared to the 5-kw Allis-Chalmers cells modeled in the RNS trade study.

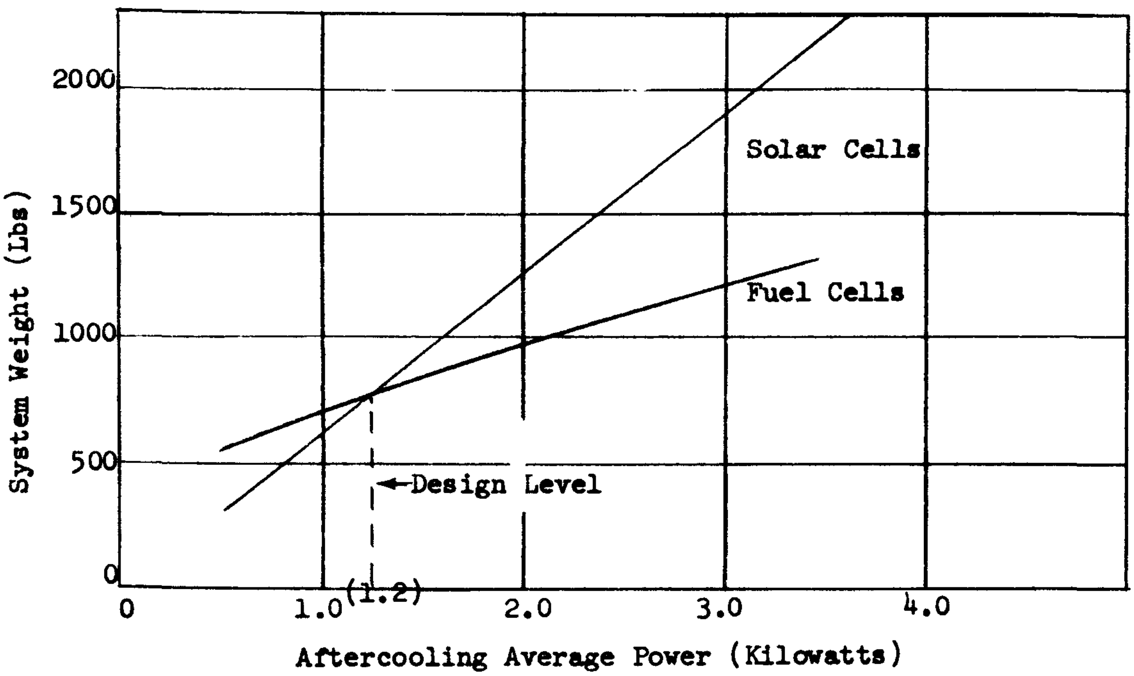

Figure 4.7-4 POWER SYSTEM WEIGHT SENSITIVITY TO AFTERCOOLING POWER

Table 4.7-12

POWER SOURCE EVALUATION

	Solar Cells	Fuel Cells
Weight (lb)	750	755
Estimated Reliability (MTBF x 10^3/RT)	37	53
Estimated System Cost ($)	1.7×10^6	0.5×10^6
Operational Requirements	Roll in during thrusting	Resupply each round trip
Technology Status	Li-doped cells under development	Baseline for Space Shuttle

4.7.5 Checkout

Checkout operations were defined in Section 3.7 according to mission phase, alternative operations, and subsystem requirements. The analysis described here concerns the checkout control concept.

Three basic concepts considered in Phase II were reviewed. The first may be characterized as autonomous. The onboard checkout system includes all of the preprogrammed procedures required to effect checkout. This would include the capability to transmit the results of the checkout operation to the ground crews. However, no requirement would exist for the ground crews to participate actively in the onboard process. This approach requires essentially real-time evaluation of all data accumulated during the checkout operation and provides for the ability of taking direct action when a malfunction is detected. Within the autonomous approach, the selection between centralized checkout and built-in test equipment (BITE) for each subsystem was considered. BITE is generally more compatible with a decentralized data management function. Section 4.7.6 considers two alternate decentralized data management subsystem architecture, however selects a centralized approach.

The second approach would be to maximize the utilization of ground facilities and transmit all commands to stimulate the vehicle and evaluate by ground computer the returning data, allowing for the decision making process on earth. This approach allows for the use of the essentially unlimited ground capability for data processing, storage, and subsequent fault prediction analyses.

The third approach is a hybrid one where the operational procedures are stored and processed onboard. The ground would get selected data and have the ability to modify procedures by uplink and transmit new procedures to the vehicle for special purpose checkout. Operational checkout and fault isolation procedures would be stored onboard while fault prediction procedures for non-space resident modules could be stored on the ground. The vehicle would then have to store some limited set of procedures, primarily operational, to stimulate and evaluate the prime subsystems. The ground would have control of the sequence of procedure execution and the timing when checkout is to be performed. This approach is closer to the autonomous concept than to the ground control approach.

The requirement for checkout exists in both earth and lunar orbit. While the RNS is at lunar distances only a limited amount of communication compatibility is available. During near earth checkout operations, communication delays occur both in transmission time and because of limited viewing time over the ground stations. Therefore, ground transmitted procedures cannot respond rapidly to anomolous situations. The ground controlled approach would preclude the use of a closed loop checkout philosophy, which was successfully used during the Saturn program and described in Reference 4-1, Section 2.3.7. Based on this and the recurring nature of checkout, hybrid approach, approximating the autonomous approach, is selected as baseline. Centralized checkout with a BITE concept for NDICE and the data management self-check is employed. The procedures required to effect the selected onboard checkout strategy are also identified and described in Reference 4-1, Section 2.3.7. Analysis of fault isolation requirements in the maintenance section suggests that only a limited amount of fault isolation is required because of the large size of the replacement modules. The ability of the man (on the ground) to provide procedure modification and create diagnostics for situations that were not anticipated or preprogrammed seems mandatory.

The processing and storage requirements associated with the requirement for onboard checkout is shown in Table 4.7-13. The primary processing mode at peak is represented by the data management self-check and the potential implementation of fault prediction algorithms (trend analysis) in real time. The diagnostic routine for the processor is assessed at 5,000 operations per second with a high speed storage requirement of 500 words. It is assumed that up to 100 functions per second will require fault prediction at an average of 27 equivalent adds for each function. A continuous scan of functions to determine in or out of limits is assumed for another 100 functions. An independent hardware emergency detection system (EDS) is baseline for the RNS and the associated emergency procedure implementation is considered to be a non-peak requirement for the primary processor. The largest implication of onboard checkout is the large bulk storage requirement for procedures. In general, these procedures are implemented during non-peak periods such as orbital coast and do not contribute to the peak load. Additionally, since these procedures deal with electromechanical devices such as valves, they generally run for long periods of time and have minimal processing requirements per unit time.

Table 4.7-13

PROCESSING AND STORAGE REQUIREMENTS

ONBOARD CHECKOUT

Function	Processing Equivalent Adds/Sec at Peak	Storage: High Speed (Words)	Storage: Bulk (Words)
Data Management Self Check	5,000	500	-
Fault Prediction (100 Functions)	2,700	350	-
Function Scan (100 Functions)	500	250	-
Emergency Detection Processor	-	100	-
Emergency Procedures	-	-	10,000
Interface Verification	-	-	2,000
Instrumentation Calibration	-	-	150
Subsystem Checkout (Including Redundancy Checks)			
Astrionics	-	-	6,500
Propulsion (Excl NERVA)	-	-	3,200
Auxiliary Propulsion	-	-	1,000
Other Subsystem	-	-	1,500
Totals	8,200	1,200	24,350

4.7.6 Data Management

A study was performed to establish the functional requirements for data management and select a baseline architecture for the RNS. Processing and storage requirements for each function are established and centralized and decentralized systems approaches evaluated.

4.7.6.1 Processing and Storage Requirements

The processing and storage requirements of the data management function are derived from the RNS instrumentation, processing, and storage requirements of the various subsystems. These are itemized in Table 4.7-14. The processing and storage requirements for navigation and guidance and onboard checkout are established in Sections 4.7.3 and 4.7.5, respectively. The NERVA instrumentation requirements are included in Table 4.7-14; however, the processing and storage for control for the engine operation are not included. Maximum processing requirements occur during a main engine burn (Reference 4-55). The processing and storage requirements for each subsystem were developed in terms of equivalent adds per second (ops) assuming a divide-multiply-add time ratio of 8:4:1 and 32-bit processor. Storage requirements are divided between high-speed, random access and bulk with a dynamic interchange capability.

The instrumentation list for an operational RNS and the distribution of frequency response requirements is shown in Section 4.7.1. These requirements translate to about 8,800 samples per second or at 10 bits/sample about 90,000 bits/sec. The upper limit for internal RNS data flow is taken as 0.5×10^6 bits/sec for the development vehicle assuming all data is transmitted during at least one mission phase. The largest contributor to the processing storage requirements for the instrumentation, command and control subsystem is the implementation of the data compression algorithm. The processing requirement shown allows for 8,800 samples per second, each of which would require 12 ops to effect the compression algorithm. To allow for calibration of the data utilized in the operational programs, 38 ops per sample are allowed, based on a second order calibration curve, and an assumed 100 samples per second. Capability for both uplink and downlink processing, control of the instrumentation mode, and a dictionary is provided. These, however, represent minimal processing requirements.

Table 4.7-14

DATA MANAGEMENT TRADE STUDY

PROCESSING AND STORAGE REQUIREMENTS

Function	Processing Equivalent Adds/Sec at Peak	Storage	
		High Speed (Words)	Bulk (Words)
Onboard Checkout			
Data Management Self-Check	5,000	500	-
Fault Prediction (100 Functions)	2,700	350	-
Function Scan (100 Functions)	500	250	-
Emergency Detection Processor	-	100	-
Emergency Procedures	-	-	10,000
Interface Verification	-	-	2,000
Instrumentation Calibration	-	-	150
Subsystem Checkout (Including Redundancy Checks)			
Astrionics	-	-	6,500
Propulsion (Excluding NERVA)	-	-	3,200
Auxiliary Propulsion	-	-	1,000
Other Subsystem	-	-	1,500
Subtotal	8,200	1,200	24,350
Instrumentation, Command and Control			
Data Compression	105,000	2,000	2,000
Downlink Processing	1,000	50	-
Uplink Processing	-	500	-
Instrumentation Mode Control	-	200	-
Calibration Data	3,800	2,500	2,500
Dictionary	-	1,500	1,500
Subtotal	109,800	6,750	6,000

Table 4.7-14 (Cont)

DATA MANAGEMENT TRADE STUDY

PROCESSING AND STORAGE REQUIREMENTS

Function	Processing Equivalent Adds/Sec at Peak	Storage High Speed (Words)	Storage Bulk (Words)
Data Management			
Executive*			
Control	15,000	2,000	
Memory Management	-	400	
I/O Processing	10,000	600	
Data Bus Controller	9,000	500	
Redundancy Switchover	-	100	
Time Base Control	1,000	100	
Procedures			
Mission Procedures	5,000		10,000
Orbital Operation Procedures	-	-	15,000
Subtotal	40,000	3,700	25,000
Navigation, Guidance and Control			
Attitude Determination and Control	19,700	2,300	-
Guidance and Navigation — Ground Processing	29,500	3,700	-
Autonomous Navigation**	30,000	10,000	
Supporting Routines***	4,000	-	15,400
Subtotal	83,200	16,000	15,400
Total	241,200	27,650	70,750

*Assumes centralized 1 + 1 processor configuration.

**Includes capability for ground update/backup — not required with ground processing.

***Assumes centralized processor — for dedicated add 15,000 adds/sec and 1800 words of high speed storage for exec plus intercomputer communication requirements.

Major contributions to the processing and storage requirements associated with the data management functions are represented by executive functions. Control is estimated to be 15,000 equivalent adds per second and input/output (I/O) processing another 10,000 adds per second. The data bus controller is assumed to be implemented in software and would require approximately 9,000 ops/sec. Allowance is made for a time base and provision is made for processor switchover control, which assumes that the processors are in a configuration that includes redundancy. This represents an overhead of about 15 percent, which is consistent with the experience of other computer system executive loads. To implement mission procedures 5,000 ops/sec were allocated. It is assumed that some portion of mission procedures will occupy high speed memory. However, it is considered feasible to use dynamic high speed storage so that a only portion of the total procedure requirement needs to be resident in high-speed storage at any one time. Orbital operation procedures are used off-peak and are allowed for in the bulk storage requirement.

In summary, the total processing requirements at peak are about 241,000 equivalent adds/sec, and the high speed, random access storage requirement is less than 28,000 words, assuming dynamic storage of the operational procedures. This would allow about 5,000 words of procedure storage with a 32,000-word memory. The bulk storage requirements are 70,000 words; however, the sensitivity to this requirement is small as a magnetic tape or analogous bulk storage device is envisioned. The total storage requirement represents a first order approximation of the software complexity of the RNS. About 15 percent of the storage requirement is data, the balance being instructions.

The major requirements for the RNS processor are for data compression navigation, guidance and control, and the overhead for the executive functions. The early estimates of the NERVA engine control processing requirements to meet their present specifications are substantially above the present stage requirements. These requirements derive in part from the present stringent specifications of the engine. Refinement of engine control processing requirements is expected in the near future.

4.7.6.2 Architecture

The data management system architecture can employ various degrees of centralization, alternative approaches to reliability enhancement, and different data bus concepts. The evaluation of the degree of centralization considered three discrete candidates:

A. Centralized -- A single processor can satisfy the speed and memory requirements of the RNS exclusive of the engine control requirements. A block diagram of the RNS with a centralized approach is shown in Figure 4.7-5.

B. Decentralized by Function -- This approach would utilize dedicated processors for each major processing function of the RNS. The N&G function, the data compression and evaluation functions, the NERVA control function, and the data bus controller are likely candidates for dedicated processors. This has the advantages of allowing a number of hardware-software tradeoffs to favor special-purpose hardware approaches and potentially reduces software requirements for each subsystem. Additionally, it is consistent with a corporate management strategy of major subcontractors, inasmuch

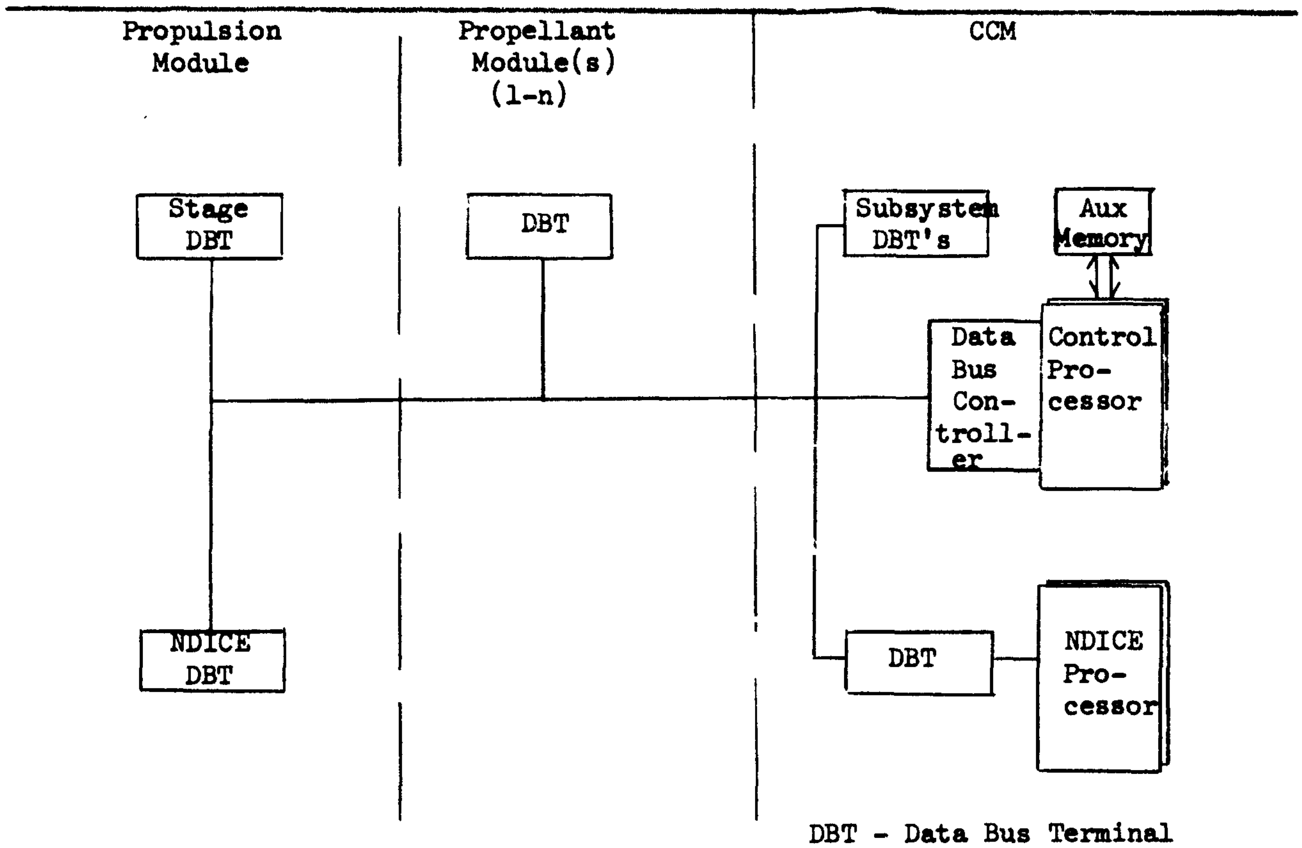

Figure 4.7-5 DATA MANAGEMENT ARCHITECTURE CENTRALIZED

as an entire N&G package, data bus, or engine subcontractor would hold total responsibility for his function. The disadvantages lie in the additional overhead penalties incurred because a single processor component or procedure is repeated rather than time shared. Reliability enhancement techniques could multiply this disadvantage. Some loss of flexibility results and the question of synchronizing computer to computer communication is a difficult one to solve. Figure 4.7-6 represents the system architecture considered for this approach.

C. Decentralized by Module -- The use of a processor in each module has the advantages of allowing autonomous checkout during the transportation phase and processing of local data during operation. The primary disadvantage is that a propellant or propulsion module, which is space resident, would have reliability requirements over three years rather than a single mission duration of 45 days. This alternative is shown in Figure 4.7-7, but is considerably less attractive than the other. The motivation for simple modules exclusive of the CCM remains.

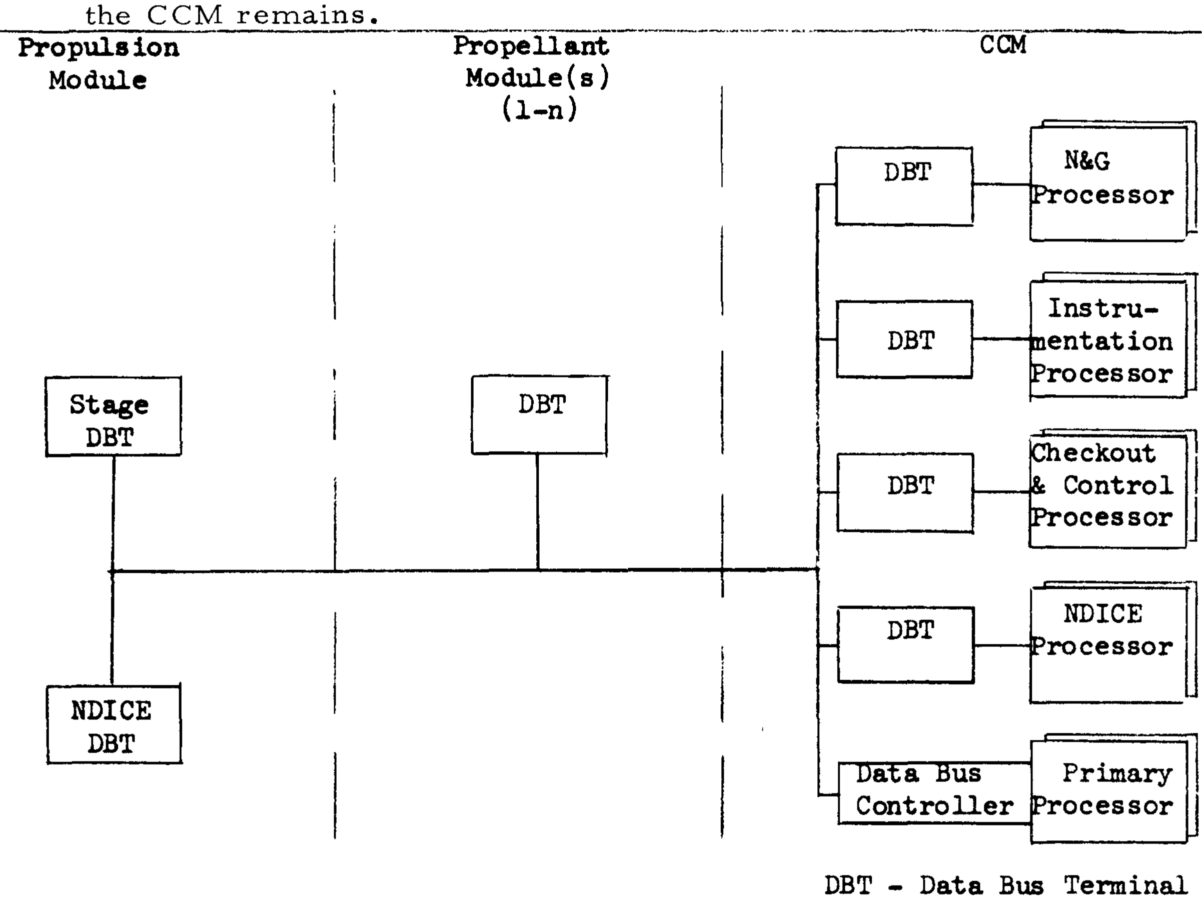

Figure 4.7-6 DATA MANAGEMENT ARCHITECTURE DECENTRALIZED BY FUNCTION

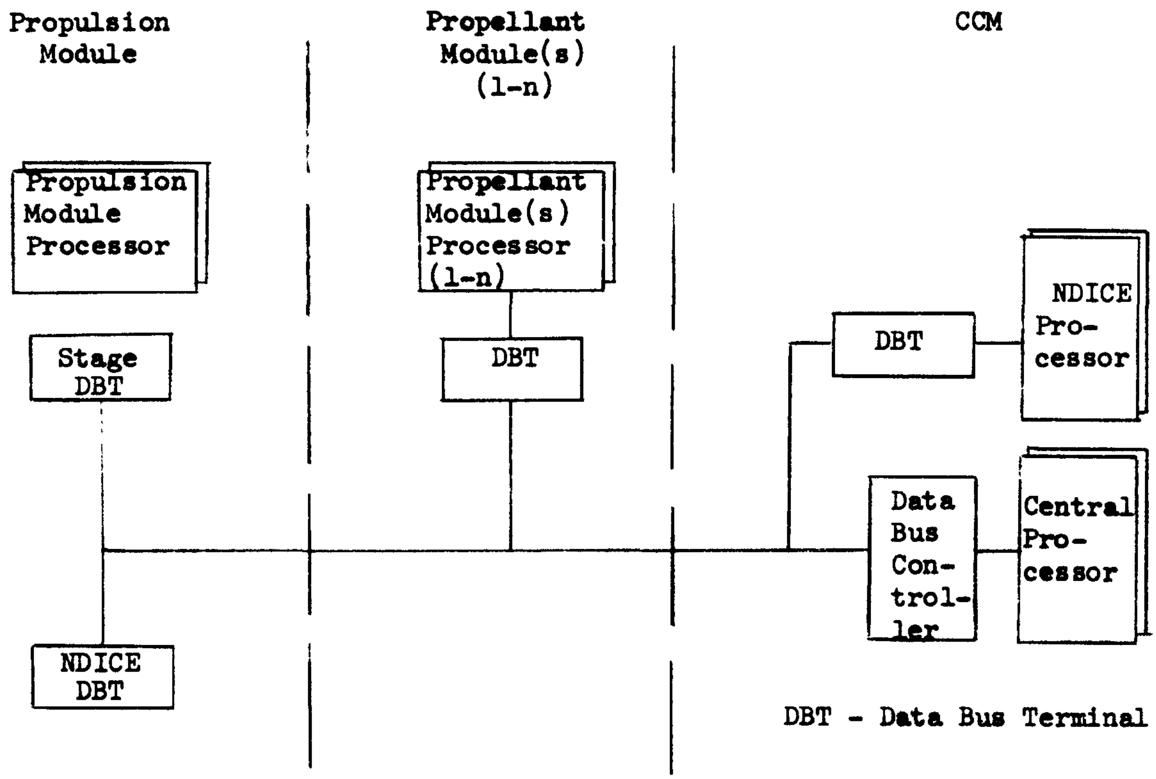

Figure 4.7-7 DATA MANAGEMENT ARCHICTECTURE DECENTRALIZED BY MODULE

The reliability of the processor configurations was evaluated, as shown in Figure 4.7-8. These curves were based on the assumption that the failure rate for the standby unit is 0.1 of the operational unit. The curves are labeled as follows: A + B (X.XX), where A represents the number of active units required to perform a function, B is the number of backup or standby units, and (X.XX) is the "coverage," which is an indication of the probability of successful detection of a fault, switchover, and start of the redundant unit. The results are highly sensitive to the coverage value.

The reliability allocation for the data management subsystem is 0.9976. Assuming that the processor configuration would have to meet this requirement exclusive of other elements of unreliability in the system, this would correspond to an MTBF of 23,700 hours assuming a 1 + 1 configuration with a switchover reliability of 0.99. If, alternately, one-half of the unreliability was attributed to other components in the systems such as the data bus controller, the reliability allocation for the computer system would be 0.9988, corresponding to an MTBF for the 1 + 1 configuration of 38,500 hours assuming a 0.99

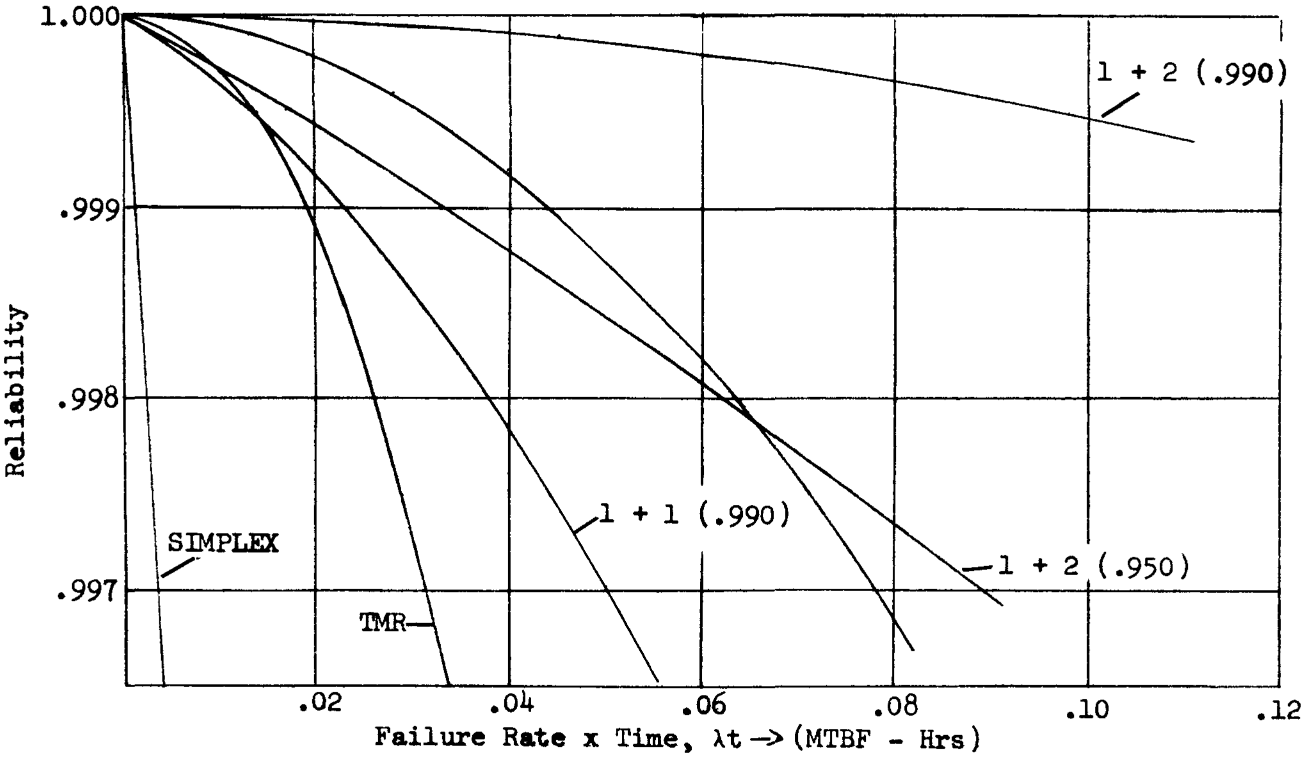

Figure 4.7-8 RELIABILITY OF ALTERNATE CONFIGURATIONS

switchover reliability. Alternately, a 1 + 2 configuration could be utilized. In this configuration the sensitivity to the switchover reliability is very high. Assuming a switchover reliability of 0.95, the processor reliability allocation would be 13,500 hours for the total allocation being attributed to the processor. Again, assuming one-half of the processor unreliability would be taken by the other components in the system, the corresponding reliability requirement for the single processor in the 1 + 2 configuration would be 26,400 hours.

The requirement for a 4-μsec add time on the computer appears well within the state of the art. Figure 4.7-9 shows the speed of several airborne computers and their year of introduction. A factor of 2 increase over the RNS speed requirement is presently available. The possibility of integrating the NERVA engine control requirements into the data management function central processor was considered. The present requirement for the NERVA control system, being substantially above the RNS requirement for the present engine specifications indicates that a parallel processor (multiprocessor)

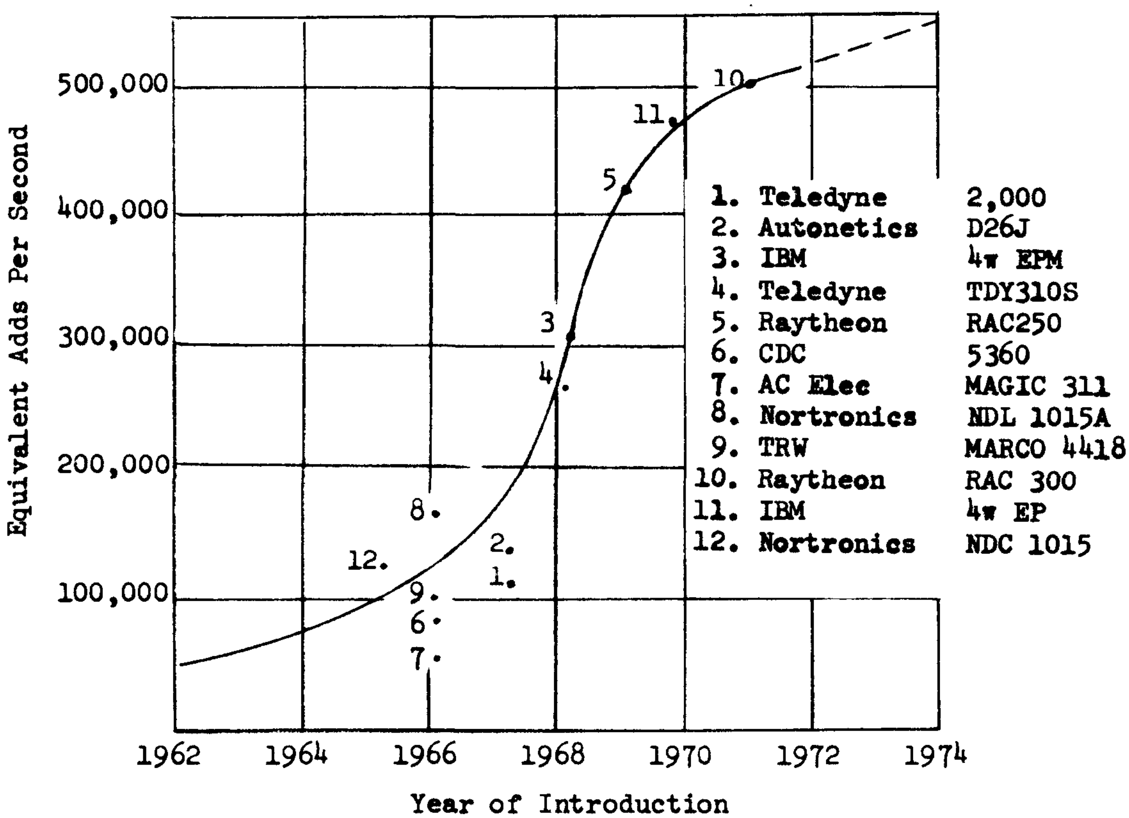

Figure 4.7-9 PROCESSOR SPEED DEVELOPMENT

approach would have to be taken. However, if the control requirements were of the same magnitude for engine control as for the sum of the balance of the RNS requirement, it would be feasible to integrate processing the requirements in a single processor concept.

The data bus concept selected in Phase II is fundamentally the time sharing of a serial digital line to transmit data over some predetermined distance. Several concepts of the data bus are presently under development. A data bus concept is accepted as baseline for the space station and the space shuttle. The present developmental efforts use from 1 to 3 lines and have transfer rates from 1 to 5 Mhz. Manchester or bipolar formats and current or voltage coupling of data bus terminals to the lines seem equally popular. Various schemes of error detection and correction are employed. Any of the data bus implimentations presently under development would satisfy the requirement of the RNS based on the requirement for the RNS developmental vehicle of 0.5×10^6 bits per second. It is expected, however, that the data bus concept selected for the space shuttle, will be adapted to the RNS requirements because RNS components must physically interface with the space shuttle data bus. For the Class 1-H RNS configuration, it is estimated that eight data bus terminals would be required. Although the data bus controller can be implemented in either hardware or software, the processing requirements for the RNS assumed the worst case--software.

A centralized approach with the data bus configuration to be used on the space shuttle was selected as baseline with an autonomous engine control processor. The system architecture for the stage uses two processors in a 1 + 1 configuration. The failure of the primary processor allows for the switchover to the secondary processor without loss of mission objectives. Although no responsibilities are assigned to the secondary processor, it is likely that as the program develops certain functions will be defined. The primary responsibility of the secondary processor is to remain in synchronization to allow for an efficient transfer of control.

Each processor has a reliability requirement of about 38, 500-hour MTBF implying that they are likely internally redundant. The processing speed requirement of a 4-μsec add is relatively modest and high-speed storage of 32, 000 words seems adequate. A shared selection of memory to insure switchover to the secondary computer and a bulk storage capability is allowed for. The data bus traffic requirement is a maximum of 0.5×10^6 bits/sec, well within the capabilities of all systems under development. The radiation environment is not constraining for the processors which will be located forward of the propellant module; however, special consideration must be given to the data bus terminals, digitizers, multiplexers, and instrumentation located on the propulsion module.

The limiting requirement for the RNS data management function appears to be the reliability of the processor and the ability to provide for an efficient switchover to a backup processor or implement other reliability enhancement techniques.

4.7.7 Radiation Effects

A literature search was performed to assess the effects of steady state radiation on semiconductors, solar cells and insulation materials. The radiation environment for the RNS is defined in Section 4.5.11. The critical location is the propulsion module aft zone, with a dose criterion for 10 round trips of 10^8 rads, which includes a factor of 10 safety margin. This is reduced to 5×10^6 rads at the top of the propulsion module.

4.7.7.1 Radiation Effects on Semiconductor Electronic Components

A study was performed to determine which classes of semiconductor components may be used in circuitry mounted near the aft end of the RNS. It was concluded that the effects of the radiation on the semiconductor devices during and after irradiation are highly predictable, and that it should be possible to select components that are useful for at least several round trips in the expected environment of the top of the run tank. To harden the circuits sufficiently, it is necessary to select components carefully, based on the fabrication process, the values of f_α and β_{in} (for bipolar transistors), and the dopant concentration (in the case of JFET's). The tolerable radiation doses for the best available devices of each type are shown in Table 4.7-15 based on a 50 percent performance degradation.

At the top of the run tank, the neutron dose is small; hence any semiconductor devices considered are considered acceptable. However, the gamma environment is relatively severe. Evacuated unpassivated mesa transistors, JFET's, or dielectrically isolated MOSFET's could be used in this environment.

If circuitry is required at the bottom of the run tank, heavy shielding and substantial development work is indicated. The neutron dose is the limiting factor in this location. Since the radiation doses at the forward end of the main tank are very small, any semiconductor devices could be used there, for many trips.

Neutron Damage

The amount of permanent degradation which neutrons cause in a bipolar transistor depends on the initial gain and the cutoff frequency, and is given approximately by:

Table 4.7-15

EFFECTS OF STEADY-STATE REACTOR RADIATION ON TRANSISTORS

Type of Device	Tolerable Neutron Dose (n/cm^2, E >10 kev)	Tolerable Dose of Ionizing Radiation (rads)	Primary Failure Modes
Bipolar -			
Planar Transistor	10^{14}	10^5	Permanent loss of gain due to neutron displacement damage.
Mesa Transistor	10^{14}	10^7	Loss of gain — Due to surface effects caused By ionizing radiation.
Bipolar Integrated Circuit	10^{14}	10^5	Increase in I_{CBO} — Due to surface effects caused By ionizing radiation.
MOSFET	10^{15}	2×10^4	Voltage shift of characteristic curves (source-to-drain current versus gate-to-source voltage) due to surface effects by ionizing radiation.
MOSFET with dielectric insulation.	10^{15}	10^6	
MOS Microcircuits	5×10^{14}	10^5	Permanent decrease in source-to-drain durrent due to neutron displacement damage.
JFET	3×10^{15}	10^7 (Estimated)	Permanent loss of gain due to neutron displacement damage.

$$\beta/\beta_{in} = 1/(1 + 0.194\ \phi\beta_{in}/f_{aco}k)$$

where β and β_{in} are the final and initial values of the common-emitter current gain, ϕ is the fast neutron fluence (n/cm^2, e >10 kev), f_{aco} is the alpha cut-off frequency (hertz), and k is the damage constant (3×10^6 for Si) (Reference 4-56). Majority-carrier devices, such as diodes, JFET's and MOSFET's, do not show significant permanent neutron damage until the dose is high enough to cause an appreciable change in the bulk conductivity of the crystal. Figure 4.7-10 shows the neutron displacement damage in JFET's (Reference 4-57).

Ionizing Radiation Damage

All of the gamma energy absorbed in a material, and at least part of the neutron energy, form ion pairs. In Si, the ionization dose contributed by fast neutrons is

$$\text{Neutron dose} = 3.3 \times 10^{-11}\ \phi\,\text{rads},$$

and in Si O_2,

$$\text{Neutron dose} = 9 \times 10^{-11}\ \phi\,\text{rads}$$

where ϕ is the integrated fast neutron flux (n/cm^2).

The neutron dose must be added to the gamma dose in calculating the ionization dose. At the top of the run tank the neutron contribution is negligible, but at the bottom of the run tank it is significant. Radiation of bipolar semiconductors will cause positive ions to accumulate on the surface of the base region, near the junction. These repel the majority carriers in the base, forming an n-type channel just under the surface. The resulting increase in the effective junction area causes I_{CBO} to increase. The ions also affect the surface states of the Si, enhancing surface recombination of majority and minority carriers, which reduces the gain.

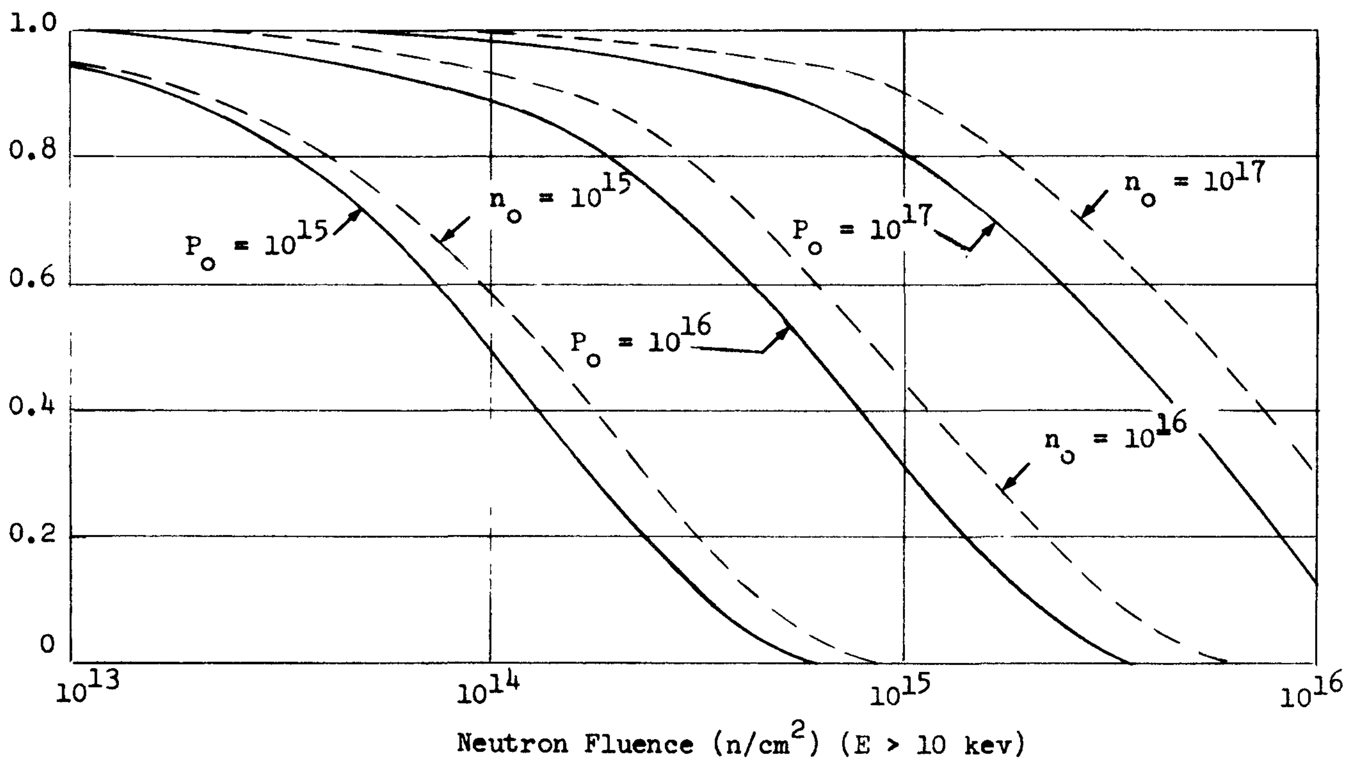

Figure 4.7-10 TRANSCONDUCTANCE DEGRADATION IN SI JFET'S DUE TO NEUTRON IRRADIATION, FOR VARIOUS INITIAL DOPING LEVELS IN CHANNEL

MOSFET's, since they are majority carrier devices, are vulnerable to ionizing radiation, which causes a positive space charge to form in the Si oxide insulation layer between the gate and the channel (Reference 4-58).

Expected Improvements in Radiation Resistance

Neutron damage causes relatively large decreases in the minority carrier lifetime in the base region of bipolar transistors, reducing the current gain. This effect can be minimized by reducing the base width. However, present technology, motivated by speed requirements, has reduced the base width to essentially the lowest practical value. Consequently, little increase can be expected in bipolar device neutron damage resistance. Lattice defects causing decreases in channel conductivity of JFET and MOSFET devices are the primary neutron damage mechanism. Changes in doping density can improve neutron hardness. However, no significant further improvement can be expected. Present limitations indicate that maximum integrated neutron doses in the 10^{14} to 10^{15} nvt range can be tolerated, with slightly better performance expected in highly doped JFET's. There will probably be very little improvement in this resistance to neutron damage over the next 10 years.

The primary damage mechanism of ionizing radiation in JFET's and bipolar planar transistors is a charge buildup in the passivating layer of the crystal and in the MOSFET's it is a charge buildup in the insulating layer between the gate and the channel. Over time substantial improvement has been made in minimizing the effect of ionizing radiation on these devices; however, JFET's have always been relatively immune to damage. It is expected that continued improvement in resistance to ionizing radiation will be seen.

Present JFET and bipolar transistors can withstand integrated doses of about 10^7 rads at a low dose rate with MOSFET devices withstanding substantially less radiation. One to two orders of magnitude improvement potential exists over the next 10 years for all three classes of devices.

4.7.7.2 Radiation Effects on Solar Cells

An literative search was conducted to determine the effects of nuclear and space radiation on the solar cells which are a candidate power source in

Section 4.7.4. The radiation environment includes neutrons and gamma rays from the nuclear engine, electrons and protons in the Van Allen belts, and protons from solar flare events.

Radiation damage, whether caused by fast neutrons, electrons, or protons, consists of lattice defects in the base region. These act as recombination traps which reduce the minority-carrier lifetime. This cuts the efficiency of the solar cell, reducing the short-circuit current (I_{sc}) and the open-circuit voltage (V_{oc}) that can be obtained from a given area of cell illuminated at a given intensity, since many of the ion pairs produced by absorbed photons will recombine before being rectified at the junction.

Expected Nuclear Environment

The radiation which the solar cells on the RNS will receive during one mission include a fast neutron dose rate of 10^8 neutrons/cm^2 (which does not include a safety factor), 50 rads of gamma rays, which will have no significant effect, a dose of electrons and protons during two passages through the Van Allen belts, and background radiation from space, which is sometimes much higher during solar flare events (Reference 4-59). Such a flare event, which occurs approximately once per year, would give a proton dose of $\sim 10^9$ p/cm^2 (E > 30 Mev). Similarly, the effect of Van Allen radiation on the cells could be calculated exactly, since the fluences and spectra of the electrons and protons in each part of the belts is known (References 4-60 and 4-61). The dose accumulated during each passage through the Van Allen belts depends on what the initial orbit is, and from what part of the orbit the ascent is begun, since the Van Allen belts are concentrated above the Earth's equator. However, it is estimated that the dose received during each passage will be equivalent to what is obtained during approximately one hour in the highest-intensity part of the belts. The solar flare dose obtained during a single large event (occurring once per year) is equivalent to roughly ten passages through the Van Allen belts (Reference 4-61).

Neutron Effects

The effect of fast neutrons on n/p Si cells (without Li) with 5 to 10 Ωcm bases is shown in Figure 4.7-10. The parameters shown are I_{sc}, V_{oc}, and maximum power (P_{max}) (Reference 4-62). With neutron irradiation, the effects on a Li-doped P/N cell would be just the same as on one which had some base donor other than Li, except that the damage in the Li-doped cell could be expected to anneal at room temperature nearly as fast as it formed, provided that the dose rate was low (about 10^{12} n/cm^2-day) and the Si was made by the float-zone process (Reference 4-61).

Damage Due to Van Allen Radiation

The effects of electrons and protons in the Van Allen belts on P/N and N/P Si solar cells, with from 0 to 60 mils of cover glass, are described in Reference 4-63. Even adding a 3-mil cover glass gives considerable improvement, increasing the useful life by a factor of 100. It was also found that heavily-shielded N/P Si cells lasted ten times as long as P/N cells with the same shielding (Reference 4-63). The relative damage rate of solar cells used in the Telstar satellite is plotted vs shield thickness (mils of sapphire) in Figure 4.7-11 (Reference 4-64).

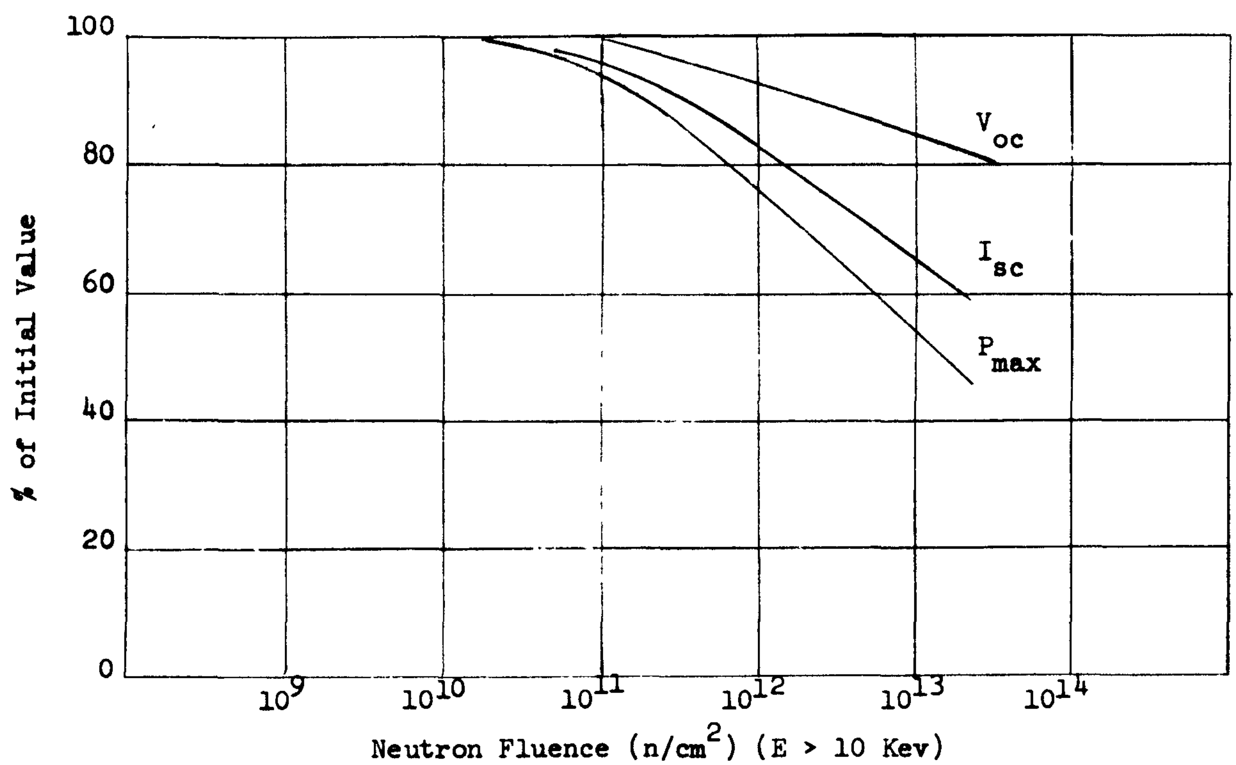

Figure 4.7-11 NEUTRON-INDUCED DEGRADATION IN N/P SI SOLAR CELLS

Hardening Solar Cells Against Radiation

The simplest way to harden cells against electron or proton damage is to add a cover glass. Depending on its thickness, it removes all the particles below a certain energy. A few mils of cover glass gives a great improvement, but increasing the thickness beyond say 60 mils will not give much additional improvement, because the proton and electron fluxes decrease rapidly with increasing energy. Figure 4.7-12 shows the relative damage rate of solar cells used in the Telstar satellite versus shield thickness. Cover glasses have no effect on neutron damage, however.

If cells are used which do not contain Li N/P cells are best, and the resistivity of the base should be low (i. e., it should be heavily doped). If Li-doped cells are used, they must necessarily be of the P/N type, the base should be heavily doped with Li (~ 1 Ωcm), and they must be made from float-zone Si. Wysocki (Reference 4-65) found that when Li cells with a 30 Ωcm base were irradiated with electrons, they received more damage than standard P/N cells with a 30 Ωcm base.

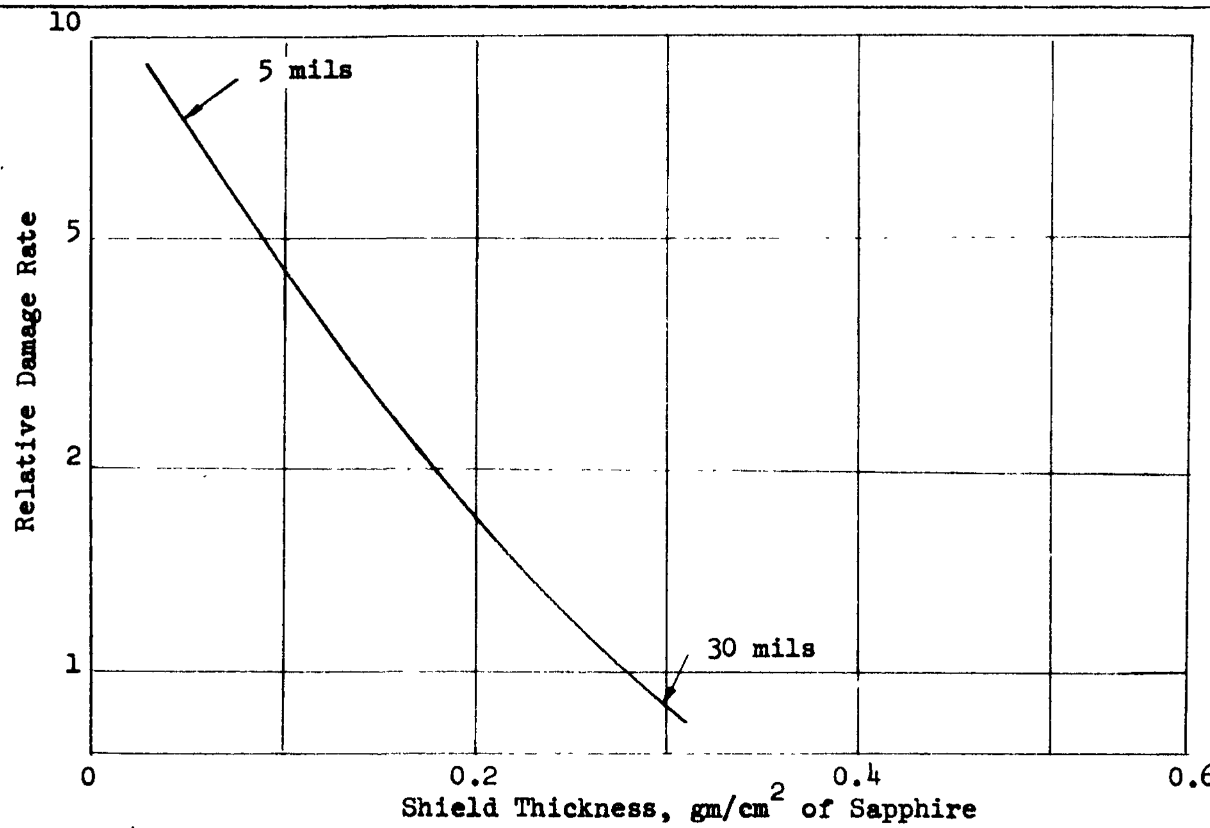

Figure 4.7-12 RELATIVE RADIATION DAMAGE RATES VS. SHIELD THICKNESS, FOR SI SOLAR CELLS IN TELSTAR

If the solar cells on the nulcear stage are to be used for 10 round trips lasting 10 years with a factor of safety of 10, the proton and electron dose equivalent will be 300 passages through the belts, or 300 hours in the heart of the belts. N/P standard cells with a 30-mil cover glass would degrade only 10 percent in this time. The neutron dose would degrade them by a negligible amount, provided the temperature of the cells is 25°C or higher. If they are colder than this, the Li could not cancel the damage as fast as it formed.

If the device must be heated to make it anneal satisfactorily, an electric heater or "black mirror" could be used. Boeing, after studying the problem, decided that an electric heater was impractical, and that the best way to heat cells would be to pull a black mirror onto the front surface (which is a sheet of material with a high absorption in the solar spectrum and low emittance in the infrared region) and aluminized insulation on the back. This heats the cell to 450°C in 1 hour. An hour or so at this temperature would anneal all the radiation-induced defects, even in a standard cell. It would be necessary to use a special cell, however, that did not contain any solder or other temperature-sensitive materials (Reference 4-66).

Conclusion

The effects of protons and electrons can be greatly reduced by using cover glasses over the cells. In general, N/P cells are more radiation-resistant than P/N cells; however, if Li is used as the base dopant in P/N cells, and the Si contains little oxygen, most of the radiation damage will anneal in a few hours at room temperature. Assuming that one large solar flare event occurs per year, and that the cells will get ten times the radiation dose that is actually expected, it is estimated that the electric power obtained from Li-doped solar cells with 30-mil cover glasses would decrease less than 10 percent in 10 years of operation.

4.7.6.3 Radiation Effects on Electrical Insulating Materials

An investigation was conducted on the radiation effects of insulation materials in conjunction with the cable and connector study under MDAC/MSFC Contract NAS8-25620 (Reference 4-67).

Radiation damage is of two types: permanent damage, which depends on the total integrated dose, and transient damage, which is a dose-rate effect. In organic materials, both neutrons and gamma rays contribute to the damage, whereas in ceramics only the neutron flux needs to be considered.

Table 4.7-16 gives the doses (in rads) at room temperature that will cause threshold damage and significant damage (~20 percent degradation of mechanical properties) to organic insulation materials. The type of damage expected is given under "Comments."

Table 4.7-17 gives the effects of radiation on ceramics. Probably any ceramic would tolerate the expected radiation, except glass containing boron.

4.7.8 NERVA Interface Implications

The primary impact of the Phase III MDAC study on this interface is related to the propulsion module concept. The present Aerojet baseline stage concept does not include a run tank, so astrionics mounted aft requires shielding. The more favorable radiation environment forward of the MDAC run tank allows for electronic component mounting in this area. Therefore, substantial changes to the presently conceived engine interface can be considered.

The routing of engine wires to the forward end of the run tank is recommended and would require approximately 3,000 wires crossing the engine/stage interface. The use of connectors as at this interface would impose a severe reliability penalty. The Phase II selection of flat cable and subsequent study of cable and connectors (Reference 4-67) has recommended that a flat conductor cable be used and a connectorless transition be made at the engine/stage interface.

It is proposed that signal conditioning, multiplexing and digitizing and control drivers be supplied with the engine instrumentation and located forward of the run tank. A data bus terminal would be provided for control and instrumentation signals that flow from the RNS and the forward mounted NDICE on the stage data bus.

Table 4.7-16

RADIATION EFFECTS ON ORGANIC ELECTRICAL INSULATION

Material	Specific Gravity	Dielectric strength (V/mil)	Initial Mechanical Properties	Radiation Damage Threshold (rads)	Dose Causing Significant Damage (rads)	Comments
Phenolic, unfilled	1.3	200-500	Hard	10^6	10^7	Becomes brittle
Epoxy (aromatic curing agent)	1.1-1.4	405		10^9	10^{10}	Becomes stiff, brittle
Polyester, unfilled	1.1 - 1.5	280-500	Flexible	10^5	10^6	Becomes brittle
Mylar film	1.4	4500	Flexible	10^6 - 10^7	10^8	Becomes brittle, cracks
Urea-formaldehyde	1.5	220-400	Stiff	2×10^6	2×10^7	Tensile str, falls
Polystyrene	1.0	600	Stiff	10^8	4×10^9	Softens, tensile strength decreases
Acrylonitrile/ Butadiene/ Styrene (ABS)	1.0- 1.1	350-500		10^8	10^9	Hardens, tensile strength falls
Polyimide film	1.43	7000	Flexible	2×10^8	10^9	Becomes brittle eventually
Polyvinyl Chloride	1.2 - 1.4	300-900		10^7	10^8	Insulation resistance and tensile strength decrease

Table 4.7-16 (Continued)

RADIATION EFFECTS ON ORGANIC ELECTRICAL INSULATION

Material	Specific Gravity	Dielectric strength (V/mil)	Initial Mechanical Properties	Radiation Damage Threshold (rads)	Dose Causing Significant Damage (rads)	Comments
Polyethylene	0.9–0.96	450-700	Flexible	$\sim 3 \times 10^7$	$\sim 10^9$	Tensile strength and breakdown voltage decrease (after first becoming more brittle)
Polycarbonate	1.2	350-400		2×10^6	3×10^7	
Kel-F (Polychlorotri-fluoroethylene)	2.1 - 2.2	400-600		10^6	2×10^7	Elongation increases, impact strength decreases
Polyvinyl Butyral	1.05	325	Flexible	2×10^6	1.5×10^7	Becomes brittle
Cellulose Acetate	1.3	200-600		10^6	1.5×10^7	
Polyamide (Nylon)	1.14	350-470	Flexible	10^6	5×10^6	Stiffens, tensile Strength increases
Teflon (TFE)	2.17	400-500	Flexible	2×10^4	4×10^4	Becomes brittle, cracks
Teflon (FEP)	2.14	500-600	Flexible	10^5	3×10^5	Becomes brittle, cracks

Table 4.7-16 (Continued)

RADIATION EFFECTS ON ORGANIC ELECTRICAL INSULATION

Material	Specific Gravity	Dielectric Strength (V/mil)	Initial Mechanical Properties	Radiation Damage Threshold	Dose Causing Significant Damage (rads)	Comments
Styrene - Butadiene (SBR)	0.93 - 1.1	420-540		10^6	10^7	Becomes brittle
Silicone Rubber	1.0 - 1.5	300-550	Flexible	10^6	3×10^6	Becomes brittle
Polypropylene	0.9	450-650	Flexible	10^6	10^7	Becomes brittle, cracks
Polypropylene Fluoride (Kynar 400)			Flexible	10^7	10^8	Becomes brittle, tensile strength falls
Diallyd Phthalate			Hard	$\sim 10^{10}$	$>10^{10}$	Becomes harder
Polyurethane	1.1-1.5	400-500	Flexible	10^9	$\sim 10^{10}$	Becomes stiffer

Table 4.7-17

RADIATION EFFECTS ON CERAMIC ELECTRICAL INSULATION

Material	Specific Gravity	Dielectric Strength (V/mil)	Mechanical Properties	Radiation Damage Threshold (n/cm^2)	Dose Causing Significant Damage (n/cm^2)	Radiation Effects
MgO	3.65	50	Hard	$4x10^{19}$	10^{20}	Dimensions change, cracks more easily
Al_2O_3	4.0	220-340	Hard	10^{19}	$2x10^{20}$	Dimensions change, cracks more easily
Glass (hard)	2.2-3.8	500	Hard	10^{16}	$>10^{16}$	Cracks form
Glass (Boron free)	2.2-3.8	500	Hard	10^{17}	10^{18}	Dimensions change, discolored, brittle
Quartz	2.65	400	Hard	10^{21}	$>10^{21}$	Dimensions change, cracks more easily
Sapphire	4.0	220-340	Hard	10^{19}	$>10^{20}$	Dimensions change, cracks more easily
Forsterite	3.2	240	Hard	10^{19}	10^{20}	Dimensions change, cracks more easily
Spinel	3.6		Hard	10^{19}	10^{20}	Dimensions change, cracks more easily
Beryllium Oxide	3.0	250-700	Hard	10^{19}	10^{20}	Dimensions change, cracks more easily

The power requirements for the engine will be included in the stage power profile and supplied as required in the form of 28 vdc. Certain stage applications require the use of ac voltage. Inverters on the propulsion module will be used to accommodate these motor requirements. Additionally, a battery integral with the stage power system would be located forward of the run tank to supply peak loads for the engine and run tank components.

Communication between the RNS data management subsystem and the NDICE would use the data bus. In addition to the signals defined in Section 7 of Book 2 it is envisioned that the control of aftercooling impulse would be required to preclude thrusting during star sightings or other specific stage operations. This would take the form of an enable or a disable signal and would take into account the modeled aftercooling profile in the stage processor.

The RNS baseline is that processing necessary for the control of the engine will be supplied by the NDICE. This is based largely on the uncertainty of the processing requirements for engine control. Should the processing requirements be comparable to the stage processing requirements, it is feasible to integrate the two processing requirements in the single, centralized processor selected for the RNS.

4.8 STRUCTURAL DYNAMICS

4.8.1 Requirements

An engine/stage structural dynamics analysis was conducted during Phase II for a simplified model of the Class 1 Standard RNS during launch to orbit, which indicated that structural loads could present a problem if the engine is launched integrally with the stage. A specific trade study was assigned to MDAC during Phase III as Subtask 9.6, to provide a more complete analysis of engine/stage structural dynamics for launch by the Saturn INT-21. Both the Class 1 Standard (a single module with NERVA attached to the conical aft bulkhead) and upright, integral launch of the Class 1-Hybrid (dual modules with NERVA attached to a propulsion module run tank) were investigated. The design criteria, method of analysis, and results for these two launch concepts are reported here. The baseline MDAC launch concept entails launch of

NERVA attached to a propulsion module run tank inside the space shuttle cargo bay. The method of analysis to be described is applicable to this case, but space shuttle launch dynamic excitations would be required to evaluate this configuration.

Figure 4.8-1 shows the RNS Class 1 Standard Hybrid configurations for the baseline 10-degree half-angle cone. In each, NERVA is cantilevered from a long, flexible beam during launch, which will combine with the high weight and flexibility of the NERVA to result in low resonant frequencies. These low frequency modes could couple with the launch vehicle bending motion at release and lift-off and during boost. Large displacements of the NERVA could result from this coupling, leading to potential engine clearance problems and excessive loads. The NERVA clearance envelope in the 33-ft-diameter interstage is adequate, but loading could be a problem both to the stage structure and NERVA. Two design approaches have been considered: (1) stiffen and strengthen the stage and NERVA structure, and/or (2) restrain the NERVA during launch and boost phase of flight with removable structure. ANSC considers that strengthening NERVA would impose a significant weight penalty (Reference 4-26), so the supported engine approach is preferred.

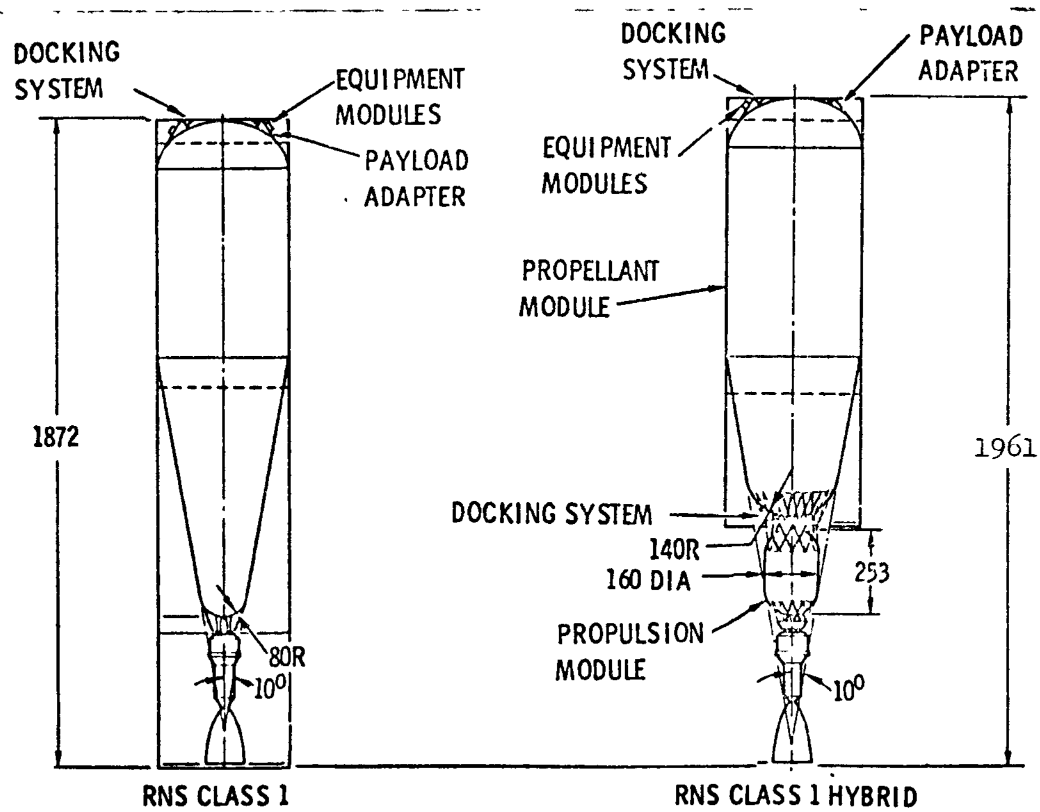

Figure 4.8-1 RNS CLASS 1 CONFIGURATIONS (300,000 Lb LH_2)

Two engine restraint concepts have been analyzed by MDAC: (1) lateral ties between the engine at the nozzle throat and ascent shell, and (2) axial struts between the thrust structure and engine pressure vessel with the gimbal actuators locked. These are illustrated in Figure 4.8-2.

The NERVA structural dynamic model defined by Reference 4-68 is depicted in Figure 4.8-3. Most of the mass points in the model have axial, lateral, an torsional degress of freedom, except for the gimbal actuators (points E through HO, which have only axial motion, and the nuclear subsystem (points W and AA through DD), which does not have rotational motion. Dynamic response data have been generated by MDAC for the three degrees of freedom of the stage/upper thrust structure interface (point B), pressure vessel/nozzle/nuclear subsystem (point V), nozzle throat (point EE), and nozzle extension/destruct subsystem (point KK). These mass points are shaded on the figure. The analyses are based on the free-free data in Reference 4-69 for the B configuration of the NERVA in the 45 to 225-degree X – Y plane. The first six resonant frequencies of this model (which are not component modes) are 3.34, 14.34, 18.14, 36.19, 44.09, and 47.96 Hz. Two percent structural damping was used in generating the dynamic response data.

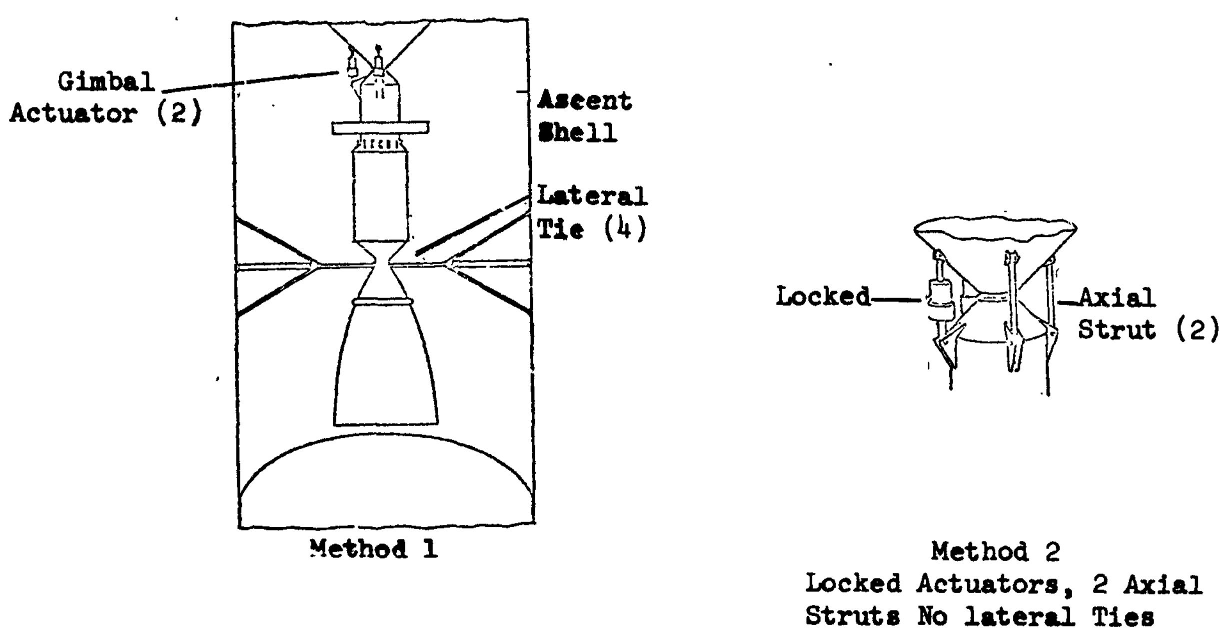

Figure 4.8-2 ENGINE SUPPORT SCHEMES

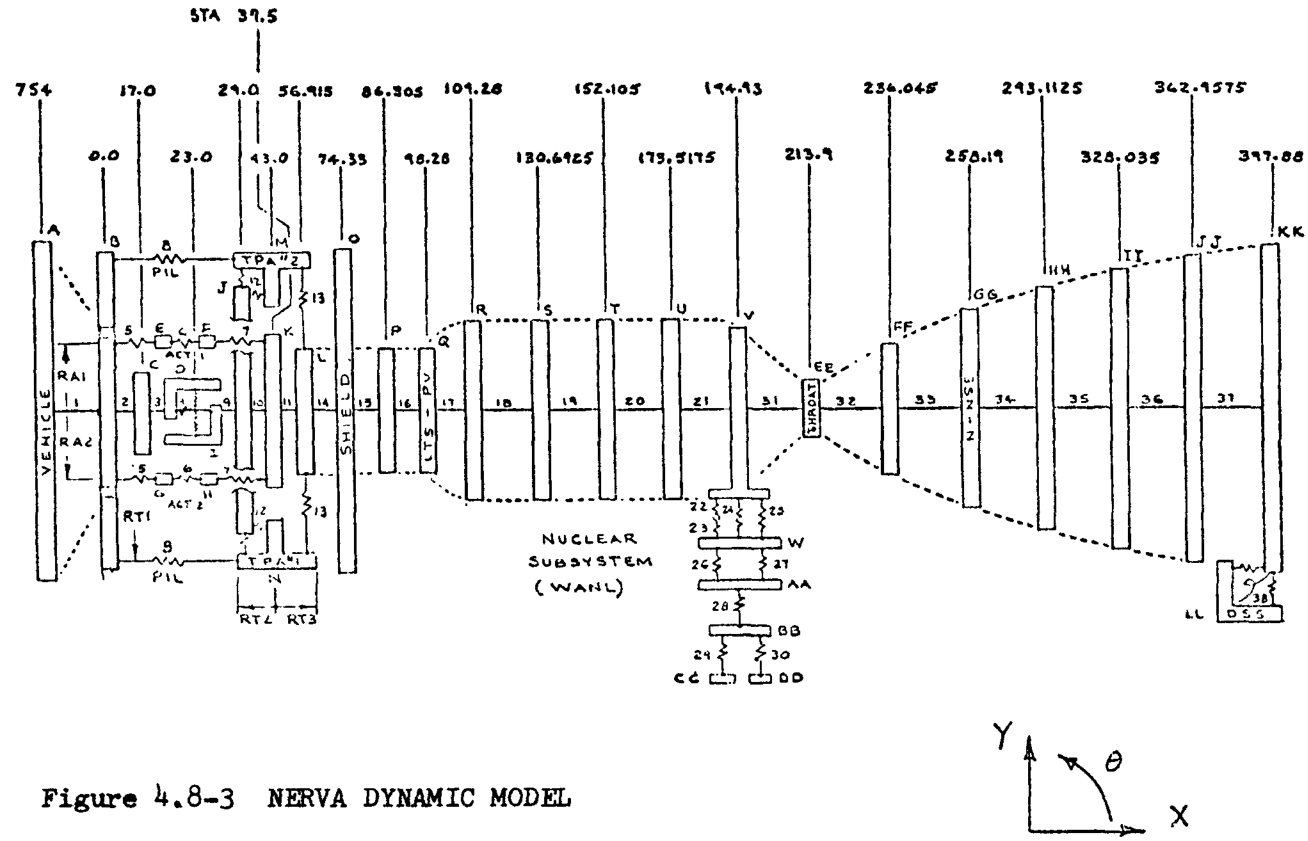

Figure 4.8-3 NERVA DYNAMIC MODEL

The lateral acceleration transient used to excite the dynamic model was based on Saturn V launch data, and is defined by Reference 4-70. The release and liftoff transient was selected since it is the most severe. It has appreciable energy at 2.46, 4.50, 5.37, 7.99, 9.30, and 11.2 Hz. The total peak lateral acceleration of the transient was 2.2 g peak. This transient was allowed to decay to zero within 6 sec.

Saturn INT 21 data obtained from Reference 4-71 list the first three resonant frequencies at lift-off as 0.89, 2.01 and 4.04 Hz. Transient acceleration levels associated with these frequencies were not provided. Therefore, without making some assumptions as to the levels, dynamic responses could not be generated using this data. However, with the frequency differences between these data and the Saturn V data used, the dynamic responses could be appreciably affected.

The results required are the resonant frequencies of the system, both without any engine restraint and with each of the two restraint concepts, and the dynamic response of the system to stimuli.

4.8.2 Method of Analysis

Figure 4.8-4 shows schematically the models used to analyze NERVA/stage dynamics for INT-21 launch and defines the coordinate system used. To excite the dynamic model a lateral acceleration transient was applied to the horizontal degree of freedom. Positive displacements are in the direction of the arrows shown.

The development of the equations of motion for the Class 1 Standard and Hybrid is similar. The Hybird, which is a more complex configuration, will be used to illustrate the technique. The intermodule structure and the propulsion module are represented as the following elements: (1) forward truss structure, (2) run tank, (3) aft thrust truss structure, and (4) NERVA.

The equations for each of the first three elements have been developed by MDAC. The dynamic description for the fourth was obtained from ANSC, as indicated above. These are combined into the equations of motion for

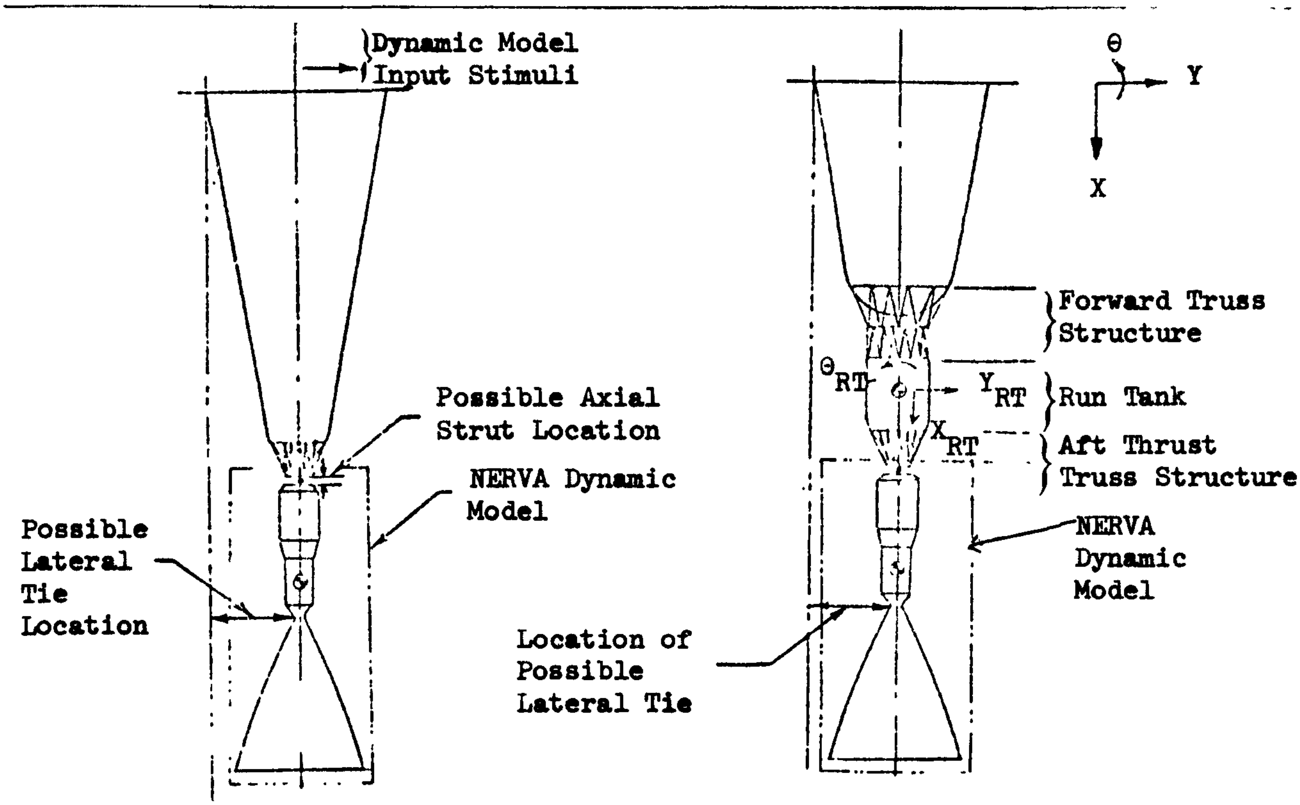

Figure 4.8-4 MODELS USED IN ANALYZING NERVA/STAGE DYNAMICS

the total system to be equating like displacements. Coordinate transformations were used to eliminate dependent coordinates. The final form of the equations of motion has fifteen degrees of freedom: (1) the three motions of the stage base, (2) the three rigid body degree of freedom of the run tank, (3) the three rigid-body degree of freedom of the NERVA, and (4) the first six bending modes of the NERVA. The matrix below outlines these equations.

For the two specific engine restraint concepts which have been analyzed submatrixes were added to this basic spring matrix. In the case of lateral ties between the engine throat and ascent shell, the horizontal input transient applied to the horizontal Y degree of freedom of the forward truss is also applied to the ascent shell attach point of the lateral tie.

To obtain the natural resonant frequencies the problem is reduced to a twelve degree of freedom problem by moving the input element submatrix ($\underline{X}_1$, $\underline{Y}_2$, $\underline{\theta}_3$) to the right side of the equal sign and solving the characteristic equation. The eigenvectors obtained are used to transform the input element submatrix to the new modal coordinates. The forced response is determined by evaluating the resulting differential equations. After the responses have been obtained in "modal" coordinates a coordinate transformation is used to convert back to "real" physical components displacements. Response curves (coordinate displacement versus time) are then generated using an automatic plot routine. One complete set of data consists of 37 response curves.

Response data was generated only for the case of an horizontal input applied on the $\underline{Y}_2$ degree of freedom. The program used could also generate responses for $\underline{X}_1$ and $\underline{\theta}_3$ inputs. However, Reference 4-70 defined only the input transient for $\underline{Y}_2$ without providing similar data for $\underline{X}_1$ and $\underline{\theta}_3$.

$$
\begin{array}{l}
\text{Stage Base} \\
\\
\\
\text{Run Tank} \\
\\
\\
\text{NERVA Rigid Body} \\
\\
\\
\text{NERVA Bending} \\
\\
\\
\\
\\
\\
\end{array}
\left[\begin{array}{cccccccccc}
0 & & & & & & & & & \\
 & 0 & & & & & & & & \\
 & & 0 & & & & \multicolumn{3}{c}{\text{All Off-Diagonal Terms Zero}} & \\
 & & & m_R & & & & & & \\
 & & & & m_R & & & & & \\
 & & & & & I_R & & & & \\
 & & & & & & \overline{m} & & & \\
 & & & & & & & \overline{m} & & \\
 & & & & & & & & \overline{I} & \\
 & & & & & & & & & \text{Modal Masses}
\end{array}\right]
\left[\begin{array}{c}
X_1 \\ Y_2 \\ \Theta_3 \\ X_R \\ Y_R \\ \Theta_R \\ \overline{X} \\ \overline{Y} \\ \overline{\Theta} \\ \xi_1 \\ \xi_2 \\ \xi_3 \\ \xi_4 \\ \xi_5 \\ \xi_6
\end{array}\right]
+
\left[\begin{array}{c}
\\
\\
\text{Structural Coupling} \\
\text{Spring Matrix} \\
\\
\\
\end{array}\right]
\left[\begin{array}{c}
X_1 \\ Y_2 \\ \Theta_3 \\ X_R \\ Y_R \\ \Theta_R \\ \overline{X} \\ \overline{Y} \\ \overline{\Theta} \\ \xi_1 \\ \xi_2 \\ \xi_3 \\ \xi_4 \\ \xi_5 \\ \xi_6
\end{array}\right]
= 0
$$

4.8.3 Dynamic Response - Class 1 Standard

Dynamic response data have been generated for the Class 1 Standard configuration for the seven cases defined in Table 4.8-1.

Table 4.8-1

STANDARD CONFIGURATION DYNAMIC RESPONSE CASES

Case	Type of Restraint	Spring Rate (lb/in.)
1	Unrestrained	—
2	Nozzle Throat/Ascent Shell Lateral Ties	5,000
3	Nozzle Throat/Ascent Shell Lateral Ties	10,000
4	Nozzle Throat/Ascent Shell Lateral Ties	25,000
5	Engine Pressure Vessel/Thrust Structure Axial Struts	1,000,000
6	Engine Pressure Vessel/Thrust Structure Axial Strust	2,000,000
7	Engine Pressure Vessel/Thrust Structure Axial Struts	4,000,000

Table 4.8.2 lists the resonant frequencies obtained for the unrestrained engine and the lateral restraint and axial strut alternatives. Both methods of restraint increase the first (cantilevered) resonant frequency. However, lateral restraint of the NERVA appears to be a far more effective method of raising the frequency. Figures 4.8-5 and 4.8-6 provide plots of the first resonant frequency versus spring rate for each of the two restraint methods.

Table 4.8-2

RESONANT FREQUENCIES (HZ)
CLASS 1 STANDARD CONFIGURATION

		Axial Struts Between the Thrust Structure and Pressure Vessel			Lateral Ties Between the Engine and Ascent Shell at Nozzle		
Mode Number	Without Restraint	1×10^6 lb/in.	2×10^6 lb/in.	4×10^6 lb/in.	5.0×10^3 lb/in.	10×10^3 lb/in.	25×10^3 lb/in.
1	0.97	1.53	1.56	1.57	1.79	2.34	3.50
2	4.92	6.26	6.26	6.26	4.92	4.92	4.92
3	6.26	7.71	8.09	8.32	6.26	6.26	6.27
4	16.12	16.12	16.13	16.13	16.12	16.12	16.12
5	17.75	17.75	17.75	17.76	17.75	17.75	17.76
6	21.45	24.01	24.43	24.09	21.45	21.47	21.48

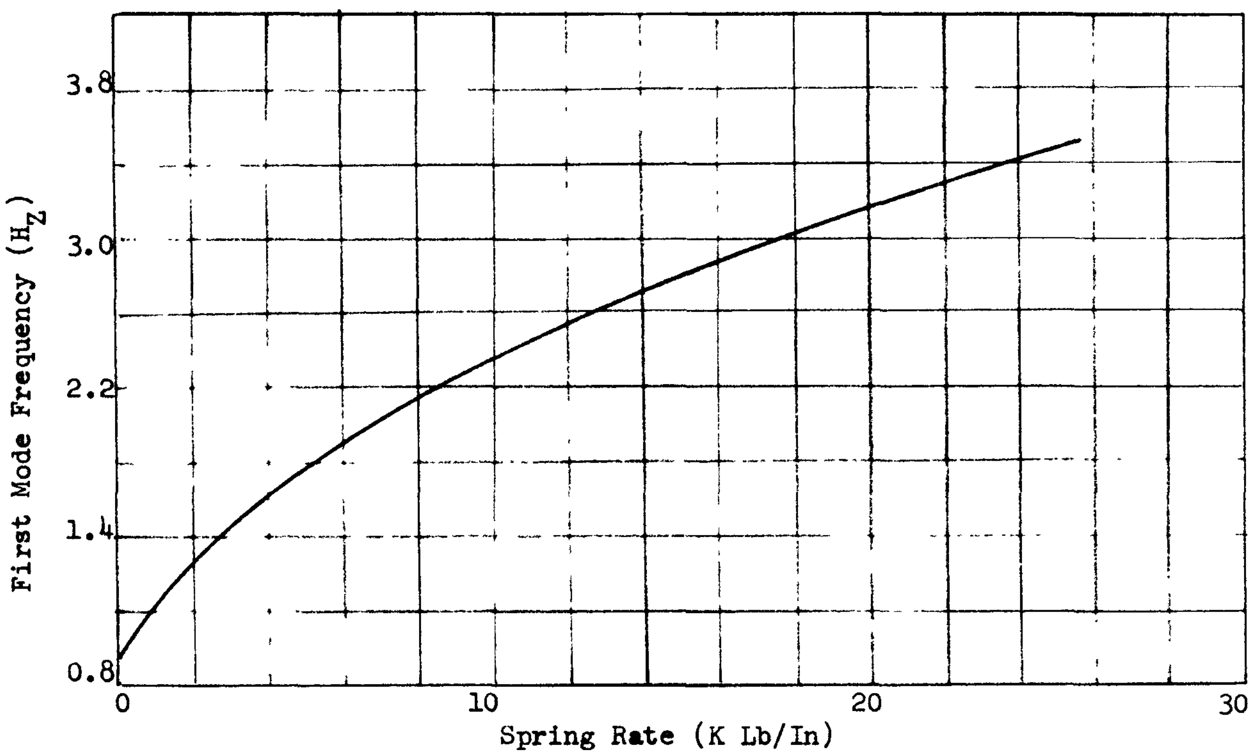

Figure 4.8-5 FREQUENCY VS. SPRING RATE FOR LATERAL TIES AT NOZZLE

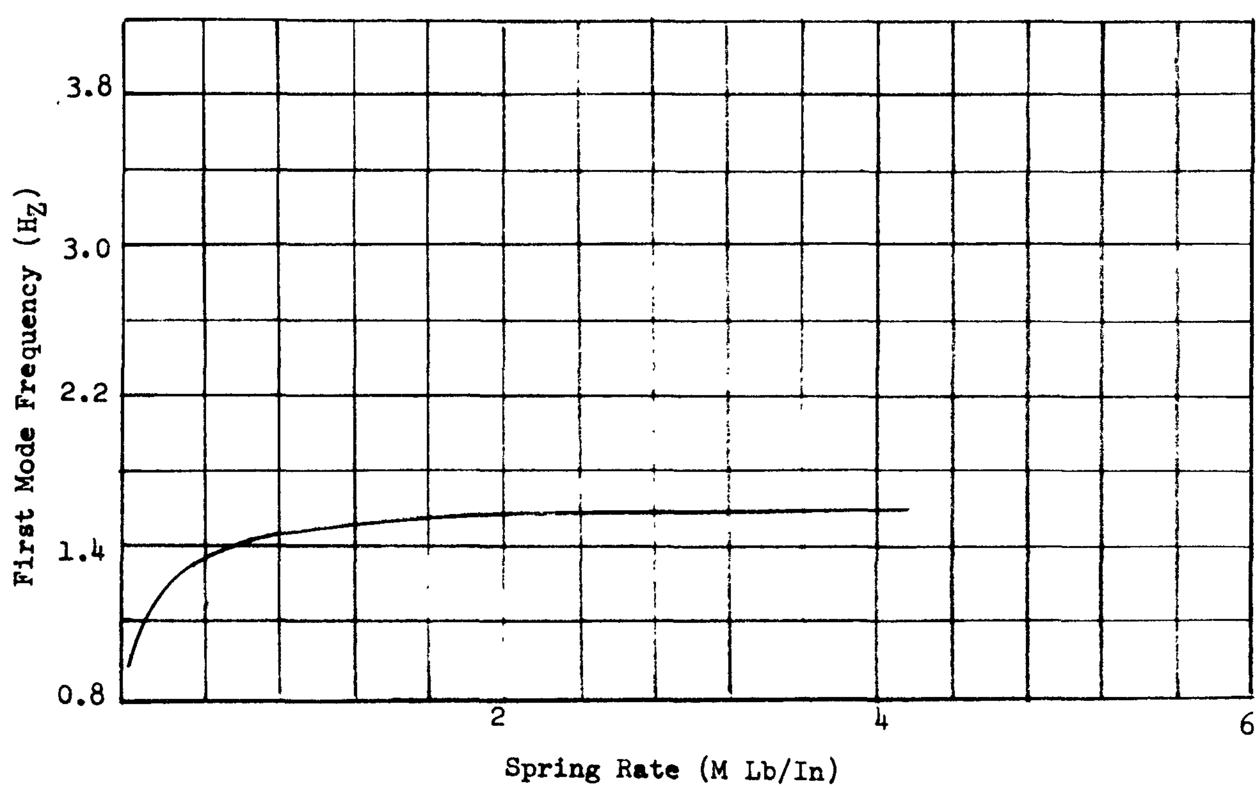

Figure 4.8-6 FREQUENCY VS. SPRING RATE FOR AXIAL STRUTS AT ACTUATORS

Tables 4.8-3 and 4.8-4 summarize the dynamic response for the cases of lateral restraint at the NERVA throat and restraint at the actuators. The unrestrained case is shown in each table for reference. For conciseness, the results are presented as the maximum positive and negative displacements of each degree of freedom for the primary NERVA mass points. The displacements resulting from the applied lateral acceleration is not considered excessive. Review of these data leads to the following conclusions:

A. Restraint of the NERVA does not necessarily reduce the displacements.

B. For the case of restraint at the actuators, increasing the restraint spring rate will decrease the displacements of the nozzle extension while increasing the displacements for the critical nuclear subsystem.

C. Lateral restraint at the throat can raise the cantilevered resonant frequently to such a level that coupling with the input transient becomes excessive. This phenomenon is displayed in the 10,000 lb/in. restraint case where the cantilevered frequency is raised to 2.34 HZ (see Table 4.8-2), very near to the 2.46 HZ frequency of the input transient. As can be seen from Table 4.8-3, the displacements for this restraint case (10,000 lb/in.) are higher than those of the other two restraint spring rate cases.

4.8.4 <u>Dynamic Response — Class 1-Hybrid Integral Launch</u>

Table 4.8-5 lists the resonant frequencies obtained for the Hybrid configuration for the unrestrained case and the case of a 10,000 lb/in. lateral tie at the nozzle. As can be seen from these data the lateral restraint increases the first cantilevered frequency from 0.63 HZ to 2.01 HZ.

Table 4.8-6 summarizes the dynamic response data obtained for this configuration. An additional mass point is shown for the run tank. Review of these data leads to the following conclusions:

A. Restraint of the NERVA at the throat does not necessarily reduce the dynamic displacements.

B. With lateral restraint the horizontal displacement of the nuclear subsystem is increased approximately from 0.34 to 1.75 inches. Whereas, the displacement of the nozzle extension is reduced

Table 4.8-3

SUMMARY OF DYNAMIC DISPLACEMENTS

CLASS 1 STANDARD - LATERAL RESTRAINT AT THROAT

Mass Point	Degree of Freedom	Unrestrained		5×10^3 lb/in. Restraint		10×10^3 lb/in. Restraint		25×10^3 lb/in. Restraint	
		Maximum Positive	Maximum Negative	Maximum Positive	Maximum Negative	Maximum Positive	Maximum Negative	Maximum Positive	Maximum Negative
Interface (Stage/UTS)	X - 4 Inches	0.073	0.064	0.066	0.061	0.075	0.068	0.096	0.103
	Y - 5 Inches	1.71	1.41	1.62	1.32	1.7	1.22	1.62	1.29
	θ - Radians	0.0037	0.0034	0.0035	0.0036	0.0048	0.0036	0.0035	0.003
PV/Nozzle/NSS	X - 56 Inches	0.116	0.72	0.14	0.14	0.23	0.195	0.148	0.18
	Y - 57 Inches	0.54	0.47	1.45	1.32	3.2	3.3	1.45	1.48
	θ - Radians	0.015	0.0187	0.02	0.024	0.028	0.023	0.015	0.016
Nozzle Throat	X - 69 Inches	0.116	0.072	0.131	0.142	0.215	0.195	0.148	0.18
	Y - 70 Inches	0.51	0.42	1.45	1.5	3.6	3.6	1.48	1.65
	θ - 71 Radians	0.015	0.019	0.021	0.024	0.028	0.023	0.0155	0.016
Nozzle Extension/DSS	X - 87 Inches	0.116	0.072	0.13	0.14	0.215	0.195	0.15	0.18
	Y - 88 Inches	3.3	3.92	5.0	6.0	8.4	7.6	3.8	4.4
	θ - 87 Radians	0.0162	0.0205	0.024	0.026	0.03	0.027	0.017	0.0175

Table 4.8-4

SUMMARY OF DYNAMIC DISPLACEMENTS

CLASS 1 STANDARD - RESTRAINT AT ACTUATORS

Mass Point	Degree of Freedom	Unrestrained		1×10^6 lb/in. Restraint		2×10^6 lb/in. Restraint		4×10^6 lb/in. Restraint	
		Maximum Positive	Maximum Negative	Maximum Positive	Maximum Negative	Maximum Positive	Maximum Negative	Maximum Positive	Maximum Negative
Interface (Stage/UTS)	X - 4 Inches	0.073	0.064	0.032	0.048	0.046	0.063	0.044	0.065
	Y - 5 Inches	1.71	1.41	0.96	0.51	1.23	0.66	1.25	0.75
	θ - 6 Radians	0.0037	0.0034	0.0013	0.0012	0.0012	0.0017	0.0014	0.0019
PV/Nozzle/NSS	X - 56 Inches	0.116	0.072	0.072	0.092	0.056	0.078	0.055	0.067
	Y - 57 Inches	0.54	0.47	0.85	1.17	0.92	1.21	0.96	1.22
	θ - 58 Radians	0.015	0.0187	0.007	0.0096	0.0065	0.0085	0.0061	0.0077
Nozzle Throat	X - 69 Inches	0.116	0.072	0.072	0.092	0.045	0.077	0.055	0.076
	Y - 70 Inches	0.51	0.42	0.92	1.36	1.03	1.35	1.07	1.25
	θ - 71 Radians	0.015	0.019	0.0072	0.0096	0.0066	0.0086	0.0062	0.0077
Nozzle Extension/DSS	X - 87 Inches	0.116	0.072	0.072	0.092	0.055	0.076	0.053	0.075
	Y - 88 Inches	3.3	3.92	2.4	3.1	2.4	2.9	2.3	2.75
	θ - 89 Radians	0.0162	0.0205	0.0086	0.0096	0.0075	0.0091	0.007	0.0084

Table 4.8-5

RESONANT FREQUENCIES (HZ)

CLASS 1 HYBRID

Mode Number	Without Restraint	10×10^3 lb/in. Lateral Tie Between the Engine and Ascent Shell Tie at Nozzle
1	0.632	2.01
2	2.28	2.47
3	4.66	4.66
4	6.55	6.55
5	9.26	9.26
6	14.25	14.25

approximately from 3.3 to 2.0 inches. The horizontal displacements of the run tank is not effected appreciably by the presence of the lateral restraint.

4.8.5 Structural Loading Implications

Dynamic response data have been presented for an INT-21 launch of the Class 1 Standard and Hybrid configurations with two engine restraint concepts and a range of restraint system spring rates. It is concluded that lateral restraint of the NERVA is far more effective in raising the cantilevered resonant frequency than axial struts. However, for the model studied restraint of the NERVA does not necessarily reduce the dynamic displacements and creates a more severe environment for the nuclear subsystem. Depending on the restraint system spring rate, the cantilevered frequency of the NERVA could be changed to the point that a correspondence with the frequency of the input transient occurred. This would lead to undesirable coupling. An analytic tool such as the one developed should be used to predict and avoid this situation.

The input lateral acceleration transient of 2.2 g peak can be significantly amplified by the cantilevered system. Table 4.8-7 below shows the peak lateral accelerations at various locations for the Standard and Hybrid integral launch configurations. Also, for reference this table shows the maximum

Table 4.8-6

SUMMARY OF DYNAMIC DISPLACEMENTS

HYBRID

Mass Point	Degree of Freedom	Unrestrained		Lateral Restraint at Throat 10,000 lb/in.	
		Maximum Positive	Maximum Negative	Maximum Positive	Maximum Negative
Interface (Stage/UTS)	X - 4 Inches	0.08	0.05	0.10	0.083
	Y - 5 Inches	1.92	1.95	1.92	2.00
	θ - 6 Radians	0.0076	0.0083	0.0105	0.078
PV/Nozzle/NSS	X - 56 Inches	0.167	0.162	0.17	0.135
	Y - 57 Inches	0.345	0.345	1.72	1.8
	θ - 58 Radians	0.0142	0.015	0.0073	0.0067
Nozzle Throat	X - 69 Inches	0.163	0.163	0.169	0.134
	Y - 70 Inches	0.61	0.61	1.73	1.75
	θ - 71 Radians	0.141	0.15	0.073	0.067
Nozzle Extension/DSS	X - 87 Inches	0.165	0.163	0.168	0.135
	Y - 88 Inches	3.25	3.4	1.91	2.06
	θ - 89 Radians	0.0145	0.016	0.0075	0.0069
Run Tank Center of Mass	X_{RT} Inches	0.055	0.031	0.061	0.051
	Y_{RT} Inches	0.84	0.92	0.77	0.67
	θ_{RT} Radians	0.007	0.0063	0.0072	0.0079

Table 4.8-7

PEAK LATERAL ACCELERATION AND DISPLACEMENT COMPARISON

Location	Class 1 - Standard		Class 1 - Hybrid	
	Unrestrained	10,000 lb/in. Restraint At Throat	Unrestrained	10,000 lb/in. Restraint At Throat
Interface (Stage/UTS)				
Peak Lateral Acceleration (g)	4.3	4.4	1.1	0.90
Maximum Lateral Displacement (in.)	1.7	1.7	1.9	1.9
Pressure Vessel/Nozzle/ Nuclear Subsystem				
Peak Acceleration (g)	2.2	2.0	0.20	0.70
Maximum Displacement (in.)	0.54	3.2	0.35	1.75
Nozzle Throat				
Peak Acceleration (g)	2.1	2.2	0.50	0.70
Maximum Displacement (in.)	0.51	3.6	0.61	1.75

lateral displacement at these locations. The second location indicated in the table is the reactor core base. The reactor fuel elements are cantilevered upward from this location. Implication of the dynamic transients on the reactor core would appear to deserve particular attention.

To assess the structural loadings associated with the dynamic displacements the changes in length (deformations) of the structural elements are required. These deformations multiplied by the known stiffness matrix of the structural elements, will provide the structural loadings. The deformations are difficult to obtain because of (1) oscillatory nature of the responses, and (2) the fact that relative instead of absolute displacements are required to determine the deformations and attendant structural loading. The analytic tool utilized does not generate these deformations, but the capability can be added.

A preliminary assessment of the loading for a few selected time points has been made using hand calculations. This assessment has indicated that in general the stage loading is not excessive. The unrestrained Class 1 - Hybrid configuration was analyzed. For this case the largest relative deflections occurred at liftoff transient and produced strut loads of 6,270 lb, 10,310 lb and 5.505 lb compression for the propulsion module thrust structure, forward skirt, and the propellant module intermodular thrust structure, respectively. Comparing these loads with those in Table 4.2-9, only the propulsion module forward skirt is affected by this dynamic loading condition, with an attendent load increase of 2,240 lb/strut. This would result in a skirt that weighed 260 lb, which is only a 10 lb increase over one designed for engine operation. The impact on the thrust structure for the unrestrained standard configuration is less severe. Thus, the major concern for stage structure would be increased stiffening for propellant tankage. Since the two integral launch configurations are not serious candidates for the RNS baseline design, the additional stress analysis required to evaluate this condition was not performed.

If the unrestrained launch case imposed excessive tank weight penalties for stiffening, the implications of lateral restraint would warrant a more careful evaluation, since it appears that reducing loads at the stage interface and gimbal assembly and actuators must be traded against a more severe dynamic environment for the nuclear subsystem. It should be emphasized that the results cited are dependent on the dynamic inputs utilized. Both the INT-21 and space shuttle are expected to have a lower spectrum of input frequencies than the reference Saturn V data; which increases the possibility for dynamic coupling of the cantilevered engine system. Thus, the baseline space shuttle launch case deserves investigation of these factors.

REFERENCES

3-1 "Nuclear Flight System Definition Study Final Report, Volume II, Part 1, RNS System Definition, System Analysis", MDC G0585, May 1970.

3-2 "Nuclear Flight System Definition Study, Final Report, Volume II, Part 2, RNS System Definition, Single Module Concept Definition," MDC GO585, May 1970.

3-3 J. B. Blackmon, J. N. Castle, and B. R. Heckman, "Propellant Settling" Douglas Report No. DAC 62263, May 1968.

3-4 B. L. Pierce and J. W. H. Chi, "An Experimental and Analytical Study of Film Boiling Heat Transfer to Hydrogen," AIAA Paper No. 70-660, June 1970.

3-5 J. W. H. Chi, "Forced Convective Boiling Heat Transfer to Hydrogen," J. Spacecraft and Rockets, Vol. 3, No. 1, page 150, January 1966.

3-6 W. A. Olsen, "Experimental and Analytical Investigation of Interfacial Heat and Mass Transfer in a Pressurized Tank Containing Liquid Hydrogen", NASA TN D-3219, March 1966.

4-1 "Nuclear Flight System Definition Study Final Report, Volume II, Part 2, RNS System Definition, Single Module Concept Definition", MDC G0585, May 1970.

4-2 "Nuclear Flight Propulsion Module Study Final Report, Part 1, NFPM Design," MDC G0586, May 1970.

4-3 "Application of Saturn V Intermediate Launch Vehicle to Space Station Missions - Final Report," Boeing Report D5-15804-2, September 1970.

4-4 "Guidelines for Strength Analysis, Test, and Assessment Requirements," MSFC Memorandum S&E-ASTN-AS-70-55, dated June 5, 1970.

4-5 "Structural Design Criteria and Interpretive Information Applicable to a Manned Space Shuttle," NASA Langley Space Vehicle Design Criteria Office, Contract NASI-6024, Review Copy, July 1970.

4-6 "Orbital Workshop, Loads and Structural Design Criteria," DAC-56612B, August 1970.

4-7 "Guidelines and Constraints Document, Nuclear Shuttle Systems Definition Study, Phase A," MSFC PD-SA-P-70-63, Rev. 2, October 1, 1970.

4-8 "NERVA Program Requirements Document," SNPO-NPRD-1, Release 7, January 19, 1970.

4-9 "Metallic Materials and Elements for Aerospace Vehicle Structures," MIL-HDBK-5A, February 8, 1966.

4-10 "Plastics for Flight Vehicles," MIL-HDBK-17, August 14, 1961.

4-11 "Structural Sandwich Composites," MIL-HDBK-23A, December 30, 1968.

4-12 "Cryogenic Materials Data Handbook," ML-TDR-64-280, July 1965.

4-13 "NERVA Reference Data (Full Flow Engine)," AGC Report S-130-CP-090290 Preliminary, April 1970.

4-14 "NERVA Status Presentation," AGC. September 1970.

4-15 "Acceleration Load Factors for Space Shuttle Payload," MSFC Memorandum S&E-ASTN-AA-70-110, November 13, 1970.

4-16 "Ground Rules for INT-21 Launch Vehicle Definition Studies, Rev. B," MSFC Letter S&E-CSE-L-70-239, dated August 24, 1970.

4-17 "Preliminary Analysis of INT-21 Launch Vehicle/McDonnellDouglas (MDAC) Space Station Payload - Mission No. 1," Boeing Report 5-1085-INT-21-07, February 23, 1970.

4-18 "CEI Detail Specification, Performance/Design and Qualification Requirements and Product Configuration and Acceptance Test Requirements," for S-IVB Stages 205 through 212, for Saturn IB Program, CP-208000 B.

4-19 "Terrestrial Environment (Climatic) Criteria Guidelines for Use in Space Vehicle Development," 1969 Revision, NASA TM-X-53872, September 8, 1969.

4-20 "Buckling of Thin-Walled Circular Cylinders," NASA SP-8007, August 1968.

4-21 R. R. Meyer, "Structural Analysis Design Note Optimization of Isogrid Cylinders and Spheres," Space Shuttle Design Note No. WEST-STR-2, Contract NAS8-26016, August 13, 1970.

4-22 S. Timoshenko and J. M. Gere, "Theory of Elastic Stability," McGraw-Hill, 1961.

4-23 G. Gerard and H. Becker, "Handbook of Structural Stability, Part I - Buckling of Flat Plates," NASA TN 3781, July 1957.

4-24 R. R. Meyer, "Constitutive Equations and Membrane Solutions for Isotropic Stiffened Shells," SM-49248, September 1965.

4-25 "Buckling of Thin-Walled Truncated Cones," NASA SP-8019, September 1968.

4-26 "NERVA Engine Structural Support," Aerojet Nuclear Systems Co. Letter 7840:0399L, May 26, 1970.

4-27 C. L. Hanks and D. J. Hamman, "The Effect of Radiation on Electrical Insulating Materials," Battelle Memorial Institute, REIC Report No. 46, dated June 16, 1969.

4-28 "Modern Plastics Encyclopedia, 1969-1970," Vol. 46, October 1969.

4-29 E. C. McKannan and R. L. Gause, "Effects of Nuclear Radiation and Cryogenic Temperatures on Engineering Materials," NASA, Huntsville, Alabama, AIAA Paper No. 64-361, 1st AIAA Annual Meeting, Washington, D.C., June 29-July 2, 1964.

4-30 D. K. Weidner, ed., "Natural Environment Criteria for the NASA Space Station Program," NASA TM X-53865, October 31, 1969.

4-31 "Terrestrial Environment (Climatic) Criteria Guidelines for Use in Space Vehicle Development," NASA TM X-53872, September 1969.

4-32 "Space Environment Criteria Guidelines for Use in Space Vehicle Development," (1969 Revision) NASA TM X-53957, October 1969.

4-33 Charles F. Schafer, Tommy C. Bannister, "Thermal Control Coating Degradation Data from the Pegasus Experiment Packages," in Progress in Astronautics and Aeronautics - Volume 20, 1967.

4-34 Carr B. Neel, "The Role of Flight Experiments in the Study of Thermal-Control Coatings for Spacecraft," AIAA Paper 67-329, Thermophysics Specialist Conference, New Orleans, Louisiana, April 17-20, 1967.

4-35 P.M. Blair, Jr., G.F. Pezdirtz and R.A. Jewell, "Ultraviolet Stability of Some White Thermal Control Coatings Characterized in Vacuum," AIAA Paper 67-345, (Presented at Thermophysics Specialist Conference, New Orleans, Louisiana, April 17-20, 1967).

4-36 John P. Millard, "Results from the Thermal Control Coatings Experiment on OSO-III," AIAA Paper 68-794, AIAA Thermophysics Conference, Los Angeles, California, June 24-26, 1968.

4-37 R. Bowman, "Rigid Polyurethane Foam Technology," Western Plastics, March 1965.

4-38 B.H. Anderson and M.J. Kolar, "Experimental Investigation of the Behavior of a Confined Fluid Subjected to Non-Uniform Source and Wall Heating," NASA TND-2079, November 1963.

4-39 "Analytical and Experimental Study of Liquid Orientation and Stratification in Standard and Reduced Gravity Fields," LMSC Report 2-05-64-1, July 1964.

4-40 D. B. Neff, "Free Convection in a Container of Cryogenic Fluid," M. S. Thesis, Denver Univ.

4-41 C. R. Easton, "Large Amplitude Free Surface Oscillations with Surface Tension," Ph. D. Thesis, UCLA, 1970.

4-42 "Space Materials Handbook, 2nd Edition," NASA Report MLTDR-64-40, January 1965.

4-43 "The Effect of Nuclear Radiation on Elastomeric and Plastic Components and Materials, " Battelle Memorial Institute, REIC Report No. 21 (Addendum), August 31, 1964.

4-44 "Radiation Effects State of the Art, 1963-1964," Battelle Memorial Institute, REIC Report No. 34, June 30, 1964.

4-45 F. Cotton, "Radiation Effects on Design Properties of Some Common Plastics and Elastomers," Picatinny Arsenal, Dover, N. J., Technical Report 3615, September 1967.

4-46 E. E. Keklin and E. T. Smith, "Measured Effects of the Various Combinations of Nuclear Radiation, Vacuum and Cryotemperatures on Engineering Materials," Annual Report, FZK-188-2, May 1964.

4-47 "Lightweight Scanning Laser Radar System for the 1975-80 Space Station and Associated Vehicles," ITT Report No. 301501, November 1969.

4-48 "Transmittal of NERVA Pump Net Positive Suction Pressure (NPSP) Conditions as a Function of Flow," ANSC Letter 7410:1075, July 15, 1970.

4-49 A. D. Wilcox, B. A. Lindsey, and M. A. Capo (WANL), "NERVA Flight Engine Common Radiation Analysis Model," RN-TM-0583, Aerojet General Corporation, May 1969.

4-50 "Final Report of Shield System Trade Study," SO54-023, Volume I, Book 2, Aerojet Nuclear Systems Co., July 1970.

4-51 R. G. Soltesz, et. al., "Radiation Measurements and Analysis in a Nuclear Rocket Propellant Tank Mockup," AIAA Paper No. 69-475, AIAA Fifth Propulsion Joint Specialist Conference, June 1969.

4-52 C. G. Collins and V. P. Calkins, "Radiation Damage to Elastomers, Plastics, and Organic Liquids," General Electric, Atomic Products Div., Aircraft Nuclear Propulsion Dept., Report APEX-261, September 1956.

4-53 G. I. Abrams, "Navigation and Guidance Alternatives on the RNS," ION proceedings, February 1971.

4-54 "Space Station Definition," NAS8-25140, MDC G0605, July 1970.

4-55 G. I. Abrams, "Data Management on the RNS," AIAA Integrated Information Systems Conference, February 1971.

4-56 J. R. Bilinski and R. Merrill, "Selecting Transistors for Radiation Environments," Electronics, p. 38 ff, dated December 25, 1959.

4-57 W. Shedd, B. Buchanan, and R. Dolan, "Radiation Effects on JFET's, IEEE Trans. On Nuclear Science, p. 88ff, dated December 1969.

4-58 L. D. Phillip and P. O. Lauritzen, "Irradiation Damage of MOSFET's Operating in the Common Source Mode," IEEE Trans. On Nuclear Science, p. 284 ff., dated December 1967.

4-59 A. E. Cariffe, "Planetary Solar Array Development," Electro-Optical Systems, Inc., Final Report, February 28, 1969.

4-60 W. E. Price, "The Simulation of Space Radiation Damage to Spacecraft Systems," IEEE Trans. on Nuclear Science, p. 2 ff. December 1965.

4-61 J. I. Vette, "The Space Radiation Environment," IEEE Trans. On Nuclear Science, p. 1 ff, October 1965.

4-62 E. J. Stofel, et al, "Neutron Damage to Si Solar Cells," IEEE Trans. on Nuclear Science, p. 27 ff., October 1969.

4-63 R. C. Waddel, "Radiation Damage to Solar Cells on Relay I and Relay II," IEEE Trans. on Nuclear Science, p. 60 ff, November 1964.

4-64 F. M. Smits, "The Degradation of Solar Cells Under Van Allen Radiation," IEEE Trans. on Nuclear Science, p. 88 ff, January 1963.

4-65 J. J. Wysocki, "Role of Li in Damage and Recovery of Irradiated Silicon Cells," IEEE Trans. on Nuclear Science, p. 103 ff. December 1967.

4-66 D. R. Clarke, et al, "Development of Solar-Panel System for Thermally Annealing Radiation-Damaged Solar Cells," Boeing, Seattle, Final Report NAS5-10445, December 1968.

4-67 "Cabling and Connectors on a Nuclear Stage," NAS8-25620, MDC G0757, February 23, 1971.

4-68 "Dynamic Analysis Report," Aerojet Nuclear System Company Report SO38-CP090290-F1, September 1970.

4-69 "Structural Information Requested by McDonnell Douglas Corporation," Aerojet Nuclear System Company Letter 7410:0214, October 12, 1970.

4-70 "Review of Loads Table and Acoustic Levels," MSFC Letter S&E-ASTN-AA-70-42, May 12, 1970.

4-71 "Report, Refined Analysis of INT-21 Launch Vehicle/Nuclear Shuttle Configuration, 187 Foot Stage," Boeing Company (Huntsville) Letter 5-9406-H-01, August 18, 1970.